FINAL REPORT

Elucidation of the Mechanisms and Environmental Relevance of cis-Dichloroethene and Vinyl Chloride Biodegradation

SERDP Project ER-1557

November 2012

Evan Cox
GeoSyntec Consultants

SERDP
DOD ▪ EPA ▪ DOE

REPORT DOCUMENTATION PAGE

Form Approved
OMB No. 0704-0188

PLEASE DO NOT RETURN YOUR FORM TO THE ABOVE ORGANIZATION.

1. REPORT DATE *(DD-MM-YYYY)*	2. REPORT TYPE	3. DATES COVERED *(From - To)*
11-2012	Final Report	04-2007-11-2012

4. TITLE AND SUBTITLE

Elucidation of the Mechanisms and Environmental Relevance of cis-Dichloroethene and Vinyl Chloride Biodegradation

5a. CONTRACT NUMBER

5b. GRANT NUMBER

5c. PROGRAM ELEMENT NUMBER

6. AUTHOR(S)

Evan Cox

5d. PROJECT NUMBER

ER-1557

5e. TASK NUMBER

5f. WORK UNIT NUMBER

7. PERFORMING ORGANIZATION NAME(S) AND ADDRESS(ES)

GeoSyntec Consultants
130 Research Lane, Suite 2
Guelph, Ontario N1G 5G3

8. PERFORMING ORGANIZATION REPORT NUMBER

9. SPONSORING/MONITORING AGENCY NAME(S) AND ADDRESS(ES)

SERDP/ESTCP
4800 Mark Center Drive, Suite 17D08
Alexandria, VA 22350-3605

10. SPONSOR/MONITOR'S ACRONYM(S)

SERDP/ESTCP

11. SPONSOR/MONITOR'S REPORT NUMBER(S)

ER-1557

12. DISTRIBUTION/AVAILABILITY STATEMENT

Unlimited

13. SUPPLEMENTARY NOTES

14. ABSTRACT

Through two decades of laboratory and field research, it has been generally believed that cis 1,2 dichloroethene (cDCE) and vinyl chloride (VC) can further degrade through a variety of mechanisms, including: i) anaerobic reductive dechlorination to ethene and/or ethane; ii) anaerobic oxidation to carbon dioxide (CO_2) under iron- and/or manganese-reducing conditions; iii) aerobic oxidation and co-oxidation to CO_2; and iv) reduction through a variety of metal and metal-oxide surface-catalyzed reactions. Knowledge of the various cDCE and VC degradation processes has led to the development and deployment of monitored natural attenuation (MNA) and enhanced in situ bioremediation (EISB) remedies at a significant number of Department of Defense (DoD) sites impacted by chlorinated solvents.

15. SUBJECT TERMS

16. SECURITY CLASSIFICATION OF:			17. LIMITATION OF ABSTRACT	18. NUMBER OF PAGES	19a. NAME OF RESPONSIBLE PERSON
a. REPORT	b. ABSTRACT	c. THIS PAGE		150	Joel Baker
					19b. TELEPHONE NUMBER *(Include area code)* 519-822-2230

Reset

Standard Form 298 (Rev. 8/98)
Prescribed by ANSI Std. Z39.18

ACKNOWLEDGEMENTS

Funding of this work was provided by the Department of Defense, Strategic Environmental Research and Development Program (SERDP).

The authors wish to thank Andrea Leeson of SERDP for her support during this study, David Freedman (Clemson University), Paul Bradley and Francis Chapelle (United States Geological Survey), Michael Singletary (U.S. Navy) for providing site materials, Kinga Révész and Claire Tiedeman (USGS Menlo Park) for use of site information for field assessment of ethene degradation. Special thanks to the Natural Sciences and Engineering Research Council (NSERC) Strategic Grants Project for the additional supporting funds provided to the University of Toronto (Barbara Sherwood Lollar and Elizabeth Edward) and Geosyntec.

The success of this work would not have been possible without the hard work, cooperation and support from the principal investigators (PI) and co-performers listed below:

- Evan Cox (PI), Natasha Barros and Michaye McMaster – Geosyntec Consultants, Inc.;
- Barbara Sherwood Lollar (CO-PI), George Lacrampe-Couloume, Scott Mundle, and Tiffany Johnson – University of Toronto;
- James Gossett (CO-PI), Laura Jennings, Cloelle Giddings, and Wan Lutfi Wan Johari – Cornell University;
- Jim Spain (CO-PI), Shirley Nishino, Rayford Payne, Kwanghee Shin, and Sarah Craven – Georgia Institute of Technology;
- Elizabeth Edwards (CO-PI), Alfredo Pérez-de-Mora, Melanie Duhamel, and Winnie Chan – University of Toronto; and
- Carey Austrins.

TABLE OF CONTENTS

LIST OF TABLES

LIST OF FIGURES

LIST OF APPENDICES

LIST OF ACRONYMS

1,1-DCE	1,1-dichoroethene
6-HHA	6-hydroxyhexanoic acid
ATSDR	Agency for Toxic Substances and Disease Registry
CAD	chloroacetaldehyde dehydrogenase
CAP	ε−caprolactone
cDCE	*cis*-1,2-dichloroethene
CHMO	ChnB, cyclohexanone monoxygenase (often abbreviated as CMO)
CMO	ChnB, cyclohexanone monooxygenase (often abbreviated as CHMO)
CYHX	cyclohexanone
DCA	1,2-dichloroethane
DCAA	2,2-dichloroacetic acid
DCAL	2,2-dichloroacetaldehyde
DCET	2,2-dichloroethanol
DNAPL	dense non-aqueous phase liquid
EDTA	ethylenediaminetetraacetic acid
Et_2O	diethyl ether
EtOAc	ethyl acetate
EtOH	ethanol
FAD	flavin adenine dinucleotide
FID	flame-ionization detector
FMO	flavin-containing monooxygenase
GC	gas chromatograph or gas chromatography
GST	glutathione S-transferase
HAD	haloacid dehalogenase
IPTG	isopropyl β-D-1-thiogalactopyranoside
ISSO	industrial site in southwestern Ontario, Canada
iTRAQ	isobaric tags for relative and absolute quantitation
KO	knockout (*chnB*-negative JS666)
LB	Luria-Bertani, Miller broth
LC	liquid chromatograph or liquid chromatography
MEHQ	hydroquinone monomethyl ether
MS	mass spectrometry or mass spectrometer
MSD	mass-selective detector
MSM	minimal salts medium
mCPBA	*meta*-chloroperoxybenzoic acid
NAD	nicotinamide adenine dinucleotide
NADH	reduced form of nicotinamide adenine dinucleotide
NADP	nicotinamide adenine dinucleotide phosphate
NADPH	reduced form of nicotinamide adenine dinucleotide phosphate
P450	cytochrome P450

PCE	tetrachloroethene (perchloroethylene)
PCR	polymerase chain reaction
RTDF	Research Technology Development Forum
RT-PCR	reverse transcription polymerase chain reaction
SABRE	Source Area BioREmediation
TAE	Tris-acetate-EDTA buffer
TCA	tricarboxylic acid
TCE	trichloroethene
tDCE	*trans*-1,2-dichloroethene
Tris	tris(hydroxymethyl)aminomethane
TRK	media containing TSA + rifampicin + kanamycin
TSA	trypticase soy agar
TSB	trypticase soy broth
TBE	Tris-borate-EDTA buffer
WT	wild-type
VC	vinyl chloride

1. ABSTRACT

Background and Objectives: Through two decades of laboratory and field research, it has been generally believed that cis-1,2-dichloroethene (cDCE) and vinyl chloride (VC) can further degrade through a variety of mechanisms, including: i) anaerobic reductive dechlorination to ethene and/or ethane; ii) anaerobic oxidation to carbon dioxide (CO_2) under iron- and/or manganese-reducing conditions; iii) aerobic oxidation and co-oxidation to CO_2; and iv) reduction through a variety of metal and metal-oxide surface-catalyzed reactions. Knowledge of the various cDCE and VC degradation processes has led to the development and deployment of monitored natural attenuation (MNA) and enhanced in situ bioremediation (EISB) remedies at a significant number of Department of Defense (DoD) sites impacted by chlorinated solvents. However, it has proven difficult to confidently and reliably quantify several of the degradation processes (mainly the oxidation and abiotic reactions) at field scale using common investigation techniques, and as such, MNA and EISB cases invoking these reactions as explanations for apparent cDCE and VC mass loss often appear speculative. The overall objective of this research program was to develop information and tools to help DoD remediation project managers (RPMs) and remediation practitioners better understand and quantify the frequency of occurrence, relative contribution, and overall environmental relevance of the various cDCE and VC degradation processes in field settings.

Technical Approach: The research program was accomplished through three research modules, including: i) elucidation of the aerobic oxidation pathway for cDCE; ii) isolation of organisms and elucidation of the anaerobic oxidation pathway(s) for cDCE and VC under iron and/or manganese-reducing conditions; and iii) improvement in the understanding of isotopic fractionation signatures related to cDCE and VC reductive dechlorination, and assessment of the isotopic signatures associated with ethene degradation. In addition, at SERDP's request, a fourth research module was added to support the Remediation Technology Development Forum's (RTDF's) Source Area BioREmediation (SABRE) project.

Results: The key results of this project can be summarized as follows: i) JS666 remains the only isolated organism known to mediate aerobic oxidation of cDCE to CO_2, and DNA-based molecular biological tools (MBTs) exist to track its presence and fate during EISB bioaugmentation projects; ii) significant advancements were made in understanding the pathway, mechanisms and enzymes associated with aerobic oxidation of cDCE in JS666; iii) anaerobic oxidation of cDCE and/or VC under iron- or manganese-reducing conditions could not be confirmed, despite substantial efforts with materials from many sites; iv) suspected anaerobic oxidation of VC may in fact be aerobic oxidation to CO_2 at extremely low levels of oxygen in the subsurface, as evidenced by research presented herein; and v) compound-specific isotope fractionation of carbon occurs in both anaerobic and aerobic microbial degradation of ethane, allowing the use of this analytical tool to assess ethene degradation as a possible means to explain poor ethene mass balance in EISB and MNA projects.

Benefits: The tools and information produced by this project will greatly assist DoD RPMs and remediation practitioners with understanding and validating EISB and MNA remedies at sites contaminated with chlorinated ethenes such as tetrachloroethene and trichloroethene.

2. BACKGROUND AND OVERALL OBJECTIVES

Through two decades of laboratory and field research, it has been generally believed that cis-1,2-dichloroethene (cDCE) and vinyl chloride (VC) can further degrade through a variety of mechanisms, including: i) anaerobic reductive dechlorination to ethene and/or ethane; ii) anaerobic oxidation to carbon dioxide (CO_2) under iron- and/or manganese-reducing conditions; iii) aerobic oxidation and co-oxidation to CO_2; and iv) reduction through a variety of metal and metal-oxide surface-catalyzed reactions. Knowledge of the various cDCE and VC degradation processes has led to the development and deployment of monitored natural attenuation (MNA) and enhanced in situ bioremediation (EISB) remedies at a significant number of DoD sites impacted by chlorinated solvents. However, it has proven difficult to confidently and reliably quantify several of the degradation processes (mainly the oxidation and abiotic reactions) at field scale using common investigation techniques, and as such, MNA and EISB cases invoking these reactions as explanations for apparent cDCE and VC mass loss often appear speculative.

The overall goal of this research program was to generate information and tools to help DoD remediation project managers (RPMs) and remediation practitioners better understand and quantify the frequency of occurrence, relative contribution, and overall environmental relevance of the various cDCE and VC degradation processes in field settings.

The specific technical objectives of this research program were to:

i) elucidate the aerobic and anaerobic oxidation pathways and reaction kinetics for cDCE and VC;

ii) identify and isolate organisms capable of mediating these reactions;

iii) develop and validate molecular biological tools (MBTs), including compound specific isotope analysis (CSIA) and Deoxyribonucleic Acid (DNA)-based analyses, for assessment of the degradation mechanisms; and

iv) determine the relevance of the various biodegradation mechanisms at field scale so that DoD RPMs and remediation practitioners can better design, implement, monitor, and validate MNA and EISB remedies.

The research program was accomplished through three research modules, including:

i) elucidation of the aerobic oxidation pathway for cDCE;

ii) isolation of organisms and elucidation of the anaerobic oxidation pathway(s) for cDCE and VC under iron and/or manganese-reducing conditions; and

iii) improvement in the understanding of isotopic fractionation signatures related to cDCE and VC reductive dechlorination, and assessment of the isotopic signatures associated with ethene degradation.

In addition, at SERDP's request, a fourth research module was added to support the Remediation Technology Development Forum's (RTDF's) Source Area BioREmediation (SABRE) project.

The remainder of this report is divided into five sections. Sections 3 through 6 provide a summary of the work conducted for each of the four research modules identified above. Each section provides background information relative to the module, objectives specific to the module, a description of the research materials and methods, results and discussion, conclusions and implications for future research and implementation, and literature cited. Section 7 presents overall study conclusions, and discusses implications for implementation of these research findings and for future research.

3. MODULE 1 – ELUCIDATION OF THE CIS-DICHLOROETHENE AEROBIC OXIDATION PATHWAY

3.1 Objective 1 – cDCE Oxidation Pathway Determination

3.1.1 Background

To date, only one organism, *Polaromonas* sp. strain JS666, has been identified as possessing the ability to grow aerobically on cDCE. It is not clear whether the lack of cDCE-degrading isolates is because they do not exist, there has been no systematic search for them, or the bacteria are difficult to culture from natural ecosystems.

cDCE found in the environment is a product of incomplete metabolism of tetrachloroethene (PCE) and trichloroethene (TCE), which are included in the top 50 Agency for Toxic Substances and Disease Registry (ATSDR) Priority List Hazardous Substances (ATSDR 2011 Substance Priority List, U.S. Department of Health and Human Services, ATSDR, Atlanta, GA). The isolation of a bacterium able to reductively dehalogenate PCE to ethene through a combination of growth-coupled dehalorespiration (Maymó-Gatell *et al.*, 1997) and cometabolism (Maymó-Gatell *et al.*, 1999) was rapidly followed by the discovery of a variety of anaerobic bacteria and genes capable of reductive dechlorination of chloroethenes. The major transformations of PCE by anaerobic bacteria are to TCE, cDCE, and VC leading to ethene (Maymó-Gatell *et al*., 1997). Despite the widespread distribution of such bacteria, degradation of PCE/TCE often "stalls" with the accumulation of cDCE and VC. Several reasons have been advanced for the phenomenon. A survey of chloroethene contaminated sites with a DNA microarray specific for known reductive dehalogenase genes found that cDCE accumulated at sites where no signals could be detected for the *bvcA* and *vcrA* genes even though *Dehalococcoides* were present and the sites were otherwise favorable for reductive dehalogenation (Dugat-Bony *et al.*, 2012). Another study (Ise *et al.*, 2011) found that at some concentration between 146 and 292 μM cDCE inhibited degradation even in the presence of *bvcA* and *vcrA* genes. Lack of electron donors and/or insufficient reducing conditions have also been suggested (Schmidt and Tiehm, 2008) as cDCE and VC require stronger reducing conditions than do PCE and TCE. Finally, oxygen is an inhibitor of reductive dechlorination, and migration of plumes to oxic sites would preclude dehalorespiration.

Research for Module 1 was primarily the responsibility of Dr. Jim Spain at the Georgia Institute of Technology, in collaboration with Dr. James Gossett at Cornell University and Dr. Barbara Sherwood Lollar at the University of Toronto.

Evidence for the involvement of a cytochrome P450 in the initial steps of cDCE oxidation by JS666 was presented. However, this did not rule out involvement of other enzymes (e.g., cyclohexanone monooxygenase and glutathione-S-transferase) in cDCE oxidation – possibly even in parallel first steps (Figure 3-1), since JS666 has been observed to exhibit two different phenotypical degradation behaviors (termed "good" and "bad" (Jennings, 2005)). Our working

hypothesis is that some of the parallel cDCE-degradation pathways (e.g., those involving monooxygenases) could potentially be harmful ("bad") to JS666 through the production of toxic, intermediate epoxides whose subsequent transformation is poorly regulated. Other pathways (e.g., those involving P450) might be less stressful to the organism (and therefore comparatively "good").

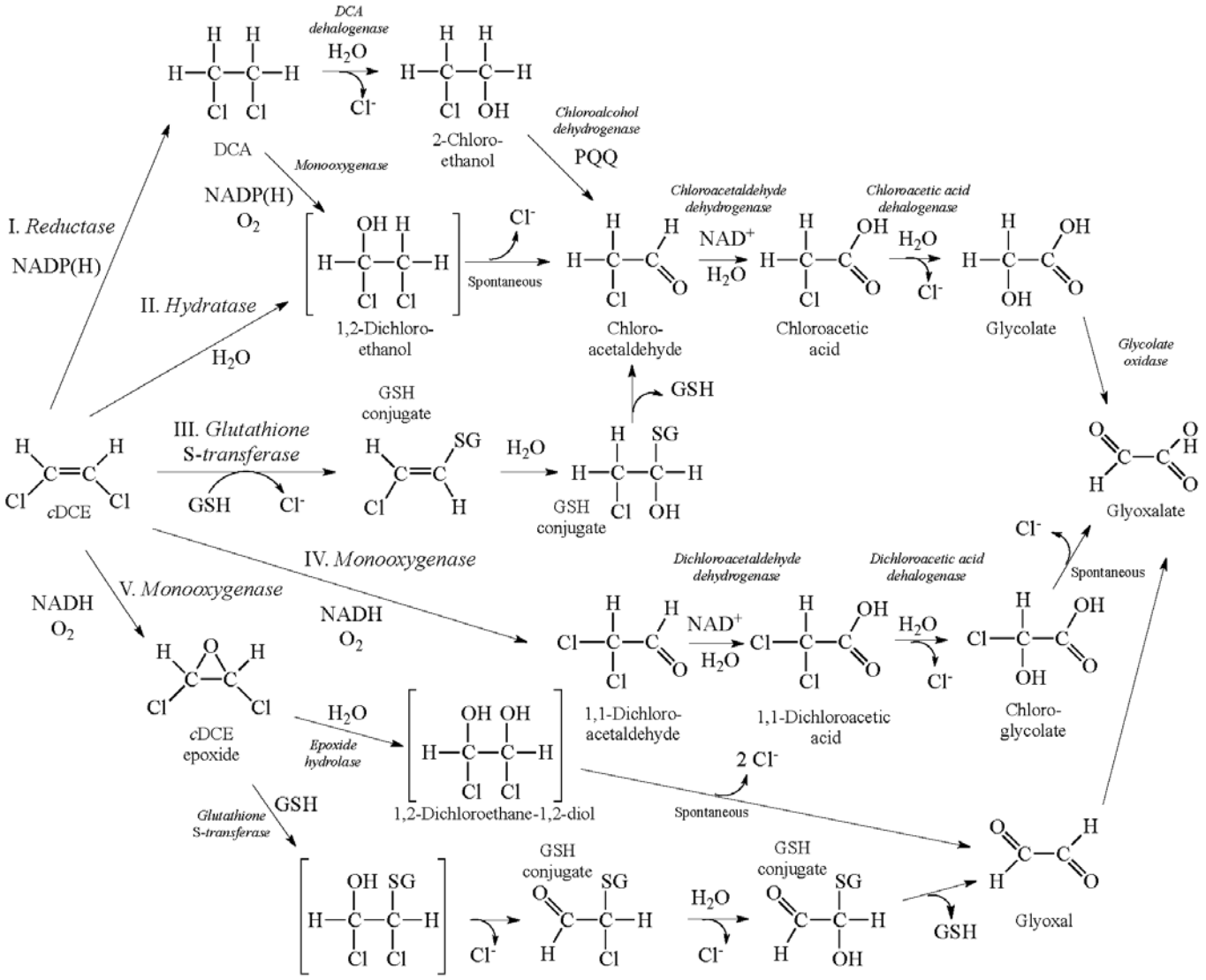

Figure 3-1: Predicted possible cDCE degradation pathways based upon bioinformatics, integrated omics approaches, and enzyme assays

3.1.2 Research Objectives

In this research module, strain JS666 was used as a model system for the aerobic oxidation of cDCE to achieve the following objectives:

1. Determine the cDCE Oxidation Pathway(s);
2. Develop DNA-Based MBTs;
3. Develop CSIA Tools; and
4. Conduct Field Validation (No-Go).

The genome of *Polaromons* sp. JS666 (Mattes, Alexander *et al.*, 2008) was elucidated in 2005, yet the finished sequence failed to reveal an obvious pathway for the degradation of cDCE. The lack of any other organisms capable of aerobic growth on cDCE meant that there are no genes in the databases annotated to directly point to a function involved in cDCE degradation in JS666. However, a number of studies of vinyl chloride degradation and related compounds suggested several potential transformations such as monooxygenation, epoxidation, reduction, hydration, and GSH-conjugate formation (de Bont, Attwood *et al.*, 1979; Liebler, Meredith *et al.*, 1985; Vogel, Criddle *et al.*, 1987; Ensign and Allen, 2003). We examined the genome for the presence of genes that might encode enzymes that catalyze such reactions. In addition, the machine annotation of JS666 completed by the Joint Genome Institute indicated the presence of a 1,2-dichloroethane (DCA) degradation pathway encoded in the genome, which suggested several potential steps in the lower pathway (http://genome.ornl.gov/microbial/bpro_js666/14oct05/RES_PRIAM/map00631_org.html).

Based on the presence of genes that might encode the potential reactions we developed a model of hypothetical pathways to guide our investigations (Figure 3-1). The model was greatly informed by the results of an integrated omics approach (proteomics, transcriptomics, and metabolomics) that was used to study gene expression in JS666 (Jennings, Chartrand *et al.*, 2009). Microarray data comparing RNA extracted from cDCE-grown versus glycolate-grown cultures confirmed five of the proteins found through proteomics study. Putative gene function was suggested using bioinformatics tools.

The intermediate steps in the aerobic degradation of cDCE by JS666 were established by a combination of oxygen uptake measurements in resting cells, and enzyme assays in cell extracts. Protein and cDNA microarray studies further corroborated a downstream pathway of cDCE degradation via (di)chloroacetaldehyde, (di)chloroacetic acid, and (chloro)glycolate similar to a pathway in bacteria able to grow on 1,2-dichloroethane (DCA) (Janssen, Scheper *et al.*, 1985; Hage and Hartmans, 1999). All the genes for DCA degradation are present in JS666 even though they do not form a recognizable operon. The initial reactions in the pathway, however, remained elusive and it became apparent that cDCE oxidation is more complex than previously anticipated.

The attempt to similarly identify the initial steps in cDCE oxidation through the combination of protein and cDNA microarray studies failed to provide a definitive answer. The microarray studies did however point to genes that might encode potential reactions that were only modestly up-regulated after growth on cDCE. One of those genes encoded a cytochrome P450 that was shown to be critical to the initial steps of cDCE oxidation through cloning, P450 specific inhibitors, and identification of metabolites. More recent work using initial growth of JS666 on cyclohexanone, to promote more rapid subsequent growth on cDCE supported additional efforts to identify the upper pathway using molecular techniques such as gene knockout and transposon mutagenesis.

We refined the cytochrome P450 studies, with regard to identification of the products and determination of the relative importance of other enzymes in cDCE oxidation. Parallel first steps (Figure 3-1) are indicated by two different degradation behaviors (termed "good" and "bad") (Jennings, 2005). To that end, we pursued dynamic-expression studies with putative genes involved in aerobic cDCE degradation and/or stress-response (more fully discussed under Section 3.2); knock-out of the cyclohexanone monooxygenase gene (*chnB*) of JS666; and heterologous expression of *chnB* and adjacent genes of the cyclohexanol operon.

As part of a separate but related research task, we attempted to enrich and identify other aerobic cDCE oxidizers via microcosms prepared using material from a number of sites. Materials from 14 sites contaminated with cDCE were tested. Although a few microcosms showed initial loss of cDCE, the degradation was not sustainable through multiple transfers as the initial soil was diluted out. The results suggest that the initial activities were due to cometabolism supported by other compounds present.

3.1.3 Materials & Methods

Growth conditions

JS666 was routinely grown with cDCE as the sole carbon and energy source in a 7-liter (L) bioreactor maintained at 20°C, pH 7.0, dissolved O_2 40%. Minimal medium (MSM)(Stanier, Palleroni *et al.*, 1966) was modified as follows: phosphate buffer, 10 millimolar (mM); all other nutrients supplied at half-strength. cDCE (Aldrich D62004) was supplied continuously by a syringe pump. To enable more rapid growth, some cultures were pre-grown on cyclohexanone (5 millimolar [mM]) or 5:1 (volume to volume ratio [v/v]) acetonitrile:cDCE. Feedstocks were changed to cDCE as the sole carbon and energy source prior to experiments either by changing the growth substrate provided to the bioreactor, or by removing portions of the culture (0.25-2 L), harvesting by centrifugation, and inoculating the cells into half-strength mineral salts medium (½-MSM) supplemented with cDCE or other appropriate carbon sources. Flasks were sealed with teflon-lined septa, then carbon sources (cDCE, DCA, ethanol, or succinate) were added to a final concentration of 0.5 mM. Cultures were grown for 24 hours at 20 degrees Celsius (°C) with shaking before being harvested for oxygen uptake experiments or for enzyme assays. Trypticase soy agar at one-quarter strength (1/4-TSA) solidified with

15 grams per liter (g/L) agar was used as a purity check.

Additional cultures were grown in serum bottles on cDCE in MSM at a pH of 7.1 to 7.2 (Giddings, Liu *et al.*, 2010). Pure cultures were maintained through a series of 5% v/v culture transfers into 100 mL MSM in 160-mL serum bottles and fed a nominal concentration of cDCE of 51 mg/L. [Concentrations of all volatiles are reported here as "nominal" – i.e., ignoring partitioning to headspace.]

Alternative growth substrates for JS666 were tested on agar plates supplemented with ethanol, acetonitrile, or cyclohexanone as the carbon source. Individual colonies were transferred into separate wells of 96-well microplates containing ¼-MSM plus a pH indicator (bromothymol blue, 10 mg/L). cDCE was provided in the vapor phase.

Cells were harvested by centrifugation and washed twice with phosphate buffer (pH 7.0, 20 mM). Cells used in enzyme assays were broken by 3 passages through a French press. Extracts were centrifuged at 26,000 × g for 1 hour at 4°C and stored on ice until used in experiments.

Enrichments

Soil and/or ground water was acquired from a variety of sites (Table 3-1) contaminated with cDCE. Microcosms were created in serum bottles containing either 50 milliliters (mL) of liquid in 160 mL bottles or, 200-250 mL liquid in 540 mL bottles. The microcosms were provided with cDCE as the sole carbon source and incubated at room temperature with shaking. cDCE was monitored by gas chromatography (GC). Microcosms were re-spiked as cDCE disappeared, or transferred to dilute the initial soil.

Table 3-1: Site location and material used for aerobic cDCE enrichment microcosms

Site	Soil/Water	Collection Date	Well ID	Sample Depth (ft)
Milledgeville, GA	Soil composite	2/11/2008	SB-1	15-17
Dover AFB (EMU), DE	Groundwater	7/1/2008	GSCP9A	11
Dover AFB (Area 5), DE	Groundwater	7/1/2008	DM3504S	12
Dover AFB (Area 6), DE	Groundwater	6/30/2008	IRO1D MW101S MW103S MW212D DM360D	13-15 10 12 12 19
Cape Canaveral AFS (LC-34), FL	Groundwater(1)	5/1/2007	IW-51S ESB-SB-1	
	Soil core(1)		ESB-SB-2	6-8, 8-10,10-12, 12-14, 14-16,16-18
NB Kitsap (OU-1), Keyport, WA	Groundwater(1)	11/29/2006	N2	
	Soil composite(1)		N2	1-3
Alamac American Knits, Lumberton, NC	Soil composite(1)	2/15/2007	SB-1 SB-2	0-0.5
Myrtle Beach AFB (SWMU 256), SC	Soil core(1)	1/25/2007	SB-MW-12-1	4-6, 6-8, 8-10, 12-14, 14-16
			SB-MW-12-3	4-6, 6-8, 14-16
Hill AFB (OU-1), UT	Microcosms(2)		4-1A 2-May 3-May	
Cecil Field NAS (Site 3), FL	Groundwater	10/9/2008	Site 3, 13S	
St. Julien's Creek Annex, VA	Groundwater	10/23/2008	IW-2	
Hill AFB (OU-1), UT	Groundwater	11/6/2008	U1-307 U1-104 U1-089 U1-103 U1-179 U1-098 U1-154 U1-151 U1-138	
NASA, FL	Groundwater	2/09/2009		
Germany	Groundwater	6/05/2009		

Notes:

(ft) - feet

(1) materials obtained from ESTCP Project No. ER-0625

(2) materials obtained from Dr. Amy Callaghan at the University of Oklahoma

Oxygen uptake assays

Oxygen uptake was measured polarographically with a Clark-type oxygen electrode connected to a YSI model 5300 biological oxygen monitor. The reaction mixtures contained resting cells at an O.D. 600 nm of 1.5 (about 0.1 milligram [mg] protein per ml) plus substrates (1 mM) in air-saturated phosphate buffer (0.02 M, pH 7.0) at 20°C.

Enzyme assays

Cell extracts were prepared as previously described in Tris/EDTA/beta-mercaptoethanol buffer (25/1/1mM), pH 8.0 (Janssen, Scheper *et al.* 1985). cDCE monooxygenase or cDCE reductase activities were monitored by measuring NAD(P)H oxidation at 340 nanometer (nm) in the presence of oxygen and cDCE. cDCE hydratase and DCA dehalogenase were followed by measuring chloride release colorimetrically (Bergmann and Sanik, 1957). PQQ-dependent chloroethanol dehydrogenase activity was measured by monitoring 2,6-dichlorophenolindophenol DCPIP reduction spectrophotometrically at 570 nm (Dijk, Gerritse *et al.* 2004). NAD(P)-type chloroethanol dehydrogenase activity was measured by monitoring NAD(P) reduction spectrophotometrically at 340 nm. Chloro- and dichloroacetaldehyde dehydrogenase activity was determined by monitoring formation of NADH from NAD at 340 nm (Hage and Hartmans, 1999).

Glutathione S-Transferase (GST) activity was assayed by the method of Habig *et al.* (Habig, Pabst *et al.*, 1974) at 25 °C. The standard reaction mixture (600 microliters [µL]) contained 0.1 M potassium phosphate buffer (pH 6.5), 1.0 mM glutathione (GSH), 1.0 mM 1-chloro-2,4-dinitrobenzene (CDNB) and 10–60 µL cell extract. Enzyme activity was calculated by using a molar absorption coefficient for the CDNB–GSH conjugate of 9600 M^{-1} centimeter^{-1} (cm^{-1}) at 340 nm.

GST activity against cDCE was determined by monitoring the disappearance of cDCE in the headspace by gas chromatography. Reactions were performed in 2 mL (high performance liquid chromatography) HPLC vials with 1 mL solution and 1 mL headspace and were crimp sealed with Teflon coated stoppers. Reactions were performed in 50 mM phosphate buffer at pH 6.5, 7.5, or 8.5 and contained 100 to 200 micrograms (µg) of protein. cDCE was diluted 1:1000 into acetonitrile and then 2 µL was immediately added to each vial, and the vials were sealed. The theoretical final concentration of cDCE in each reaction was 18 µM. Reactions were performed in duplicate. One replicate was analyzed at time zero; the second replicate was placed on its side and shaken vigorously at room temperature for 3 hours before analysis.

Cytochrome P450 was assayed by monitoring substrate disappearance and/or product formation by gas chromatograph-electron capture detector (GC/ECD) headspace analysis. Reaction mixtures (1 mL) consisted of cell extracts (1 to 4 mg protein) and substrates (80 to 160 nanomoles [nmol]) in phosphate buffer (50 mM, pH 7.2) in 4 mL bottles sealed with Teflon-coated butyl rubber stoppers. Reactions were started by addition of NADH or NADPH (2.5 mM) and the bottles were incubated at 25°C. At appropriate intervals, the reactions were

stopped by the addition of $ZnSO_4$ (30 mM) and were extracted with ethyl ether. Dichloroacetaldehyde dehydrogenase (van der Ploeg, Smidt *et al.*, 1994) and chloroacetate dehalogenase (Janssen, Scheper *et al.*, 1985) were measured by following the reduction of NAD to NADH at 365 nm.

Whole genome expression arrays

Whole genome expression arrays with 192,000 features were designed and produced by NimbleGen from the JS666 genome (http://genome.ornl.gov/microbial/bpro_js666/14oct05/), with 10 probes per open reading frame (ORF) and 50 base pair (bp) tiling of the intergenic regions. Cultures were grown on glycolate or cDCE and the total ribonucleic acid (RNA) was extracted from the frozen pellets. Complementary deoxyribonucleic acid (cDNA) was synthesized from the RNA and submitted to NimbleGen for hybridization. Results were analyzed using Genespring (Agilent Technologies) at the Genomics Core at Montana State University. Samples were filtered to identify differential expression on cDCE compared to glycolate.

2D-Protein expression gel analysis

2-D gel electrophoresis was conducted essentially as described previously (Sauer and Camper 2001). Frozen cell pellets (800 µg) were suspended in tris(hydroxymethyl) aminomethane (Tris)-ethylene diamine tetraacetic acid (EDTA) buffer (TE) and disrupted by sonication. Proteins were precipitated from crude extracts and resolubilized in commercial buffer (Amersham 3-10 NL IPG [non-linear immobilized pH gradient]). Soluble proteins were applied to Immobiline 3-10 NL or 3-11 NL IPG strips by in-gel rehydration. Isoelectric focusing separated the proteins in the first dimension. Proteins were equilibrated and separated in the second dimension by gel electrophoresis using a Hoefer Dalt vertical system with 12 percent (%) acrylamide gels at 17°C. Gels were stained with coomassie brilliant blue, destained, and scanned. Differentially expressed proteins were digested with trypsin and analyzed using liquid chromatography coupled to tandem mass spectrometry (LC/MS/MS) and/or matrix assisted laser desorption ionization tandem time-of flight mass spectrometry (MALDI-TOF/TOF). LC/MS/MS analyses were conducted at the Mass Spectrometry Laboratory at Montana State University or at the Mass Spectrometry Core (MSC) at Cornell University. MALDI-TOF/TOF was conducted at the MSC at the University of Texas. The MASCOT search engine was used to compare peptide masses determined from mass spectrometry to that of sequences in the National Center for Biotechnology Information (NCBInr) bacterial database. Acceptable protein identifications required expectation values of 0.01 and 0.001 for LC/MS/MS and MALDI-TOF/TOF respectively. The protein match was verified by comparing the molecular weight or isoelectric point of the protein spot to values in the database.

Cloning and expression of GST and P450 enzymes

Glutathione-*S*-transferase (GST)

Primers were designed to amplify the gene encoding glutathione-*S*-tranferase (Bpro_0645). The polymerase chain reaction (PCR) product was cloned into the pET21 vector according to the manufacturer's instructions (Novagen pET System Manual), then transformed into the competent *E. coli* host. Expression was induced by isopropyl β-D-1-thiogalactopyranoside (IPTG).

Cytochrome P450

Genomic DNA was extracted with a Genomic DNA purification system (Promega, Madison, WI). Both individual genes and a 3.5 kb fragment containing cytochrome P450 (Bpro_5301, here and throughout this section the locus tags [Bpro_xxxx] for the genes in JS666 are provided), ferredoxin reductase (Bpro_5300), and ferredoxin (Bpro_5299) was amplified by PCR using 017F (CACCACGCTGCACCGTGTTATGTTTCAC) and 017R (TCAGTGCTGGCCGAGCG GCG) primers. The PCR products were treated with DNA Polymerase I, Large (Klenow) Fragment, then cloned into the pET101/D-TOPO vector (Novagen, Gibbstown, NJ). The constructs were transformed into *E. coli* BL21 Star (DE3) or *E. coli* Rosetta 2 for expression. Clones were grown in 30 ml of trypticase soy broth media containing Overnight Express Autoinduction Systems I (Novagen) at 37 °C. When the optical density at 600 nm (OD_{600}) reached 0.8 to 0.9, the temperature was reduced to 25 °C, the cultures were supplemented (Scheps, Honda Malca *et al.* 2011) with δ-aminolevulinic acid (0.5 mM) and $FeSO_4$ (0.1 mM) and the cultures were incubated until OD_{600} reached 16 to 18 (approximately 16 hours). Cells were harvested by centrifugation, washed twice with phosphate buffer (20 mM, pH 7.5) and stored on ice until used.

Substrate transformation by whole cells

Cells were suspended to an OD_{600} of 10 to 40 in ½-MSB (5 mL) in 35-mL serum bottles. Reactions were initiated by the addition of substrates and cultures were incubated at 25 °C with shaking (250 rpm). Substrate disappearance was monitored by gas chromatography (GC).

For mass balance measurements, cDCE and its metabolites were measured in ether extracts of cultures provided with cDCE. All manipulations were carried out without a headspace in gas-tight, glass and teflon syringes equipped with mini-valves. Prior to addition of cDCE, the medium was sparged to saturation with O_2 then drawn into a 50 ml syringe containing 2 glass beads (4 mm). Neat cDCE was injected into the syringe through the valve opening, and the contents were mixed by inversion. 8 ml of the stock were transferred to a 10 ml syringe through a female-female luer fitting and mixed with 2 ml of washed cells (aided by 1 glass bead). The reaction was stopped by the transfer of 1 ml of the mixture to a 5 ml syringe containing 3 ml of ethyl ether. The syringe was inverted for 1 min to extract cDCE and its metabolites, then placed upright in a beaker to allow the phases to separate. 0.5 µL of the ether phase was drawn directly from the syringe through the valve opening and analyzed by GC/FID. Following the initial

analysis, the ether phase was pushed out of the syringe and the aqueous phase was extracted with 3 more ml of ether and analyzed as before.

Creation of a chnB*-negative, knockout strain*

A suicide translational fusion vector, pVIK110 (Kalogeraki and Winans 1997) was used to disrupt the *chnB* gene in JS666 wild-type strain (Figure 3-2). All bacterial strains, vectors, plasmids and primer sets used in the present study are listed in Table 3-2.

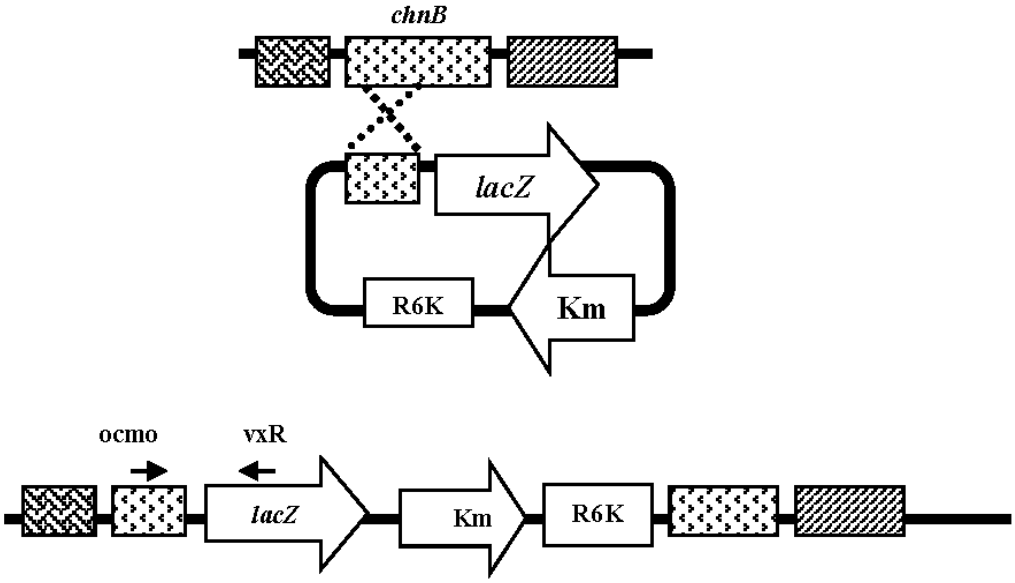

Figure 3-2: Suicide vector was integrated into the genome of JS666 through homologous recombination. Primers ocmo and vxR were used to confirm the integration of the plasmid into the genome at the designated location. Km is kanamycin resistance gene. R6k is the origin of replication. The resulting protein is a ChnB-LacZ fusion.

Table 3-2: Bacterial strains, vectors and primers used in this study

Name of strain, plasmid, or primer	Relevant characteristics or sequence		Source or reference(s)
Strains			
Polaromonas sp.			
JS666	cDCE aerobic degrader (WT)		This study
JS666 Δ*chnB::kan*	*chnB*-knockout strain (KO)		This study
JS666 Δ*chnB::kan*, *chnB*	*chnB*-complement strain		This study
E. coli			
SY327 λ*pir*	Host for pVIK110, contain λ*pir* for *pir* plasmids		Madsen, E.
S17-1 λ*pir*	Contains λ*pir* for *pir*-dependent plasmids, conjugal donor;		Madsen, E.
Rosetta 2 (DE3)	Host for gene expression		Novagen
BL21 Star™ (DE3)	Host for gene expression		Invitrogen
Plasmids or vector			
pVIK110	*lacZY* for translational fusions, R6K oriV, suicide vector; kan^R		Kalogeraki/Winans
pVcmo	Suicide vector construct containing fragment of *chnB* gene		This study
pET101/D-TOPO®	Expression vector, amp^R		Invitrogen
pCOLADuet™-1	Expression vector, kan^R		Novagen
pET21(a)+	Expression vector, amp^R		Novagen
pJB866	Expression vector, tet^R		NBRP-*E.coli* at NIG, Japan
pJcmo	Expression vector with Bpro_5565		This study
p15TV-L	Expression vector with Bpro_4478		Chan et al.
pJS597	Expression vector with Bpro_5299 – Bpro_5301		Shin et al.
PCR primers [a]		bp [b]	
VcmoF (SalI)	5'-CCCTCTAGACAACATCAAGGGCATCGAG-3'	427	This study
VcmoR (XbaI)	5'-CCCGTGGACTTCTTCGCTGGTGGCAATG-3'		This study
ocmoF	5'-GAAATCCAGACCGATACCGA-3'	823	This study
vxR	5'-TTGACCGTAATGGGATAGGT-3'		This study
isoF	5'-TGCCGCTGACAACAACAC-3'	139	Jennings
isoR	5'-ATCAATGCCTTTGGAGTGC-3'		Jennings
Protein overexpression			
66F	5'-CACCATGAAACCTTCAACCGAGGC-3'		This study
66H	5'-AGCAGCCTTAAACCATTGGG-3'		This study
65F	5'-CACCATGACCCTGGCAACACAAGA-3'		This study
65R	5'-TTAGCGGATCTCAAAACCTGG-3'		This study
63F	5'-CACCATGAATTACCGCTGCGCCCA-3'		This study
63R	5'-TCAAGGCTGCAGCACCACG-3'		This study
E6566F (BamHI)	5'-CCCGGATCCATGACCCTGGCAACACAAGA-3'		This study
E6566R (XhoI)	5'-CCCCTCGAGTCAAGCAGCCTTAAACCATT-3'		This study
C6364F (EcoRI)	5'-CCCGAATTCATGAAACGCGTACAAGA-3'		This study
C6364R (HindIII)	5'-CCCAAGCTTTCTTCAAGGCTGCAGCA-3'		This study
Reverse transcription PCR		bp [b]	
RT-RpoF	5'-GCCTATTCCTATACCGAACGC-3'	387	This study
RT-RpoR	5'-GTAGACTTCCTGCTCCTTGAC-3'		This study
RT-ISOF	5'-GAAATTCAGCACTCCAAAGGC-3'	397	This study
RT-ISOR	5'-TCTTGTAGAAACCTTCGGCG-3'		This study
RT-p450F	5'-ACCCCGTGCATTACTGTAAG-3'	370	This study
RT-p450R	5'-CAAGGGAAATCAAACAGCGTC-3'		This study
RT-GSTF	5'-TTGAACGGGTGGAGATTGAC-3'	411	This study
RT-GSTR	5'-AGCTGTAGTTGGCAATATCGG-3'		This study
RT-CMOF	5'-GAAATCCAGACCGATACCGA-3'	572	This study

Name of strain, plasmid, or primer	Relevant characteristics or sequence		Source or reference(s)
RT-CMOR	5'-TCCGGGTCTTTGACAATCTC-3'		This study
RT-HYDF	5'-GCAAACAACATCACCACCAG-3'	330	This study
RT-HYDR	5'-AGGAACGGGAACACATGCT-3'		This study
RT-ALDF	5'-AATCTCGGCATCCAGTTACC-3'	419	This study
RT-ALDR	5'-GGCTTCATTCGGGTCAAAAG-3'		This study
RT-HADF	5'-AGATGGTCAGCAAGATGTGG-3'	322	This study
RT-HADR	5'-AAGTGATCGAAGGAGTTGGTC-3'		This study

[a] nucleotide sequences for restriction enzyme sites are underlined

[b] bp: resulting amplicon sizes in base-pairs.

Preliminary assessment of antibiotic resistance

Antibiotic resistances of strains used in the knockout construction were determined. JS666 was resistant to rifampicin, but sensitive to kanamycin, ampicillin, chloramphenicol and tetracycline. The *E. coli* strains were resistant to kanamycin, ampicillin, chloramphenicol, and tetracycline but sensitive to rifampicin.

Vector preparation

pVIK110 was extracted from *E. coli* SY327 pVIK110 using the PureYield plasmid purification kit (Promega). An internal fragment of *chnB* was PCR-amplified from JS666 genomic DNA using the VcmoF and VcmoR primer pair (T_m = 60°C) with a Mastercycler Gradient (Eppendorf). The resulting amplicons and pVIK110 were cut using *Xba*I and *Sal*I restriction enzymes (Fermentas), ligated and transformed into chemical competent *E. coli* S17-1 λ*pir* cells using heat-shock treatment. Chemical competent *E. coli* S17-1 λ*pir* cells were prepared using a rubidium chloride method (Douglas, 1983).

Conjugation

JS666 cells were harvested by centrifugation, suspended in ¼-TSB and grown without shaking for 24-48 hours before mating. To improve vector transfer to the recipient strain, *E. coli* S17-1 λ*pir* pVcmo cells were grown in LB broth at 30°C overnight before the cells were harvested and suspended in ¼-TSB. Suicide vector containing the internal *chnB* fragment, pVcmo, was transferred into rifampicin-resistant JS666 by conjugation with *E. coli* S17-1 λ*pir* pVcmo cells on ¼-TSB at 23°C for 24-48 hours. 100-µL aliquots of the bacterial mixtures were spread on ¼-TSA plates containing rifampicin (60 µg/mL) and kanamycin (30 µg/mL) (TRK plates) and incubated for 5-7 days at 23°C. The resulting colonies were transferred to a fresh TRK plate. The transconjugants (KO) were confirmed by PCR with isoF-isoR, ocmoF- vxR and 65F-65R (or RT-CMOF and RT-CMOR) primer pairs (T_m = 60°C) and visualized on 1% TBE or TAE gels. The isoF-isoR primers are specific for JS666. The ocmoF-vxR primers detect the insert in the *chnB* gene that disrupts the function. The remaining primers hybridize to the *chnB* sequences

before and after the insert, to yield a 572-bp amplicon for wild-type JS666 (WT) and none for KO (because of an extra 9.3-kbp insert and short PCR extension time). The resulting amplicons were excised and purified for sequencing. KO colonies were maintained in 50-mL MSM containing 10 mM succinate, 51 mg/L cDCE, and 30 μg/mL kanamycin. As control, JS666 was similarly inoculated into 50-mL MSM containing 10 mM succinate, and 51 mg/L cDCE, but without kanamycin. Occasionally, both KO and WT cultures were checked for purity by streaking on a fresh ¼-TSA plate and several colonies were selected for PCR-testing using ocmoF-vxR and isoF-isoR primer sets, looking specifically for KO characteristics in the KO and JS666 characteristics in both strains.

Growth and substrate-utilization comparisons between KO and WT strains

Stock cultures of the WT and KO strains were grown in 5-mL ¼-tripticase soy broth (TSB) with 1.3 μmol/bottle cDCE. To generate inocula for WT assays, aliquots (0.1 mL) from the TSB+cDCE WT culture were transferred into 5-mL MSM containing 1.3 μmol/bottle cDCE with 10 mM succinate, 10 mM acetate, 1 mM cyclohexanone (CYHX), or 10 mM EtOH. The KO strain did not grow on the same range of substrates as the WT. Inocula for KO assays was generated by transferring aliquots (0.1 mL) from its TSB+cDCE culture into 5-mL MSM containing 1.3 μmol/bottle cDCE with 10 mM acetate.

For growth substrate assays, approximately 0.2-mL aliquots of the WT or KO inocula were transferred into 100-mL MSM containing test substrates plus cDCE at 3 different concentrations (132 μmol/bottle, 52 μmol/bottle, or no cDCE). cDCE and optical density at 600 nm (OD_{600}) were monitored. All experiments were conducted with biological duplicates. When ε-caprolactone (CAP) was the growth substrate, cultures were grown in 100 mL MSM with 1 mM CAP at three concentrations of cDCE (106 μmol/bottle, 52 μmol/bottle, or none). The cultures were also assayed for their ability to grow on cyclohexanol. In the cyclohexanol test 5 mL of succinate-grown inocula (with cDCE exposure to both strains during growth) were transferred into 95-mL fresh MSM with 0.5 mM cyclohexanol in 160-mL serum bottles.

To assay possible TCE, VC, DCA and ethene transformations, WT and KO cultures were grown in 1-L serum bottles containing 400-mL MSM plus 1 mM CAP and 52 μmol/bottle of cDCE. When the OD_{600} reached 0.3 – 0.5 or at mid-cDCE degradation, the cells were harvested by centrifugation, washed once with MSM, and suspended in 160-mL serum bottles containing 50 mL MSM. TCE, DCA, VC and ethene were added and then monitored (via headspace sampling) at appropriate intervals. Formation of epoxyethane from ethene-fed cultures was also noted. The experiments were conducted with biological duplicates. Standard curves were generated from TCE, DCA, VC and ethene in 160-mL serum bottles containing 50-mL MSM.

Overexpression of genes in the cyclohexanol operon of JS666

Background

The cyclohexanol degradation pathway has been well characterized biochemically (Donoghue and Trudgill, 1975) and genetically (Chen, Peoples *et al.*, 1988). Cyclohexanol is transformed into its dicarboxylic acid through a five-step conversion (Figure 3-3): cyclohexanol is reduced to CYHX by cyclohexanol dehydrogenase (ChnA). CYHX is oxidized to CAP via Baeyer-Villiger oxidation by the flavin-containing cyclohexanone monooxygenase (ChnB). The cyclic lactone is then hydrolyzed by 1-oxa-2-oxocycloheptane lactonase (ChnC) into 6-hydroxyhexanoic acid (6-HHA), before being converted into 6-oxohexanoic acid by 6-hydroxyhexanoate dehydrogenase (ChnD). 6-Oxohexanoate dehydrogenase (ChnE) converts 6-oxohexanoic acid into adipic acid, which is further oxidized to acetyl-CoA and succinyl-CoA through a β-oxidation pathway.

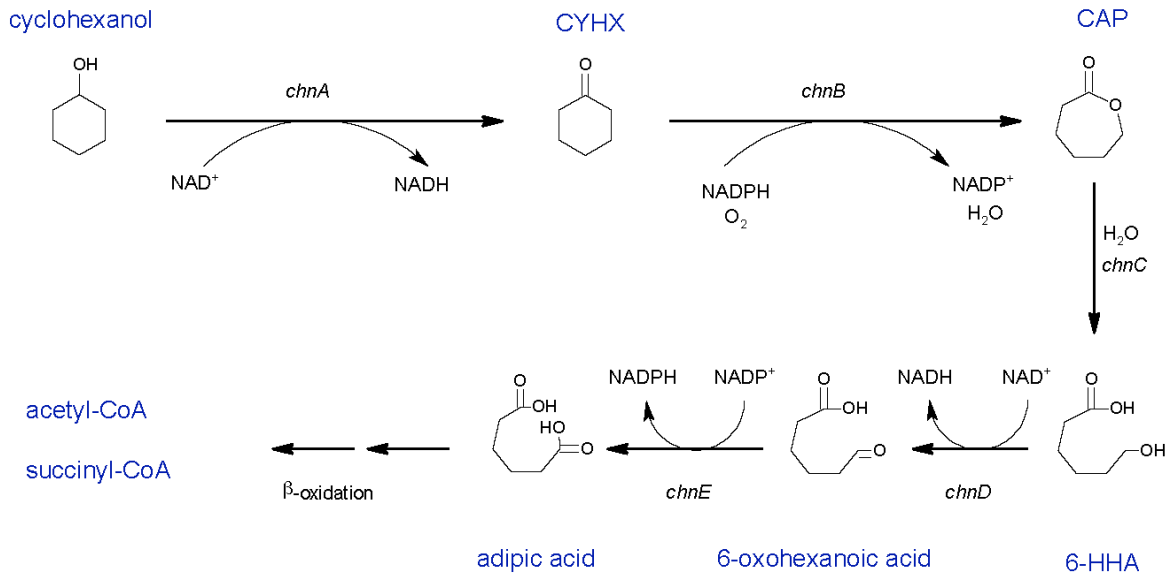

Figure 3-3: Biodegradation of cyclohexanol in Acinetobacter sp. NCIMB 9871. Adapted from Donoghue and Trudgill (1975).

Genes of a putative cyclohexanol-degradation pathway are present in JS666 (Figure 3-4) on the larger of the 2 megaplasmids. In JS666 the genes are rearranged compared to the canonical operon in *Acinetobacter* NCIMB 9871 and *chnE* is located on the chromosome. The genes in JS666 were overexpressed in *E. coli* in order to: (i) confirm their functions; and (ii) ascertain whether any of the proteins encoded by them are active on cDCE or its expected metabolites.

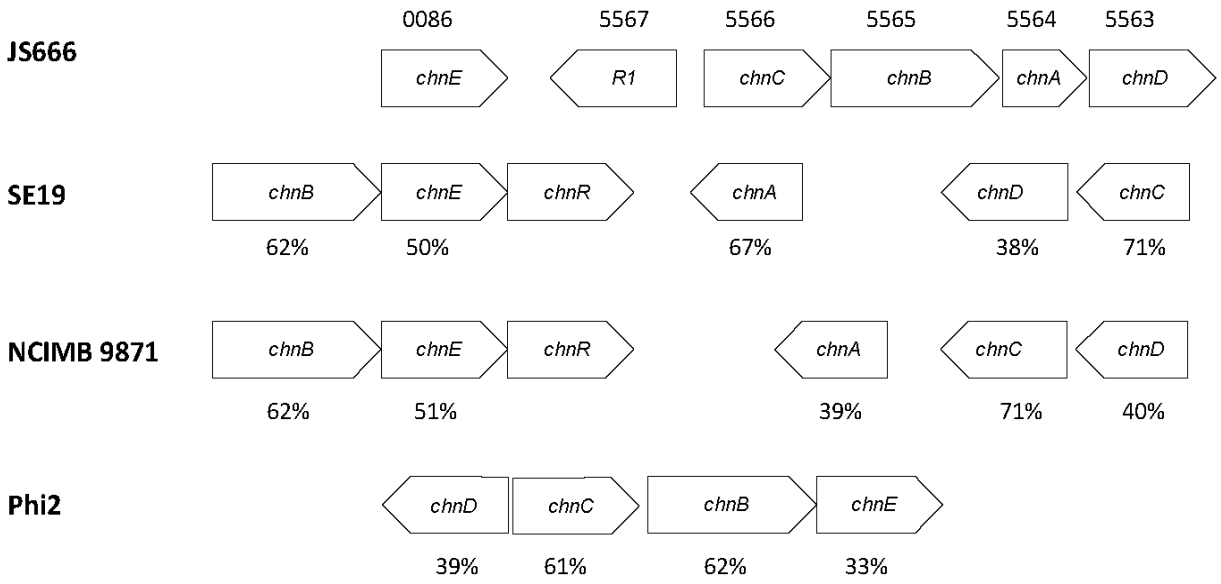

Figure 3-4: Organization of the genes that catalyze cyclohexanol biodegradation in *Polaromonas* sp. JS666, *Acinetobacter* spp. SE19, NCIMB 9871 and *Rhodococcus* sp. Phi2. JS666 gene loci (Bpro) are shown above the genes and percent amino acid identities are shown under other bacterial genes (Iwaki *et al.*, 2002a; Brzostowicz *et al.*, 2003; Mattes *et al.*, 2008). *chnR* encodes the transcriptional activator. *R1* is the Fis-family transcriptional regulator.

Cloning

Genes were cloned — separately or in tandem with neighboring genes — into the pET101/D-TOPO expression vector (Invitrogen). *chnC* (Bpro_5566) was amplified by PCR from WT genomic DNA with *Pfu*Ultra II Fusion HS DNA polymerase (Agilent Technologies, Inc.) and 66F-66R primer pairs. The resulting amplicons were cloned into the expression vector and transformed into *E. coli* BL21 Star™ (DE3). *chnB* (Bpro_5565) and *chnD* (Bpro_5563) were similarly amplified using 65F-65R and 63F-63R primer pairs.

chnC and *chnB* were cloned in tandem into the pET21a(+) cloning vector, and *chnA* and *chnD* genes were cloned in tandem into pCOLADuet™-1 (Novagen). The *chnC-chnB* gene pair was amplified by PCR with the E6566F-E6566R primer pair, containing BamHI and XhoI restriction sites, respectively. The amplified product and pET21a(+) were excised with FastDigest®, BamHI, and XhoI (Fermentas) and ligated, resulting in the recombinant plasmid designated pJMG6566. The *chnA-chnD* gene pair was amplified with the C6463F-C6463R primer pair containing EcoRI and HindIII restriction sites, respectively. The amplicons were excised with FastDigest®, EcoRI and HindIII (Fermentas) and ligated into pCOLADuet™-1, resulting in pJMG6463. Sequences were checked and errors were corrected using QuickChange Multi Site-Directed Mutagenesis Kit (Agilent Technologies).

Enzymatic assay of overexpressed proteins from the cyclohexanol pathway of JS666

ChnB enzyme overexpression and assays

For assaying overexpression of the *chnB* in *E. coli*, whole-cell studies were adopted based on previous studies (Iwaki, Hasegawa *et al.*, 2002; Alexander, 2010). *E. coli* Bl21 Star™ strains containing pJGM65R or pJGM6566 were grown in LB broth supplemented with 100 μg/mL ampicillin and 1 μg/mL riboflavin on a rotary shaker at 30°C. When the optical density reached 0.4 – 0.5, IPTG was added to the media (0.1 mM), and the cultures agitated for 5 minutes before the substrates were added and the temperature reduced to 23°C. The disappearance of the substrates and the appearance of products were monitored. Substrates tested were CYHX, cDCE, styrene and DCAL), and the expected products were CAP, cDCE-epoxide and DCAA, respectively. Uninduced cultures and plasmid-free *E. coli* strains were used as controls.

Hydrolase enzyme overexpression and assays

chnC was overexpressed using a method similar to that described above for ChnB. In a separate experiment, *E. coli* Bl21 Star™ strains containing pJMG66H were grown in LB broth supplemented with 100 μg/mL ampicillin at 30°C. When the optical density reached 0.4 - 0.5, 0.1 IPTG was added (0.1 mM) to the media, and the cultures were agitated for 5 minutes before the substrate (10 μL CAP, 10 μL styrene oxide, 0.5 mL epoxyethane or 5 μL chemically-synthesized cDCE-epoxide), was injected into 20-mL cultures in 160-mL serum bottles. Subsequent incubation to assay growth was conducted at 23°C.

A chromosomally encoded hydrolase from strain JS666 (Bpro_4478) was tested with chemically-synthesized cDCE-epoxide (Chan, Wong *et al.* 2010). The gene was cloned into ampicillin-resistant p15TV-L, and the plasmid was transformed into *E. coli* BL21 Star™. In a preliminary experiment, the cells were grown in LB broth containing 100 μg/mL ampicillin at 30°C. When OD_{600} reached 0.5 – 0.6, IPTG was added (0.5 mM), and the culture was shaken at 23°C overnight. The cells were harvested and washed once with phosphate buffer. The pellets were suspended in 20 mM phosphate buffer supplemented with 1 mM succinate. Chloride ions were measured after 1 and 4 hours. At 5-hours, 1 mM succinate was added and the incubation was continued overnight. Final readings were taken in the morning. An uninduced control accompanied all the steps.

The experiment was repeated but with the addition of a culture provided with 0.5% glucose. When OD_{600} reached 0.5 - 0.6, IPTG was added (1 mM). After 4-hour induction at 30°C, the cells were harvested and washed twice in phosphate buffer. The cells were suspended in 20 mM phosphate buffer and chemically synthesized cDCE-epoxide (in acetonitrile) was introduced to the cultures. Uninduced cells were assayed for background activity and chloride release. Phosphate buffer with no cells was used as blank control.

Dehydrogenase enzyme overexpression and assay

E. coli BL21 Star™ (DE3) strains containing either pJMG6364 or pJMG63R were grown on LB broth with 0.5% glucose and 30 μg/mL kanamycin or 100 μg/mL ampicillin, respectively, at 30°C. A plasmid-free host strain was used as negative control. When OD_{600} reached 0.4 – 0.5, IPTG was added (1 mM) and the cultures were shaken overnight at 23°C. The cultures were harvested by centrifugation and washed once with phosphate buffer. The pellets were suspended in 20 mM phosphate buffer (pH 7.5) and aliquots (10-mL) of the culture (containing approximately 20 mg of cells) were transferred into 25-mL serum bottles, and substrates were added. Uninduced cells were used as control. ChnD (6-hydroxyhexanoate dehydrogenase) was tested for activity with cyclohexanol, 6-HHA, EtOH, acetaldehyde, glycolate and DCET. The tandomly cloned ChnA (cyclohexanol dehydrogenase) and ChnD were tested with cyclohexanol, 6-HHA, EtOH, and acetaldehyde. Acetaldehyde was added from a stock (5.25 g/L) of 155 μL acetaldehyde dissolved in 23.2 mL cold phosphate buffer.

iTRAQ proteomics comparison between WT and KO strains

Both WT and KO strains were grown in 2 mM CAP, with or without cDCE (52 μmol/bottle). CAP was chosen as secondary carbon source because both WT and KO strains can utilize it while allowing WT cells to sustain the "good" cDCE-degradation behavior (Figure 3-5). Substrates were monitored by gas chromatography. The cultures were harvested by centrifugation when the cells were actively degrading cDCE and/or CAP. The cells were washed once with phosphate buffer then suspended in 20 mM phosphate buffer (pH 7.5), and broken by passage through a French press at 20,000 psi. In between cultures, the French press cell was cleaned with a 3x rinse with distilled water, a 70% ethanol rinse, followed by 3x distilled water. To minimize protein cross-contamination, the cultures were broken in the order: WT grown on CAP-only, WT on CAP and cDCE, KO on CAP-only, and KO on CAP and cDCE. The French press cell and the lysates were kept at 4°C. WT and KO pellets were stored at -80°C for RNA extraction. Subsequent procedures (i.e. protein digestion, iTRAQ labeling, fractionation, chromatography, spectrometry and data processing) were performed by James McCardle, Wei Chen and Sheng Zhang at The Proteomics and Mass Spectrometry Core Facility, Cornell University. Details of the procedures are in Appendix A-1.

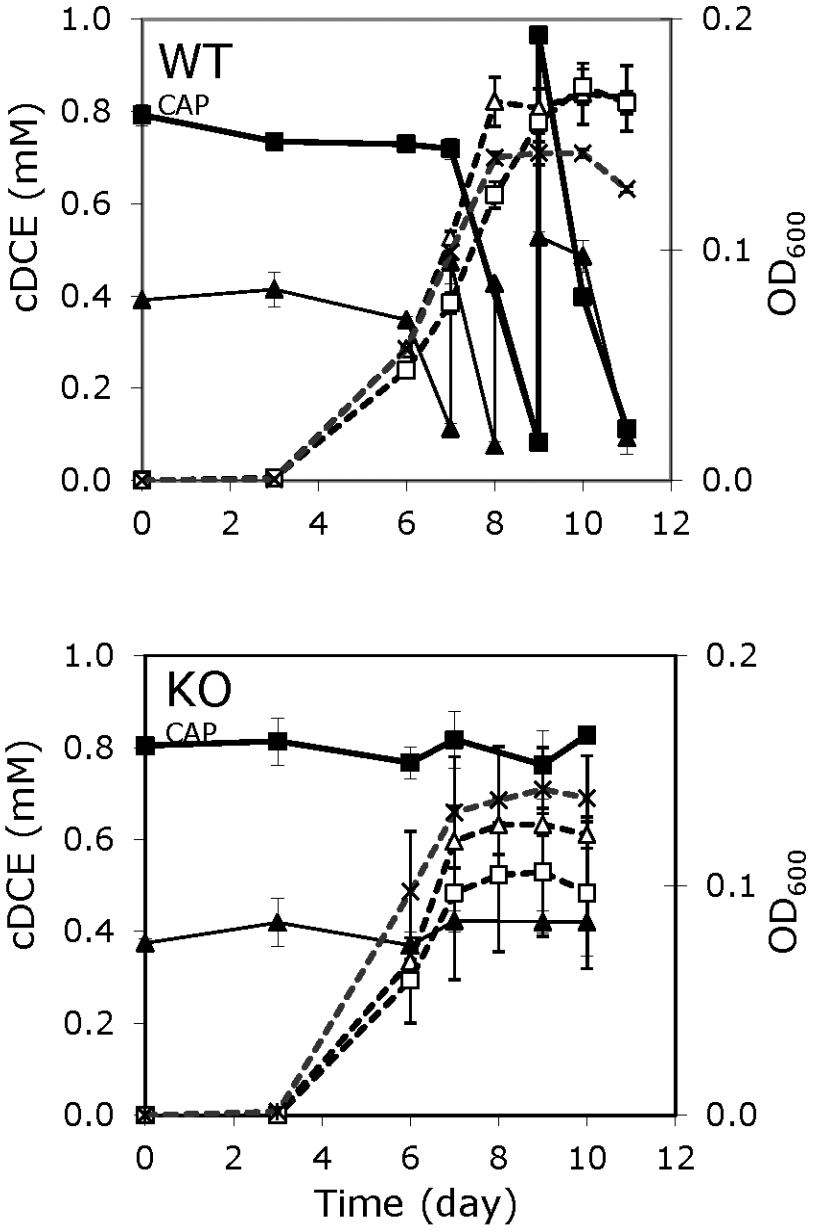

Figure 3-5: Growth of WT and KO strains on MSM and 1 mM CAP with or without cDCE. Bars depict standard errors of experimental biological duplicates. Solid lines with closed markers are cDCE, and dotted lines with opened markers are OD_{600}. Cultures were supplied with 106 μmol/bottle cDCE (squares), 52 μmol/bottle cDCE (triangles) or no cDCE (stars).

Reverse transcription polymerase chain reaction (RT-PCR)

WT and KO cultures were grown in MSM containing 10 mM succinate, with or without cDCE (52 μmol/bottle). When the OD_{600} reached 0.6 - 0.8 (or mid-degradation of succinate), the cells were harvested and total RNA was extracted using the Qiagen Allprep RNA/DNA Mini Kit and treated twice with RNase-free DNase I (Qiagen and Promega). Total RNAs were measured and checked for DNA contamination using an Agilent RNA Nano chip analyzed in an Agilent 2100 Bioanalyzer.

100 ng of RNA was used as a template for the reverse transcription reaction. The first strand of complementary DNA (cDNA) was primed using a cocktail of gene-specific primers (2 pmol/primer, 8 primers total). A two-step RT-PCR protocol was used: a mixture of RNA template and primers was incubated at 65°C for 5 min and then chilled on ice. Reverse transcriptase and buffer (Bio-rad iScript) were added to the RNA, centrifuged and incubated at 42°C for 60 min. The reaction was terminated by heating at 85°C for 5 min. The cDNA was measured and checked for purity with a NanoDrop 2000C (Thermo Scientific). 300 ng of cDNA was used as template with the RT-PCR primers listed in Table 3-2. Melting temperature used for the PCR reaction was 60°C, and the reaction was run for 30 or 35 cycles.

Analytical Methods

Spain Laboratory, Georgia Institute of Technology

cDCE, DCA, and cyclohexanone were monitored by GC using an Agilent 6890N GC equipped with a Supelco 60/80 Carbopack B column (6 feet by 1/8 inches). Inlet temperature was 200°C with helium flow at 13 mL $minute^{-1}$ (min^{-1}), the flame ionization detector (FID) was maintained at 275°C with hydrogen gas (H_2) and air flow at 40 and 460 mL min^{-1}, respectively. The oven temperature was ramped at 20°C min^{-1} from 100°C to 150°C, then at 10°C min^{-1} to a maximum of 175°C and held until all compounds eluted. cDCE epoxide, dichloroacetaldehyde (DCAL), and chloroacetaldehyde were analyzed by an HP6890 GC equipped with either an ECD or a 5973 mass detector. Compounds were separated on a DB-5MS column (30 centimeters [cm] × 0.25 millimeter [mm], 0.25 micrometer [μm] film thickness; J&W scientific, CA). The oven temperature was initially held at 35 °C for 10 min, ramped at 20 °C/min to 175 °C, and held at the final temperature for 3 min. For more rapid separation of cDCE and DCAL samples were run isothermally at 60°C. Headspace samples (100 microliters [μL]) were analyzed directly. Aqueous samples were spiked with TCE, mixed with equal volumes of ethyl ether and shaken for 10 min. The phases were separated by centrifugation and the ether extracts were analyzed by GC/ECD or GC/mass spectrometry (MS). Oxygen and carbon dioxide were monitored using a thermal conductivity detector (TCD).

Protein was measured using a Pierce Bicinchonninic acid protein assay kit (Rockford, IL). Chloride was measured by the method of Bergmann (Bergmann and Sanik, 1957).

DCAL hydrate was converted to DCAL trimer and thence to DCAL by the method of Wakasugi (Wakasugi, Miyakawa *et al.*, 1993). cDCE epoxide was synthesized chemically (Verce, Gunsch *et al.*, 2002) and biologically (Fox, Borneman *et al.*, 1990) by transformation of cDCE by the cytochrome P450 clone. Products produced by both methods had parent masses [M^+] at *m/z* 112, 114, and 116 which corresponds to those of cDCE epoxide (Janssen, Grobben *et al.*, 1988). cDCE epoxide could not be accurately measured because of the lack of a reported extinction coefficient. A rough estimate was obtained by measuring A_{530} in extracts after derivitization with 4-(*p*-nitrobenzyl)pyridine (Fox, Borneman *et al.*, 1990).

Gossett Laboratory, Cornell University

TCE, cDCE, VC, DCA, ethene and epoxyethane were analyzed by 0.1-mL headspace samples injected (using a locking gas-tight syringe, VICI Pressure-Lok® Series A) into a gas chromatograph (Perkin-Elmer Autosystem) equipped with a flame-ionization detector (FID) and a 8-ft x 1/8-inch stainless-steel column packed with 1% SP-1000 on 60/80 Carbopack B (Supelco) that was operated isothermally at 160°C. For detecting cDCE-epoxide, headspace samples up to 2 mL were injected. Oxygen and carbon dioxide levels were measured with a Perkin-Elmer GC equipped with a thermal-conductivity detector and a 80" × 1/8" column packed with 60/80-mesh 13X molecular sieve (Supelco), operated at 90˚C. Substrate levels were quantified by comparison to standards prepared using known-amount additions in serum bottles containing phosphate buffer.

Cyclohexanol, CYHX and CAP were analyzed by GC after extraction of aqueous samples with EtOAc (1:1 = sample: EtOAc), and 2 μL of the organic layer was injected into a gas chromatograph (Hewlett Packard HP5890 Series II) equipped with an FID and a SPB™-5 column (15 m × 0.53 mm × 1.5 μm; Supelco). The column temperature was maintained at 50°C for 2 min, then ramped 15°C/min to 215°C. The injector and detector temperatures were both 250°C. Standards for these substrates were made gravimetrically and extracted using EtOAc for GC measurements.

DCAL, DCET, styrene and styrene oxide concentrations were analyzed by GC after extraction of aqueous samples with Et_2O (2:1 = sample:Et_2O), and 3 μL of organic extract was injected into a gas chromatograph (Hewlett Packard HP5890) equipped with a FID and a DB-5ms column (30 m × 0.53 mm × 1.0 μm; Agilent Technologies) that was operated with column at 40°C for 4 min, then ramped 40°C/min to 200°C until all had been eluted. The injector and detector temperatures were 200°C and 250°C, respectively. Standards for these substrates were made gravimetrically and extracted using Et_2O for GC measurements.

For EtOH and acetaldehyde measurements, direct aqueous injection (3 μL) was made to the GC (HP5890) with FID and DB-5ms column, operated with similar program conditions described above with a longer final temperature (200°C) to remove excess water. Prior to analyses, samples were centrifuged to remove cell debris and kept on ice between measurements to ensure stability of EtOH and acetaldehyde. Standards for both EtOH and acetaldehyde were made by

adding 45.2 μL and 42.7 μL of substrates into 9.54 mL and 9.95 mL of distilled water, respectively.

The concentrations of acetate, succinate, chloride, 6-HHA and glycolate, were measured using a Dionex Ion Chromatograph (AS50) equipped with Dionex AS14A analytical and guard ion-exchange columns with suppressed conductivity detection in an isocratic CO_2-free, 40-mM NaOH eluent at 1 ml/min for 15 minutes. Samples were centrifuged to remove cell debris prior to analyses. Standards for chloride concentrations were prepared gravimetrically through known amount of additions into volumetric flasks.

3.1.4 Results & Discussion

Enrichments for new cDCE-degrading bacteria

Microcosms were constructed with soil and groundwater from a variety of cDCE-contaminated sites (Table 3-1) in order to enrich for additional aerobic cDCE-degrading bacteria. Such organisms could enable a variety of comparative studies with JS666 at all levels (gene, enzyme, microcosm).

Microcosms constructed with materials from a site in Milledgeville, GA and Dover Air Force Base (AFB), DE were repeatedly spiked with cDCE with subsequent disappearance of the added cDCE. Disappearance of cDCE continued after 20% transfers into fresh media (Figure 3-6). After a second transfer, cDCE disappearance continued, but a third transfer failed to show cDCE loss greater than in uninoculated controls. The disappearance of cDCE from the Milledgeville and Dover microcosms is consistent with biodegradation because the removal of cDCE was increasingly rapid with each additional cDCE spike. It is possible that essential nutrients were diluted or removed along with the original soil. Attempts to rescue the cultures by adding back some of the original microcosm material and by testing for nutrient requirements such as vitamins and amino acids failed to restore growth and attempts to rescue the microcosms were discontinued after 200 days. No other microcosms showed cDCE loss in excess of uninoculated controls.

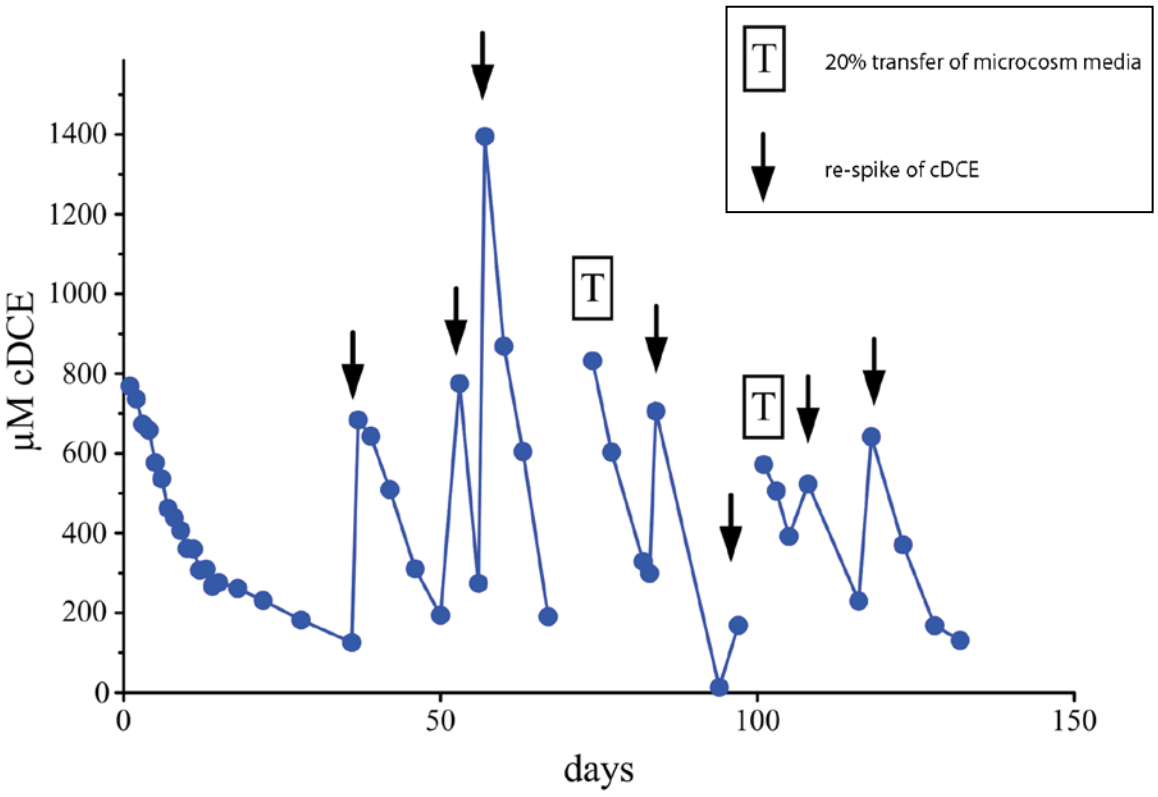

Figure 3-6: Microcosm trend plot of aerobic cDCE removal (Milledgeville, GA)

Additional microcosms were constructed with cDCE contaminated groundwater from a site in Germany reported to have the isotopic fractionation signature for aerobic cDCE degradation (Blessing, Schmidt *et al.*, 2009) as well as from a NASA site in Florida. However, no cDCE degradation was detected in the new microcosms. All microcosms were discontinued after 100 to 290 days when they failed to be enriched for cDCE-degrading bacteria. The results suggest that the ability to grow aerobically on cDCE is a rare trait.

Oxygen uptake assays

Resting cell assays can indicate potential intermediates in aerobic degradation pathways (Stanier, 1947). Initial tests of washed, resting cells of JS666 grown on cDCE showed a strong, inducible oxygen uptake activity, compared to controls grown on succinate, when provided with cDCE, DCA, 2-chloroethanol, or ethanol as substrates (Table 3-3). Research sponsored by ESTCP (ER-0516) revealed that DCA is a growth substrate for JS666 (Major, 2008) in contrast to the original report (Coleman, Mattes *et al.*, 2002) in which DCA was tested at a concentration that is toxic to the organism. Cells grown in the presence of DCA showed very little oxygen uptake activity in general, likely due to the high toxicity of DCA to JS666. The addition of chloroacetaldehyde, and to a lesser extent dichloroacetaldehyde, also strongly stimulated oxygen uptake by cDCE-grown JS666. The resting cell assays were later repeated in order to assess the

response of cyclohexanone-grown cells to the same potential pathway intermediates (Table 3-4).

Table 3-3: Oxygen uptake[a] by resting cells of JS666 grown with various carbon sources

Test Substrate	Growth Substrate			
	cDCE	cDCA	Ethanol	Succinate
cDCE	9.3	0.7	2	2
cDCA	5.5	0.7	2.7	0
2-Chloroethanol	2.4	0	1.7	0
Chloroacetyl chloride	0	0.4	1.7	1.5
Chloroacetaldehyde	13.1	8.5	11.4	11
Dichloroacetaldehyde	6.6	2.9	4.7	1
Chloroacetic Acid	0.3	0.4	1.3	3.5
Dichloroacetic Acid	4.1	0.7	2.3	4
Glyoxal	3.1	2.2	1	8
Glycolate	0.3	1.5	3.7	8.5
Succinate	0.7	0	1	18.1
Ethanol	8.3	0.7	6.4	1

Notes:

[a]Rates are nmol $O_2 \cdot min^{-1} \cdot$mg cell $protein^{-1}$ and are the average of two to four measurements. Test substrates were added at 1 mM final concentration from a 100 mM stock in 50% acetonitrile.

Table 3-4: Oxygen uptake by whole cells of JS666

Test Substrate	Growth Substrate[1]		
	cDCE	DCA	Cyclohexanone
cDCE	16.4	1.0	0
DCA	10.8	1.0	0
Cyclohexanone	12.1	1.4	21.1
2-chloroethanol	2.5	0	2.4
Chloroacetaldehyde	13.8	8.0	14.8
Dichloroacetaldehyde	6.6	2.0	2.4
Chloroacetic acid	0.4	0	2.0
Dichloroacetic acid	4.1	1.0	0
Glyoxal	3.1	2.0	0
Glycolate	3.0	1.0	2.6
Succinate	1.0	1.0	8.0
Ethanol	8.8	1.0	5.6

Notes:

cDCE - cis-1,2-dichloroethene

DCA - dichloroethane

(1) - nmol min^{-1} mg-$protein^{-1}$

The combined oxygen uptake results indicated that:

1) DCA degradation is induced in cDCE-grown cells whereas DCA-grown cells only showed moderate induction of cDCE degradation. The result suggested that DCA might be an intermediate in cDCE degradation.

2) The activity with chloracetaldehyde appeared to be constitutive, and is roughly equivalent when JS666 is grown on succinate, whereas the activity with dichloracetaldehyde was upregulated about six-fold by growth on cDCE. The data suggested that the pathway for cDCE degradation proceeds through chloro-, or dichloroacetaldehyde. Multiple aldehyde dehydrogenases are annotated in the genome of JS666, one or more of which could be responsible for this activity.

3) Cyclohexanone-grown cells are unable to degrade cDCE or DCA immediately, whereas cDCE- and DCA-grown cells both show activity with cyclohexanone. The result suggests that cyclohexanone monooxygenase is not the initial enzyme in the cDCE or DCA degradation pathway, but does not rule out participation in other reactions. Another possibility is that cDCE or some metabolite of cDCE degradation is a non-specific inducer of cyclohexanone 1,2-monooxygenase.

Enzyme Assays

JS666 exhibits an extended lag time before resumption of growth upon transfer of succinate-grown cultures to cDCE (Major, 2008). Together with the above oxygen uptake studies, the results indicate that growth on cDCE, but not succinate, induces the expression of one or more enzymes responsible for the degradation of cDCE and its subsequent oxidation products. Enzyme activities in cell extracts (Table 3-5) confirmed the lower pathway of cDCE degradation suggested by the oxygen uptake experiments. Both chloro- and dichloracetaldehyde dehydrogenase activities were readily detected in extracts of cDCE-grown JS666 at rates sufficient to account for growth. The rate of chloroacetaldehyde dehydrogenase was about twice that of dichloroacetaldehyde dehydrogenase. This was originally interpreted to mean that chloroacetaldehyde is the true biological intermediate while the activity observed with dichloroacetaldehyde is a fortuitous reaction. However, if the initial reaction is monooxygenation to an aldehyde then the true intermediate would be dichloroacetaldehyde. Chloracetaldehyde is highly reactive with DNA and tRNA (Biemat, Ciesiołka *et al.*, 1978; Kohwi and Kohwi-Shigematsu, 1988; Kohwi-Shigematsu and Kohwi 1991), binding permanently at specific sites. The high up-regulation of chloroacetaldehyde dehydrogenase in PCB-stressed *Burkholderia xenovorans* LB400 has been proposed as a detoxification mechanism (Parnell, Park *et al.*, 2006). JS666 might constitutively express chloroacetaldehyde dehydrogenase as a detoxification mechanism or as a part of the DCA pathway to quickly remove the most toxic intermediate of DCA degradation.

Table 3-5: Enzyme activities in cell extracts of JS666

Enzyme Assayed	Rate[a] per Growth Substrate cDCE
cDCE Monooxygenase	ND[b]
cDCE Reductase	ND
cDCE Hydratase	ND
cDCA Dehalogenase	ND
2-Chloroethanol Dehydrogenase, PQQ type	ND
2-Chloroethanol Dehydrogenase, NAD(P) type	ND
Chloroacetaldehyde Dehydrogenase	58[c]
DiChloroacetaldehyde Dehydrogenase	29[c]
Chloroacetic Acid Dehalogenase	15[d]
Dichloroacetic Acid Dehalogenase	15[d]

Notes:

[a]Rates are the average of two to four measurements.

[b]Not detected.

[c]nmol NADH produced·min^{-1}·mg cell $protein^{-1}$.

[d]nmol Cl^- released·min^{-1}·mg cell $protein^{-1}$.

In addition, both chloro and dichloroacetic acid dehalogenase activities were detected. Haloacid dehalogenases (HADs) catalyze the removal of the halogen from a molecule, cleaving the carbon-halogen bond. HADs replace the halogen with a hydroxl through the hydrolysis of α-halogenated carboxylic acid. The product of chloroacetic acid dehalogenation is glycolate. Glycolate is likely oxidized to the central metabolite glyoxalate by the flavoprotein glycolate oxidase, the presence of which is indicated in the sequenced genome. There are two paralogous HADs in the JS666 genome, one of which is on a plasmid (Bpro_5186). They share a 58% and 54% amino-acid identity with *Agrobacterium tumefacians* RS5 and *Pseudomonas* sp., respectively. Both enzymes were expressed in *E. coli* (Jennings, Chartrand *et al.*, 2009).

No evidence for transformation of cDCE was detected in cell extracts (Table 3-5). cDCE did not increase the rate of NAD(P)H oxidation by cell extracts of cDCE-grown JS666, which suggested that an initial transformation by a monooxygenase or reductase was unlikely, however later studies with cloned enzymes revealed great difficulty in expressing the monooxygenase activity in cell extracts despite high activity in the whole cells. Chloride release from cDCE was not detected; suggesting that a hydratase does not act on cDCE.

Determination of Growth Conditions for Molecular Biology

The genes that initiate the cDCE degradation pathway were not readily determined, in part because many of the molecular tools could not be used because of difficulties with screening.

Many techniques, such as knockouts, complementation, mutation, conjugation, plasmid curing require the ability to discriminate between the growth of the wild-type and the manipulated strain after applying the technique. JS666 often failed to grow with cDCE following any exposure to growth substrates other than cDCE. Thus screening based on growth differences following genetic manipulations, which typically require a growth phase on media such as LB agar, was not possible. JS666 will grow with a short lag period in liquid cultures on cDCE or cyclohexanone when the growth substrate is switched between the two compounds. Colonies can similarly be grown on plates with cyclohexanone as the carbon source then inoculated into ¼-MSM with acid indicator and provided cDCE in the vapor phase, turned yellow, indicating chloride release from cDCE. Colonies are large enough to manipulate in 2-3 weeks after growth on cyclohexanone agar plates vs 2-3 months on plates provided with cDCE.

Extension of the new growth methods allowed the application of a limited number of molecular techniques to the pathway determination. JS666 could grow on agar plates containing cyclohexanone without losing the ability to grow on cDCE. However, matings on cyclohexanone plates between *E. coli* and JS666 failed to yield organisms with knockouts in the GST or cyclohexanone monooxygenase genes and attempts were discontinued at Georgia Tech, however a *chnB* knockout was successfully created at Cornell.

mRNA and Protein Expression

The lower pathway of cDCE oxidation was determined through a combination of resting cell assays and enzyme assays. The lower pathway of cDCE degradation comprises (di)chloroacetaldehyde dehydrogenase, followed by (di)chloroacetic acid dehalogenase, which together convert (di)chloroacetaldehyde to (di)chloroacetic acid and then finally to glycolate. Enzyme assays did not reveal the initial enzymatic attack on cDCE. Enzymes assayed, but not detected, were: (i) cDCE monooxygenase, (ii) cDCE reductase, and (iii) cDCE hydratase.

Transcriptomics (microarrays) and proteomics (2-D protein gels) are complementary techniques that can provide a snapshot of the genes and proteins that are induced when JS666 is grown on cDCE versus glycolate controls. Genes and proteins upregulated or expressed in cDCE-grown cells compared to glycolate-grown cells are candidates for involvement in cDCE degradation, including the unknown initial steps. 590 genes and 265 intergenic regions were upregulated in cells grown on cDCE compared to glycolate. A list of the twenty most highly upregulated transcripts (Table 3-6) has several notable congruences with the list of highly expressed protein spots identified by LC/MS/MS and MALDI-TOF/TOF (Table 3-7).

Table 3-6: Genes highly upregulated by cDCE compared to glycolate

Gene Annotation	Fold Change	Locus Tag
Extracellular ligand-binding receptor	111	Bpro_3336
Glutathione S-transferase	100	Bpro_0645
Pyridoxamine 5'-phosphate oxidase	87	Bpro_0646
Inner-membrane translocator	70	Bpro_3335
Haloacid dehalogenase, type II	53	Bpro_0530
Haloacid dehalogenase, type II	51	Bpro_5186
Hypothetical	43	Bpro_0532
Sodium solute transporter superfamily	41	Bpro_0531
Sodium solute transporter superfamily	40	Bpro_0530
Inner-membrane translocator	31	Bpro_3334
ABC transporter related	27	Bpro_3333
Conserved hypothetical	24	Bpro_0529
Hypothetical	19	Bpro_5184
ABC transporter related	18	Bpro_3332
Conserved hypothetical	18	Bpro_2731
Chromate transporter	16	Bpro_2503
Amidase	15	Bpro_3330
Animal haem peroxidase	15	Bpro_2396
Carbon monoxide dehydrogenase	10	Bpro_0577
Cyclohexanone monooxygenase	10	Bpro_5565

Table 3-7: Proteins upregulated by cDCE compared to glycolate

Protein Annotation	Peptide Score	Locus Tag
Glutathione S-transferase-like	325	Bpro_0645
2-C-methyl-D-erythritol 2,4-cylodiphosphate synthase	109	Bpro_2715
Haloacid dehalogenase, type II	663	Bpro_5186
Haloacid dehalogenase, type II	638	Bpro_0530
Pyridoxamine 5'-phosphate oxidase-related	280	Bpro_0646
2-Isopropylmate synthase	146	Bpro_2322
Cyclohexanone monooxygenase	186	Bpro_5565
Chaperonin GroEL	70	Bpro_0759
Trigger factor	404	Bpro_2029
Protein of unknown function DUF404	265	Bpro_3157
Cyclohexanone monooxygenase	70	Bpro_5565
Glutamine synthetase, type I	68	Bpro_1807

The proteomics experiments detected the expression of GST, pyridoxamine 5'-phosphate oxidase (PNPO), cyclohexanone monooxygenase (ChnB) and two genes annotated as haloacid dehalogenase (HAD). The activity of a haloacid dehalogenase in the lower pathway of cDCE degradation was previously identified by biochemical assays. The other three enzymes were candidates as initial enzymes for cDCE degradation based upon functions associated with known enzymes with similar annotations. However, machine annotation only suggests function based on sequence, and may be incorrect. Nonetheless, the proteins were among the most highly upregulated when JS666 was grown on cDCE, and provided a starting point for examining the role of specific genes during the degradation of cDCE.

Glutathione S-Transferase

Bpro_0645 was one of the most highly upregulated genes and its product GST, one of the most highly upregulated proteins (Tables 3-6 and 3-7). GST could potentially attack cDCE (Figure 3-1 pathway III) to form a glutathione-dichloroethane conjugate (Vuilleumier, 1997; Vuilleumier and Pagni, 2002). We tested the hypothesis with whole cell and enzyme assays using JS666 and with *E. coli* clones that overexpressed the GST encoded by Bpro_0645. An alternate role for GST could be conversion of an epoxide intermediate (Figure 3-1 pathway V) rather than cDCE to a glutathione-dichloroethane conjugate.

Extracts of cells grown on cDCE showed activity with 1-chloro-2,4-dinitrobenzene (CDNB), the standard test substrate for GST activity (Lee, Toung *et al.*, 1995), but no detectable transformation of cDCE when incubated with glutathione (Table 3-8). It remained possible that the inability to detect the proposed GST attack on cDCE was due to a low specific activity of the wild type enzyme towards cDCE. Therefore, we overexpressed the protein in *E. coli* and tested the recombinant cell extracts for relevant enzyme activity. Cell extracts of *E. coli* expressing GST exhibited a 50-fold increase in activity versus CDNB as the substrate (Table 3-9). Control *E. coli* cells containing the vector without the insert showed no activity versus CDNB. GST did not attack cDCE or propylene epoxide (a surrogate for cDCE epoxide), as monitored by substrate disappearance by GC. The result was not due to poor expression of the JS666 GST in *E. coli*, as evidenced by the activity of the recombinant protein versus CDNB. cDCE epoxide was unavailable for the assay, but the data suggest that the biological substrate of the JS666 GST is not cDCE or cDCE epoxide. The true biological function of GST, and its role in cDCE metabolism, remain to be determined.

Table 3-8: Glutathione S-Transferase activity in extracts of JS666

Test Substrate	Growth Substrate[(1)]		
	cDCE	DCA	Cyclohexanone
1-chloro-2,4-dinitrobenzene	210	0	0
cDCE	0	0	0

Notes:

cDCE - cis-1,2-dichloroethene

DCA - dichloroethane

(1) - nmol min^{-1} mg-$protein^{-1}$

Table 3-9: Glutathione S-Transferase in recombinant *E. coli* cell extracts

Test Substrate	Growth Substrate[(1)]	
	GST1 (Bpro_0645)	No Insert
1-chloro-2,4-dinitrobenzene	13,200	0
cDCE	0	0
Propylene epoxide	0	0

Notes:

cDCE - cis-1,2-dichloroethene

(1) - nmol min^{-1} mg-$protein^{-1}$

Cyclohexanone monooxygenase

Unlike cDCE-degrading bacteria, aerobic VC-degrading bacteria (Hartmans and de Bont, 1992; Coleman and Spain, 2003) are widespread in the environment and the pathway for VC degradation is well established (de Bont, Attwood *et al.*, 1979; Allen, Clark *et al.*, 1999; Ensign and Allen, 2003) to occur via epoxidation catalyzed by monooxygenases. Because cyclohexanone monooxygenase is upregulated by cDCE (Tables 3-6 and 3-7) we tested the hypothesis that the first step is an epoxidation catalyzed by a monooxygenase. Cyclohexanone stimulated high oxygen uptake by cells grown on cDCE, confirming the microarray results (Table 3-4). However, cDCE did not stimulate oxygen uptake by cyclohexanone-grown cells, although they readily oxidized cyclohexanone. The results suggest that cyclohexanone monooxygenase is not involved in epoxidation of cDCE. On the same plasmid, but not linked to the cyclohexanone monooxygenase gene, is a gene that encodes a protein related to cytochrome P450 cyclohexane monooxygenase. Such enzymes have the potential to catalyze the same types of transformations of chlorinated alkenes as cyclohexanone monooxygenase.

Simultaneous Degradation of cDCE and DCA

cDCE-grown cells of JS666 degraded DCA with no lag period. In the presence of DCA, cDCE degradation was inhibited by an amount equivalent to the DCA degradation. DCA degradation was unaffected by the presence of cDCE (Figure 3-7). The inhibition of cDCE degradation by DCA might be explained by competitive inhibition of an enzyme that catalyzes the initial transformation of cDCE; however, it is unclear why DCA degradation was unchanged.

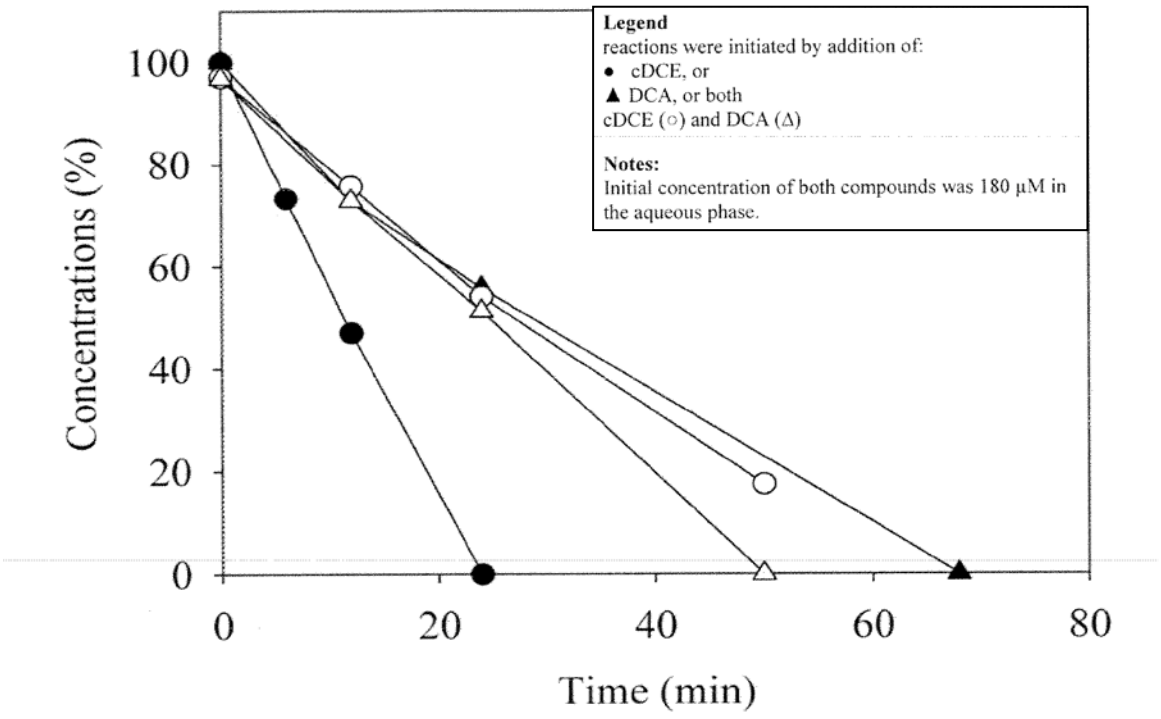

Figure 3-7: Biodegradation of cDCE and DCA by cells of JS666 (JS666 grown on cDCE)

Involvement of Oxygen in Transformation of cDCE

The inability to detect the disappearance of NAD(P)H in cell extracts provided with cDCE (enzyme assays above) directed attention away from the possibility that the initial reaction is a monooxygenation. However, negative results of initially more promising reactions called for an alternative approach to the involvement of oxygenases in the transformation cDCE and DCA (Figure 3-1). In order to determine whether cDCE could be degraded in the absence of oxygen, cDCE-grown cultures of JS666 were sparged with N2. Following a 5 min incubation to deplete the oxygen in the aqueous phase, the cultures were provided with cDCE. No cDCE degradation was observed in the absence of oxygen, but degradation began immediately after the addition of air (Figure 3-8). Aerobic control cultures degraded cDCE with no lag. The results suggest the involvement of an oxygenase in the initial steps of cDCE degradation.

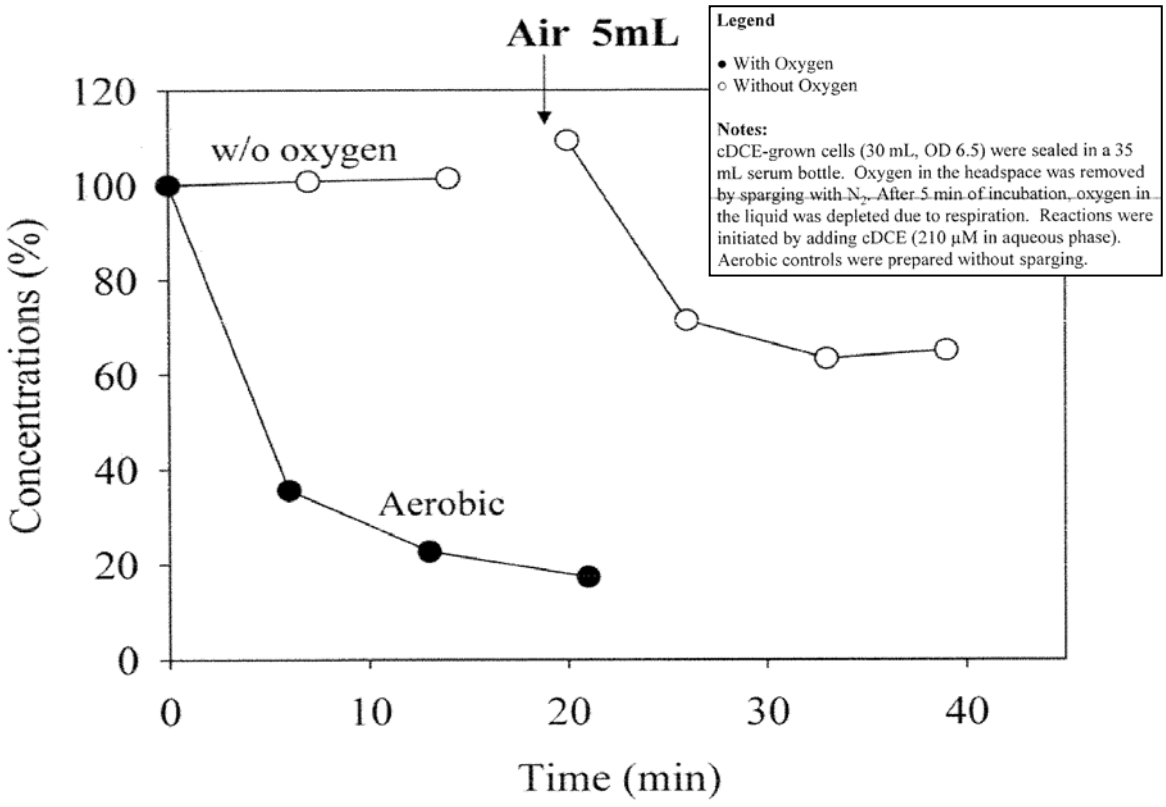

Figure 3-8: Biodegradation of cDCE with and without oxygen

Effect of Cytochrome P450 Inhibitors

Cytochrome P450 enzymes catalyze a wide variety of oxygenation reactions including the epoxidation of double bonds and the hydroxylation of saturated C-H bonds (Guengerich, 2001). Metyrapone (Williams, Cosme *et al.*, 2004) and phenylhydrazine (Raag, Swanson *et al.*, 1990) are specific cytochrome P450 inhibitors. cDCE and DCA degradation by intact cells of JS666 was inhibited over 90% by 200 µM metyrapone or phenylhydrazine when measured by oxygen uptake. The oxygen uptake rates with chloroacetaldehyde and cyclohexanone were unchanged. The degree of inhibition of the initial rates of cDCE and DCA degradation was proportional to the amount of metyrapone (Figure 3-9). The results indicate that cytochrome P450 catalyzes cDCE and DCA biodegradation in JS666.

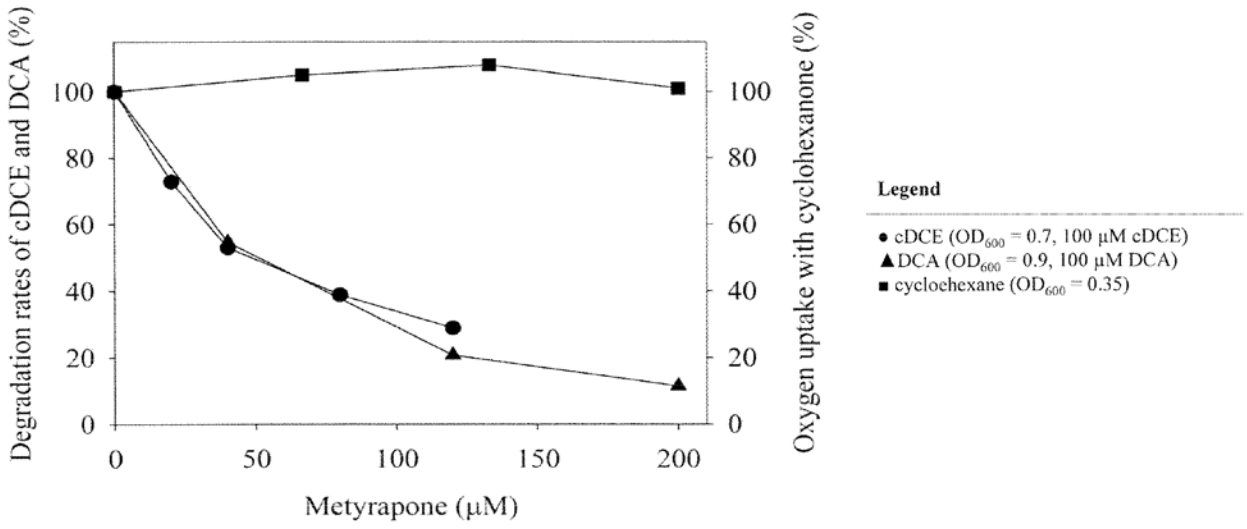

Figure 3-9: Metyrapone inhibition of cDCE and DCA degradation

Cloning and Expression of Cytochrome P450

There are four genes annotated as cytochrome P450s in the genome of JS666 (Mattes, Alexander *et al.* 2008). Three of the four are upregulated by growth on cDCE. Bpro_5301, which was upregulated 3.5 fold, showed 76% amino acid identity to a cytochrome P450 alkane hydroxylase (CYP153A) from *Mycobacterium* sp. HXN-1500 (van Beilen, Holtackers *et al.* 2005; Jennings, Chartrand *et al.* 2009). The gene was immediately upstream of the ferredoxin reductase (Bpro_5300) and ferredoxin (Bpro_5299) on one of the large plasmids of JS666. The three genes were cloned into *E. coli* and expressed. The clone catalyzed the transformation of DCA and cDCE at 4.1 and 2.3 nmol/min, respectively. No degradation was observed in the absence of oxygen, but degradation was immediate upon the addition of oxygen. The results support the hypothesis that cytochrome P450 catalyzes the initial steps of cDCE biodegradation in JS666.

Dichloroacetaldehyde and cDCE epoxide were produced from cDCE transformation by dialyzed extracts of the *E. coli* clone only when NADH or NADPH was present in the reaction (Figure 3-10). When DCA was the substrate, chloroacetaldehyde was produced in the presence of NADH. The P450-catalyzed epoxidation of terminal olefins is not a fully concerted process. The formation of a porphyrin N-alkylation product between a substrate and the enzyme results in an irreversible enzyme inactivation (Meunier, de Visser *et al.* 2004). The cytochrome P450 in JS666 is specialized for dichloroacetaldehyde production from cDCE, possibly as a means to prevent accumulation of a toxic and reactive epoxide.

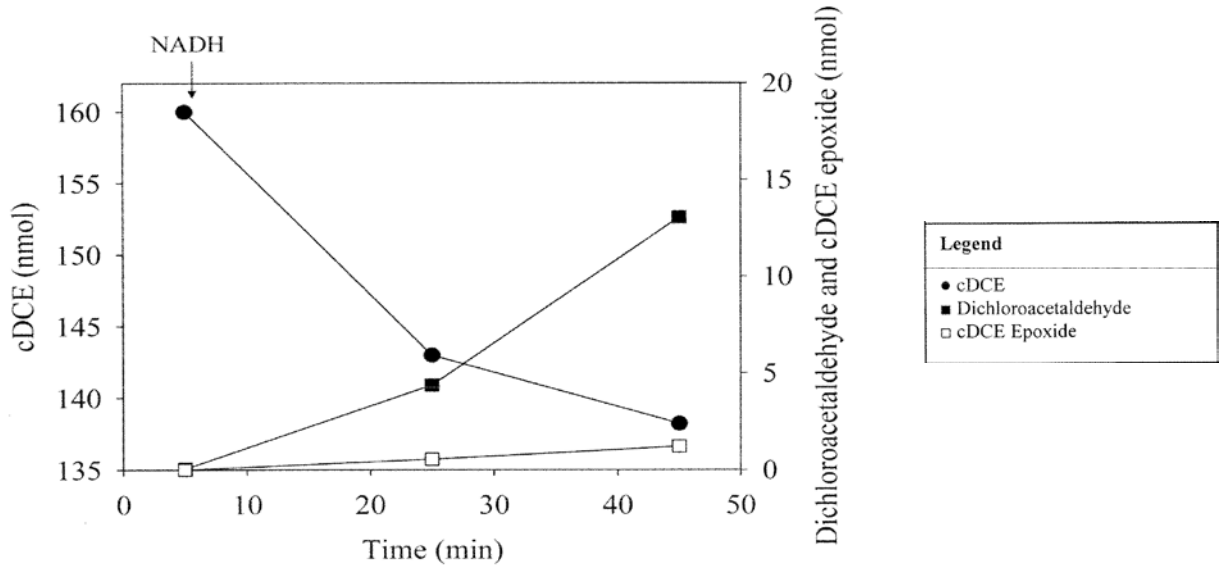

Figure 3-10: Biotransformation of cDCE in cell extracts of *E. coli* clone expressing cytochrome P450

cDCE Epoxide and Dichloroacetaldehyde Accumulation During cDCE Degradation

When cDCE-grown cells of JS666 were transferred to fresh media and supplied with cDCE, dichloroacetaldehyde and cDCE epoxide accumulated (Figure 3-11). The transient accumulation of dichloroacetaldehyde suggests that it is an intermediate of cDCE degradation.

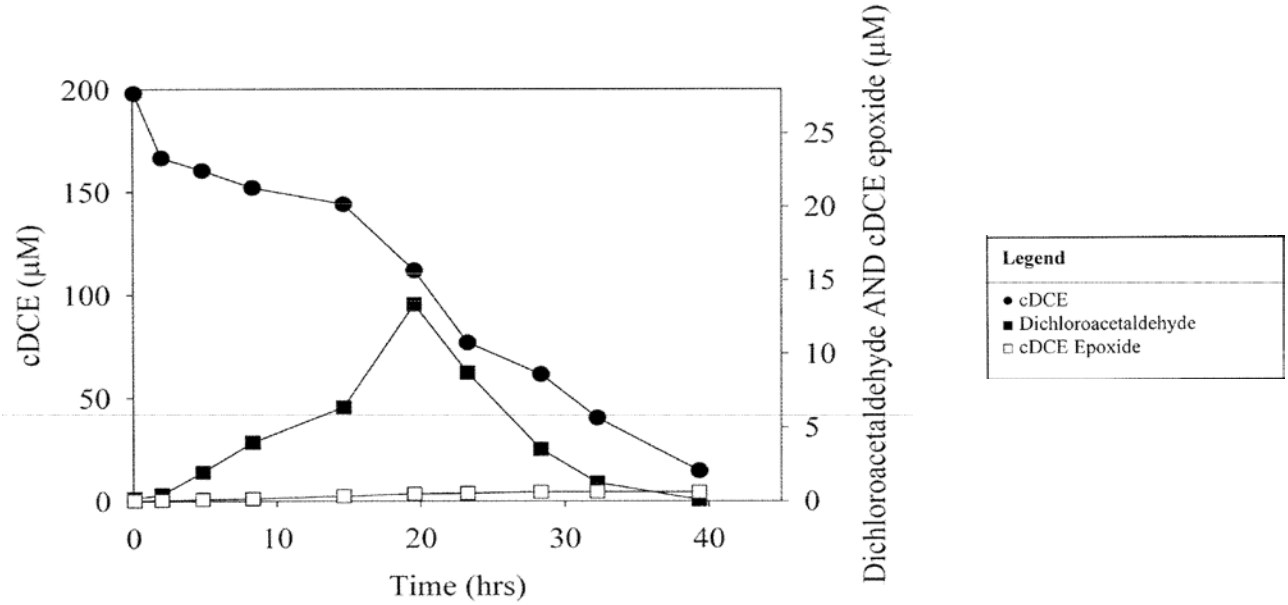

Figure 3-11: cDCE degradation kinetics during the growth of JS666 on cDCE

When all cDCE was degraded, the rate of cDCE epoxide disappearance from the culture medium was similar to the rate in cell-free culture medium prepared by filtration. In both instances the half lives of cDCE epoxide was roughly 72 hours, similar to the abiotic half life of cDCE epoxide in liquid (Janssen, Grobben *et al.* 1988). Sequential addition of cDCE (350 μmol total) over 74 hours resulted in further accumulation of cDCE epoxide. Approximately 0.1% of the cDCE epoxide was lost during the incubation period. The accumulation of cDCE epoxide may explain the high expression of GST during the growth on cDCE (Jennings, Chartrand *et al.* 2009) in that GST functions primarily as a detoxification mechanism (Armstrong 1997; van Hylckama Vlieg and Janssen 2001). The results suggest that the cDCE epoxide spontaneously decomposes in cultures, but that it is a dead end metabolite not productively transformed by JS666.

cDCE clone improvement

The genes that encode the three components of the cytochrome P450 holoenzyme were cloned and expressed individually. However the reconstituted enzyme failed to transform cDCE. Two additional plasmids that each encoded all three components were constructed, and in intact cells, transformed cDCE as described above. The difference between the clones is the presence of a large portion of the intergenic region between Bpro_5301 and Bpro_5302 on the more active clone (Figure 3-12). Despite the tantalizing evidence above, the studies were plagued by the rapid loss of activity of the clones, and an uncertain mass balance. The ability of the clones to transform cDCE was enhanced by moving the constructs from *E. coli* BL21 into *E. coli* Rosetta 2, a host that supports the expression of genes that require rare codons. The new constructs degrade cDCE more rapidly relative to the BL21 Star host.

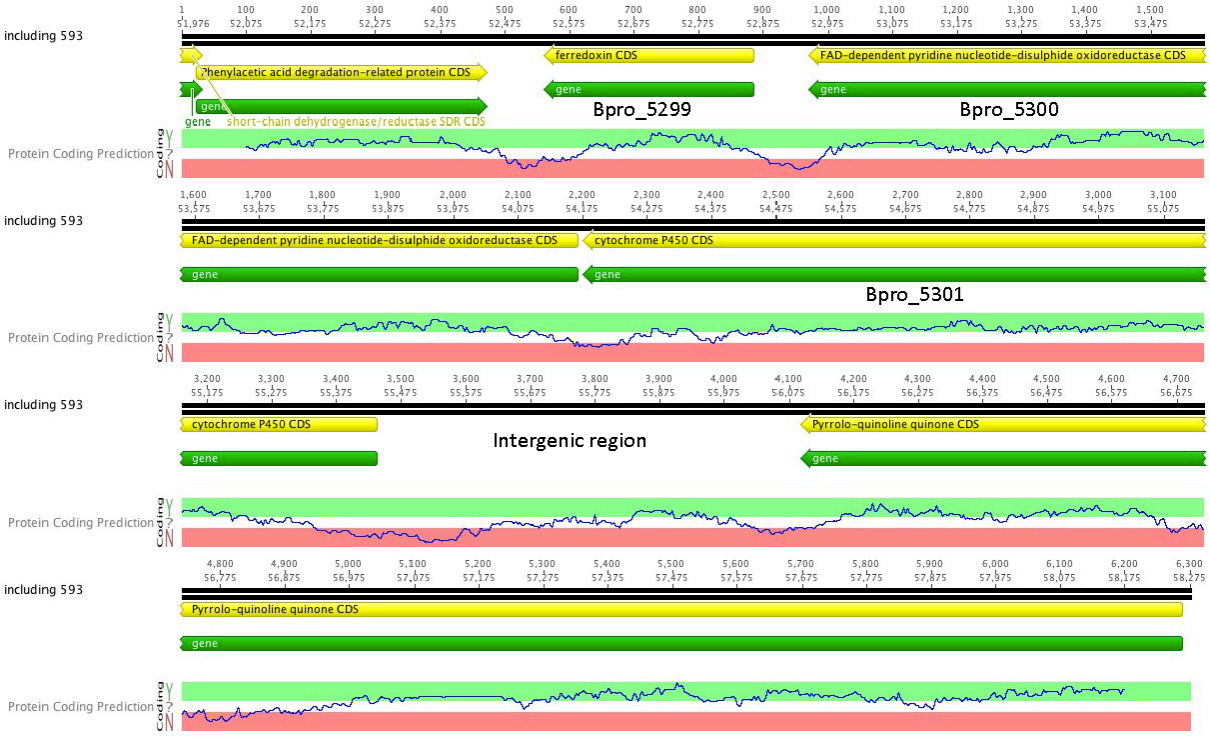

Figure 3-12: Organization of genes in clones expressing cytochrome P450. Two clones were constructed incorporating Bpro_5301, 5300, and 5299. The more active clone incorporated much of the intergenic region between Bpro_5301 and Bpro_5302.

cDCE mass balance

cDCE transformation by the clones is accompanied by the accumulation of dichloroacetaldehyde in the aqueous phase and a major unidentified peak in the gas phase (Figure 3-13). Accurate mass spectroscopy indicated that the composition of the unknown is $C_2H_2OCl_2$. The formula is consistent with any of several DCE epoxides or chloroethene alcohols. Epoxides synthesized from cDCE, tDCE, and 1,1-DCE had different GC retention times from the unknown. A chlorinated ether also proved not to be the unknown. We have not ruled out the possibility that the compound is 2,2-dichloroethenol. The compound had not been previously considered due to its limited, but still rather high predicted solubility (40 mM) in aqueous solutions. However, recent papers suggest that the compound predominantly exists in the gas phase (Werner and Cool, 1998).

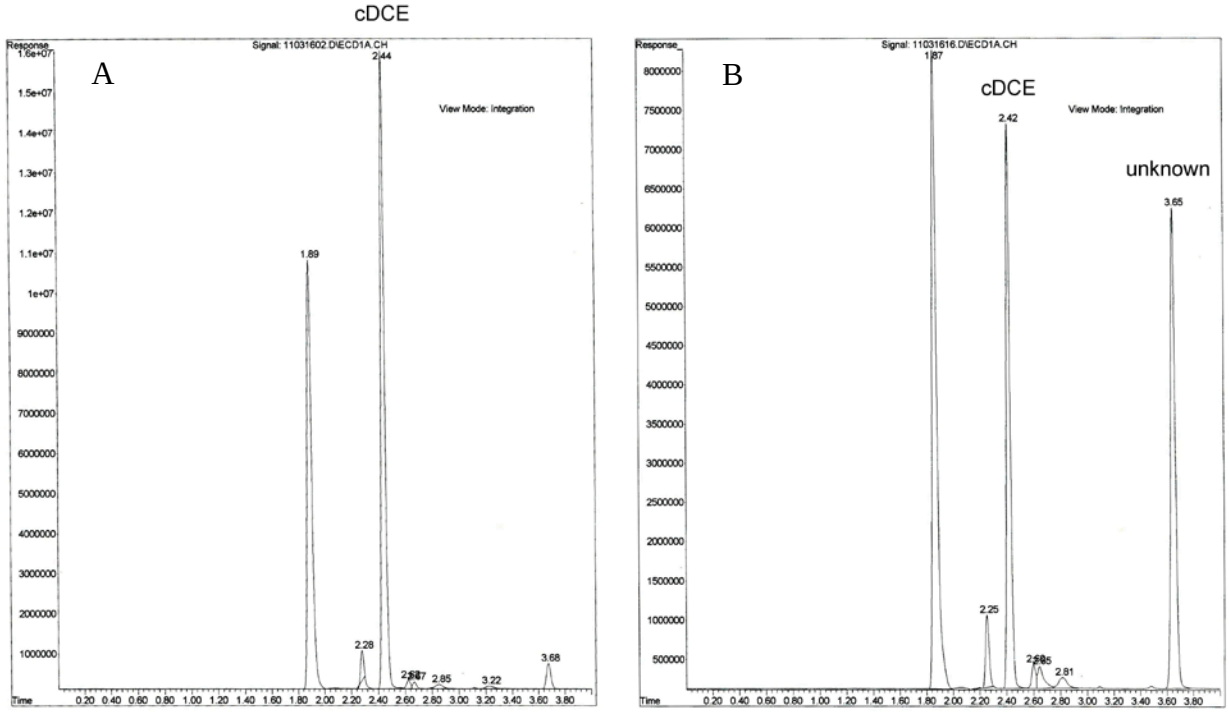

Figure 3-13: A. Initial analysis of headspace of P450 clone provided with cDCE. B. Appearance of the unknown peak accompanying the disappearance of cDCE

Further improvements were made to the growth conditions by the addition of iron and a heme precursor to the cultures during induction (Jansson, Stoilov *et al.*, 2000). We had previously observed that only pinkish cultures were induced, presumably due to the ferredoxin. With the new additives, induced cultures of the clones were much redder, but not more active in cDCE transformation. They do however produce less of the unknown metabolite and much more dichloroacetaldehyde.

Establishing a mass balance between cDCE degradation and dichloroacetaldehyde has been problematic due to lack of a means to quantify the unknown or cDCE epoxide. Although the epoxide can be derivatized to give a blue color, there are no reported extinction coefficients for cDCE epoxide, and extinction coefficients for related epoxides vary greatly among compounds. The transformation of cDCE by the clones is initially rapid with equally rapid production of dichloroacetaldehyde. After a short period, the rate of transformation slows dramatically, along with the production of dichloroacetaldehyde, while the unknown continues to accumulate (Figure 3-14). JS666 also produces the unknown metabolite during degradation of cDCE, but to a much lesser degree than the *E. coli* clones (Figure 3-15). These observations suggest that dichloroacetaldehyde is the true product of cDCE transformation by the P450 and that the unknown might be an artifact caused by the loss of activity of the P450 enzyme.

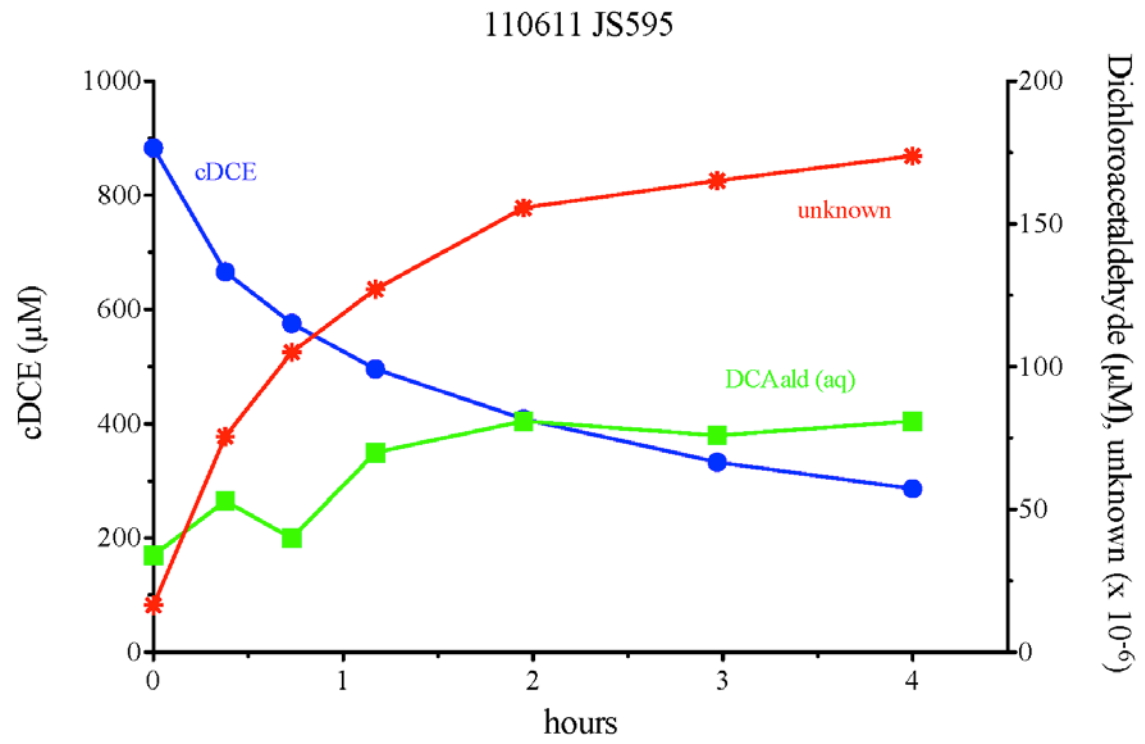

Figure 3-14: Time course of disappearance of cDCE and appearance of unknown in the headspace of a clone expressing P450. Dichloroacetaldehyde was extracted from the aqueous phase.

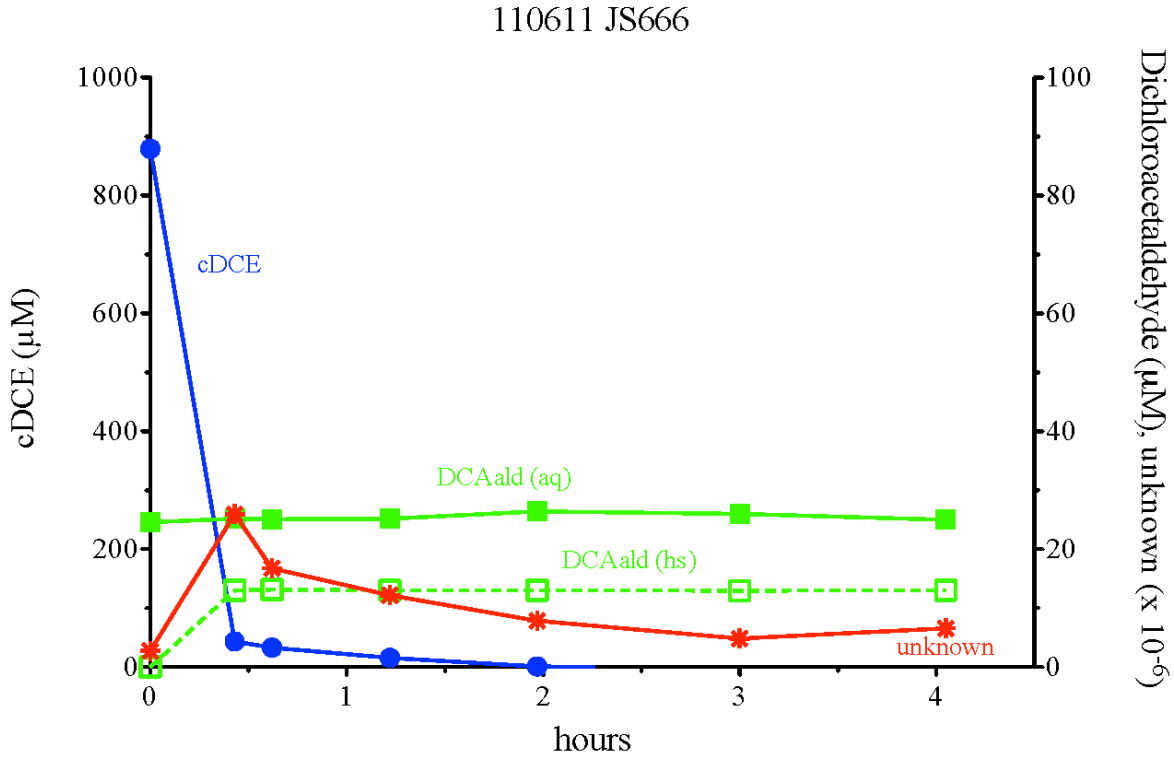

Figure 3-15: Time course of degradation of cDCE by JS666. cDCE was degraded completely with accumulation of trace levels of the unknown.

To establish a mass balance, it is therefore necessary to only consider initial transformation, when the reaction is still rapid and little of the unknown is produced. When there is a headspace present, the cDCE and unknown partition to the headspace while dichloroacetaldehyde partitions to the aqueous phase. The rapidity of the initial transformation renders taking separate samples for aqueous and headspace analyses inaccurate. Accordingly, we developed a no headspace protocol that enabled us to sample cDCE and all its metabolites simultaneously. Of the several extraction solvents examined, only ethyl ether extracted both cDCE and dichloroacetaldehyde quantitatively without interfering with the GC/ECD analysis. However, the analysis was complicated by the lysis of the cells by ether, and the inefficient extraction of dichloroacetaldehyde from the DNA and protein released by lysis.

Nevertheless, preliminary experiments have raised the recovery of dichloroacetaldehyde from 12% in early experiments to 35 to 70% of the cDCE consumed.

chnB *Knockout studies*

Homologous recombination was used to generate a *chnB* knockout (Figure 3-16). The top gel shows results from samples of WT strain and two replicates of *chnB*-negative (KO) strains. Both were positive for the isocitrate lyase (*iso*) gene of JS666. The bottom gel shows that the *chnB*-negative strains contained an amplicon (830bp) of the appropriate size to indicate successful disruption of the intended location.

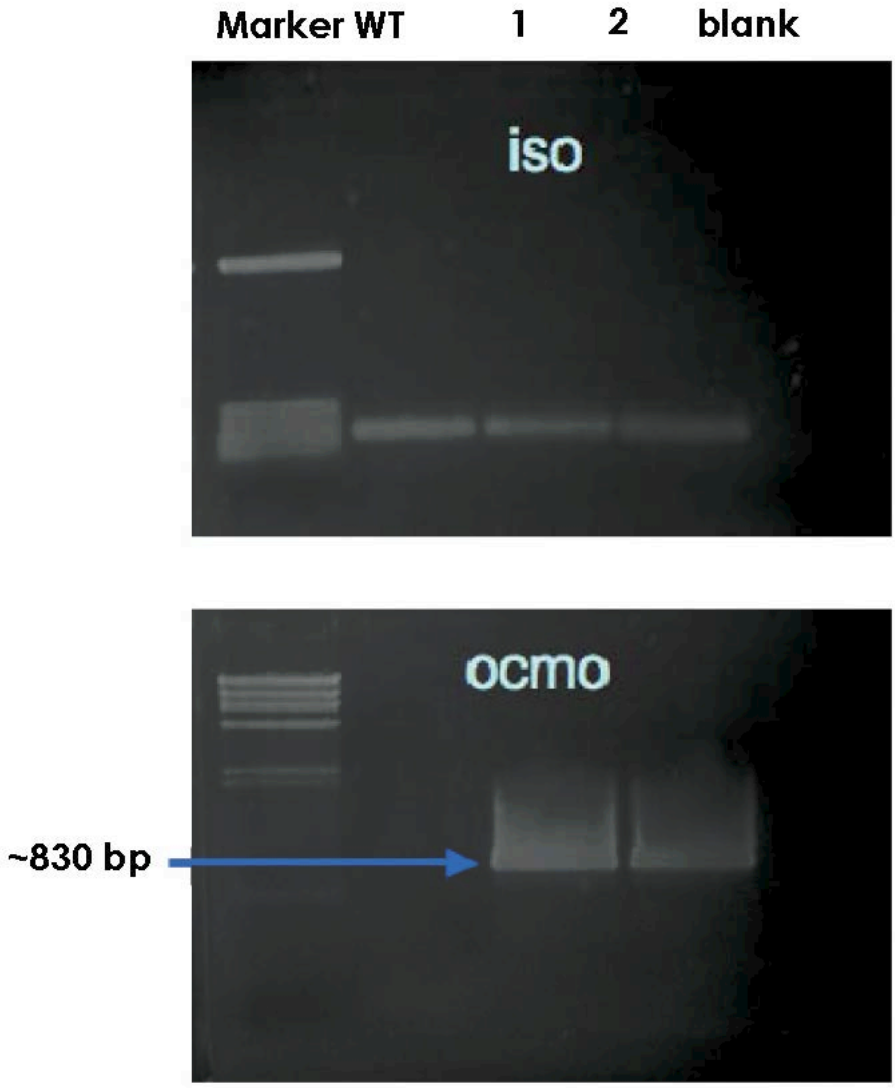

Figure 3-16: Gel results from wild-type strain ("WT" lane) and two *cmo*-negative strains (lanes "1" and "2")

The growth of WT and KO strains on different substrates

The primary purpose of this set of experiments was to ascertain what metabolic capabilities – if any – had been lost in the KO strain, versus the WT strain. Additionally, we hoped: (i) to determine which growth co-substrates might best induce cDCE-degradation; (ii) to investigate the inhibitory effects of cDCE on bacterial growth; and (iii) to determine the extent to which cDCE *degradation* (producing potentially toxic metabolites) matters to observed cDCE toxicity, versus the mere *presence* of cDCE.

Five growth substrates were assayed: acetate (10 mM), succinate (10 mM), CYHX (1 mM), EtOH (10 mM), or CAP (1 mM). The WT cultures grew on all five substrates, and the KO cultures grew only on acetate, succinate, or CAP (Figures 3-5, 3-17 to 3-21). When WT and KO

cultures were grown on acetate, the presence of cDCE had virtually no effect. It did not impact bacterial growth by either strain, nor was cDCE degraded by either (Figure 3-17). While final cell densities were apparently highest in WT cultures at the higher cDCE level, the size of the error bars precludes such a conclusion. In essence, cDCE was irrelevant to strains growing on acetate.

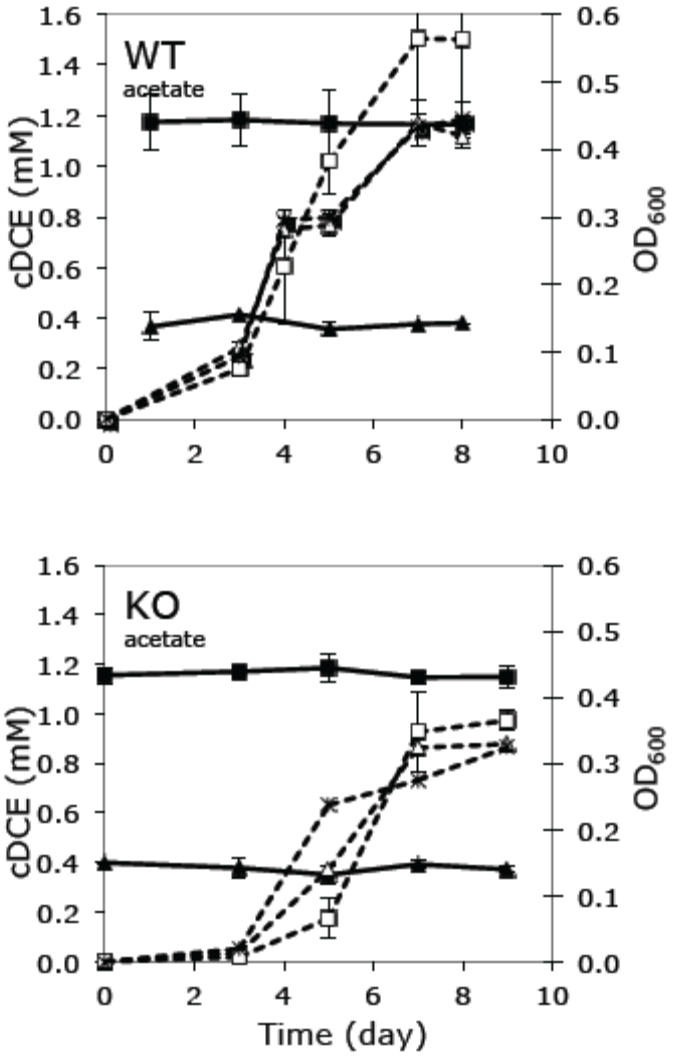

Figure 3-17: Growth of WT and KO strains on MSM and 10mM acetate with or without cDCE. Bars depict standard errors of experimental biological duplicates. Solid lines with closed markers are cDCE, and dotted lines with opened markers are OD_{600}. Cultures were supplied with 132 µmol/bottle cDCE (triangles) or no cDCE (stars).

In contrast, when cultures were growing on succinate, high concentrations of cDCE inhibited growth of both strains. At the higher concentration of cDCE (132 μmol/bottle), minimal growth was observed in WT or KO cultures provided with succinate (Figure 3-18). The WT cultures provided with succinate degraded cDCE degradation at the lower cDCE concentration; however, it was not sustained through further additions of cDCE. This bottle exhibited the "bad behavior" with respect to cDCE degradation often observed with JS666. The observation with succinate-grown WT cultures indicates that high concentrations of cDCE (and/or possibly the presence of cDCE metabolites produced from cDCE oxidation) inhibit growth, although succinate was supplemented in excess (10 mM). We currently have no explanation for the lack of cDCE toxicity in acetate-fed cultures, versus the obvious toxicity observed in succinate-fed cultures. Since cDCE was transformed in succinate-fed WT cultures at the lower cDCE level, it might also have been partially transformed in cultures at the higher cDCE level – at least to an extent that toxic metabolites resulted. However, we have never seen any evidence of cDCE transformation by the KO strain, although it is possible that the KO strain partially metabolizes cDCE to a highly inhibitory intermediate (e.g., an epoxide) that accumulates, yet does not represent a significant loss of the fed level of cDCE. This could occur, for example, if genes involved in steps other than the initial step of cDCE degradation were adversely affected in the KO strain. It is also possible that the explanation lies in some physiological difference between acetate and succinate metabolisms — possibly differences in their transmembrane transport mechanisms that could account for the observations, since high levels of cDCE would likely disrupt membrane function.

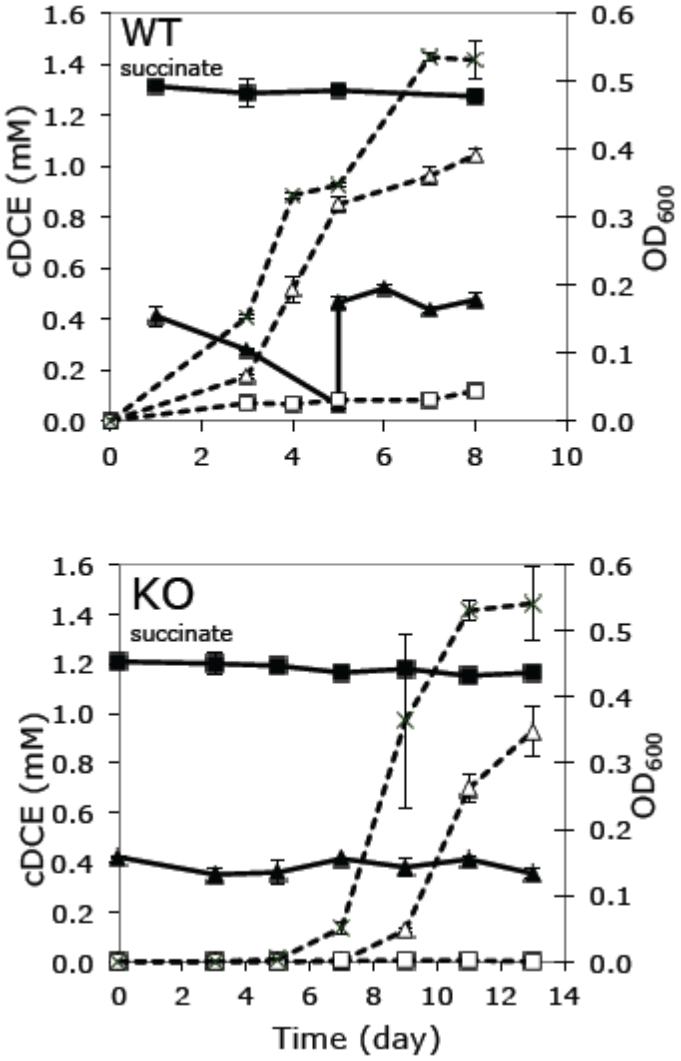

Figure 3-18: Growth of WT and KO strains on MSM and 10 mM succinate with or without cDCE. Bars depict standard erros of experimental biological duplicates. Solid lines with closed markers are cDCE, and dotted lines with opened markers are OD_{600}. Cultures were supplied with 132 µmol/bottle cDCE (squares), 52 µmol/bottle cDCE (triangles) or no cDCE (stars).

Neither CYHX nor EtOH could support growth by the KO strain (Figures 3-19, 3-20); nor was cDCE degraded by the KO strain in these bottles. On the other hand, when WT cultures were provided with CYHX or EtOH as co-substrates, the cells relatively quickly exhibited cDCE degradation and sustained it through multiple additions, even at the higher cDCE level.

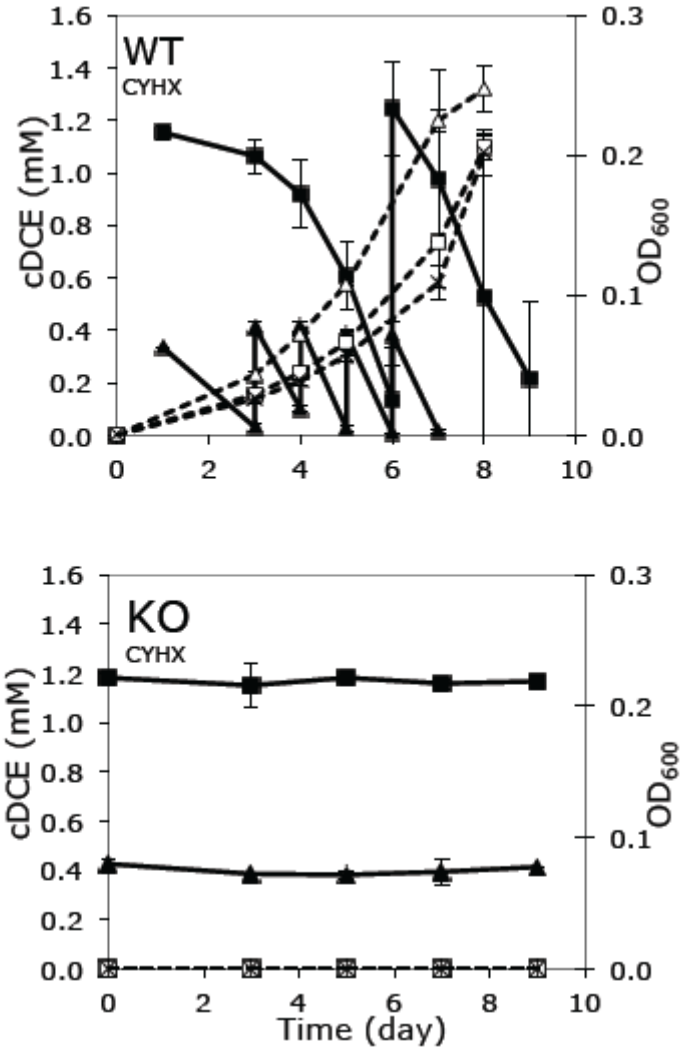

Figure 3-19: Growth of WT and KO strains on MSM and 1 mN CYHX with or without cDCE. Bars depict standard errors of experimental biological duplicates. Solid lines with closed markers are cDCE, and dotted lines with opened markers are OD_{600}. Cultures were supplied with 132 µmol/bottle cDCE (squares), 52 µmol/bottle cDCE (triangles) or no cDCE (stars).

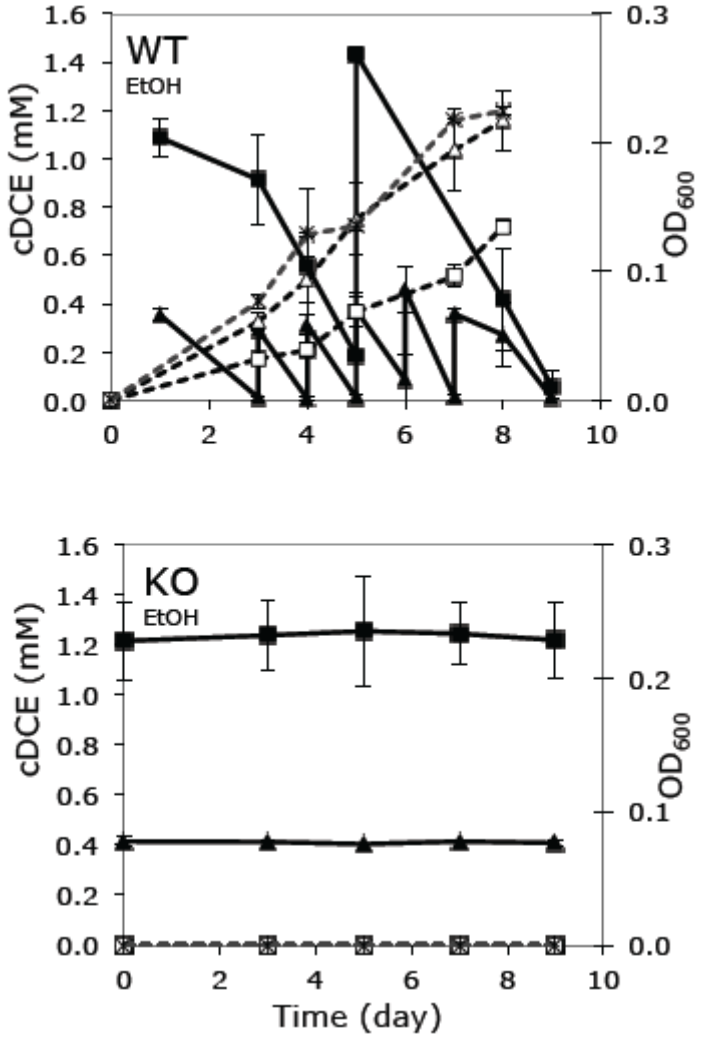

Figure 3-20: Growth of WT and KO strains on MSM and 10 mM EtOH with or without cDCE. Bars depict standard errors of experimental biological duplicates. Solid lines with closed markers are cDCE, and dotted lines with opened markers are $_{OD600}$. Cultures were supplied with 132 µmol/bottle cDCE (squares), 52 µmol/bottle cDCE (triangles) or no cDCE (stars).

WT cultures grown on mixed substrates started degrading cDCE after 6-8 days of incubation when CAP was present (Figure 3-5), whereas degradation of cDCE began after 1-2 days when CYHX or EtOH was present. When cDCE-degradation started, the densities of the WT cultures grown on CAP were higher than those of EtOH or CYHX cultures. The WT cultures grown on CAP and cDCE showed higher final culture density than cultures grown on CAP only, suggesting that cDCE was utilized for bacterial growth. In KO cultures fed CAP, there was no cDCE degradation. Final densities in bottles provided with CAP alone were similar in KO and

WT cultures, but final densities were lower in the KO cultures in presence of cDCE than in absence of cDCE, suggesting inhibition of bacterial growth. The final density for the KO culture amended with the highest amount of cDCE was the lowest among the three, suggesting that high concentrations of cDCE may stress the cells. As there was no evidence of cDCE transformation in the KO cultures, the inhibition caused by cDCE is presumed to be the result of something other than inhibitory metabolites. However, it is difficult to rule such out, because enzymes other than ChnB might be capable of producing inhibitory levels of cDCE metabolites without resulting in a detectable loss of the high, initial cDCE level. Still, there is no basis from these data to support such a hypothesis.

WT and KO cultures were assayed for growth on 1 mM cyclohexanol (Figure 3-21). After a few days the WT culture accumulated 0.04 mM CYHX. After an additional 10 days, the CYHX in the WT culture nearly doubled. No formation of CYHX was observed in the KO culture.

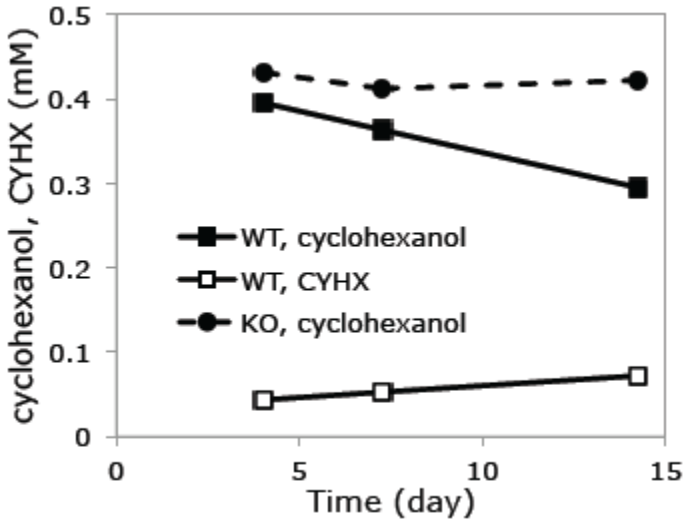

Figure 3-21: Preliminary results for WT and KO cultures tested with 0.5 mM cyclohexanol. Formation of CYHX was detected only in WT culture.

Transformation of other ethenes and of 1,2-dichloroethane

A purpose of the knockout study was to determine whether inactivation of the *chnB* gene would affect the transformation of other ethenes and of DCA. Figure 3-22 shows the transformation of other substrates by WT culture that was grown on CAP in the presence of cDCE. DCA was initially supplied at a nominal concentration of 160 μM which the WT culture immediately transformed. After two additions of DCA, the concentration of DCA added to the WT cultures was increased. Degradation of DCA showed co-metabolic-like (slowed) behavior after a total addition of approximately 75 μmol of DCA. VC was also readily degraded by WT cells. Almost 99% of VC supplied was transformed by WT cells in 21 hours. With a second addition of VC, the rate of VC transformation steadily decreased. Similar results were observed in WT

cultures transforming TCE or ethene. These 50-mL WT cultures reached their maximum transformation capacity after transforming 0.05 μmol of TCE and 2.4 μmol of ethene. The formation of epoxyethane was observed in ethene-fed bottles. The plateau may be due to formation of reactive metabolites, such as epoxides, chlorinated aldehydes and chlorinated acetates that may slow the degradation rates. KO cultures, in contrast, showed no ability to transform any of these compounds.

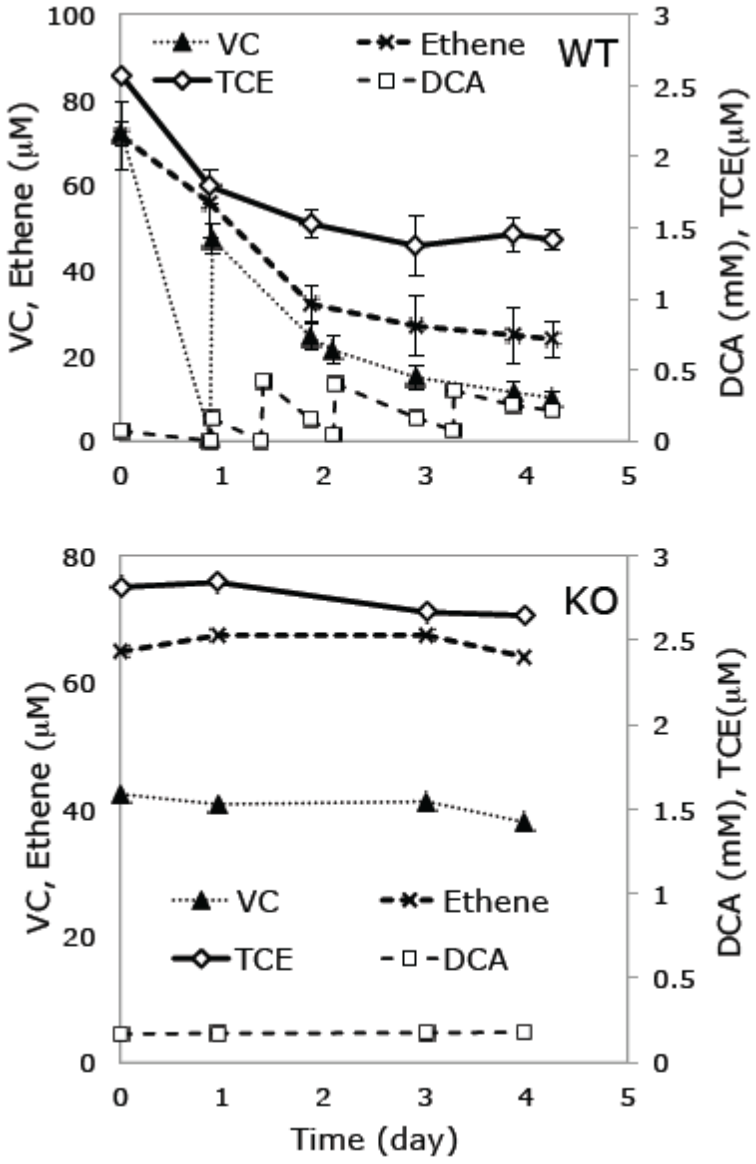

Figure 3-22: Transformation of other ethenes and of DCA by WT and KO cultures. Bars depict standard errors of biological duplicates.

Cloning and characterization of genes in the operon involved in cyclohexanol metabolism.

Four genes in the operon involved in cyclohexanol metabolism were cloned in IPTG-inducible plasmids as individual genes or in tandem (Figures 3-3, 3-4). The constructed plasmids in *E. coli* BL21 Star™ (DE3) cells contained *chnB* (pJMG65, *chnB*), *chnC* (pJMG66, the hydrolase), *chnBC* (pJMG6566, the hydrolase and monooxygenase in tandem), *chnD* (pJMG63, a long-chain dehydrogenase), or *chnAD* (pJMG6364, the short- and long-chain dehydrogenases in tandem). Attempts to amplify the whole operon (approximately 5.0 kbp, including 414 bp upstream of *chnC*) at once using *Pfu* DNA polymerase were unsuccessful. This may be due to the uneven length and GC distribution of forward and reverse primers. The GC content of the operon is similar to that of the whole genome (62%). Enzyme activities were all conducted in whole cells. Both pJMG6566 and pJMG6364 were co-transformed into *E. coli* BL21 Star™ (DE3) cells, carrying ampicillin and kanamycin resistance genes, respectively.

Summary results from enzymatic assays are presented in Table 3-10. We overexpressed ChnB, ChnC, and ChnD enzymes in *E. coli*, and confirmed their previously putative functions. Namely, ChnB converts CYHX to CAP; the hydrolase is active on CAP, and the long-chain dehydrogenase is active on 6-HHA, cyclohexanol, EtOH, and DCAL (though reducing DCAL to DCET, rather than oxidizing it). Activity of the short-chain dehydrogenase could not be distinguished from that of the long-chain dehydrogenase because the short-chain dehydrogenase was expressed only in tandem with its long-chain neighbor, and the tandem had the same activity profile as the long-chain dehydrogenase alone. None of the enzymes showed activity on cDCE, and none showed activity on epoxides above that observed in uninduced controls.

Table 3-10: Summary of substrates tested on different overexpressed enzymes. The study was conducted on whole-cell *E. coli*. (+) indicates an activity was observed, (++) indicates high activity was observed, (-) indicates no activity was observed, and (0) indicates both induced and uninduced cells transformed the substrate. N.T means not tested.

Clones [a]	pJMG63R	pJMG6364	pJMG65R	pJMG66H	pJMG6566	4478
cDCE	N.T.	N.T.	-	N.T.	-	N.T.
cDCE-epoxide	N.T.	N.T.	N.T.	-	-	-
epoxyethane	N.T.	N.T.	N.T.	-	-	-
cyclohexanol	+	+	N.T.	N.T.	N.T.	N.T.
CYHX	N.T.	N.T	++	N.T	++	N.T.
CAP	N.T.	N.T.	N.T.	++	++	N.T.
6-HHA	++	++	N.T.	N.T.	N.T.	N.T.
glycolate	-	N.T	N.T.	N.T.	N.T.	N.T.
styrene	N.T.	N.T.	-	N.T.	-	N.T.
styrene oxide	N.T.	N.T.	N.T.	-	-	N.T.
DCET	-	N.T	-	N.T	N.T	N.T
EtOH	+	+	N.T.	N.T.	N.T.	N.T.
acetaldehyde	0	0	N.T.	N.T.	N.T.	N.T.
DCAL	+	N.T.	0	N.T.	N.T.	N.T.

[a] pJMG63R = alcohol dehydrogenase; pJMG6364 = short-chain dehydrogenase + alcohol dehydrogenase tandem; pJMG65R = CMO; pJMG66H = hydrolase; pJMG6566 = hydrolase + CMO tandem; 4478 = Bpro_4478, chromosomally encoded hydrolase. All constructs were expressed in *E. coli* BL21 Star (DE3).

ChnB enzymatic assay

ChnB (pJMG65) utilized CYHX after 12 hours with production of CAP (Figure 3-23a). In *E. coli* pJMG6566, CYHX was completely transformed, and the lack of CAP accumulation suggests it was immediately hydrolyzed by the hydrolase (ChnC). In a separate experiment, CAP was delivered to *E. coli* pJMG6566 and was completely utilized (presumably by ChnC) within several hours (Figure 3-23b). There was no activity on cDCE in strains containing *chnB* (pJMG65) or *chnC-chnB* (pJMG6566), confirming the study by another research group (Alexander 2010). ChnB also showed no activity towards styrene. Thus, while we successfully cloned a functional ChnB, it showed no activity towards cDCE.

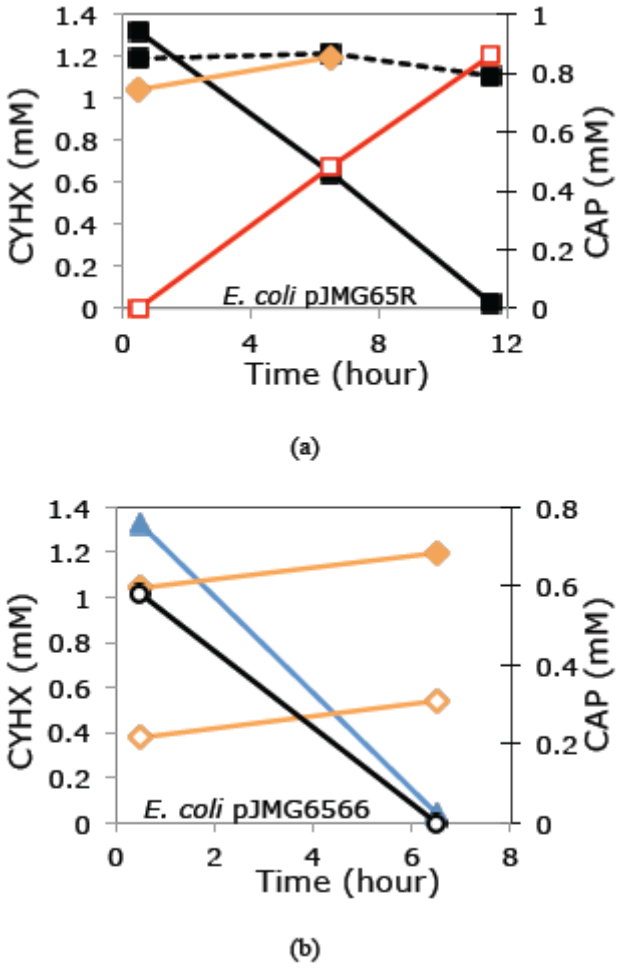

Figure 3-23: Transformation of CYHX and CAP by *E. coli* pJMG65R (CMO) or pJMG6566 (hydrolase and CMO in tandem). (a) The induced *E. coli* pJMG65 cells were given CYHX (-■-) and formation of CAP (-□-) was monitored. Uninduced *E. coli* pJMG65 cells tested with CYHX were used as control (- -■- -). (b) The induced *E. coli* pJMG6566 cells were given CYHX (-▲-) or CAP (-○-). Induced *E. coli* BL21 cells containing no plasmid were given CYHX (-◆-) or CAP (-◇-) as a negative control.

An aldehyde is another possible substrate for ChnB, and perhaps this explains the upregulation of *chnB* by cDCE in JS666. DCAL was reported as one of the major oxidation products of P450 (Shin 2010), and it is possible that DCAL could be converted into DCAA by ChnB. A whole-cell assay was conducted to test this hypothesis; however, interpretation of results was complicated by the rapid transformation of DCAL to DCET by *E. coli* controls.

Hydrolases

Lactone hydrolase catalyzes breakage of the C-O bond, forming hydroxyl acid. A putative 1-oxa-2-oxocycloheptane lactonase (Bpro_5566, ChnC) was postulated to break the C-O bond of CAP,

forming 6-HHA. *E. coli* cells harboring pJMG66h (hydrolase) were assayed with 2 mM of CAP, and the disappearance of the substrate was recorded (Figure 3-24). The induced cells completely utilized CAP within 16 hours of incubation (and perhaps even much earlier, as the CAP was completely depleted by the time of first measurement after the experiment was initiated). The slight reduction of CAP in uninduced cells may due to the leaky T7-promoter in the *E. coli* (DE3) cells after incubating the cells to stationary phase (Novy and Morris 2001).

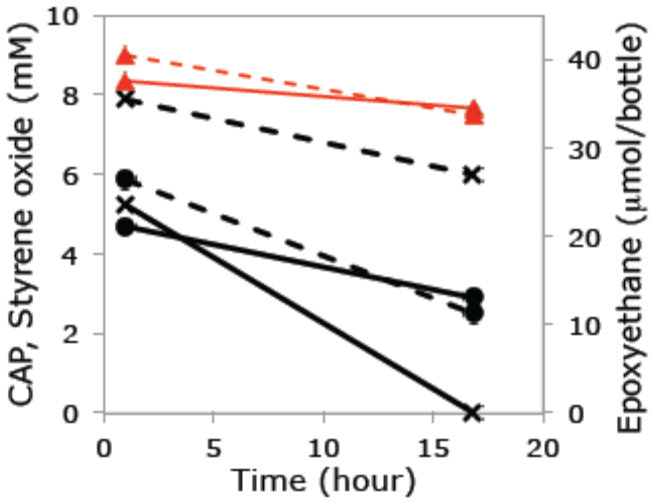

Figure 3-24: *E. coli* pJMG66h (hydrolase) cells subjected to different substrates and conditions: CAP, induced (-x-) and not induced (- - x - -); styrene oxide, induced (-●-) and not induced (- -●- -); epoxyethane, induced (-▲-) and not induced (- -▲- -).

Other substrates tested on *E. coli* expressing the hydrolase (pJMG66H) were epoxyethane and styrene oxide (Figure 3-24), and chemically-synthesized cDCE-epoxide (Figure 3-25). Slight decreases were observed for all substrates in both induced and uninduced *E. coli* cells. Results from whole-cell assays of *E. coli* containing pJMG6566 (hydrolase and monooxygenase, in tandem) with and without 0.1 mM IPTG-induction agreed with the results from the hydrolase only clone. The slow, though significant, disappearance of cDCE-epoxide in both cell cultures suggests abiotic transformation of epoxide.

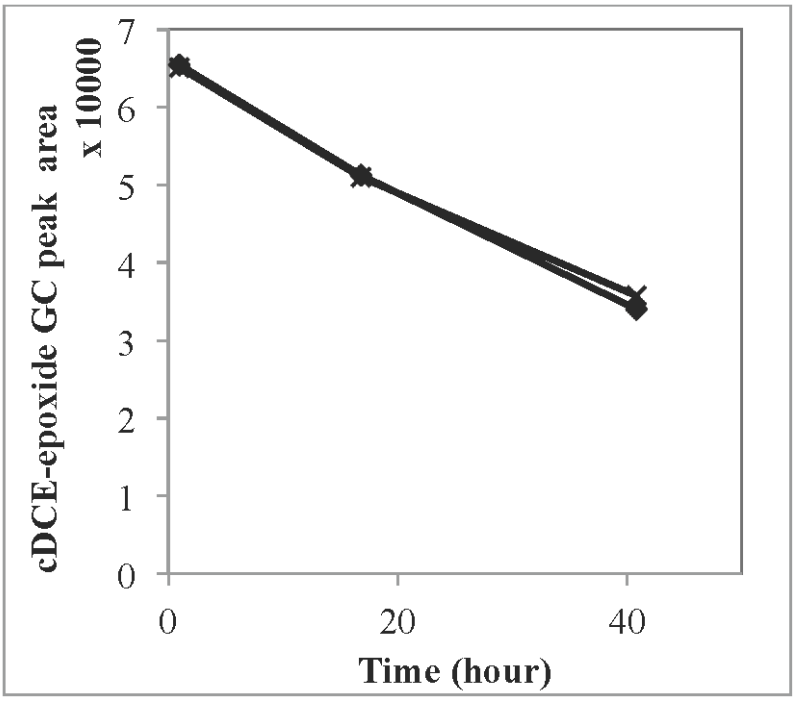

Figure 3-25: *E. coli* pJMG66h cells subjected to different conditions: cDCE-epoxide, induced (◆) and not induced (x).

A chromosomally encoded hydrolase from strain JS666 (Bpro_4478) that has been reported to dehalogenate haloacetates (Chan, Wong *et al.*, 2010) was tested with chemically synthesized cDCE-epoxide. A very slow, steady loss of cDCE-epoxide was observed, with chloride release, in all cultures without regard to hydrolase induction (data not shown).

Thus, while ChnC has demonstrated activity on CAP, the evidence presented here indicates that neither of the two hydrolases has significant activity with any of the epoxides assayed.

Dehydrogenases

Two dehydrogenases are encoded by genes located downstream of *chnB*: a short-chain dehydrogenase (*chnA*, Bpro_5564) and a long-chain, putative alcohol dehydrogenase (*chnD*, Bpro_5563). ChnA shares 39% amino-acid identity with cyclohexanol dehydrogenase from *Acinetobacter* sp. NCIB 9871 that catalyzes the transformation of cyclohexanol to CYHX. ChnD shares 40% amino acid identity with 6-HHA dehydrogenase from strain NCIB 9871. The dehydrogenase assays were conducted in *E. coli* whole-cells containing pJMG6364 (the tandem of the two JS666 dehydrogenases) or pJMG63R (the putative alcohol dehydrogenase) at 23°C. [We were unsuccessful in creating a clone that overexpressed *chnA* alone.] Test substrates included cyclohexanol, EtOH, acetaldehyde, 6-HHA, glycolate, DCAL and DCET.

Cyclohexanol was degraded in *E. coli* cells containing either pJMG6364 or pJMG63R, with both strains transforming approximately 30% of cyclohexanol to CYHX after 2 days (Figure 3-26).

No formation of CYHX was observed in uninduced cells and negative controls (induced and uninduced *E. coli* cells with no plasmids).

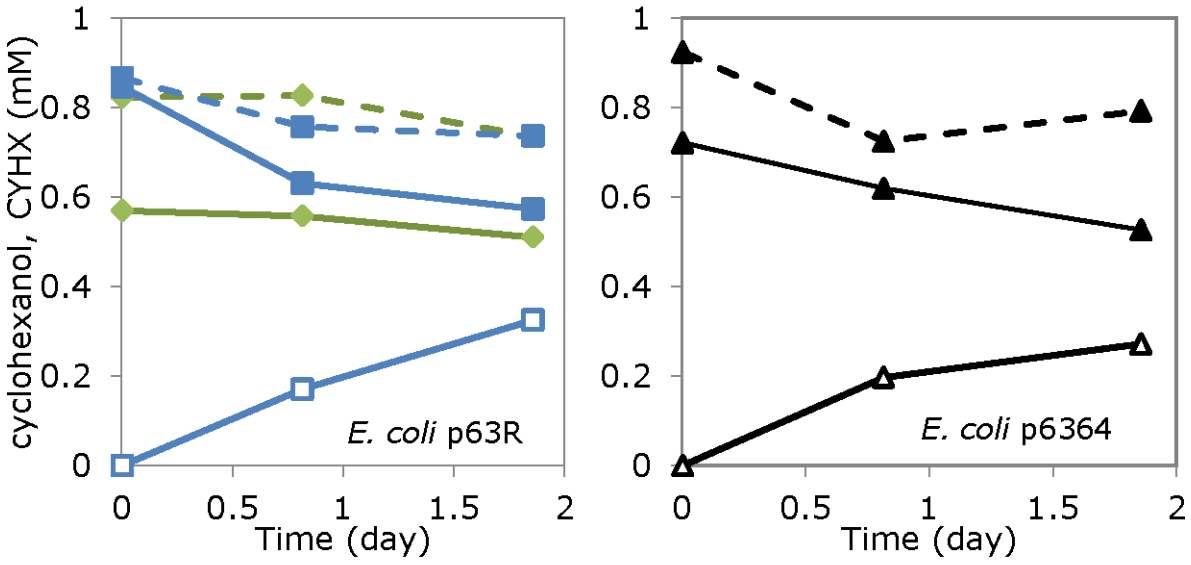

(a) (b)

Figure 3-26: Transformation of cyclohexanol to CYHX by *E. coli* strains containing either pJMG63R (alcohol dehydrogenase) or pJMG6364 (short-chain and alcohol dehydrogenases in tandem). (a) The induced (-■-) and uninduced (- -■- -) *E. coli* pJMG63R cells were given cyclohexanol and the formation of CYHX by induced cells (-□-) was monitored. The induced (-◆-) and uninduced (- -◆- -) *E. coli* cells with no plasmid tested with cyclohexanol were used as negative control. (b) The induced *E. coli* pJMG6364 cells were given cyclohexanol (-▲-) and formation of CYHX by induced cells (-△-) was monitored. Uninduced *E. coli* pJMG6364 cells were used as control (- -▲- -).

6-HHA was also degraded by the induced *E. coli* cells containing either pJMG63R or pJMG6364 (Figure 3-27a). After 20-hour incubation, only 12% and 8% of 6-HHA initial concentration remained in the *E. coli* cells cultures containing pJMG63R and pJMG6364, respectively. No degradation was observed in the uninduced cells and negative controls (*E. coli* with no plasmids). The product (i.e. 6-oxohexanoate) is not commercially available for chromatography peak identification and according to Brzostowicz and coworkers (2002), 6-oxohexanoate was spontaneously oxidized to adipate. When all *E. coli* cultures were tested with glycolate (an α-hydroxy acid), no apparent degradation was observed (Figure 3-27b).

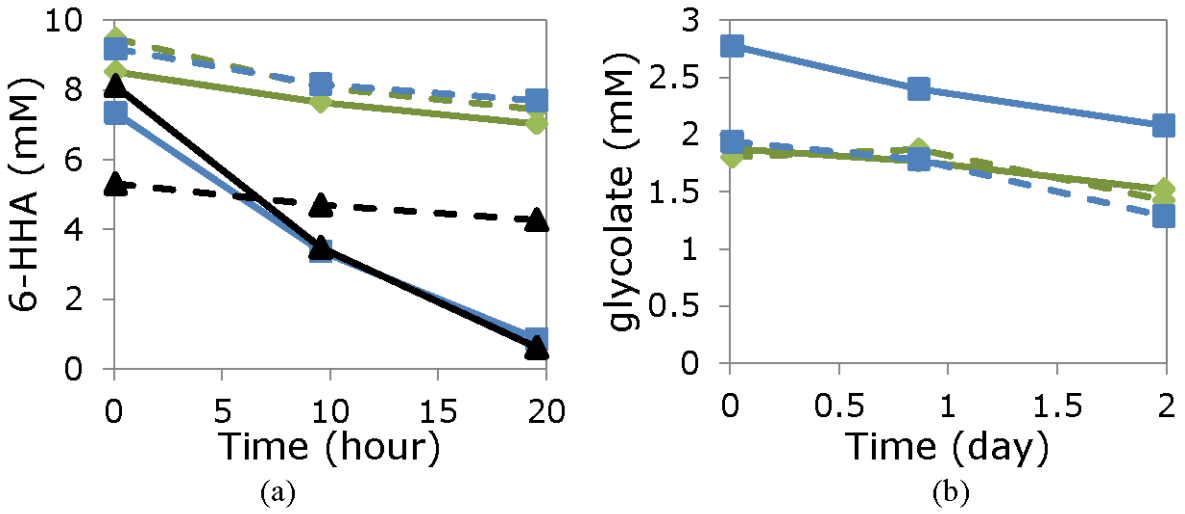

Figure 3-27: Enzymatic assays by whole-cell *E. coli* containing pJMG63R (alcohol dehydrogenase) or pJMG6364 (short-chain and alcohol dehydrogenases in tandem), tested with (a) 6-HHA and (b) glycolate. Blue lines and squares (■) represents *E. coli* pJMG63R cells and black lines and triangles (▲) represents *E. coli* pJMG6364 cells. The IPTG-induced cells are represented by solid lines, and uninduced cells by dashed lines. IPTG-induced (-◆-) and uninduced (- -◆- -) *E. coli* BL21 cells were used as negative controls.

EtOH was assayed with these two dehydrogenases, and the production of acetaldehyde monitored. The cells were incubated with EtOH for approximately 10 hours and acetaldehyde was detected in all cultures (Figure 3-28). The induced cells containing pJMG63R or pJMG6364 produced higher amounts of acetaldehyde than the rest of the cell cultures. *E. coli* pJMG63R and pJMG6364 cells produced 1.5 mM and 1.6 mM acetaldehyde, respectively, after 3 hours of incubation. The cultures were then left for an additional 6.5 hours, and the final concentration of acetaldehyde produced by *E. coli* pJMG63R cells was 3.2 mM, while with *E. coli* pJMG6364, the production remained constant. In acetaldehyde assays, all *E. coli* cultures immediately reduced it to EtOH with no distinction between induced and uninduced cell cultures or the negative controls (data not shown).

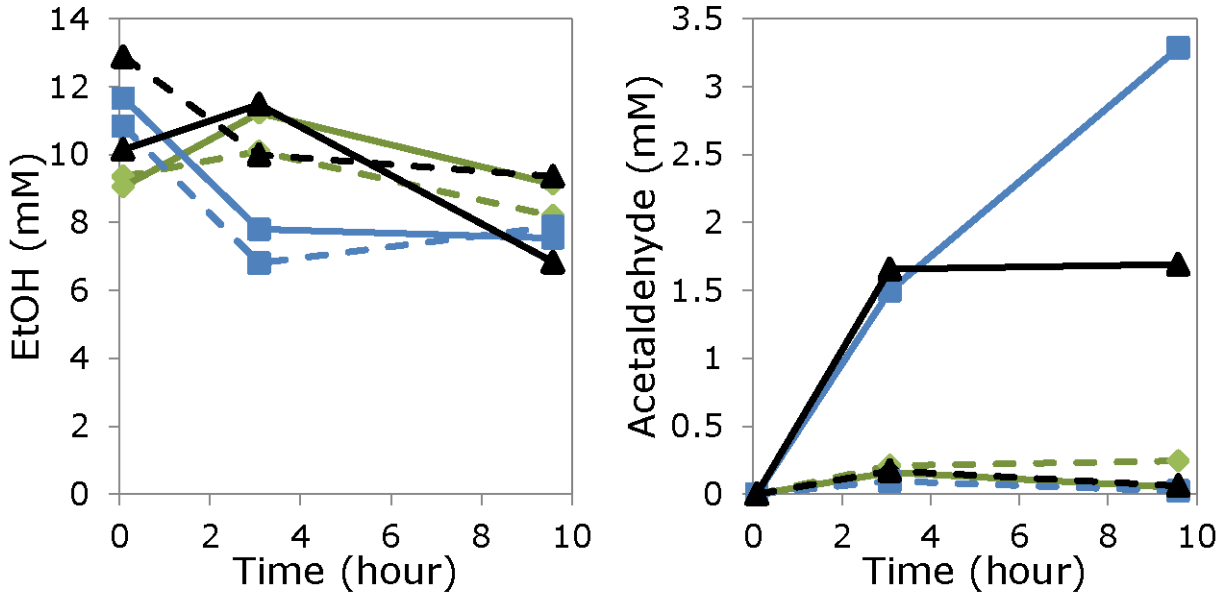

Figure 3-28: Production of acetaldehyde in whole-cell *E. coli* cultures containing pJMG63R (alcohol dehydrogenase) or pJMG6364 (short-chain and alcohol dehydrogenases in tandem) that were assayed with EtOH. Blue line and squares (■) represents *E. coli* pJMG63R cells and black lines and triangles (▲) represents *E. coli* p6364 cells. The IPTG-induced cells are represented by solid lines, and uninduced cells by dashed lines. IPTG-induced (-◆-) and uninduced (- -◆- -) *E. coli* BL21 cells were used as negative controls.

Transformation of DCAL to DCET was observed in induced *E. coli* pJMG63R cultures (Figure 3-29). Initial concentration of DCAL supplied to the induced *E. coli* pJMG63R cells was 5.3 mM, and approximately 4.2 mM of DCET was measured after 20 hours of incubation. The loss of mass balance may be due to the inconsistent Et_2O extractions and different sensitivities of DCAL vs. DCET GC peaks. DCET gives a higher peak area than from the equivalent concentration of DCAL, thus making DCET easier to quantify at lower concentration. When the cells were assayed with DCET, the formation of DCAL was not observed. It could be that the kinetic equilibrium of the reversible dehydrogenase strongly favors the alcohol over the aldehyde, as was the case with acetaldehyde assays.

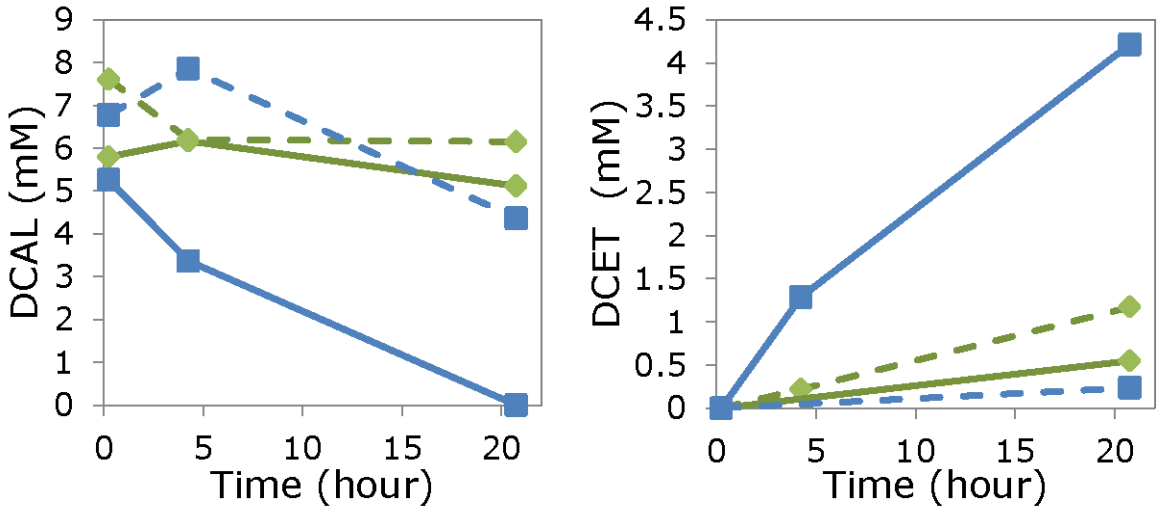

Figure 3-29: Transformation of DCAL to DCET in whole-cell *E. coli* containing pJMG63R (alcohol dehydrogenase) that have been IPTG-induced (-■-) and not induced (- -■- -). IPTG-induced *E. coli* BL21 cells were used as blank controls (-◆-) and uninduced cells (- -◆- -) were used as negative controls.

Proteome changes in WT and KO cultures, as assessed using iTRAQ

Both WT and KO cultures were grown in CAP with the presence or absence of cDCE. The concentrations of these compounds were monitored, and the cells were harvested, extracted, trypsin-digested, and iTRAQ-labeled when the cultures were actively degrading CAP and/or cDCE. The peptides from the four culture-types were labeled with reporter groups as follows:

- 114.1 (WT on cDCE + CAP);
- 115.1 (WT on CAP only);
- 116.1 (KO on cDCE + CAP); and
- 117.1 (KO on CAP only).

There were 1302 proteins identified, based on 5627 peptides using the Mascot program for all four samples. Detailed results are presented in Appendix A-2. More than 60% of the total proteome identified consisted of acidic proteins. Intensities of the reporter ions from iTRAQ tags upon fragmentation were used for quantification, and the relative quantitation ratios were normalized to the median ratio for the 4-plex in each set of experiments. The amounts of RNA polymerase were around the same throughout the four samples, inferring that the levels of housekeeping proteins, involved in the basic functioning of the cells, were similar (Table 3-11).

Table 3-11: Ratios of selected proteins identified in iTRAQ study

Locus Tag	Protein Description	115/114	116/114	117/114
Bpro_5301	P450	1.587	0.180	0.370
Bpro_5566	α/β hydrolase fold-containing protein, ChnC	10.493	0.282	0.485
Bpro_5565	ChnB	2.994	0.140	0.148
Bpro_5563	zinc-binding alcohol dehydrogenase	0.770	0.100	0.139
Bpro_5186	HAD, type II	0.155	0.142	0.150
Bpro_0056	HAD, type II	0.804	0.651	0.828
Bpro_2101	isocitrate lyase	2.494	2.114	2.177
Bpro_0645	GST	0.724	0.017	0.024
Bpro_0646	PNPox-related protein	1.165	0.450	0.401
Bpro_4442	RNA polymerase subunit beta, RpoB	1.088	0.949	0.909
Bpro_0086	2,5-dioxopentanoate dehydrogenase, ChnE	0.738	0.702	0.654
Bpro_4478	α/β hydrolase fold-containing protein	0.507	0.806	1.033
Bpro_4561	glyoxylate carboligase	0.293	0.335	0.335
Bpro_4563	2-hydroxy-3-oxopropionate reductase	0.239	0.051	0.060

In this iTRAQ report, a ratio for the 115/114 groups that is less than one (WT cultures grown in CAP vs. grown in cDCE+CAP) implies that the presence of the tagged protein is correlated to cDCE-degradation (or at least to its presence in the culture). Examination of the ratio for the 116/114 groups (WT grown on cDCE+CAP vs. KO grown on cDCE+CAP) helps to separate the effects of mere presence of cDCE (in KO) from the effects of actual cDCE degradation (in WT).

The principal objective of the iTRAQ study was to determine whether knock out of *chnB* affected translation of adjacent genes. That is, did insertion of the vector sequence within *chnB* affect only the production of ChnB protein? Results show that peptides from all genes of the cyclohexanol operon were detected at significant levels in both WT and KO strains, with the exception of the short-chain dehydrogenase (ChnA), which was not detected in any of the four culture samples (WT or KO). Five peptides associated with ChnB that are upstream and downstream of the plasmid insertion point were identified in KO cultures, and two of them yielded weak spectra or negative intensities. ChnB peptide fragments in the KO culture are not

unexpected, since there is no stop codon to prevent transcription, though a functional ChnB should not result.

For the genes adjacent to *chnB*, the abundance of peptides from the upstream hydrolase (Bpro_5566, ChnC) were reduced in KO cultures to 28% and 25% of the abundance in corresponding WT cultures (i.e., iTRAQ ratios from labels 116/114 and 117/115). On the other hand, abundance of peptides encoded by *chnB* (Bpro_5565) was reduced in KO cultures to only 14% and 5% of abundance in corresponding WT cultures. Five peptides in KO samples were attributed to the downstream alcohol dehydrogenase (Bpro_5563, ChnD). Abundance of peptides from chnD were reduced in KO cultures to 10% and 18% of abundance in corresponding WT cultures. The relative levels suggest that translation of genes downstream of the insert were affected more than translation of the upstream hydrolase. While proteome data corresponding to the short-chain dehydrogenase (*chnA*) is lacking, the intermediate position of *chnA* between *chnB* and *chnD* would predict similar reduced abundance levels.

Since the KO strain is capable of growth on CAP, the 70-75% reduction in abundance of the hydrolase (Bpro_5566, ChnC), which was shown in enzyme assays to be active on CAP, is either insufficient to cause deleterious effect on growth, or else there are other hydrolases in JS666 that serve this same purpose. On the other hand, the approximately 80-90% reduction in abundance of the alcohol dehydrogenase (Bpro_5563, ChnD) in the KO strain appears to exert a much greater effect, since the KO strain cannot grow on EtOH. Of course, peptide abundance does not tell the whole story; protein conformation matters, and the proteomics results do not address this potentially important factor. In the end, what we know is that *chnB* was knocked out, and downstream translation of the alcohol dehydrogenase (and by deduction, the short-chain dehydrogenase also) was reduced.

Jennings *et al.* (Jennings, Chartrand *et al.* 2009) identified proteins elevated by cDCE (Table 3-7), including GST-like protein (Bpro_0645), Type II HAD (Bpro_5186), 2-hydroxy-3-oxopropionate reductase (Bpro_4563) and glyoxylate carboligase (Bpro_4561). Jennings *et al.* also reported cDCE-induced transcripts, such as *chnB* (Bpro_5565), hydrolase (encoded by Bpro_5566), P450 (Bpro_5301), ABC transporters and several hypothetical proteins (Table 3-6). Our iTRAQ results (Table 3-11) generally are in accord with these previous studies.

There were higher protein levels of P450 in cDCE-degrading WT cells than in both KO strains; however, protein levels were 60% higher in CAP-grown WT cultures. The lower abundance of P450 in cDCE-degrading cells, versus CAP-only WT cells may be due to inactivation of the protein as a result of covalent-binding of the cDCE-intermediates to the heme-containing proteins (Costa and Ivanetich 1982).

Most noteworthy is the much higher abundance (i.e., low ratios 115/114, 116/114, and 117/114) of HAD (Bpro_5186) protein in WT cultures degrading cDCE than in any of the other cultures. As will be shown later (Section 3.2), HAD expression appears to correlate well with cDCE degradation and will therefore be proposed as a marker for cDCE degradation in JS666.

GST (Bpro_0645) abundance was elevated in WT cultures, compared with levels in KO cultures, with abundance about 40% higher in CAP+cDCE-degrading WT culture than in CAP-only WT culture.

The presence of chlorinated alcohols and alkanals (aldehydes) resulting from cDCE degradation might be expected to affect the abundances of several alcohol and aldehyde dehydrogenases. iTRAQ results for several are presented in Table 3-12. When comparing cDCE-degrading WT cultures and cDCE-exposed KO cells (116/114), a ratio that is less than 1 suggests that the protein expression levels were elevated by the presence of cDCE-metabolites and not by just the presence of cDCE. Aldehyde dehydrogenases may be involved in the conversion of DCAL to DCAA (Sharpe and Carter 1993), and based on the iTRAQ data, proteins encoded by Bpro_3952 and Bpro_2298 are candidates. The Bpro_2298 encoded protein shares 24% amino acid identity with ChnE from strain NCIMB9871.

Table 3-12: Ratio of aldehyde and alcohol dehydrogenases from iTRAQ study

Locus Tag	Protein Description	115/114	116/114	117/114
Bpro_3952	**aldehyde dehydrogenase**	**0.385**	**0.055**	**0.081**
Bpro_2290	aldehyde dehydrogenase	1.141	1.057	1.061
Bpro_3422	aldehyde dehydrogenase	1.379	1.038	1.014
Bpro_4691	aldehyde dehydrogenase	0.849	1.334	1.329
Bpro_2298	**aldehyde dehydrogenase**	**0.824**	**0.828**	**0.854**
Bpro_4702	aldehyde dehydrogenase	0.934	1.377	1.655
Bpro_3129	zinc-binding alcohol dehydrogenase	0.387	0.906	0.757
Bpro_2526	iron-containing alcohol dehydrogenase	0.546	0.834	1.081
Bpro_0360	zinc-binding alcohol dehydrogenase	0.735	1.176	1.132
Bpro_5563	**zinc-binding alcohol dehydrogenase chnD**	**0.770**	**0.100**	**0.139**
Bpro_3853	zinc-binding alcohol dehydrogenase	0.800	1.907	1.987
Bpro_3259	zinc-binding alcohol dehydrogenase	0.806	0.710	0.789
Bpro_2634	zinc-binding alcohol dehydrogenase	1.122	5.900	5.295
Bpro_4700	iron-containing alcohol dehydrogenase	1.129	1.604	1.857
Bpro_2565	zinc-binding alcohol dehydrogenase	1.536	1.400	1.438
Bpro_3062	zinc-containing alcohol dehydrogenase	2.949	1.519	1.545
Bpro_2135	zinc-binding alcohol dehydrogenase	3.422	0.901	0.859

The levels of the alcohol dehydrogenase encoded by Bpro_5563 was elevated by cDCE-metabolites (Table 3-12). Alcohol dehydrogenases may catalyze the interconversion of DCET and DCAL. The transformation of chloral hydrate to trichloroethanol by alcohol dehydrogenases has been reported in many studies (Friedman and Cooper ,1960; Newman and Wackett, 1991; Forkert, Baldwin *et al.*, 2005); nevertheless the exact functions of the aldehyde reduction during degradation of chlorinated ethene compounds were not elaborated. An ortholog of an alcohol dehydrogenase (Bpro_3129) is *S*-(hydroxymethyl)glutathione dehydrogenase, which catalyzes the conversion of *S*-hydroxymethyl glutathione (GS-CH_2OH) to *S*-formyl glutathione (GS-CHO). The protein encoded by Bpro_3129 was elevated in abundance in WT cells degrading CAP+cDCE, versus WT cells degrading CAP only (115/114).

WT cultures degrading both cDCE and CAP produced up to 4-fold 2-hydroxy-3-oxopropionate reductase and glyoxylate carboligase than WT degrading CAP only (Table 3-13). The enzymes catalyze the two-step conversion of glyoxylate to D-glycerate (Figure 3-30). The transformation of glyoxal into glycolate can be catalyzed by glyoxalase I (encoded by *gloA*) and hydroxyacyl glutathione hydrolase (encoded by *gloB*), which were both modestly elevated in WT degrading cDCE+CAP vs. WT degrading CAP only. The elevated abundance of glyoxalase I was observed in an *E. coli* strain overexpressing monooxygenase and hydrolase (Lee, Cao *et al.* 2006). The primary function of glyoxalase I is the conversion of methylglyoxal into D-lactate. Our result confirmed the hypothesis that cDCE-epoxide hydrolysis leads to formation of glyoxal (Rui, Cao *et al.* 2004; Lee, Hiibel *et al.* 2010). A D-2-hydroxyacid dehydrogenase (Bpro_4156, EC: 1.1.1.81) catalyzes the conversion of D-glycerate to hydroxypyruvate and interconversion of glycolate and glyoxylate.

Table 3-13: Proteins involved in proposed glyoxal transformation pathway

Locus Tag	Protein Description	115/114	116/114	117/114
Bpro_0187	glycolate oxidase FAD binding subunit	1.153	1.757	1.404
Bpro_4561	glyoxylate carboligase	0.293	0.335	0.335
Bpro_4563	2-hydroxy-3-oxopropionate reductase	0.239	0.051	0.060
Bpro_4562	hydroxypyruvate isomerase	0.009	0.059	0.053
Bpro_3549	glyoxalase I	0.830	0.524	0.637
Bpro_2055	hydroxyacyl glutathione hydrolase	0.785	1.162	1.065
Bpro_4156	D-2-hydroxyacid dehydrogenase, NAD-binding	0.861	0.982	1.052

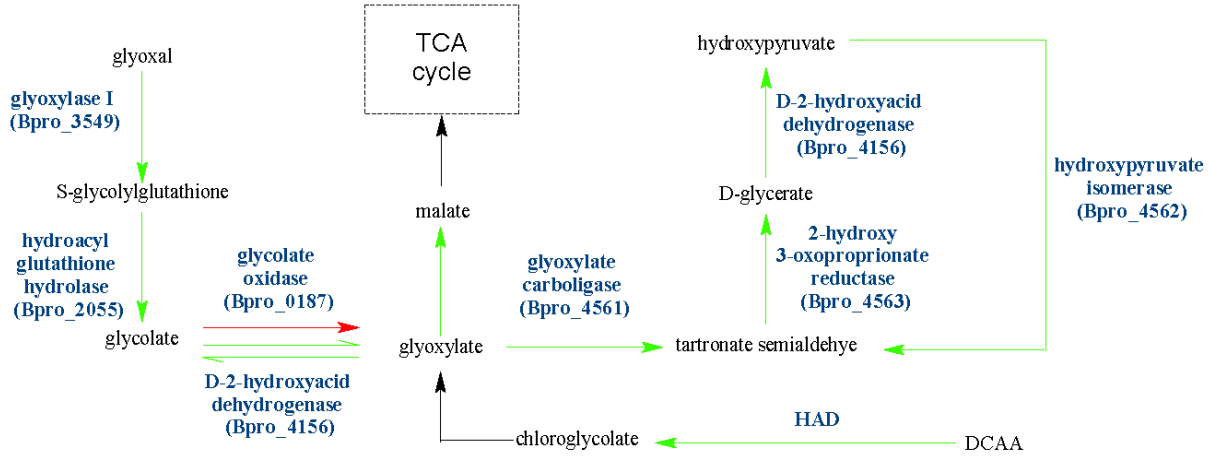

Figure 3-30: Pathways involved in glyoxylate transformation. Green and red arrows indicate protein abundances elevated and reduced, respectively, by cDCE in WT cultures.

As a quality control, we looked for proteins expected from genes present in the KO insert. Kanamycin was not added in the second transfer to avoid the expression of stress-related proteins due to the presence of kanamycin instead of cDCE. Despite this, the abundance of kanamycin-resistance protein (neomycin phosphotransferase) was elevated in both KO cultures (Appendix A-2). Another protein associated with the insert that was seen in only the KO cultures was the OriT binding protein (Appendix A-2). No formation of LacZ was reported, consistent with the sequence results because of a one-nucleotide addition in the insert.

From iTRAQ data and RT-PCR work (Figure 3-31), it can be judged that there was insignificant cross-contamination among the samples. WT is kanamycin-sensitive and KO was initially grown in media containing kanamycin. Kanamycin resistance in the KO strains is catalyzed by neomycin phosphotransferase. This protein was identified by one peptide and its MS/MS intensity peaks were 6772, 944, 79372 and 32096 for 114, 115, 116 and 117, respectively. The presence of small peaks in the 114 and 115 samples of neomycin phosphotransferase may be due to background noise and impurities of iTRAQ reagents (Wiese, Reidegeld *et al.* 2007) or minimal percentage error of impurities even after correction. The iTRAQ report shows ChnB protein was reduced almost 7-fold in KO cultures compared to WT cultures (Table 3-11). Furthermore, based on RT-PCR work, where primers were designed to target the intact region of the native *chnB* before and after the KO insertion point, intact *chnB* amplicons were not seen in KO samples even after 35 cycles. The detection limit of the gel is approximately 10 ng as indicated by the marker at 564 bp. Alcohol dehydrogenase (*chnD*), a gene in the same operon, was 10-fold lower in KO cultures vs. cDCE-degrading WT cultures; nevertheless RT-PCR work shows *chnD* amplicons in all samples (30 and 35 cycles).

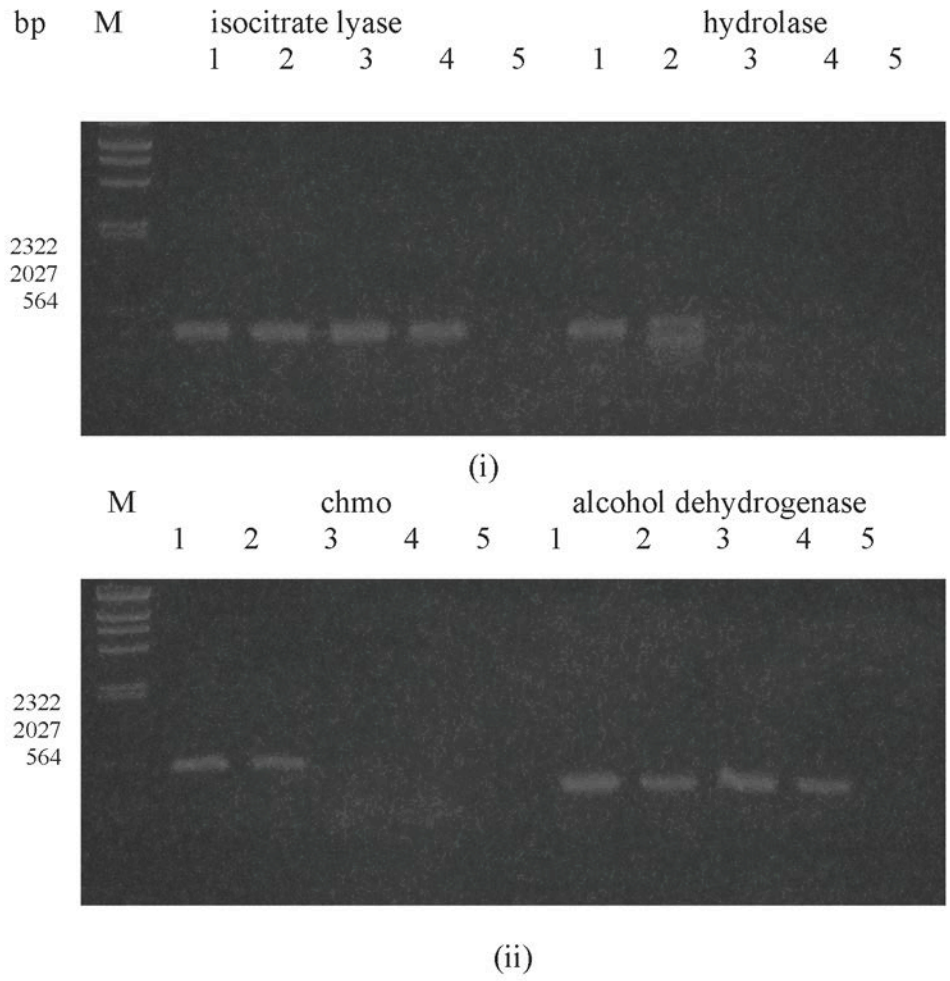

Figure 3-31: RT-PCR of 35 cycles using 300 ng of cDNA template and corresponding primer pairs for WT and KO cultures grown for iTRAQ study. cDNA was synthesized with a mixture of gene-specific reverse primers. M: Lambda DNA/HindIII marker; 1: WT grown in CAP and cDCE; 2: WT grown in CAP; 3: KO grown in CAP and cDCE; 4: KO grown in CAP; 5: water blank.

In Figure 3-31, multiple amplicons were observed in lane 2 (hydrolase) with 35-cycle but not with 30-cycle RT-PCR (data not shown). This implies that there were unintentional priming sites or high levels of *chnD* transcripts. The proteome level of hydrolase in CAP-grown WT cultures was 10-fold higher than in cultures grown on cDCE and CAP. The absence of hydrolase amplicons from KO strains in RT-PCR but detectable protein in iTRAQ may be due to lack of correlation between transcripts and proteins. mRNA in bacteria degrades rapidly (within minutes) whereas proteins can survive much longer (Taniguchi, Choi *et al.* 2010). The additional sequence of the insert in the polycistronic mRNA may hinder the formation of secondary structure of original mRNA at the 5'-end, thus limiting its stability, which leaves mRNA open for endoribonuclease E attack (Rauhut and Klug 1999). The *chnC* (hydrolase) gene

transcript is at the 5'-terminal of the polycistronic mRNA, followed by the transcript from the *chnB* gene.

In summary, the iTRAQ studies confirmed that the genes flanking the *chnB* in the KO strain were translating proteins, though protein abundance was reduced about four-fold for the upstream hydrolase (ChnC), and about ten-fold for fragments of the compromised ChnB and a downstream alcohol dehydrogenase (ChnD). We presume that translation of a short-chain dehydrogenase (ChnA) -- encoded at a position between *chnB* and *chnD* -- is similarly, highly affected. It is possible that this significant reduction in translation of the dehydrogenase genes downstream of the *chnB* KO might be more responsible for loss of the KO's ability to degrade cDCE and EtOH than is the loss of the functional ChnB itself.

3.1.5 Conclusions and Implications for Future Research / Implementation

cDCE Degradation Pathway (Figure 3-32)

Several lines of evidence suggest that cytochrome P450 catalyzes the initial steps of cDCE degradation: 1) cDCE-grown cells of JS666 degrade cDCE and DCA simultaneously, 2) oxygen is required for degradation, 3) degradation is inhibited by cytochrome P450 inhibitors, 4) an *E. coli* clone containing the cytochrome P450 (Bpro_5299-5301) from JS666 transformed cDCE, and 5) extracts of the *E. coli* clone converted cDCE to dichloroacetaldehyde, cDCE epoxide and an unknown metabolite. The subsequent pathway for degradation of dichloroacetaldehyde was confirmed by the following lines of evidence: 1) enzyme assays in cell extracts, 2) dynamic expression of HAD transcripts.

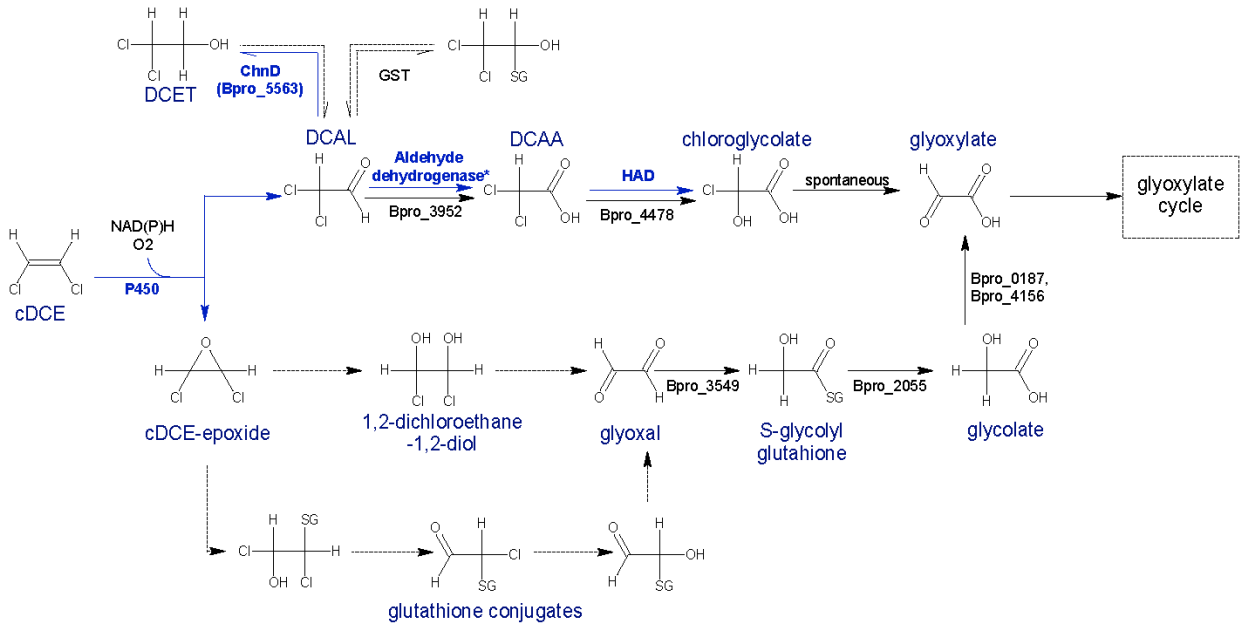

Figure 3-32: cDCE-degradation pathway(s) in strain JS666. ChnD (Bpro_5563): zinc-binding alcohol dehydrogenase; Bpro_3952: aldehyde dehydrogenase; Bpro_4478: 1-oxa-2-oxocycloheptane lactonase; Bpro_3549: glyoxylase I; Bpro_2055: hydroxyacylglutathione hydrolase (glyoxylase II); Bpro_0187: glycolate oxidase; Bpro_4156: D-2-hydroxyacid dehydrogenase. Blue arrows indicate pathways that have been confirmed biochemically. Black arrows indicate pathways that are supported by iTRAQ study. Dotted arrows indicate proposed but as yet unconfirmed transformations.

The cytochrome P450 also catalyzes the initial reactions in DCA degradation. The pathway for the aerobic oxidation of cDCE by *Polaromonas* JS666 appears to converge with the pathway for the aerobic oxidation of DCA by the well-characterized DCA degrading bacteria *Xanthobacter autotrophicus* GJ10 (Janssen, Pries, *et al.*, 1989) and *Pseudomonas* sp. DCA1 (Hage and Hartmans, 1999). *dhlA*, the gene that encodes the enzyme that catalyzes the first step in the DCA pathway in GJ10 via hydrolytic dehalogenation to an alcohol has no homolog in JS666. The gene that encodes the initial enzyme in the monooxygenase mediated pathway of DCA1 has never been identified. The cytochrome P450 from JS666 is thus the first oxygenase that catalyzes DCA degradation for which the genes have been identified and expressed.

The enzyme assays support the hypothesis that chloroacetaldehyde from cDCE is oxidized by a constitutive and highly active chloroacetaldehyde dehydrogenase to chloroacetic acids. Chloroacetic acid is then hydrolytically dehalogenated to produce glycolate. Glycolate is likely oxidized by a flavoprotein glycolate oxidase, and enters central metabolism at the level of glyoxalate.

Gene and protein expression studies revealed a number of genes that are upregulated in cDCE-grown cells compared to glycolate-grown cells. However, the biochemical studies did not support the involvement of GST or cyclohexanone monooxygenase in the initial attack on cDCE. The rationale for focusing on the two genes was that the most highly upregulated of the differentially expressed genes would be involved in cDCE degradation, an inducible function. The dynamic expression studies, however, indicate that the most highly upregulated genes are not directly involved in cDCE degradation but are necessary for a number of ancillary functions such as transport or stress response.

Alternative sets of genes that are only slightly upregulated by cDCE or are constitutively expressed seem to be involved in the actual cDCE degradation pathway. The conclusion is based on the observation that although cDCE degradation is inducible, growth on cDCE is slow, the fastest doubling time on cDCE is about 72 hours. The results suggest that the pathway is in the early stages of evolution.

cDCE degradation is the first productive pathway in which cytochrome P450 catalyzes formation of an aldehyde rather than an epoxide. Early studies of mammalian P450s attack on non-chlorinated and mono-chlorinated olefin substrates such as ethene and vinyl chloride, identified epoxides as the major products (Ortiz de Montellano, Kunze, *et al.*, 1982), however reactions with TCE predominantly produced trichloroacetaldehyde and only traces of epoxide (Miller and Guengerich, 1983). cDCE with its intermediate number of chlorine substitutions, clearly is converted by JS666 to dichloroacetaldehyde as the predominant metabolite.

The lack of a complete mass balance with cDCE transformation catalyzed by P450 expressed in *E. coli* reflects both inactivation of the enzyme through formation of a heme-substrate complex (Dolphin, 1985; Miller and Guengerich, 1983; Ortiz de Montellano, Kunze, *et al.*, 1982) and formation of covalently bound dichloroacetaldehyde protein and DNA complexes. In rat liver microsomes 40% of the P450 activity was lost within 30 minutes in the presence of TCE (Miller and Guengerich, 1983). Destruction of the heme in rat liver microsomes by 2-isopropyl-4-pentenamide is reported to limit the turnovers to 250 molecules of substrate (Ortiz de Montellano, Kunze, *et al.*, 1982). The requirement for synthesis of new enzyme molecules would be a substantial constraint contributing to the slow growth rate on cDCE if the same rate of inactivation is associated with the P450 catalyzed degradation of cDCE in JS666.

What of the possible involvement of cyclohexanone monoxygenase (ChnB) in cDCE degradation? When overexpressed in *E. coli*, ChnB showed no activity on cDCE, though it transformed cyclohexanone to ε–caprolactone, demonstrating the production of active enzyme. We were unable to determine any direct role for ChnB in cDCE-degradation by strain JS666, confirming the results from the simultaneous induction studies. On the other hand, there appear to be important roles for other genes of the cyclohexanol operon in cDCE degradation; namely, dehydrogenase genes (*chnA* and *chnD)* adjacent to – and downstream of – *chnB*.

The *chnB*-knockout study demonstrated that the mutant strain could not degrade cDCE, cyclohexanone, cyclohexanol or ethanol. Enzyme assays with the dehydrogenases (ChnA and

ChnD), encoded downstream of *chnB,* demonstrated that these enzymes transform cyclohexanol to cyclohexanone and ethanol to acetaldehyde. The knockout results thus suggest some impairment of ChnA and/or ChnD in the knockout strain, in addition to the loss of functional ChnB. Enzyme assays also showed that ChnD can interconvert 2 2-dichloroacetaldehyde and 2,2-dichloroethanol, pointing to a possible role in cDCE degradation.

Several lines of evidence indicate that the dehydrogenase genes downstream of *chnB* were transcribed and translated in the knockout strain, but with 10-fold decrease in abundance, suggesting an explanation for the knockout strain's inability to grow on ethanol. Protein conformation matters to function, and iTRAQ studies cannot reveal whether the ChnD was functional in the knockout strain.

In this study, we also investigated the possible role of an α/β hydrolase-fold coding sequence homolog of 1-oxa-2-oxocycloheptane lactonase (ChnC) as an epoxide hydrolase. Failure of ChnC to hydrolyze epoxides suggests involvement of other hydrolases or of abiotic hydrolysis. Preliminary evidence from another α/β hydrolase-fold coding sequence (Bpro_4478) was insufficient to conclude anything about involvement of epoxide hydrolases as detoxification agents.

Taken together, our results suggest that cytochrome P450 carries out the first step of cDCE degradation by JS666, but that dehydrogenases (probably ChnA and/or ChnD) in the cyclohexanol pathway might play important roles in succeeding steps (e.g., in transforming alcohol and aldehyde intermediates). The critical involvement of metabolic genes from separate pathways under separate regulation might explain often-encountered difficulty in initiating cDCE degradation by JS666. The results also suggest that the cDCE degradation pathway in JS666 is recently evolved because the genes for cDCE degradation are not in an organized operon and are not highly upregulated. Lack of a well-regulated operon could account for the various behaviors (good versus bad) observed in cDCE-grown JS666 cultures, as well as the long lag times often seen before cDCE degradation begins. The current understanding of pathway evolution is that pathways and operons evolve from extant pathways. Little is invented, but much is borrowed and adapted to new functions. In the case of the cDCE pathway, it appears that at least some of the genes were from an alkane degradation pathway (the cytochrome P450 gene), a DCA-degradation pathway, and a cyclohexanol degradation pathway. It is possible that the ChnB activity observed in cDCE-grown cells is a vestige of former function in a cyclohexanol pathway. It appears that multiple pathways might be involved and that competing processes might divert some of the carbon skeleton. The evolution, regulation and potential for improvement of the cDCE pathway are compelling mysteries that can be explored now that the basic biochemistry and molecular biology of the pathway has been established.

Many of the genes that were identified as involved in cDCE degradation are carried on a megaplasmid belonging to the MOB_H family of conjugative plasmids (Garcillán-Barcia, Francia, *et al.*, 2009). Although the MOB_H family has not been functionally characterized, the JS666 plasmid bears all components required to initiate conjugation with other bacteria, and thus has the potential to transfer the degradative pathway to other organisms. That we have not been able

to replicate aerobic oxidation of cDCE using material obtained from a variety of cDCE-contaminated sites suggests that dispersal of the cDCE pathway is a rare event. The factors that constrain transmission to other strains should be investigated to enable increased effectiveness of bioaugmentation.

No toxic metabolites other than chloride accumulate during cDCE degradation. The traces of epoxide produced during cDCE mineralization decompose spontaneously and never reach toxic levels. The fact that the decomposition rate is similar in the presence or absence of cells supports the argument above that no epoxide hydrolase is involved. It thus appears that *Polaromonas* sp. JS666 is a safe candidate for use in bioremediation, bioaugmentation or monitored natural attenuation.

3.1.6 Literature Cited

Alexander, A. K. (2010). Bioremediation and Biocatalysis with *Polaromonas* sp. strain JS666. PhD Dissertation, University of Iowa.

Allen, J. R., D. D. Clark, J.G. Krum and S. A. Ensign. (1999). "A role for coenzyme M (2-mercaptoethanesulfonic acid) in a bacterial pathway of aliphatic epoxide carboxylation." Proceedings of the National Academy of Sciences, USA **96**: 8432-8437.

Armstrong, R. N. (1997). "Structure, catalytic mechanism, and evolution of the glutathione transferases." Chemical Research in Toxicology **10**: 2-18.

Bergmann, J. G. and J. Sanik, Jr. (1957). "Determination of trace amounts of chlorine in naphtha." Analytical Chemistry **29**: 241-242.

Biemat, J., J. Ciesiołka, P. Gomicld, R. W. Adamiak, W. J. Krzyzosiak and M. Wiewiorowski. (1978). "New observations conceming the chloroacetaldehyde reaction with some tRNA constituents. Stable intermediates, kinetics and selectivity of the reaction." Nucleic Acids Research **5**: 789-804.

Blessing, M., T. C. Schmidt, R. Dinkel and S. B. Haderlein. (2009). "Delineation of multiple chlorinated ethene sources in an industrialized area. A forensic field study using compound-specific isotope analysis." Environmental Science and Technology **43**(8): 2701-2707.

Brzostowicz, P. B., M. B. Blasko and P. E. Rouvière. (2002). "Identification of two gene clusters involved in cyclohexanone oxidation in *Brevibacterium epidermidis* strain HCU." Applied Microbiology and Biotechnology **58**(6): 781-789.

Chan, W. Y., M. Wong, J. Guthrie, A. V. Savchenko, A. F. Yakunin, E. F. Pai and E. A. Edwards. (2010). "Sequence- and activity-based screening of microbial genomes for novel dehalogenases." Microbial Biotechnology **3**(1): 107-120.

Chen, Y.-C. J., O. P. Peoples and C. T. Walsh. (1988). "*Acinetobacter* cyclohexanone monooxygenase: gene cloning and sequence determination." Journal of Bacteriology **170**(2): 781-789.

Coleman, N. V., T. E. Mattes, J. M. Gossett and J. C. Spain (2002). "Biodegradation of *cis*-dichloroethene as the sole carbon source by a β-proteobacterium." Applied and Environmental Microbiology **68**(6): 2726-2730.

Coleman, N. V. and J. C. Spain (2003). "Distribution of the coenzyme M pathway of epoxide metabolism among ethene- and vinyl chloride-degrading *Mycobacterium* strains." Applied and Environmental Microbiology **69**: 6041-6046.

Costa, A. K. and K. M. Ivanetich (1982). "The 1,2-dichloroethylenes: Their metabolism by hepatic cytochrome P-450 in vitro." Biochemical Pharmacology **31**(11): 2093-2102.

de Bont, J. A. M., M. M. Attwood, S. Primrose and W. Harder. (1979). "Epoxidation of short chain alkenes in *Mycobacterium* E20: the involvement of a specific mono-oxygenase." FEMS Microbiology Letters **6**: 183-188.

Dijk, J. A., J. Gerritse, G. Schraa and A. J. Stams. (2004). "Degradation pathway of 2-chloroethanol in *Pseudomonas stutzeri* strain JJ under denitrifying conditions." Archives of Microbiology **182**(6): 514-519.

Dolphin, D. (1985). "Cytochrome P 450: substrate and prosthetic-group free radicals generated during the enzymatic cycle." Philosophical Transactions of the Royal Society B **311**(1152): 579-591.

Donoghue, N. A. and P. W. Trudgill (1975). "The metabolism of cyclohexanol by *Acinetobacter* NCIB 9871." European Journal of Biochemistry **60**(1): 1-7.

Douglas, H. (1983). "Studies on transformation of *Escherichia coli* with plasmids." Journal of Molecular Biology **166**(4): 557-580.

Dugat-Bony, E., C. Biderre-Petit, F. Jaziri, M. M. David, J. Denonfoux, D. Y. Lyon, J.-Y. Richard, C. Curvers, D. Boucher, T. M. Vogel, E. Peyretaillade, and P. Peyret. (2012). "In situ TCE degradation mediated by complex dehalorespiring communities during biostimulation processes." Microbial Biotechnology **5**(5):642-653.

Ensign, S. A. and J. R. Allen (2003). "Aliphatic expoxide carboxylation." Annual Review of Biochemistry **72**: 55-76.

Forkert, P.-G., R. M. Baldwin, B. llen, L. H. Lash, D. A. Putt, M. A. Shultz and K. S. Collins. (2005). "Pulmonary Bioactivation of Trichloroethylene to Chloral Hydrate: Relative Contributions of CYP2E1, CYP2F and CYP2B1." Drug Metabolism and Disposition **33**(10): 1429-1437.

Fox, B. G., J. G. Borneman, L. P. Wackett and J. D. Lipscomb. (1990). "Haloalkene oxidation by the soluble methane monooxygenase from *Methylosinus trichosporium* OB3b: mechanistic and environmental implications." Biochemistry **29**(27): 6419-6427.

Friedman, P. J. and J. R. Cooper (1960). "The Role of Alcohol Dehydrogenase in the Metabolism of Chloral Hydrate." Journal of Pharmacology and Experimental Therapeutics **129**(4): 373-376.

Garcillán-Barcia, M. P., M. V. Francia, and F. de la Cruz (2009). "The diversity of conjugative relaxases and its application in plasmid classification." FEMS Microbiology Reviews **33**(3): 657-687.

Giddings, C. G. S., F. Liu, and J. M. Gossett (2010). "Microcosm assessment of *Polaromonas* sp. JS666 as a bioaugmentation agent for degradation of *cis*-1,2-dichloroethene in aerobic, subsurface environments." Ground Water Monitoring and Remediation 30(2): 106-113.

Guengerich, F. P. (2001). "Common and uncommon cytochrome P450 reactions related to metabolism and chemical toxicity." Chemical Research in Toxicology **14**: 611-650.

Habig, W. H., M. J. Pabst and W. B. Jakoby. (1974). "Glutathione S-transferases. The first enzymatic step in mercapturic acid formation." Journal of Biological Chemistry **249**(22): 7130-7139.

Hage, J. C. and S. Hartmans (1999). "Monooxygenase-mediated 1,2-dichloroethane degradation by *Pseudomonas* sp. strain DCA1." Applied and Environmental Microbiology **65**: 2466-2470.

Hartmans, S. and J. A. M. de Bont (1992). "Aerobic vinyl chloride metabolism in Mycobacterium aurum L1." Applied and Environmental Microbiology **58**: 1220-1226.

Ise, K., K. Suto, and C. Inoue. (2011). "Microbial diversity and changes in the distribution of dehalogenase genes during dechlorination with different concentrations of *cis*-DCE." Environmental Science and Technology **45**(12):5339-5345.

Iwaki, H., Y. Hasegawa, S. Wang, M. M. Kayser and P. C. Lau. (2002). "Cloning and Characterization of a Gene Cluster Involved in Cyclopentanol Metabolism in *Comamonas* sp. Strain NCIMB 9872 and Biotransformations Effected by *Escherichia coli*-Expressed Cyclopentanone 1,2-Monooxygenase." Applied and Environmental Microbiology **68**(11): 5671-5684.

Janssen, D. B., G. Grobben, R. Hoekstra, R. Oldenhuis and B. Withold. (1988). "Degradation of trans-1,2-dichloroethene by mixed and pure cultures of methanotrophic bacteria." Applied Microbiology and Biotechnology **29**(4): 392-399.

Janssen, D. B., F. Pries, J. van der Ploeg, B. Kazemier, P. Terpstra, and B. Witholt (1989). "Cloning of 1,2-dichloroethane degradation genes of *Xanthobacter autotrophicus* GJ10 and expression and sequencing of the *dhlA* gene." Journal of Bacteriology **171**(12): 6791-6799.

Janssen, D. B., A. Scheper, L. Dijkhuizen and B. Witholt. (1985). "Degradation of halogenated aliphatic compounds by *Xanthobacter autotrophicus* GJ10." Applied and Environmental Microbiology **49**(3): 673-677.

Jansson, I., I. Stoilov, M. Sarfarazi and J. B. Schenkman. (2000). "Enhanced expression of CYP1B1 in Escherichia coli." Toxicology 144: 211-219.

Jennings, L. K. (2005). Culturing and enumeration of *Polaromonas* sp. strain JS666 for its use as a bioaugmentation agent in the remediation of *cis*-dichloroethene-contaminated sites. M.S., Cornell University.

Jennings, L. K., M. M. G. Chartrand, G. Lacrampe-Couloume, B. S. Lollar, J. C. Spain, J. M. Gossett (2009). "Proteomic and transcriptomic analyses reveal genes upregulated by *cis*-dichloroethene in *Polaromonas* sp. strain JS666." Applied and Environmental Microbiology **75**(11): 3733-3744.

Kalogeraki, V. S. and S. C. Winans (1997). "Suicide plasmids containing promoterless reporter genes can simultaneously disrupt and create fusions to target genes of diverse bacteria." Gene **188**(1): 69-75.

Kohwi, Y. and T. Kohwi-Shigematsu (1988). "Magnesium ion-dependent triple-helix structure formed by homopurine-homopyrimidine sequences in supercoiled plasmid DNA." Proceedings of the National Academy of Sciences, USA **85**: 3781-3785.

Kohwi-Shigematsu, T. and Y. Kohwi (1991). "Detection of triple-helix related structures adopted by poly(dG)-poly(dC) sequences in supercoiled plasmid DNA." Nucleic Acids Research **19**: 4267-4271.

Lee, H.-C., Y.-P. S. Toung, Y. S. Tu and C. P. Tu. (1995). "A molecular genetic approach for the identification of essential residues in human glutathione S-transferase function in *Escherichia coli*." Journal of Biological Chemistry **270**(1): 99-109.

Lee, J., L. Cao, S. Y. Ow, M. E. Barrios-Llerena, W. Chen, T. K. Wood and P. C. Wright. (2006). "Proteome Changes after Metabolic Engineering to Enhance Aerobic Mineralization of *cis*-1,2-Dichloroethylene." Journal of Proteome Research **5**(6): 1388-1397.

Lee, J., S. R. Hiibel, K. F. Reardon and T. K. Wood. (2010). "Identification of stress-related proteins in *Escherichia coli* using the pollutant *cis*-dichloroethylene." Journal of Applied Microbiology **108**(6): 2088-2102.

Liebler, D. C., M. J. Meredith and F. P. Guengerich. (1985). "Formation of glutathione conjugates by reactive metabolites of vinylidene chloride in microsomes and isolated hepatocytes." Cancer Research **45**(1): 186-193.

Major, D. W. (2008). Laboratory study report. Enhancing natural attenuation through bioaugmentation with aerobic bacteria that degrade *cis*-1,2-dichloroethene, SERDP**:** 125.

Mattes, T. E., Alexander, A. K., Richardson, P. M., Munk, A. C., Han, C. S., Stothard, P. and N. C. Coleman (2008). "The Genome of Polaromonas sp. JS666: Insights into the Evolution of a Hudrocarbon- and Xenobiotic-Degrading Bacterium, and Features of Relevance to Biotechnology." Applied and Environmental Microbiology **74**(20): 6405-6416.

Maymó-Gatell, X., Y.-t. Chien, J. M. Gossett, and S. H. Zinder. (1997). "Isolation of a bacterium that reductively dechlorinates tetrachloroethene to ethene." Science **276**(5318):1568-1571.

Maymó-Gatell, X., T. Anguish, and S. H. Zinder. (1999). "Reductive dechlorination of chlorinated ethenes and 1,2-dichloroethane by '*Dehalococcoides ethenogenes*' 195." Applied and Environmental Microbiology **65**(7)**:**3108-3113.

Meunier, B., S. P. de Visser and S. Shaik. (2004). "Mechanism of oxidation reactions catalyzed by cytochrome P450 enzymes." Chemical Reviews **104**(9): 3947-3980.

Miller, R. E., and F. P. Guengerich (1983). "Metabolism of trichloroethylene in isolated hepatocytes, microsomes, and reconstituted enzyme systems containing cytochrome P-450." Cancer Research **43**(3): 1145-1152.

Newman, L. M. and L. P. Wackett (1991). "Fate of 2,2,2-trichloroacetaldehyde (chloral hydrate) produced during trichloroethylene oxidation by methanotrophs." Applied and Environmental Microbiology **57**(8): 2399-2402.

Novy, R. and B. Morris (2001) "Use of glucose to control basal expression in the pET system innovations." inNovations, 16.

Ortiz de Montellano, P. R., K. L. Kunze, H. S. Beilan, and C. Wheeler (1982). "Destruction of cytochrome P-450 by vinyl fluoride, fluroxene, and acetylene. Evidence for a radical intermediate in olefin oxidation." Biochemistry **21**(6): 1331-1339.

Parnell, J. J., J. Park, V. Denef, T. Tsoi, S. Hashsham, J. Quensen 3rd and J. M. Tiedje. (2006). "Coping with polychlorinated biphenyl (PCB) toxicity: physiological and genome-wide responses of *Burkholderia xenovorans* LB400 to PCB-mediated stress." Applied and Environmental Microbiology **72**(10): 6607-6614.

Raag, R., B. A. Swanson, T. L. Poulos and P. R. Ortiz de Montellano. (1990). "Formation, crystal structure, and rearrangement of a cytochrome P-450$_{cam}$ iron-phenyl complex." Biochemistry **29**(35): 8119-8126.

Rauhut, R. and G. Klug (1999). "mRNA degradation in bacteria." FEMS Microbiology Reviews **23**(3): 353-370.

Rui, L., L. Cao, W. Chen, K. F. Reardon and T. K. Wood. (2004). "Active Site Engineering of the Epoxide Hydrolase from *Agrobacterium radiobacter* AD1 to Enhance Aerobic Mineralization of *cis*-1,2-Dichloroethylene in Cells Expressing an Evolved Toluene *ortho*-Monooxygenase." Journal of Biological Chemistry **279**(45): 46810-46817.

Sauer, K. and A. K. Camper (2001). "Characterization of phenotypic changes in *Pseudomonas putida* in response to surface-associated growth." Journal of Bacteriology **183**(22): 6579-6589.

Scheps, D., S. Honda Malca, H. Hoffmann, B. M. Nestl and B. Hauer. (2011). "Regioselective ω-hydroxylation of medium-chain *n*-alkanes and primary alcohols by CYP153 enzymes from *Mycobacterium marinum* and *Polaromonas* sp. strain JS666." Organic and Biomolecular Chemistry **9**(19): 6727-6733.

Schmidt, K. R., and A. Tiehm. (2008). "Natural attenuation of chloroethenes: identification of sequential reductive/oxidative biodegradation by microcosm studies." Water Science Technology **58**(5):1137-1145.

Sharpe, A. L. and D. E. Carter (1993). "Substrate specificity of rat liver aldehyde dehydrogenase with chloroacetaldehydes." Journal of Biochemical Toxicology **8**(3): 155-160.

Shin, K. (2010). Biodegradation of Diphenylamine and *cis*-dichloroethene. PhD Dissertation, Georgia Institute of Technology.

Stanier, R. (1947). "Simultaneous adaptation: a new technique for the study of metabolic pathways." Journal of Bacteriology **54**: 339-348.

Stanier, R. Y., N. J. Palleroni and M. Doudoroff. (1966). "The aerobic pseudomonads: a taxonomic study." Journal of General Microbiology **43**: 159-271.

Taniguchi, Y., P. J. Choi, G. W. Li, H. Chen, M. Babu, J. Hearn, A. Emili and X. S. Xie. (2010). "Quantifying *E. coli* Proteome and Transcriptome with Single-Molecule Sensitivity in Single Cells." Science **329**(5991): 533-538.

van Beilen, J. B., R. Holtackers, D. Lüscher, U. Bauer, B. Witholt and W. A. Duetz. (2005). "Biocatalytic production of perillyl alcohol from limonene by using a novel *Mycobacterium* sp. cytochrome P450 alkane hydroxylase expressed in *Pseudomonas putida*." Applied and Environmental Microbiology **71**(4): 1737-1744.

van der Ploeg, J., M. P. Smidt, A. S. Landa and D. B. Janssen. (1994). "Identification of chloroacetaldehyde dehydrogenase involved in 1,2-dichloroethane degradation." Applied and Environmental Microbiology **60**(5): 1599-1605.

van Hylckama Vlieg, J. E. T. and D. B. Janssen (2001). "Formation and detoxification of reactive intermediates in the metabolism of chlorinated ethenes." Journal of Biotechnology **85**(2): 81-102.

Verce, M. F., C. K. Gunsch, A. S. Danko and D. L. Freedman. (2002). "Cometabolism of *cis*-1,2-dichloroethene by aerobic cultures grown on vinyl chloride as the primary substrate." Environmental Science and Technology **36**(10): 2171-2177.

Vogel, T. M., C. S. Criddle and P. L. McCarty. (1987). "Transformations of halogenated aliphatic compounds." Environmental Science and Technology **21**: 722-736.

Vuilleumier, S. (1997). "Bacterial glutathione S-transferases: what are they good for?" Journal of Bacteriology **179**(5): 1431-1441.

Vuilleumier, S. and M. Pagni (2002). "The elusive roles of bacterial glutathione *S*-transferases: new lessons from genomes." Applied Microbiology and Biotechnology **58**: 138-146.

Wakasugi, T., T. Miyakawa, F. Suzuki, S. Itsuno and K. Ito. (1993). "Preparation of dichloroacetaldehyde cyclic trimer and its depolymerization." Synthetic Communications **23**(9): 1289-1294.

Werner, J. H. and T. A. Cool (1998). "Flame sampling photoionization mass spectrometry of dichloroethenol." Chemical Physics Letters **290**(1-3): 81-87.

Wiese, S., K. A. Reidegeld, H. E. Meyer and B. Warscheid. (2007). "Protein labeling by iTRAQ: A new tool for quantitative mass spectrometry in proteome research." Proteomics **7**(3): 340-350.

Williams, P. A., J. Cosme, D. M. Vinkovic, A. Ward, H. C. Angove, P. J. Day, C. Vonrhein, I. J. Tickle and H. Jhoti. (2004). "Crystal structures of human cytochrome P450 3A4 bound to metyrapone and progesterone." Science **305**(5684): 683-686.

3.2 Objective 2 – Development of DNA-Based Molecular Biological Tools

3.2.1 Background

When we commenced this project, our intent was to develop a DNA-based tool to prospect for growth-coupled, aerobic cDCE-oxidizing activity at contaminated sites. Had we discovered other isolates beyond strain JS666, we would have performed comparative analysis of their cDCE-degradation pathways and developed molecular biological tools (MBTs) based on genes they shared. Since we are left with strain JS666 as the only isolated representative of growth-coupled aerobic cDCE-degraders, that approach is not possible.

Instead, being the only representative, JS666 has potential as an effective bioaugmentation agent at sites where cDCE has accumulated in aerobic environments. In this context, DNA-based MBTs are useful to track its migration after bioaugmentation. Furthermore, it might be useful to develop mRNA-based MBTs that would correlate well with cDCE-degradation activity of JS666.

DNA-based MBTs for JS666 were developed in previous, ESTCP-sponsored research and have been published (Giddings, Jennings, *et al.*, 2010). They are based on JS666 genes encoding the enzymes isocitrate-lyase (abbreviated “ISO” in this report) and cyclohexanone monooxygenase

(properly designated as ChnB, but commonly abbreviated “CMO” here), and the primer sequences were selected based on uniqueness to that strain.

In this present, SERDP-sponsored project, we examine the possibilities for using mRNA targets as MBTs for monitoring cDCE-degradation *activity*, rather than the mere *presence* of JS666. Selection of potential mRNA targets was based on results presented in Section 3.1 of this report, but are summarized here.

Targets of Putative Function

Jennings *et al.* (Jennings, Chartrand, *et al.*, 2009) used an integrated omics approach (proteomics, transcriptomics, and metabolomics) to study gene expression in JS666. Microarray data comparing RNA extracted from cDCE-grown versus glycolate-grown cultures confirmed five of the proteins found through proteomics study (see earlier Table 3-7 [presented in Section 3.1]). Putative gene function was suggested using bioinformatics tools. A number of transcripts that were highly up-regulated in the presence of cDCE share sequence homology with proteins that could be involved in degradation [e.g., cyclohexanone monooxygenase (CMO — or ChnB, as it is now more formally designated), cytochrome P450 (P450), haloacid dehalogenase (HAD), and glutathione S-transferase (GST)] or stress response [e.g., pyridoxamine 5'-phosphate oxidase (PNP) and GST]. JS666 is known to produce an epoxide in oxidation of ethene (Coleman, Mattes, et a., 2002); epoxidation is therefore one of the plausible first steps in cDCE oxidation. Epoxides are highly reactive and can be quite damaging to cellular components. It is therefore understandable if there is an up-regulation of genes associated with oxidative stress caused by cDCE degradation. Further, cDCE, being an organic solvent, might be expected at high concentrations to compromise the membrane of JS666. Thus, some of these transcripts might be up-regulated as a response to solvent stress (Isken and de Bont ,1998). Up-regulated gene transcripts warrant further scrutiny to better understand how they are (or are not) correlated to up-regulation of metabolic genes.

The omics approaches raised many hypotheses and suggested alternative pathways, but did not clearly elucidate the cDCE degradative pathway(s). For the work conducted here, we chose to target the genes that were identified as up-regulated by cDCE in both the microarray and proteomic experiments. Additionally, we targeted cytochrome P450, because our work (Section 3.1) has suggested a role for this enzyme in the initial step of cDCE oxidation. We also targeted isocitrate lyase (the target of our DNA probe for JS666 abundance in bioaugmentation) (Giddings, Jennings *et al.*, 2010) and the beta-subunit of RNA polymerase (RpoB) as potential "housekeeping genes" for possible use in normalizing mRNA data.

Predicted Protein Function

Work conducted with bioinformatics, integrated omics approaches, and enzyme assays (Section 3.1) has lead to several hypothetical pathways to cDCE oxidation by JS666 with various initial steps (Figure 3-32 from end of Section 3.1). The reader is referred to Section 3.1 for more detailed discussion of the possible role(s) played by these proteins in JS666.

Cyclohexanone Monooxygenase (CMO or ChnB), Bpro_5565
Monooxygenases catalyze the reaction between molecular oxygen and an organic substrate, resulting in the addition of one oxygen atom to the substrate and reduction of the other oxygen atom to water. These enzymes require a cofactor, such as NAD(P)H. Jennings *et al.* (Jennings, Chartrand, *et al.*, 2009) postulated that the function of CMO in JS666 is to catalyze DCE epoxidation, though through our later studies (Section 3.1) we found no evidence for this.

Glutathione S-Transferase (GST), Bpro_0645
GSTs have many functions. There is evidence of bacteria producing GST to relieve epoxide stress, and glutathione is involved in protein synthesis, degradation, and folding, as well as protection against oxidative stress, and a number metabolic processes (van Hylckama Vlieg and Janssen, 2001). In JS666, GST could be involved in epoxide transformation, direct dehalogenation of cDCE, or simply to relieve oxidative stress (Jennings, Chartrand, *et al.*, 2009).

Haloacid Dehalogenase (HAD), Bpro_0530, Bpro_5186
Dehalogenases catalyze the removal of the halogen from a molecule, cleaving the carbon-halogen bond. HADs replace the halogen with a hydroxyl through the hydrolysis of α-halogenated carboxylic acid. There are two paralogous HADs in the JS666 genome, one of which is on a plasmid (Bpro_5186). Both have confirmed activity by expression in *E. coli* (Jennings, Chartrand, *et al.*, 2009). In purified cell extracts from JS666, putative HAD enzyme transformed chloroacetic acid to glycolate (Jennings, Chartrand, *et al.*, 2009).

Pyridoxamine 5'-Phosphate Oxidase (PNP), Bpro_0646
PNP is an oxidase that catalyzes the final step in the vitamin B6 metabolism pathway. Vitamin B6 is thought to be involved in a number of important metabolic processes including sustaining glutathione (GSH) levels, and alleviating oxidative stress (Jennings, Chartrand, *et al.*, 2009).

Cytochrome P450 (P450), Bpro_5301
P450 is a widely occurring monooxygenase with other actions as well. The reaction that is catalyzed by P450 acting upon an alkene (such as cDCE) produces an epoxidation, an aldehyde rearrangement and/or a suicide complex that deactivates the protein (de Visser, Kumar, *et al.*, 2004). In Section 3.1, a major role for P450 was demonstrated in the initial step of cDCE oxidation by JS666.

3.2.2 Research Objectives

The primary objective of this phase of study was to assess the potential of several genes in JS666 as targets for mRNA-based MBTs that might correlate with cDCE-degradation activity in strain JS666.

Our strategy for addressing this objective was to examine the pattern of expression of putative, cDCE-pathway degradative genes (and other genes found to be up-regulated during cDCE degradation) under dynamic conditions. Examining transcripts under conditions of both successful and unsuccessful degradation of cDCE – and during the process of adaptation to

cDCE degradation – should allow the development of MBTs for JS666 *activity*, supplementing the already-developed, DNA-based MBTs that have been used to detect *presence* of JS666 (Giddings, Jennings *et al.*, 2010). By extension, such mRNA-based and DNA-based tools might be useful in prospecting for in-situ cDCE-oxidation activity at sites not amended with JS666; however, absent any other isolated cDCE-oxidzers, this extended utility of the JS666-derived MBTs remains undetermined.

3.2.3 Materials & Methods

Chemicals and Media

cDCE (>99%, stabilized with MEHQ) and 1,2-dichloroethane (DCA, 99.5%) were obtained from TCI. Ethanol (EtOH, anhydrous ethyl alcohol, 95.27%; methyl isobutyl ketone, 1.0%; ethyl acetate, 1.0%; hydrocarbon, 1.0%) and glycolic acid (gly, 70% aqueous solution) were obtained from Fisher Scientific. Minimal salts media (MSM) was used to grow JS666 as described elsewhere (Giddings, Liu, *et al.*, 2010).

Culturing Technique

JS666 cultures were grown on neat cDCE in MSM at a pH of approximately 7.1 to 7.2, as described elsewhere (Giddings, Liu, *et al.*, 2010). Pure cultures were maintained through a series of 5% v/v culture transfers into 100 mL MSM in 160-mL serum bottles and fed a nominal concentration of cDCE of 51 mg/L. [Note: concentrations of all volatiles are reported herein as "nominal" – i.e., ignoring partitioning to headspace.] Additionally, purity checks by streak-plating were routinely carried out.

Analytical Methods

Total quantities of cDCE and DCA in bottles were measured from 100-µL headspace samples by gas chromatography (Perkin-Elmer, Autosystem GC) with a flame-ionization detector and a packed column (1% SP-1000 on 60/80 Carbopack B [Supelco]). Levels were quantified through comparison to standard curves created from known additions to replicate serum bottles containing distilled water (dH_2O). Additionally, oxygen and carbon dioxide were monitored using a thermal conductivity detector (TCD).

Nucleic Acid Extraction and Isolation

RNA and DNA were isolated using the QIAGEN AllPrep DNA/RNA Mini Kit. Prior to cell lysis, each sample was amended with 2×10^{10} copies of luciferase control RNA (Promega) as exogenous internal reference mRNA, in order to ascertain extraction efficiency of the protocol (Johnson, Lee, *et al.*, 2005). To remove DNA contamination, the RNA was treated with RNase-free DNase I (Fisher) digestion protocol. The quality and quantity were assessed using an Agilent 2100 bioanalyzer RNA 6000 Nano assay (Agilent Technologies).

RT cDNA Synthesis

cDNA was synthesized from 0.2 μg of RNA using an iScript cDNA synthesis kit (Bio-Rad) with random hexamer primers according to the manufacturer's instructions.

Quantitative Polymerase Chain Reaction (qPCR)

The cDNA levels, and therefore the number of transcripts from target genes in each sample, were quantified by real-time polymerase chain reaction (RT-PCR) with a thermocycler (iCycler Detection System, BIO RAD) with the intercalation agent iQ SYBR Green (BIO RAD), and primers specific for *Polaromonas* sp. JS666 targets and for the luciferase control). The reactions were carried out under the following conditions: 2 min at 50ºC followed by 3 min at 95ºC; next 40 cycles (denaturation at 95ºC for 15 sec, annealing and extension at 63ºC for 1 min), where fluorescence was measured after every cycle. Each reaction was performed in triplicate, and a melt curve was completed following the amplification reactions to confirm the specificity of the primers and the reactions. Primers for JS666 degradative, stress response, and housekeeping genes (Table 3-14) were designed using the PrimerQuest software available at the IDT website (http://scitools.idtdna.com/Primerquest/). Primer specificity was checked by BLAST analysis. BLAST analysis of the primer pairs designed for either HAD showed that they were indistinguishable at the nucleic acid level.

Table 3-14: Gene targets and primer sets

Locus Tag	Gene Description	Primers (F/R)
Bpro2101	isocitrate lyase (ISO)	5'TGCCGCTGACAACAACAC/ 5'ATCAATGCCTTTGGAGTGC
Bpro0645	glutathione S-transferase-like (GST)	5'CAAGCTTTACCGTGTCGCCATTTC/ 5'CAGGTCAATCTCCACCCGTTCAAA
Bpro5565	cyclohexanone monooxygenase (CMO)	5'ATTGTCAAAGACCCGGAAACTGCC/ 5'TAAATGGCGTAGTAGCCGCTGTCA
Bpro0646	pyridoxamine 5'-phosphate oxidase-related (PNP)	5'GTGCCGGATTTCATGGGCAACTTT/ 5'CAGATAGAGCAGGTCGCCATTGTCA
Bpro_0530/ Bpro_5186	haloacid dehalogenase, type II (HAD)	5'GTTGACGAAGTGCGGCTGTTCAAA/ 5'TCTGATTCACCCAAGTGCAGGGTA
Bpro5301	cytochrome P450 (P450)	5'AGGACAGCTTGTTTGGTCCGTACT/ 5'ATCCATCGCAATGAACATCGGCAG
Bpro4442	beta subunit of RNA polymerase (RpoB)	5'TTGTGGAAGCCGATGCATTTGACC/ 5'ATCGCGTTCTTGATGCTTTCCAGC
	exogenous internal reference luciferase (LUC)	5'TACAACACCCCA ACATCTTCGA/ 5'GGAAGTTCACCGGCGTCAT

By enumerating luciferase as well as target transcripts, recovery efficiency and reverse transcription losses can be accounted for (Johnson, Lee, *et al.*, 2005; Rahm, Morris, *et al.*, 2006). Additionally, by monitoring a housekeeping gene alongside up-regulated genes, increases in the transcripts of interest can be attributed to cell activity during experimental conditions and not simply an increase in cell numbers. It is difficult to know *a priori* which, if any, gene will be stably expressed (Sharkey, Banat, *et al.*, 2004), and so two possible housekeeping genes were chosen. These were isocitrate lyase (ISO) and the beta-subunit of RNA polymerase (RpoB). However, upon further investigation we found the RpoB expression levels to be difficult to quantify precisely and too variable for this purpose. For these reasons, ISO was chosen as the housekeeping gene.

Expression Data Analysis (DART)

To damp-out errors associated with plate-to-plate variation in standard curves, fluorescence data generated by the iCycler was analyzed using the DART-PCR technique as outlined and developed by Pierson *et al.* (Peirson, Butler, *et al.*, 2003) and described previously (Giddings, Liu, *et al.*, 2010).

Experimental Conditions

All batch reactors were prepared aseptically in autoclaved 1-L serum bottles and contained 500 mL of MSM. Amendments were administered and samples taken via sterile syringe through ethanol-swabbed, flamed septa. All experiments were conducted at 22ºC in the dark, agitated at 60 RPM. Cultures were sampled for both RNA and DNA by withdrawing 10 mL of liquid by sterile disposable syringe. The samples were centrifuged at 10,000x*g* for 10 min at 4°C, and most of the supernatant discarded. They were then centrifuged again at 21,000*g* for an additional 5 min. The cell pellets were stored at –80°C until extraction unless otherwise noted. Because such large culture volumes were removed for RNA isolation, significant cDCE and DCA were also removed during the sampling. To account for such substrate losses that were not due to biodegradation, we present the GC-plots of degraded cDCE or DCA as the sum of incremental masses degraded, each divided by applicable liquid volume remaining during the incremental period (sum[-ΔMdeg/V]) vs. time. The values are negative so that the degradation line trends down. Note that without such a reporting method, remaining mass of cDCE or DCA would decline due to sampling losses alone, making it difficult to detect intervals during which no degradation occurred.

RNA Extraction Reproducibility and Precision

As RNA extraction and reverse transcription can be a significant source of imprecision (Johnson, Lee, *et al.*, 2005), the reproducibility of RNA extraction and comparison of freeze-thaw at various points during the extraction and reverse transcription, were examined. RNA extractions were performed in quadruplicate on a pure JS666 culture that was actively degrading cDCE. Cell pellets were either frozen or further processed according to Table 3-15, for a total of four treatments (A-D). We found that RNA was degraded beyond quantification when it was not

frozen before RNA isolation (treatments A & B). This is most likely due to how unstable RNA is at ambient temperatures. Freeze-thaw was less detrimental to the samples than letting them stay on ice between process steps, most likely due to the time required for the set-up of each step. There was no significant difference between cDNA synthesized from RNA that had been frozen or not (treatments C & D). To be efficient in sample processing, it was desirable to accumulate samples for nucleic acid isolation and then reverse transcription. Therefore, treatment D was chosen for all subsequent samples. The total copies of ISO recovered (accounting for the exogenous internal reference LUC recovery) had a coefficient of variation (CV) of 28.5%. The relative expression of GST/ISO had a CV of 44.7%.

Table 3-15: Cell pellet freezing or processing by treatment

Treatment	Cell Pellet Frozen	RNA Frozen	cDNA Frozen
A	-	-	✓
B	-	✓	✓
C	✓	-	✓
D	✓	✓	✓

Notes:
✓ - Indicate when in the RNA isolation and reverse transcription process samples were frozen at -80°C (RNA) or -20°C (cDNA).
- Processing without freezing
cDNA - complimentary deoxyribonucleic acid
RNA - ribonucleic acid

Dynamic Expression Studies

To monitor highly up-regulated transcripts, such as those possibly associated with cDCE degradation and/or stress, we conducted batch experiments with JS666 exposed to changing conditions.

The JS666 culture was either grown up on cDCE and subjected to starvation before re-exposure to cDCE or grown on the alternate substrate glycolate before being exposed to cDCE, DCA, or EtOH (Figure 3-33). Additionally, the second set of batch experiments included a glycolate-fed control culture. Both starvation and growth on glycolate have been demonstrated to create an extended lag prior to subsequent cDCE degradation.

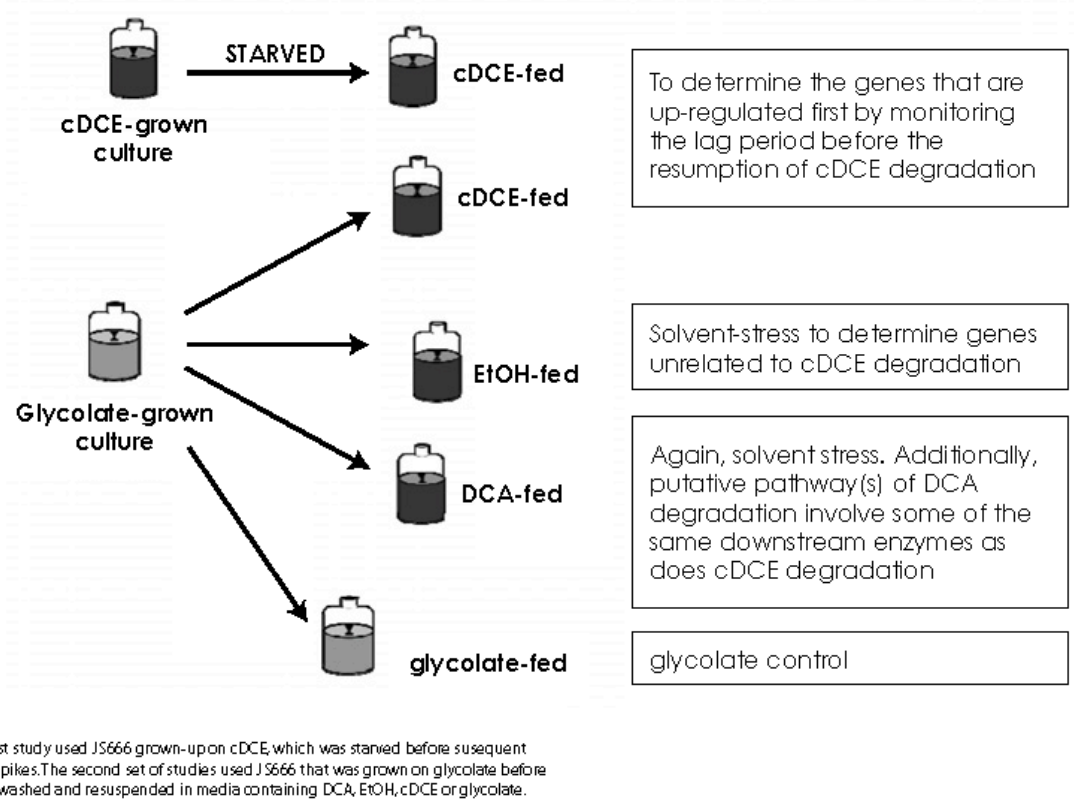

Figure 3-33: Experimental set-up for dynamic expression studies

Response Following Starvation

The hypothesis of this experiment was that the lag created by cDCE-starvation was the result of down-regulation of critical genes associated with cDCE-degradation. By monitoring transcript levels before starvation and throughout the lag period before resumption of cDCE degradation, it would reveal genes whose up-regulation is coincident with the onset of cDCE degradation, and therefore associated with the determinative (presumably initial) steps of the metabolic pathway.

The cDCE-starved cultures were prepared in duplicate and simply allowed to consume all the cDCE present (two spikes of 20 μL neat cDCE or approximately 100 mg/L total), and no additional cDCE was administered for approximately 72 hours, after which a third spike of cDCE was delivered. The cultures were sampled in triplicate for RNA before starvation, during starvation, during the lag prior to degradation, and as degradation commenced. Transcript expression is reported as total copies/mL (accounting for luciferase internal reference recovery) and also normalized to the housekeeping gene ISO to account for cell activity.

Response Following Change of Substrate

When JS666 is grown on glycolate, it does not immediately degrade cDCE. It would seem that some of the genes required for cDCE degradation are down-regulated in the absence of cDCE and in the presence of glycolate. By switching these "down-regulated" cultures to various substrates, we hoped to observe which genes are associated with the critical steps of cDCE degradation and which are more general indicators of activity or are possibly stress-related. For this purpose, we selected cDCE, EtOH, and DCA as substrates provided to cultures immediately following growth on glycolate. All are "solvents," and might evidence up-regulation of genes unrelated to cDCE degradation. Though growth on EtOH has been shown to reduce lag to subsequent cDCE degradation, it does not eliminate lag. The putative pathway(s) of DCA degradation (Figure 3-32 from end of Section 3.1) involve some of the same downstream enzymes as does cDCE degradation (Mattes, Alexander, *et al.*, 2008).

A total of 1500 mL of JS666 culture was grown to high density on 10 mM of glycolate. The pH was adjusted to approximately 7.1 to 7.2 with 5N NaOH. After two days, another 1.35 mL of glycolic acid was administered and pH adjusted. The cultures were also aseptically amended with pure oxygen as needed. The culture was washed and resuspended in duplicate in MSM and given 260 μM DCA (25 mg/L), 3 mM EtOH, 520 μM cDCE (50 mg/L), or 10 mM glycolate. The cultures were streak-plated to confirm culture purity after any handling that could have introduced contamination. Each batch culture was sampled in triplicate for RNA approximately 12 hours post inoculation and as they degraded the substrates. The glycolate controls were sampled for RNA approximately 16 hours post-inoculation. The mean transcript level of each target gene in the controls was normalized to the mean transcript level of the housekeeping gene ISO for that sample. Then for each experimental-treatment sample, its measured transcripts were normalized to ISO transcripts in that individual sample, and then reported relative to the ISO-normalized transcript values of the glycolate control. The standard deviation, σ, of a ratio of two averages of samples, $\left(\frac{\mu_Y}{\mu_X}\right)$, each with their own standard deviations, σ_Y and σ_X, is found with the following equation:

$$\sigma = \left(\frac{\mu_Y}{\mu_X}\right) \times \left(\sqrt{\left(\frac{\sigma_Y}{\mu_Y}\right)^2 + \left(\frac{\sigma_X}{\mu_X}\right)^2}\right).$$

3.2.4 Results & Discussion

Experiments were conducted in an attempt to understand how the expression of selected genes in JS666 will vary with successful or unsuccessful degradation of cDCE (i.e., during adaptation following starvation or growth on non-cDCE substrate).

Response Following Starvation

JS666 cultures suffer a long cDCE degradation lag following a brief starvation period (Figure 3-34). It was hoped that in recovery from starvation, one or more of the gene transcripts that had been previously found to be up-regulated when JS666 is growing on cDCE would coincide with the observed onset of cDCE degradation. This response would be strong indication that this gene is most likely critical to degradation. However, this response was not observed (Figure 3-35). During the starvation of the culture, there was a sharp drop in all transcript levels, no doubt reflecting generally low activity. As degradation resumed, all the targeted transcripts came up simultaneously, with the possible exception of GST and P450, which may have been up-regulated later. Most likely the window of time for the up-regulation of critical gene(s) in this suite was too short relative to sampling intervals to observe any differences in time-points at which upregulation occurred among the targeted genes.

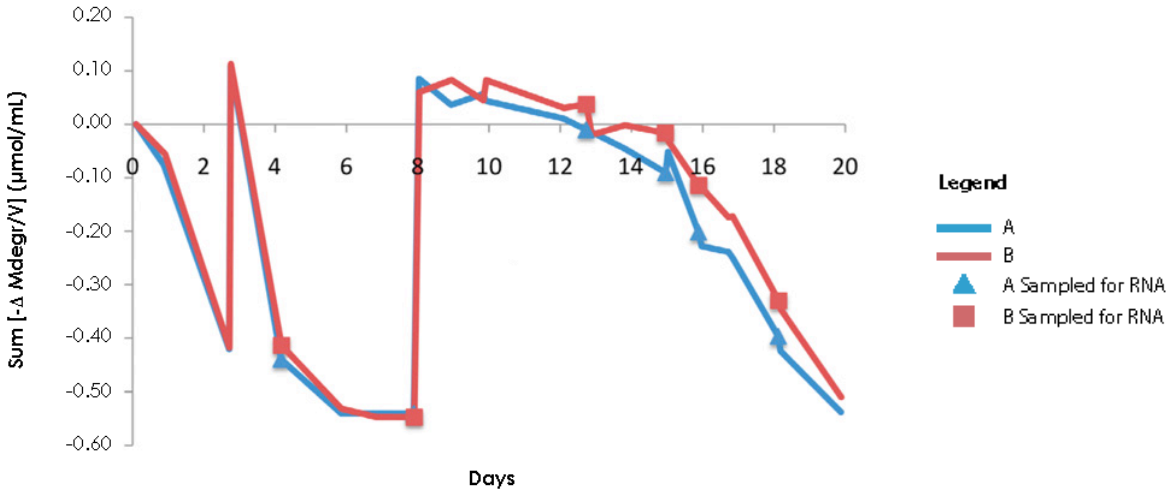

Figure 3-34: cDCE degradation in biological replicates subjected to starvation at day 6

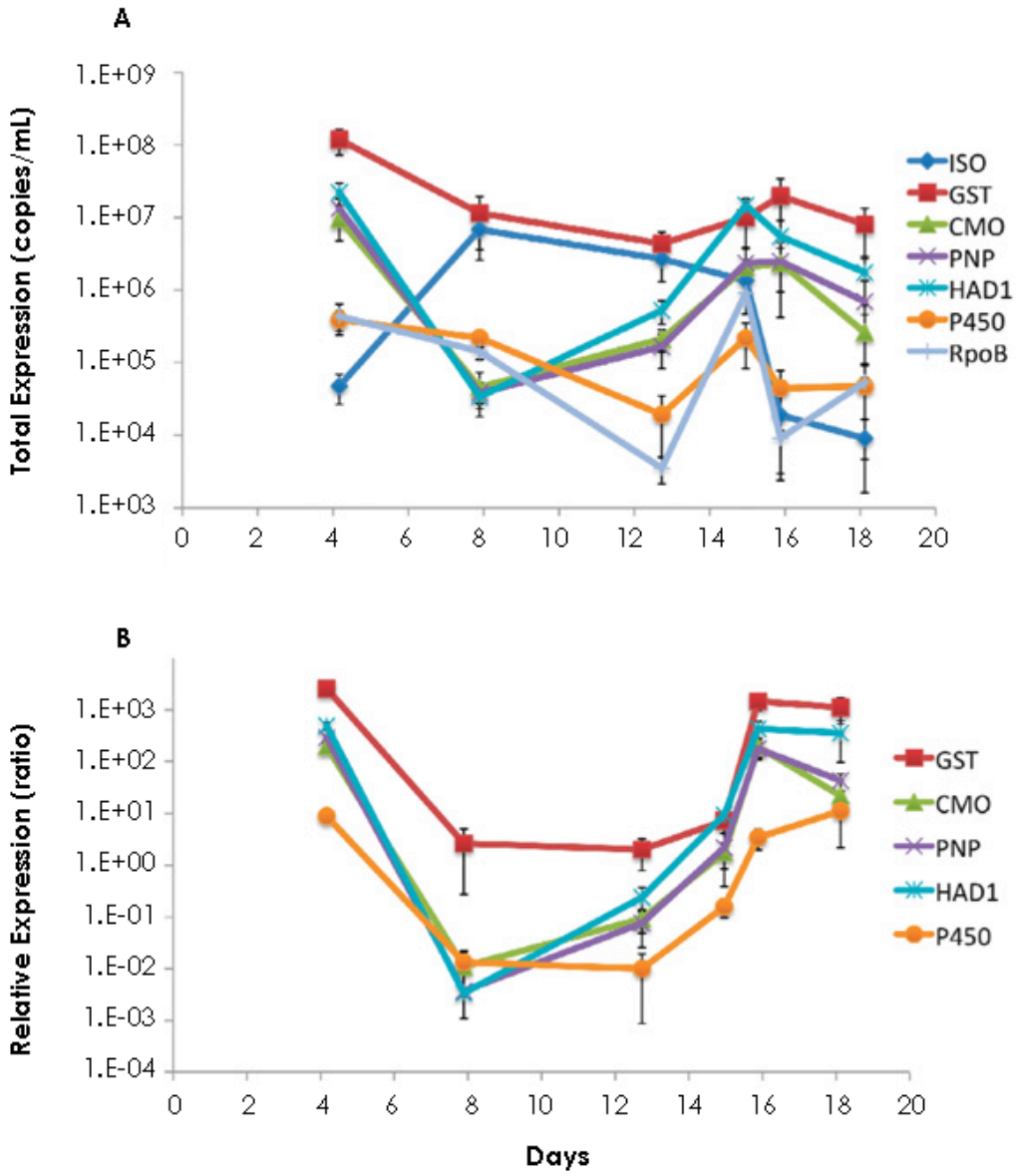

Figure 3-35: Gene expression profile for cDCE-starved cultures. A) Total Expression Accounting for Internal Reference RNA (Luciferase RNA). B) Relative Gene Expression Normalized to ISO mRNA.

Response Following Change of Substrate

cDCE

When the culture grown on glycolate was switched to cDCE, the expected lag before degradation was observed. The two biological replicate cultures did not closely track each other; thus results for each are plotted (Figure 3-36). We postulated that one or more of the gene transcripts that had been previously identified as being up-regulated on cDCE would rise coincident with onset of cDCE degradation. We observed that GST and HAD were up-regulated first (Figure 3-37). Next, the CMO and PNP came up, which was right around the onset of cDCE degradation. Bottle B showed a sharp decrease in the relative expression of HAD at the final sampling point. A possible explanation is that bottle B degraded the cDCE present before bottle A, which would suggest that HAD transcripts are down-regulated quickly after cDCE degradation.

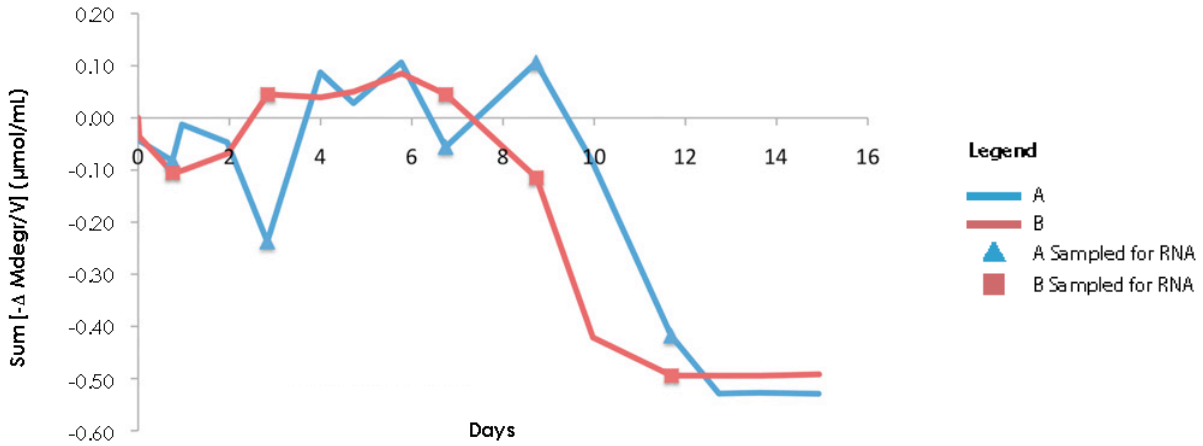

Figure 3-36: cDCE degradation in biological replicates inoculated with culture grown on glycolate

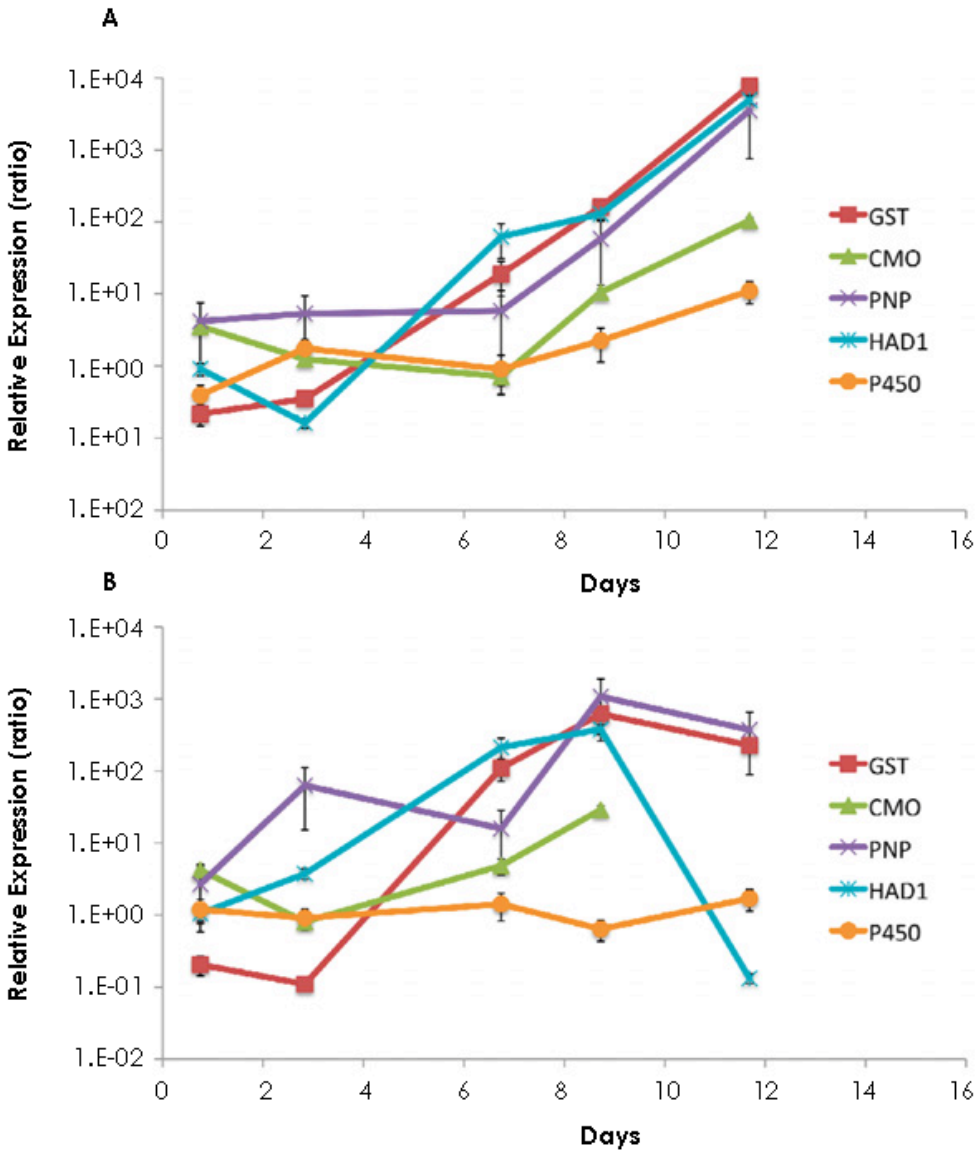

Notes:

The final data point for CMO in bottle B is not available. The cultures were initially grown on glycolate before being washed and resuspended in media containing cDCE. Relative gene expression normalized to the housekeeping gene, ISO, reported relative to the glycolate control. Error bars indicate the standard deviations of triplicate extractions.

Figure 3-37: Relative gene expression of the target transcripts, when grown on cDCE for replicates A and B

EtOH

JS666 is known to be able to utilize ethanol as a substrate; moreover ethanol generally shortens the lag leading to cDCE degradation after re-exposure to cDCE (Jennings, Chartrand, *et al.*, 2009). We did not measure ethanol directly, but measured both oxygen and carbon dioxide as surrogates for ethanol depletion. As ethanol was oxidized, there was an increase in carbon dioxide and a decrease in oxygen (Figure 3-38). The corresponding transcript expression showed a relative increase of GST almost immediately (Figure 3-39), however degradation was delayed, suggesting that the GST may be involved in solvent or stress protection rather than degradation. The CMO and PNP transcripts both showed a relative increase that appears to correspond with onset of ethanol oxidation. While this could indicate that CMO is associated with degradation in the case of ethanol, it is more likely that CMO is being co-upregulated with the nearby alcohol dehydrogenase downstream from the CMO in the same operon. PNP is most likely involved with alleviating the stress associated with the added ethanol mixture.

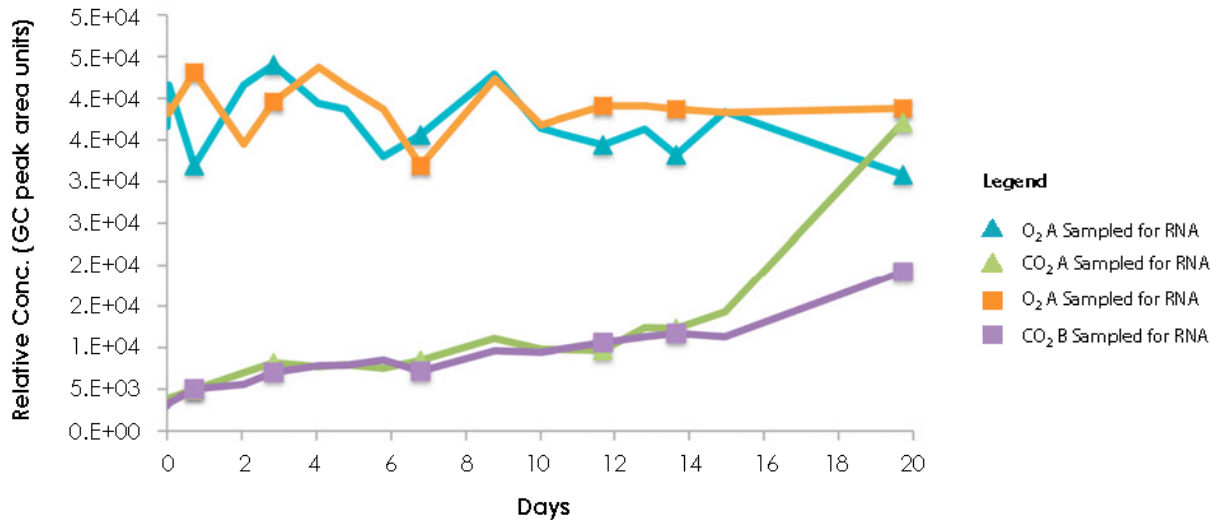

Figure 3-38: EtOH-degradation in biological replicates inoculated with culture grown on glycolate, using oxygen and carbon dioxide as surrogate measurements

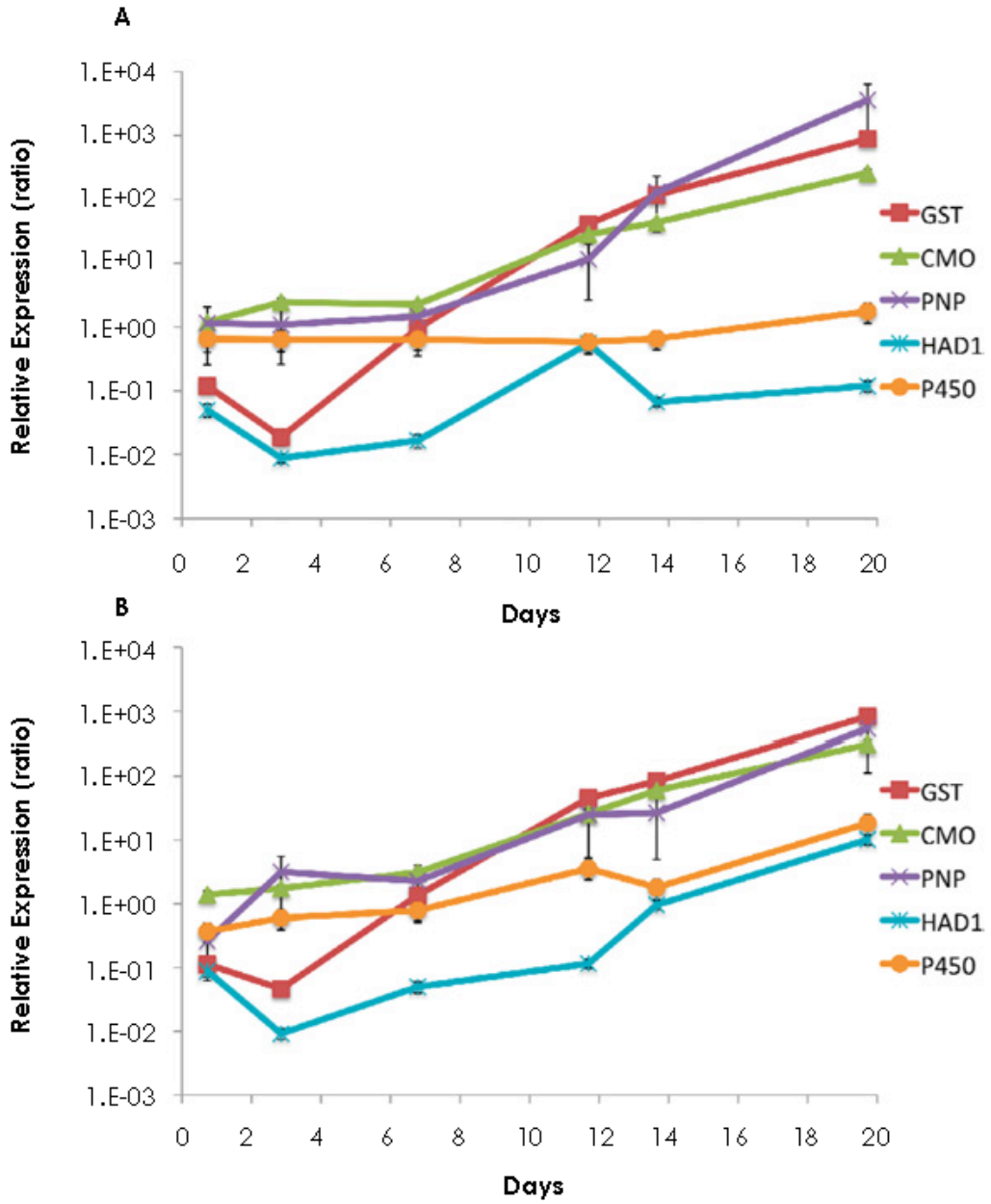

Notes:

The cultures were initially grown on glycolate before being washed and resuspended in media containing EtOH. Relative gene expression normalized to the housekeeping gene, ISO, reported relative to the glycolate control. Error bars indicate the standard deviations of triplicate extractions.

Figure 3-39: Relative gene expression of the target transcripts, when grown on EtOH for replicate A and B

DCA

According to the bioinformatic study conducted by Mattes *et al.* (Mattes, Alexander, *et al.*, 2008) JS666 possesses what seems to be a set of genes that are able to transform DCA. Presumably, the initial oxidation of cDCE would feed into this pathway. Additionally, JS666 has demonstrated sustained degradation of DCA (Jennings, Chartrand, *et al.*, 2009). By giving JS666 DCA as a substrate, after having down-regulated the cDCE degradation pathway by growing the culture on glycolate, we hoped to understand which genes were associated with the later steps in cDCE degradation. However, our culture did not degrade DCA (Figure 3-40); therefore we decided to concentrate on the expression profiles of the first few days of DCA exposure in an attempt to capture the initial reaction of JS666 to this new substrate. Moreover, midway through GC-sampling of DCA, there was a change in the instrument response, adding to the erratic DCA-degradation profile. However, it is obvious that there was little to no DCA degradation, which can be seen clearly in the later GC-sampling. In the days following the culture's exposure to DCA, the relative expression of PNP and GST rose, and the relative expressions of CMO, HAD and P450 all fell (Figure 3-41).

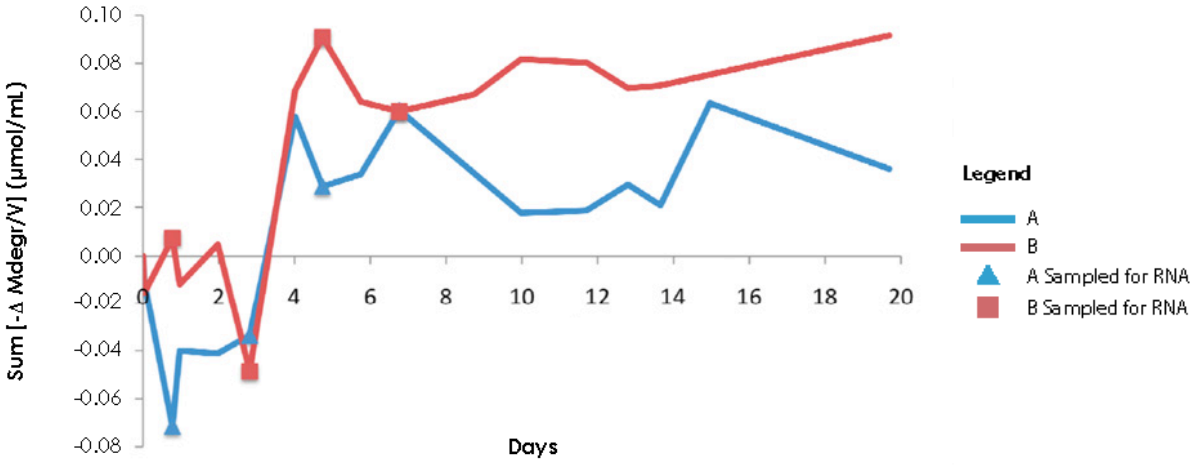

Figure 3-40: DCA-degradation in biological replicates inoculated with culture grown on glycolate

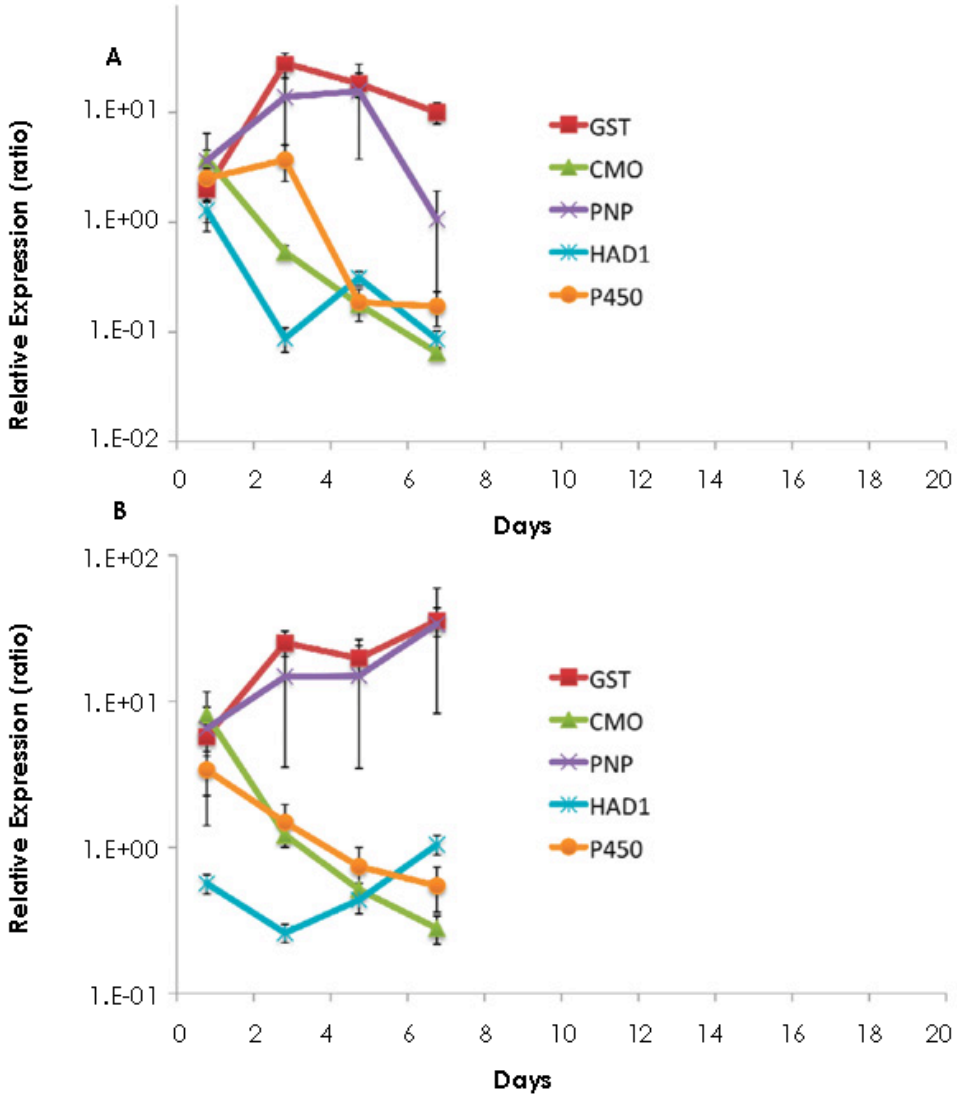

Notes:

The cultures were initially grown on glycolate before being washed and resuspended in media containing DCA. Relative gene expression when normalized to the housekeeping gene, ISO, reported relative to the glycolate control. Error bars indicate the standard deviations of triplicate extractions.

Figure 3-41: Relative gene expression of the target transcripts, when grown on DCA for replicate A and B

3.2.5 Conclusions and Implications for Future Research / Implementation

Taken together, these studies appear to confirm that HAD is involved in cDCE degradation because it was up-regulated with cDCE degradation and down-regulated with the lack of cDCE degradation. This result is consistent with what we concluded from cell-free extract studies, which is that cDCE degradation occurs through HAD catalyzed degradation of (di)chloroacetic acid (Section 3.1). It is also consistent with the iTRAQ proteomics study (Section 3.1) that showed higher abundance of HAD protein in cDCE-degrading JS666 than in JS666 growing on ε-caprolactone. While this HAD up-regulation is correlated with cDCE, it is undoubtedly not the first step in the process. However, since HAD seems to be down-regulated quickly after cDCE ceases, this may be a good gene for a MBT to look for JS666 degradation activity.

GST and PNP seem to be up-regulated to alleviate solvent and/or oxidative stress, as rise in their transcription occurred under circumstances of exposure to – but not degradation of – substrates such as EtOH and DCA. GST was up-regulated almost immediately in all treatments when there was no associated degradation. However, there is no way to rule out a role for GST in dechlorination, as GST could be involved in epoxide transformation, direct dehalogenation of cDCE, or simply to relieve oxidative stress (Jennings, Chartrand, *et al.*, 2009). PNP is an enzyme primarily associated with oxidative stress relief, and as it was up-regulated with degradation, it is most likely associated with relieving stress due to oxidation. Though results from Section 3.1 demonstrate that P450 I is capable of mediating the first step of cDCE degradation, it has such a low degree of up-regulation under any circumstances that it appears not to be a good candidate for tracking cDCE-degradation activity of JS666.

Other dynamic conditions could be explored; however with this experimental strategy (as evidenced from the results obtained to date), the window of interest when up-regulation occurs has been demonstrated to be too small to make the approach useful. The lags prior to degradation are long and unpredictable, necessitating far-too-frequent (infeasible) sampling to capture the region of interest. Therefore, we believe we have learned all we can from this line of investigation.

3.2.6 Literature Cited

Coleman, N. V., T. E. Mattes, J. M. Gossett and J. C. Spain (2002). "Biodegradation of *cis*-dichloroethene as the sole carbon source by a β-proteobacterium." Applied and Environmental Microbiology **68**(6): 2726-2730.

de Visser, S. P., D. Kumar and S. Shaik (2004). “How do Aldehyde Side Products Occur During Alkene Epoxidation by Cytochrome P450? Theory Reveals a State-Specific Multi-State Scenario where the High-Spin Component Leads to all Side Products.” Journal of Inorganic Biochemistry **98**(7): 1183-1193.

Freeman, W. M., Walker, S. J. and K. E. Vrana (1999). “Quantitative RT-PCR: Pitfalls and Potential.” Biotechniques **26**(1): 125.

Giddings, C. G. S., L. K. Jennings, and J. M. Gossett (2010). “Microcosm Assessment of a DNA Probe Applied to Aerobic Degradation of cis-1,2- Dichloroethene by Polaromonas sp. strain JS666.” Ground Water Monitoring & Remediation **30**(2): 97-105.

Giddings, C. G. S., F. Liu, and J. M. Gossett (2010). "Microcosm assessment of *Polaromonas* sp. JS666 as a bioaugmentation agent for degradation of *cis*-1,2-dichloroethene in aerobic, subsurface environments." Ground Water Monitoring and Remediation **30**(2): 106-113.

Isken, S. and J. A. de Bont (1998). “Bacteria Tolerant to Organic Solvents.” Extremophiles **2**(3): 229-238.

Jennings, L. K., M. M. G. Chartrand, G. Lacrampe-Couloume, B. S. Lollar, J. C. Spain, J. M. Gossett (2009). "Proteomic and transcriptomic analyses reveal genes upregulated by *cis*-dichloroethene in *Polaromonas* sp. strain JS666." Applied and Environmental Microbiology **75**(11): 3733-3744.

Johnson, D. R., Lee, P. K. H., Holmes, V. F. and L. Alvarez-Cohen (2005). “An Internal Reference Technique for Accurately Quantifying Specific mRNAs by Real-Time PCR with Application to the tceA Reductive Dehalogenase Gene.” Applied and Environmental Microbiology **71**(7): 3866-3871.

Mattes, T. E., Alexander, A. K., Richardson, P. M., Munk, A. C., Han, C. S., Stothard, P. and N. C. Coleman (2008). “The Genome of Polaromonas sp. JS666: Insights into the Evolution of a Hudrocarbon- and Xenobiotic-Degrading Bacterium, and Features of Relevance to Biotechnology.” Applied and Environmental Microbiology **74**(20): 6405-6416.

Peirson, S. N., Butler, J. N. and R. G. Foster (2003). “Experimental Validation of Novel and Conventional Approaches to Quantitative Real-Time PCR Data.” Nucleic Acids Research **31**(14): e73.

Rahm, B. G., Morris, R. M., and R. E. Richardson (2006). “Temporal Expression of Respiratory Genes in an Enrichment Culture Containing Dehalococcoides ethenogenes.” Applied and Environmental Microbiology **72**(8): 5486-5491.

Sharkey, F. H., Banat, I. M. and R. Marchant (2004). “Detection and Quantification of Gene Expression in Environmental Bacteriology.” Applied and Environmental Microbiology **70**(7): 3795-3806.

van Hylckama Vlieg, J. E. T. and D. B. Janssen (2001). "Formation and detoxification of reactive intermediates in the metabolism of chlorinated ethenes." Journal of Biotechnology **85**(2): 81-102.

4. MODULE 2 – ELUCIDATION OF CIS-DICHLOROETHENE AND VINYL CHLORIDE ANAEROBIC OXIDATION

4.1 Objective 1 – Anaerobic Oxidation

4.1.1 Background

Microcosm studies by other researchers have shown that cDCE and VC can be oxidized under iron- and manganese-reducing conditions (Bradley and Chapelle, 1996; Bradley and Chapelle, 1997; Bradley and Chapelle, 1998; Bradley, Chapelle, *et al.*, 1998a; Bradley, Chapelle, *et al.*, 1998b), but the pathways and microorganisms involved in such processes have not yet been identified, nor has the role of iron- and/or manganese-reduction in these processes been adequately delineated. A better understanding of the metal-linked oxidative mechanisms of cDCE and VC degradation is required to improve the authenticity of these reactions, and to improve stakeholder acceptance of the important role of these degradation mechanisms in MNA and EISB of cDCE and VC.

4.1.2 Research Objectives

The sub-objectives of Objective 1 (anaerobic oxidation) within this research module were the following:

1.1 Enrich/Isolate, Characterize & Pathway Determination

(Go/No-Go decision point);

1.2 Develop DNA-Based MBTs;

1.3 Develop CSIA Tools; and

1.4 Conduct Field Validation.

Research to address Objective 1 of Module 2 was primarily the responsibility of Dr. James Gossett at Cornell University, with collaborative support from Dr. Jim Spain at the Georgia Institute of Technology and Dr. Barbara Sherwood Lollar at the University of Toronto.

Studies in satisfaction of Objective 1.1 were unable to produce any enrichments or isolates capable of anaerobic oxidation. Therefore, Objectives 1.2, 1.3, and 1.4 were "no-go." Subsequently, the emphasis of Module 2 was redirected to the study of the aerobic oxidation of VC under extremely low oxygen conditions — conditions that would be easily confused with "anaerobic" (see Section 4.2 below).

4.1.3 Materials & Methods

Description of Candidate Materials

For this task, microcosms were constructed with materials from 17 separate sample locations obtained from nine sources. These are (in chronological order of set-up): (1) contents from two different columns operated by John Wilson (Shen and Wilson, 2007; USEPA-Kerr Lab), simulating a permeable reactive barrier constructed with magnetite and bark-mulch at Altus AFB, OK; (2) supernatant from the anaerobic sludge digester of the Ithaca Area Wastewater Treatment Plant, Ithaca, NY; (3) groundwater from three locations influenced by a chloroethene plume from a former fire-training pit (FT-02) at Plattsburgh AFB, NY: (4) sediments obtained from Paul Bradley (United States Geological Survey [USGS]) from Kingsbay Naval Air Station (NAS), GA outcrop and Kingsbay KBA-11-13A; (5) sediment obtained from Paul Bradley from NAS Jacksonville, FL; (6) sediments and adjacent groundwater from three Superfund sites (confidential), courtesy of Dr. David Freedman (Clemson University); (7) old microcosms (courtesy of Dr. Elizabeth Edwards, University of Toronto) from Cardinal Landfill, NH, that had been operated under anoxic conditions; (8) sediments from two locations at Aberdeen Proving Ground, MD; and (9) stream sediment and nearby groundwater from Cecil Field NAS, FL, the location being one where Bradley and Chapelle observed anaerobic oxidation of VC and cDCE many years ago under Fe(III)-reducing conditions (Bradley and Chapelle, 1996; Bradley and Chapelle, 1997; Bradley and Chapelle, 1998; Bradley, Chapelle, *et al.*, 1998a; Bradley, Chapelle, *et al.*, 1998b).

Laboratory Preparation

Each material was used to construct anoxic microcosms with or without freshly precipitated ferric iron (Fe[III]), and, quantity of material permitting, some were also prepared with freshly precipitated quadvalent manganese (Mn[IV]) (Table 4-1). Autoclaved (killed) controls accompanied all live bottles. The quantity we were provided of some materials was too limiting to prepare microcosms using the material for anything more than "inoculum" (in some cases, as low as 5 to 10 grams (g) per microcosm, with the balance consisting of approximately 50 to 100 mL of an anaerobic minimal salts medium).

Table 4-1: Summary of anaerobic cDCE microcosm set-up and results

Facility or Source	Sample Designation	Microcosm Setup	Duration (days)	Results
Magnetite/Mulch (PRB study, John Wilson, Altus AFB, OK)	Column B2, Effluent end (solids)	Material + Medium Fe(III) w/ and w/o	158	No loss of VC or cDCE
	Column B4, Effluent end (solids)	Material + medium Fe(III) w/ and w/o	152	1 live bottle w/o Fe(III) showed reductive dechlor of cDCE
Ithaca Area Wastewater Trmt Plant, NY	Anaerobic Digester Supernatant (liquid)	10% supernatant + medium Fe(III) w/ and w/o Mn(IV) w/ and w/o	131	1 live bottle w/o Fe(III) showed reductive dechlor of cDCE
Plattsburgh AFB Fire Training Pit Plume (FT-02), NY	Influent to groundwater treatment plant (water)	Site water + medium Fe(III) w/ and w/o	218	2 live bottles w/o Fe(III) showed reductive dechlor of VC
	Idaho Ave. Collection Trench (water)	Site water + medium Fe(III) w/ and w/o	174	2 live bottles w/o Fe(III) showed reductive dechlor of VC
	East Flightline Collection Trench (water)	Site water + medium Fe(III) w/ and w/o	172	1 live bottle w/o Fe(III) showed reductive dechlor of cDCE; 1 live bottle w/o Fe(III) showed reductive dechlor of VC
Kingsbay NAS sediments (Paul Bradley), GA	Kingsbay Outcrop (sediment)	Site sediment + medium Fe(III) w/ and w/o	171	No loss of VC or cDCE
	Kingsbay KBA-11-13A (sediment)	Site sediment + medium Fe(III) w/ and w/o	182	No loss of VC or cDCE
NAS Jacksonville sediment (Paul Bradley), FL	(sediment)	Site sediment + medium Fe(III) w/ and w/o	178	No loss of VC or cDCE
Superfund Site Materials (David Freedman)	"Clemson" site 1 (sediment and water)	Sediment + site water + medium Fe(III) w/ and w/o	145	No loss of VC or cDCE
	"Clemson" site 3 (sediment and water)	Sediment + site water + medium Fe(III) w/ and w/o	90	1 live bottle w/o Fe(III) showed minor reductive dechlor of cDCE; 1 live bottle w/o Fe(III) showed minor reductive dechlor of VC
	"Clemson" site 4 (sediment and water)	Sediment + site water Fe(III) w/ and w/o	145	No loss of VC or cDCE
	"Clemson" site 4 (sediment and water)	Sediment + site water + medium Fe(III) w/ and w/o	130	No loss of VC or cDCE

Facility or Source	Sample Designation	Microcosm Setup	Duration (days)	Results
Microcosms from Cardinal Landfill (Elizabeth Edwards), NH	Cardinal SO4 microcosms	Material + medium Fe(III) w/ and w/o	133	2 live bottles w/o Fe(III) showed minor reductive dechlor of cDCE
Aberdeen Proving Ground (West Canal Creek), MD	Aberdeen WB23 (sediment)	Sediment + medium Fe(III) w/ and w/o	45	Extensive reductive dechlor of cDCE and VC in all live bottles w/ or w/o Fe(III)
	Aberdeen WB30 (sediment)	Sediment + medium Fe(III) w/ and w/o	32	Extensive reductive dechlor of cDCE and VC in all live bottles w/ or w/o Fe(III)
Cecil Field NAS (Site 3), FL	Stream sediment (Rowell Creek) and Groundwater (MW-31S)	Sediment + groundwater Fe(III) w/ and w/o	26	Reductive dechlor of cDCE and VC in all live bottles w/ and w/o Fe(III) (except for one VC+Fe live)
	Stream sediment (Rowell Creek) and Groundwater (MW-31S)	Sediment + groundwater + medium Fe(III) w/ and w/o	24	1 live bottle w/ Fe(III) showed minor reductive dechlor of cDCE. All live bottles w/o Fe (III) showed reductive dechlor of cDCE and VC
	Stream sediment(Rowell Creek)	Sediment + medium (w/o YE) Fe(III) w/ and w/o Mn(IV) w/ and w/o	Pending set-up	not applicable

Notes:
cDCE - cis-1,2-dichloroethene
dechlor - dechlorination
Fe (III) - ferric iron
Mn(IV) - manganese
MW - monitoring well
SO4 - sulfate
VC - vinyl chloride
w/ - with
w/o - without

A strategy we employed was to add yeast extract (10 kilograms) to provide electron donor to establish suitable low redox conditions to encourage metal-reduction; by maintaining low H_2 concentrations, the presence of Fe(III) or Mn(IV) was expected to suppress undesired reductive dechlorination.

Microcosms were prepared in 160-mL serum bottles with total aqueous volume of 100 mL. The aqueous volume was either site water or medium – or a mixture of site water and medium. The freshwater enrichment medium was prepared according to a modified recipe of Lovley and Phillips (Lovley and Phillips, 1986). The medium contained 2.5 grams per liter (g/L) $NaHCO_3$, 0.1 g/L $CaCl_2 \cdot 2H_2O$, 0.1 g/L KCl, 1.5 g/L NH_4Cl, 0.69 g/L $NaH_2PO_4 \cdot H_2O$, 0.1 g/L NaCl, 0.1 g/L $MgCl_2 \cdot 6H_2O$, 0.01 g/L $MgSO_4 \cdot 7H_2O$, 0.005 g/L $MnCl_2 \cdot 4H_2O$, 0.001 g/L $Na_2MoO_4 \cdot$

$2H_2O$, and 0.01 g/L yeast extract. The medium was purged with N_2/CO_2 (80/20) gas for 30 min, as were empty serum bottles prior to their filling. Under continuous N_2/CO_2 purge, site material was delivered to each serum bottle, followed by the anaerobic delivery of medium (where used). The serum bottles were capped with Teflon-lined, butyl-rubber septa and crimped with aluminum caps. Where Fe(III) or Mn(IV) was added, 5-mL volume of freshly-precipitated Fe(III) oxyhydroxide or Mn(IV) stock suspension was injected to the Fe- or Mn(IV)-amended serum bottles to yield a final total Fe or Mn(IV) concentration of 10 mM; 5 mL additional, anoxic medium was added to bottles that did not receive Fe- or Mn(IV)-amendment. VC or cDCE was delivered to the designated microcosms to give a final nominal concentration of 10.5 milligrams per liter (mg/L) (108 μM) for cDCE or 10.1 mg/L (162 μM) for VC as electron donors. Microcosms were then incubated in the dark, unshaken, at 22˚C.

Preparation of Fe (III) Suspension

Freshly prepared Fe(III) oxyhydroxide suspension was prepared following the method of Lovley and Phillips (Lovley and Phillips, 1986). A $FeCl_3$ solution of 0.4 M was neutralized with NaOH solution to reach pH 7. The resulting Fe (III) oxyhydroxide solution was rinsed with deionized water and centrifuged repeatedly to remove Cl^-. The stock solution achieved a final concentration of 200 mM. Microcosms amended with Fe(III) were dosed at the 10-mM level.

Preparation of Mn(IV) Suspension

Freshly prepared, amorphous MnO_2 was employed in a few experiments with site materials that were not obviously candidates for Fe(III) reduction. The MnO_2 was synthesized according to the procedure of Lovley and Phillips (Lovley and Phillips, 1988) by slowly adding a solution of $MnCl_2$ (30 mM) to a basic solution of $KMnO_4$ (20 mM) which was stirred with a magnetic stir bar. This yields a poorly crystalline MnO_2 that was formed, was allowed to settle, and then washed with distilled, deionized water by centrifugation. It was dosed to microcosms at the same, 10-mM level as was used with Fe(III)-amended microcosms.

Analytical Methods

100-μL headspace samples were analyzed for cDCE and VC with a PerkinElmer Autosystem gas chromatography equipped with a FID. The temperature program was 90°C for 2.5 min, increased at 30°C/min to 195°C.

A 0.1-mL aliquot of the mixed microcosm contents was taken from each Fe-amended bottle, diluted with deionized water as needed, and analyzed with a ferrozine colorimeter method for total Fe and a phenanthroline method for ferrous iron (Fe[II]) analysis (Hach Company, Loveland, CO). Soluble Mn was assayed in Mn(IV)-amended bottles using Hach Method 8034.

4.1.4 Results & Discussion

A summary of the results is presented in Table 4.1, showing that the earliest microcosm sets were monitored for over 7 months; others just a couple of weeks. The strategy of adding a small concentration of yeast extract to establish good metal-reducing conditions in live microcosms to which oxidized forms of Fe or Mn were added proved quite successful, as evidenced by increases in reduced forms of these metals as seen in the treatment for microcosms prepared from influent to a groundwater-treatment plant at the former Plattsburgh AFB, NY (Figure 4-1).

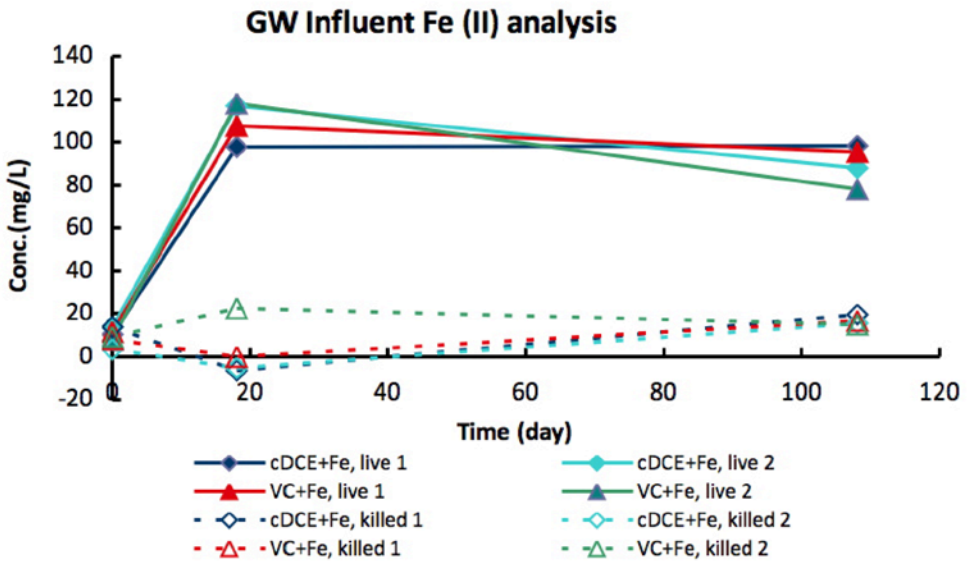

Figure 4-1: Microcosm trend plot for anaerobic oxidation study – Fe(II) (Plattsburg AFB, NY)

With the exception of a few of the live microcosms without Fe(III) or Mn(IV) that showed reductive dechlorination of cDCE to VC, none of the microcosms has shown any transformation of the chlorinated compounds. Examples of typical results for cDCE and VC are shown in Figures 4-2 and 4-3, respectively, for microcosms prepared from influent to a groundwater-treatment plant at the former Plattsburgh AFB, NY. Note that conditions suitable for Fe-reduction are evident from the Fe(II) data (Figure 4-1). The amount of freshly precipitated Fe(III) we added to Fe-amended microcosms was about 560 mg Fe/L, and from the plateau in Fe(II) (*ca.* 100 mg/L), it is apparent that Fe(III) was not depleted. Visually, there remained an orange color in these microcosms. The amount of yeast extract provided (10 mg/L) was purposefully chosen not to deplete all of the Fe(III) after the yeast extract was spent, ensuring long-term sustenance of Fe-reducing conditions in the bottles. This was quite successful, as the only reductive dechlorination observed was in microcosms without added Fe(III). In fact, in all microcosms that were run, the only Fe(III)-amended ones that evidenced reductive

dechlorination were from muck-like materials that supplied so much native electron donor that Fe(III) did become depleted.

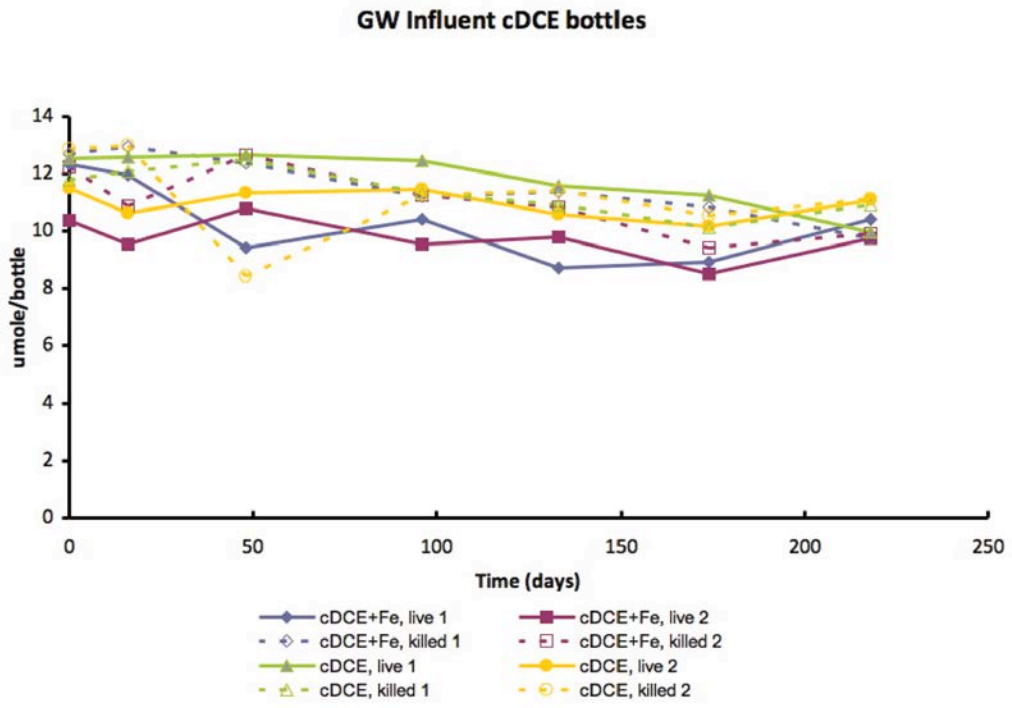

Figure 4-2: Microcosm trend plot for anaerobic oxidation study - cDCE (Plattsburg AFB, NY)

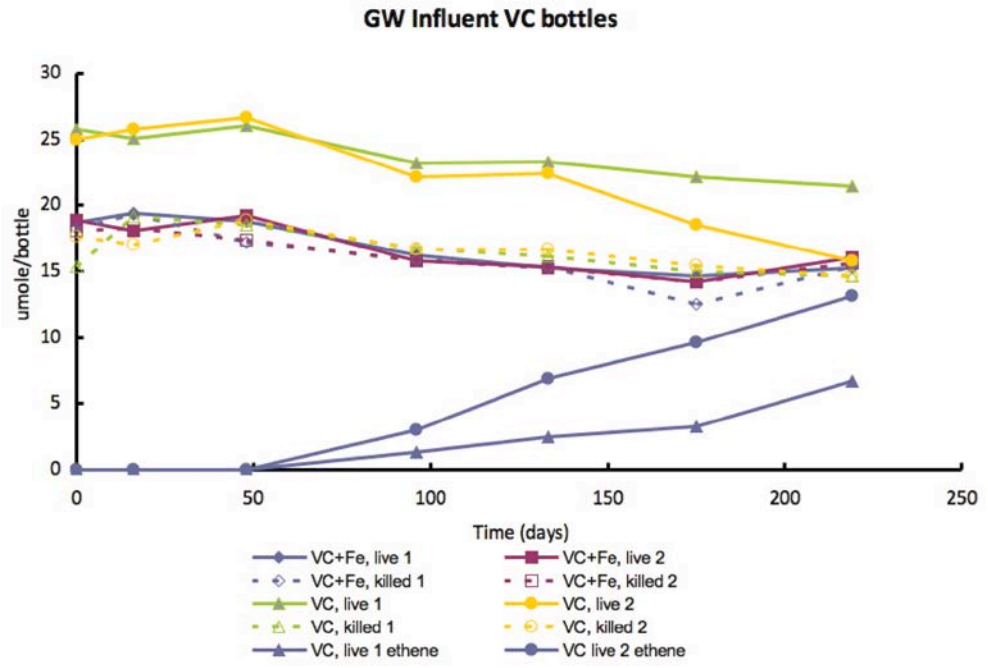

Figure 4-3: Microcosm trend plot for anaerobic oxidation study - VC (Plattsburg AFB, NY)

4.1.5 Conclusions and Implications for Future Research / Implementation

Unfortunately, though excellent metal-reducing conditions were established in microcosms, none evidenced the slightest oxidation of cDCE or VC. The only transformation of chloroethenes we observed were their reductive dechlorination in anoxic microcosms lacking oxidized Fe or Mn.

To date, we have now monitored (including current bottles) 352 individual microcosms, with no evident anaerobic oxidation of cDCE or VC. Since no enrichments capable of anaerobic oxidation of cDCE and VC could be developed from materials collected, then the subsequent steps of Objective 1 of this module were not implemented (Go/No-Go Decision Point).

4.1.6 Literature Cited

Bradley, P. M. and F. H. Chapelle (1996). "Anaerobic mineralization of vinyl chloride in Fe(III)-reducing aquifer sediments." Environmental Science & Technology **30**(6): 2084-2086.

Bradley, P. M., and F. H. Chapelle (1997). "Kinetics of DCE and VC mineralization under methanogenic and Fe(III)-reducing conditions." Environmental Science & Technology **31**(9): 2692-2696.

Bradley, P. M., and F. H. Chapelle (1998). "Microbial mineralization of VC and DCE under different terminal electron accepting conditions." Anaerobe **4**(2): 81-87.

Bradley, P. M., F. H. Chapelle, and D. R. Lovley (1998a). "Humic acids as electron acceptors for anaerobic microbial oxidation of vinyl chloride and dichloroethene." Applied and Environmental Microbiology **64**(8): 3102-3105.

Bradley, P. M., F. H. Chapelle, and J. T. Wilson (1998b). "Field and laboratory evidence for intrinsic biodegradation of vinyl chloride contamination in a Fe(III)-reducing aquifer." Journal of Contaminant Hydrology **31**(1): 111-127.

Lovley, D. R., and E. J.P Phillips (1986). "Organic matter mineralization with reduction of ferric iron in anaerobic sediments." Applied and Environmental Microbiology **51**(4): 683-689.

Lovley, D. R., and E. J.P. Phillips (1988). "Novel mode of microbial energy metabolism: Organic carbon oxidation coupled to dissimilatory reduction of iron or manganese." Applied and Environmental Microbiology **54**(6): 1472-1480.

Shen, H., and J. T. Wilson (2007). "Trichloroethylene removal from groundwater in flow-through columns simulating a permeable reactive barrier constructed with plant mulch." Environmental Science & Technology **41**(11): 4077-4083.

4.2 Objective 2 – Aerobic Oxidation of Vinyl Chloride at Extremely Low Oxygen Concentrations

4.2.1 Background

As reported above (Section 4.1), no anaerobic oxidation activity on cDCE or VC was found after approximately 400 microcosms had been constructed with materials from 17 separate sample locations, obtained from nine candidate sites, and microcosms were incubated for greater than 6 months.

An alternative explanation for disappearance of VC at some sites, in what are thought to be anaerobic subsurface environments, is that the environments are, in fact, not anaerobic. Rather, they might be subject to low, steady influx of oxygen, and aerobic oxidation could be occurring at extremely low oxygen concentrations.

Several previous reports provide the genesis for this hypothesis. First, the half-velocity constants and oxygen thresholds measured for five different pure cultures of aerobic VC-degraders were all extremely low (Coleman, Mattes, *et al.*, 2002). Thresholds for oxygen use ranged from 0.02 to 0.1 mg/L – concentrations low enough that comparable subsurface environments would likely be classified as "anaerobic" in field assessments. Additionally, Schmidt and Tiehm (Schmidt and Tiehm, 2008) observed that aerobic VC-oxidizing bacteria survived anaerobic conditions for up to a year and maintained their ability for aerobic degradation, which they observed at dissolved oxygen concentrations between 0.1 and 0.3 mg/L. Finally, an aerobic, VC-oxidizing Mycobacterium was isolated from what was thought to be an anaerobic microcosm (Fullerton, High, *et al.*, 2009).

4.2.2 Research Objectives

The revised focus (Objective 2) of Module 2 was to test the hypothesis of sustained vinyl chloride oxidation at low oxygen concentrations. Research for Objective 2 of Module 2 was primarily the responsibility of Dr. James Gossett at Cornell University.

4.2.3 Materials & Methods

This work has been published in Environmental Science and Technology (Gossett, 2010). Therefore, only a summary of methods and results are presented here.

Influenced by these previous reports of aerobic VC-oxidation, we selected several microcosms that had been incubated anaerobically for five months and subsequently amended them with oxygen. VC-oxidation commenced within 42 days in three of them, and a second addition of VC was degraded completely within an additional 8 days.

Studies were then conducted with VC-oxidizing transfer cultures derived from two chloroethene-contaminated sites, as well as with microcosms constructed from sediment and groundwater from one of these sites. Oxygen was steadily delivered to the experimental systems using LDPE permeation tubes to maintain low dissolved oxygen throughout the time-course of investigation.

4.2.4 Results & Discussion

With VC-oxidizing transfer cultures and microcosms derived from authentic site materials, VC oxidation was sustained at DO concentrations below 0.02 and 0.1 mg/L, respectively. This supports the possibility that – at least at some sites – apparent loss of VC from what are thought to be anaerobic zones might, in fact, be due to aerobic pathways occurring under conditions of low oxygen flux (e.g., via diffusion from surrounding aerobic regions and/or from recharge events). Groundwaters with DO concentrations of 0.1 mg/L would likely be labeled "anaerobic;" and those with DO of 0.02 mg/L, most assuredly. Field measurement of dissolved oxygen is generally accomplished with membrane electrodes, and low DO concentrations are typically considered to indicate "anaerobic conditions," since the time-constant of the membrane electrode is rather long (i.e., the approach of the reading to the true value is increasingly slow as the true value approaches zero). Furthermore, DO instrumentation is typically calibrated at high DO, not at low DO concentrations. If geochemical data show typical end-products of anaerobic processes (e.g., methane, reduced iron, sulfide), that usually solidifies a conclusion of anaerobic conditions. However, monitoring wells are often screened over >1 meter depth intervals; and the depth interval of an aquifer contributing water to a pumped sample can exceed the screened interval considerably, resulting in a sample that represents a mix of different in-situ strata (some anaerobic and some aerobic), complicating assessment of biogeochemical conditions.

Very little oxygen would be required for aerobic degradation to have significant impact. The stoichiometry measured in this study (2.025 mol O_2/mol VC) converts to almost exactly 1:1 on a

mass basis. Thus, a VC concentration of 100 ppb would require only 0.1 mg/L DO for its complete degradation by aerobes. Furthermore, reports suggest that aerobic VC-oxidizers are common at chloroethene-contaminated sites (Coleman, Mattes, *et al.*, 2002), and can survive prolonged exposure to truly anaerobic conditions (Schmidt and Tiehm, 2008). One of the aerobic, VC-oxidizing cultures in this present study (Cecil Field) was derived from a microcosm that had exhibited reductive dechlorination and methane production over 140 days of anaerobic incubation, before it was administered oxygen to commence aerobic oxidation of VC.

What of the potential for aerobic oxidation in studies intended to be anaerobic? Bradley *et al.* recognized the potential problem with oxygen contamination of experiments designed to investigate "anaerobic oxidation" (Bradley, Chapelle, *et al.*, 2008). To avoid such artifacts, they suggested that many investigators had gone to the alternate extreme of establishing excessively high reducing conditions, incompatible with processes such as iron or manganese reduction. And therein lies the dilemma: experiments designed to study the role of iron- or manganese-reducing bacteria in chloroethene transformation must operate under conditions only slightly more reducing than microaerophilic regimes. The potential for artifact resulting from small amounts of oxygen introduction is therefore significant. In the context of a typical experimental microcosm with 100 mL liquid, a nominal concentration of 100 ppb VC (0.16 µmol VC) would require only 0.32 µmol O_2 for its aerobic degradation. That requirement would be met by the cumulative introduction of only 40 µL of air over the course of microcosm operation. Given multiple sampling events and the possibility of developing a vacuum in bottles from repeated sampling, introduction of such quantities of air is not unreasonable. Obviously, the potential for significant aerobic contribution to observed VC disappearance increases at lower VC levels.

4.2.5 Conclusions and Implications for Future Research / Implementation

The idea that aerobic oxidation can be significant mechanism for chloroethene remediation in zones previously classified as “anaerobic” has gained traction. Since the paper by Gossett was published in 2010, it has now been cited 12 times in published papers by other authors, including Bradley’s, “Reinterpreting the importance of oxygen-based biodegradation in chloroethene-contaminated groundwater” (Bradley, 2011).

Our studies underscore both the need to assess the potential for aerobic VC oxidation at sites, as well as the difficulty in doing so. Given that sustained VC oxidation was observed at DO concentrations below 0.02 mg/L, it is not practical to exclude its possibility through measurement of DO. Assessment of aerobic VC oxidation activity can be done with microcosms, of course. However, aerobic VC-degraders are likely to be limited in distribution to a relatively small zone at the interface between truly anaerobic and aerobic portions of a contaminant plume – i.e., degradation is so rapid that VC might not persist far into the aerobic zone. Microcosm studies are relatively expensive, a factor tending to restrict the number of sampling locations investigated. Given the number of sampling points required to detect an activity likely to be narrowly distributed at an ill-defined anaerobic/aerobic interface, the most cost-effective way would seem to be through application of molecular biological tools targeting

aerobic processes. DNA-based tools would enable investigators to determine the current (or at least recent) presence of aerobic VC-oxidizers. Better still, tools based on transcription (mRNA) of VC-degradative genes would allow detection of on-going activity in otherwise mischaracterized "anaerobic" environments. One apparent impediment to development of such tools is the lack of distinguishing genotypical features between aerobic ethene-degraders capable of VC-oxidation and those that are not (Coleman and Spain, 2003). However, a recent study (Yang and Mattes, 2008) found that extended exposure of ethene-oxidizers to VC caused their adaptation to use of VC as growth substrate, perhaps making it less important to distinguish among phenotypes of ethene-oxidizers. Detection of generic, aerobic, "ethenotrophic" bacteria would likely be sufficient to distinguish low-oxygen aerobic plumes from truly anaerobic ones.

4.2.6 Literature Cited

Bradley, P. M., Chapelle, F. H. and F. E. Löffler (2008). "Anoxic mineralization: environmental reality or experimental artifact?" Ground Water Monitoring & Remediation **28**(1): 47-49.

Bradley, P. M. (2011). "Reinterpreting the importance of oxygen-based biodegradation in chloroethene-contaminated groundwater." Ground Water Monitoring and Remediation **31**(4): 50-55.

Coleman, N. V. and J. C. Spain (2003). "Distribution of the Coenzyme M pathway of epoxide metabolism among ethene- and vinyl chloride-degrading Mycobacterium strains." Applied and Environmental Microbiology **69**(10): 6041–6046.

Coleman N. V., Mattes, T. E., Gossett, J. M. and J. C. Spain (2002). "Phylogenetic and kinetic diversity of aerobic vinyl chloride-assimilating bacteria from contaminated sites." Applied and Environmental Microbiology **68**(12): 6162-6171.

Fullerton, H., High, J., Reid, A., Lehmicke, L., Freedman, D. L., and S. H. Zinder (2009). "Isolation of aerobic vinyl chloride oxidizing microorganisms from anaerobic groundwater microcosms." Abstracts from the 109th General Meeting of the American Society of Microbiology Philadelphia, May 17-21.

Gossett, J. M. (2010). "Sustained aerobic oxidation of vinyl chloride at low oxygen concentrations." Environmental Science & Technology **44**(4): 1405-1411.

Schmidt, K. R. and A. Tiehm (2008). "Natural attenuation of chloroethenes: identification of sequential reductive/oxidative biodegradation by microcosm studies." Water Science & Technology **58**(5): 1137-1145.

Yang, O. J. and T. E. Mattes (2008). "Adaptation of aerobic, ethene-assimilating Mycobacterium strains to vinyl chloride as a growth substrate." Environmental Science & Technology 42(13): 4784-4789.

5. MODULE 3 – REDUCTIVE DECHLORINATION

5.1 Background and Objectives

The process of reductive dechlorination of chloroethenes to ethene has been extensively studied over the last decade, and considerable understanding about the microorganisms and mechanisms involved has been achieved. However, there remains some uncertainty about the relationship between observed carbon isotope fractionation and the underlying mechanisms of cDCE and VC reductive dechlorination. The results from this research module are essential for determining the appropriate enrichment factors to apply in field studies for quantification of biodegradation, and for distinguishing between different processes degrading cDCE and VC.

In addition, the fate of ethene produced by reductive dechlorination of VC is not completely understood. At many sites, the molar concentration of ethene produced is far lower than would be expected from the stoichiometric conversion of parent chlorinated ethenes. The lack of mass balance is often attributed vaguely to further reduction of ethene to ethane or anaerobic or aerobic oxidation of ethene to CO_2.

The objectives of this research module are the following:

1. Investigate the applicability of laboratory-derived enrichment factors for microbially mediated reductive dechlorination reactions to field conditions; and

2. Investigate the fate of ethene produced by reductive dechlorination.

5.2 Objective 1 – Carbon Isotope Fractionation Variability during Reductive Dechlorination

5.2.1 Background

Objective 1 attempts to answer the question of how well laboratory-derived fractionation factors can be extrapolated to the field. To date, all laboratory studies have been conducted for cDCE and VC when they were present as the parent compounds spiked into microcosms, rather than produced as daughter products from more chlorinated precursors. Recent research by Morrill *et al.* (in review) suggests that for VC in particular, the fractionation factors for VC degrading as a parent compound may be significantly different than for VC which is first produced from a more chlorinated parent and subsequently degraded. These findings might be explained by a two-step process of fractionation where the overall observed fractionation is the combined effect of fractionation due to enzymatic reaction as well as fractionation due to transport across the cell membrane. This hypothesis was tested by comparing isotopic fractionation in free cell extracts to the values obtained in whole cell microcosm studies. The results are essential for determining the appropriate fractionation factors to apply in field studies for quantification of biodegradation, and for distinguishing between different processes degrading cDCE and VC.

5.2.2 Research Objectives

These experiments were initially designed to test the hypothesis that transport of VC across the cell membrane might result in a depression of the observed fractionation effect. Recent literature has discussed a variety of processes that might account for such masking effects, but transport across the cell membranes was an obvious potential hypothesis given its well-known role in depressing the observed carbon isotope effects during photosynthesis (O'Leary, 1988). Nijenhuis *et al.* (2005) observed this effect for PCE dechlorination. Previous work in our own group (Morrill *et al.*, 2006) had also suggested that fractionation during VC dechlorination was significantly less if VC was the initial substrate, compared to if VC was an intermediate in dechlorination, suggesting a possible effect due to transport or diffusion.

5.2.3 Materials & Methods

In early 2009, we refined our cell-free extract techniques to improve reproducibility, and understand kinetic differences between extracts taken at different conditions (with presumably a different enzyme content) and assayed under different conditions.

These experiments were prepared using a series of vials, each containing buffer solution, cell free extracts, and chlorinated electron acceptor and inhibitor. The experiments were run twice, allowing the chlorinated compound to degrade 95 to 99%. Experiments with KB-1® culture whole cells were also performed, to repeat the experiments of Slater *et al.* Duplicate bottles, each containing media, KB-1® culture, and 1 mL VC were prepared. The experiment was run three times, for approximately 15 to 28 hours each time, which allowed VC to degrade 48 to 95%. Concentrations and $\delta^{13}C$ values were measured throughout each experiment using headspace analysis on GC and gas chromatography-combustion-isotope ratio mass spectrometry (GC/C/IRMS).

5.2.4 Results & Discussion

For this milestone, several experiments were conducted to compare fractionation in cell-free extracts (CFE) and whole cell cultures of KB-1® amended with vinyl chloride. The measured fractionation in whole cell cultures in these experiments was entirely consistent with published literature from various sources on VC fractionation (Table 5-1, right column). Interestingly, and somewhat unexpectedly, the enrichment factors in cell-free extracts were consistently lower than in the corresponding whole cell experiments (Table 5-1, left column).

Table 5-1: Summary of vinyl chloride enrichment factors

Cell-Free Extracts		Whole Cells	
ε	95% CI	ε	95% CI
-19.5	1.4	-25.0	1.8
-19.2	1.1	-25.7	1.5
-20.1	0.7	-25.5	1.6

Notes:
ε - enrichment factor
CI - confidence interval
VC - vinyl chloride

The results obtained in our experiments also indicate that, for VC, fractionation during biodegradation may in fact be smaller in cell-free extracts than in whole cell cultures. This finding rules out a significant role for membrane transport as a rate limiting step during VC dechlorination. Similar results showing no effect of transport have now been observed in comparable studies conducted more recently on TCE (Cichocka *et al.*, 2007) and on 4 other chlorinated compounds (1,2-DCA, chloropentane, 1,3-dichloropentane and chlorobutane) (Abe *et al.*, 2009).

The finding of smaller fractionation in cell-free extracts is consistent with recent results also obtained by the University of Toronto in a separate study carried out for both whole cell and cell-free extract degradation of 1,1,1-TCA and 1,1-DCA (Sherwood Lollar *et al.*, 2010), where again we observed lower fractionation in cell-free extracts compared to whole cell cultures. These findings are important as they suggest another mechanism, other than membrane transport, is controlling the observed fractionation patterns, possibly related to enzymatic efficiency effects of the type previously demonstrated by Mancini *et al.* (2006).

Another possible explanation for variable fractionation factors in dechlorinating cultures such as KB-1® is the fact that multiple reductive dehalogenases are expressed simultaneously in the culture, even by a single *Dehalococcoides* strain, and that during our experiments, we may very well be assaying different enzymes, and thus not making accurate comparisons. Therefore we have shifted our emphasis to attempting to purify these enzymes and to determine experimental protocols to reliably express the same enzyme complement, work which is outside the scope of this project. Until we have a reasonable method to systematically assess enzyme efficiency for individual and specific reductive dehalogenases, we cannot further evaluate this new hypothesis about enzymatic efficiency.

In the free cell extract experiments, the average enrichment factor for the five vials was found to be approximately -30.l ‰. Each vial fit the Rayleigh model with R^2 values of greater than 0.99.

In contrast, in the whole cell experiments, the fractionation factor ranged from -21.5‰ ± 4.8‰ to -29.4‰ ± 1.0‰ with R^2 values greater than 0.96. These fractionation factors span the range between the values observed by Slater *et al.*[(1)] for whole cells, and the values obtained in the cell free extract experiments.

5.2.5 Conclusions and Implications for Future Research / Implementation

Our experiments have ruled out a significant role for membrane transport as a rate-limiting step during VC dechlorination. Observed small differences in fractionation between whole cells and cell free extracts for VC dechlorination may relate to the presence of multiple enzymes, and changes in enzymatic efficiencies, but in order to test these hypotheses, more pure enzyme preparations are required. Purifying reductive dehalogenases is a very significant undertaking that was not part of the scope of work.

5.2.6 Literature Cited

Abe, Y.; Zopfi, J.; Hunkeler, D. (2009). "Effect of molecule size on carbon isotope fractionation during biodegradation of chlorinated alkanes by Xanthobacter autotrophicus GJ10." Isotopes in Environmental and Health Studies **45**(1): 18-26.

Cichocka, D.; Siegert, M.; Imfeld, G.; Andert, J.; Beck, K.; Diekert, G.; Richnow, H. H.; Nijenhuis, I. (2007). "Factors controlling the carbon isotope fractionation of tetra- and trichloroethene during reductive dechlorination by Sulfurospirillum ssp. and Desulfitobacterium sp. strain PCE-S." FEMS Microbiology Ecology **62**(1): 98-107.

Mancini, S. A.; Hirschorn, S. K.; Elsner, M.; Lacrampe-Couloume, G.; Sleep, B.; Edwards, E. A.; Sherwood Lollar, B. (2006). "Effects of trace element concentration on enzyme controlled stable isotope fractionation during aerobic biodegradation of toluene." Environmental Science & Technology **40**(24): 7675-7681.

Morrill, P. L.; Sleep, B. E.; Slater, G. F.; Edwards, E. A.; Sherwood Lollar, B. (2006). "Evaluation of isotopic enrichment factors for the biodegradation of chlorinated ethenes using a parameter estimation model: toward an improved quantification of biodegradation." Environmental Science & Technology **40**(12): 3886-3892.

Nijenhuis, I.; Andert, J.; Beck, K.; Kastner, M.; Diekert, G.; Richnow, H. H. (2005). "Stable isotope fractionation of tetrachloroethene during reductive dechlorination by Sulfurospirillum multivorans and Desulfitobacterium sp. strain PCE-S and abiotic reactions with cyanocobalamin." Applied and Environmental Microbiology **71**(7): 3413-3419.

O'Leary, M. H. (1988). "Carbon Isotopes in Photosynthesis." Bioscience **38**(5): 328-336.

Sherwood Lollar, B., S. Hirschorn, S.O.C. Mundle, A. Grostern, E.A. Edwards, and G. Lacrampe-Couloume. (2010). "Insights into Enzyme Kinetics of Chloroethane Biodegradation Using Compound Specific Stable Isotopes." Environmental Science & Technology **44**(19): 7498–7503.

Slater, G. F., B. Sherwood Lollar, B. E. Sleep, and E. A. Edwards. (2001). "Variability in carbon isotopic fractionation during biodegradation of chlorinated ethenes: Implications for field applications." Environmental Science & Technology **35**(5): 901-907.

5.3 Objective 2 – Fate of Ethene and Impact on Mass Balance during Reductive Dechlorination

5.3.1 Background

Objective 2 attempted to address concerns of the fate of ethene produced by reductive dechlorination of VC. At many sites, the molar concentration of ethene produced is far lower than would be expected from the stoichiometric conversion of parent chlorinated ethenes. The lack of mass balance is often attributed vaguely to further reduction of ethene to ethane or anaerobic or aerobic oxidation of cDCE, VC and/or ethene to CO_2. We attempted to verify these claims by measuring the isotopic composition of ethene produced in a variety of different microcosms and under a variety of different conditions to determine if further degradation of ethene could be stimulated or not. If ethene was further transformed, it was assumed that the residual ethene would become progressively more enriched in ^{13}C, to an extent beyond that found in the parent chloroethenes. If such enrichment was observed, we intended to identify the mechanisms (reductive dechlorination or anaerobic/aerobic oxidation) and through a broader survey in conjunction with work in other modules, establish how common a process it was, and how best to validate its occurrence in the field. Reduction of ethene to ethane has been observed in previous microcosm studies in our own lab and by others[1], so it was anticipated that we would be able to obtain positive results to compare to new field data.

Microbial degradation of ethene is commonly observed in aerobic systems, with fewer cases reported in anaerobic systems; however, limited information is available on the isotope enrichment values (ε) associated with these processes. Aerobic degradation of ethene is thought to occur via oxidative processes that lead to CO_2. Anaerobic degradation processes have been shown to transform ethene quantitatively to ethane. If either process is sensitive to isotopic fractionation on carbon, to the extent that ethene is degraded at a contaminated field site the isotope signature of ethene may reveal that further degradation is taking place.

5.3.2 Research Objectives

The overall goal of this study was to test the hypothesis that carbon isotope fractionation during degradation of ethene can be used to evaluate compositional and isotopic mass balance during dechlorination, so as to explain poor ethene mass balance. This hypothesis was tested through a combination of microcosm studies using materials from several sites, and field data from a contaminated field site in southwestern Ontario (Canada) currently undergoing EISB. The goal was to determine whether or not ethene biodegradation was occurring in addition to reductive dechlorination, to explain poor ethene mass balance.

5.3.3 Microcosm Studies - Materials & Methods

Laboratory media used to initiate the study of ethene degradation was obtained from discussions with colleagues. Two prior microcosm studies derived from contaminated site material were identified where significant transformation of ethene to ethane was noted. One set of microcosms was from a study initiated by Dr. David Freedman of Clemson University in 2003. Another set of microcosms was identified from the archives of Dr. Elizabeth Edwards from a 1998 study in conjunction with Geosyntec Consultants. These microcosms were retrieved and amended with substrates and were monitored for transformation of ethene to ethane, as described below.

5.3.3.1 Freedman Microcosms (CRP48 Lac 1-3, CRP50 Lac 1-3)

Microcosms were prepared in the laboratory of Dr. David Freedman at Clemson University using soil and groundwater from two locations in a wetland downgradient of a former TCE disposal pit. Three replicate microcosms (labeled 1-3) were prepared from each location in 2003 and monitored since that date with re-feeding as necessary. Ethane production was noted early in the study but soon ceased with ethene being the sole end product of dechlorination (D. Freeman, email communication with E. Edwards, July 2007). Microcosm bottles (6) were shipped to the University of Toronto in the summer of 2007 for the current study which commenced on October 19, 2007 (Day 1), when they were amended with sodium lactate as a potential electron donor, and neat VC.

5.3.3.2 Landfill Microcosms (L-A, L-B, L-C)

Three replicate microcosms were constructed in 1998 using soil and groundwater from a former industrial landfill in New Hampshire. Contaminants included TCE as well as benzene, toluene, xylenes, and other chlorinated aliphatic compounds. Microcosms were incubated anaerobically and were amended with sodium acetate, sodium lactate, methanol, and ethanol as potential electron donors; dechlorination of TCE to ethane was noted. After the study, the microcosms were sealed and archived in the dark at room temperature until Day 1 of the current study (November 16, 2007). Headspace was purged with a CO_2/NO_2 mix, then cultures were fed VC to a target concentration of 0.2 mg/L aqueous (1 µmol/bottle) and methanol, ethanol, and lactate as potential electron donors.

5.3.3.3 Negative Control Sample (KB-1®)

An enrichment of KB-1® on VC was maintained as a negative control for future isotope studies, as this culture does not degrade ethane (i.e., ethene is a stable end product of VC dechlorination).

5.3.4 Microcosm Studies - Results & Discussion

We determined the enrichment values (ε) associated with microbial degradation of ethene in both anaerobic and aerobic microcosms using CSIA. We compared these results to the $\delta^{13}C$ isotope signatures of trichloroethene, cis-dichloroethene, vinyl chloride, and ethene measured from a field site undergoing active EISB in Ontario, Canada, to determine if CSIA is an effective approach to assess the accumulation of daughter products and the fate of ethene in contaminated groundwater.

5.3.4.1 Freedman Microcosms (CRP48 Lac 1-3, CRP50 Lac 1-3)

Ethene production was observed in all cultures within two weeks of amendment. Ethane production was observed only in the CRB 48 microcosms. Between Days 20-22, the headspace of the microcosms was purged with CO_2/NO_2 (20:80), then the microcosms were amended with VC to a target concentration of 1 mg/L aqueous (2 µmol/bottle). Ethene and ethane production were observed within one week of the second feeding. Headspace was purged again on Day 34 and cultures were amended with ethene to a target concentration of 0.1 mg/L aqueous (3 µmol/bottle). Ethane production was observed within 2 days of feeding (Figure 5-1). Measurements made on Day 42 showed continued ethane production in the CRP48 microcosms but not in the CRP50 microcosms. These data suggest that ethane production from ethene is not stoichiometric (i.e. 1 mole per mole), suggesting that another mechanism for ethene removal may be operative.

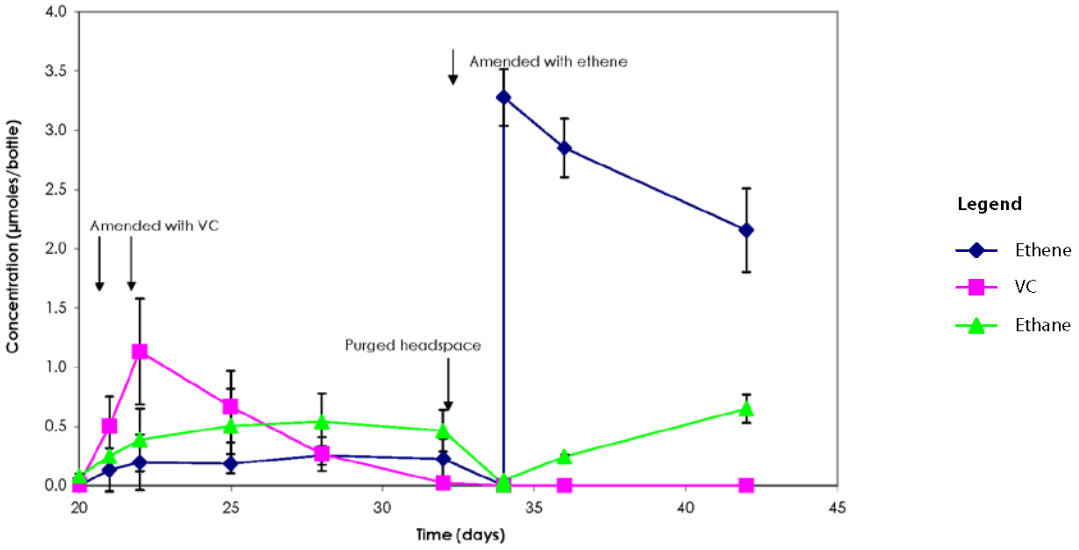

Notes: Vinyl Chloride (VC), ethene and ethane concentrations, reported in µmoles per bottle, as a function of time in CRP 48 Microcosms. Data are average +/- standard deviation of 3 replicate microcosms derived from the original bottles sent from Clemson University in July 2007. Microcosms were purged on Day 20 to remove accumulated ethane, ethene and methane, and amended with VC (twice since first time the concentration was lower than expected). On Day 32, the microcosms were purged again and this time amended with ethene.

Figure 5-1: CRP 48 microcosms: average values (n=3) after headspace purge on day 20

Microcosms obtained from Dr. Freedman however indicated ethene disappearance over time, accompanied by the appearance of ethane and methane. The appearance of ethane was near-stoichiometric with the disappearance of ethene. Isotopic balance consistent with the degradation of ethene to ethane was also observed, with the starting $\delta^{13}C$ value of ethene and the final $\delta^{13}C$ value of ethane both equal to -30‰ ± 0.5‰ in each replicate. The ε value of all replicates was identical within 95% confidence intervals, and was equal to -5.6‰ ± 0.5‰, with an R^2 value of 0.93 (Figure 5-2).

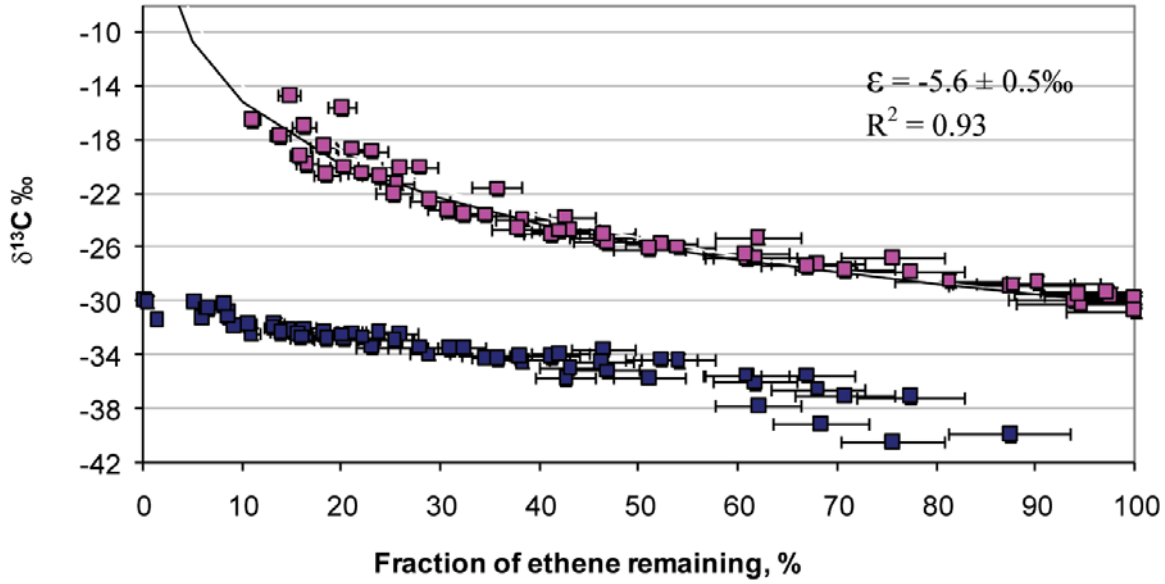

Note: Isotopic fractionation of stable carbon isotopes during the degradation of ethene to ethane. Pink squares represent ethene; Blue squares represent ethane. Values for ethene fit the Rayleigh model with an R2 value of 0.93.

Figure 5-2: Isotopic fractionation of ^{13}C during anaerobic degradation of ethene

5.3.4.2 Landfill Microcosms (L-A, L-B, L-C)

By Day 12, none of the cultures had shown any significant activity. This was not unexpected given how long these microcosms had been dormant. The Landfill microcosms were monitored over a period of six months, and showed no evidence of ethene degradation. These were therefore rejected as suitable microcosms for this study.

5.3.5 Field Studies - Site Description, Materials and Methods

TCE was historically used as a degreasing agent and was released to the subsurface at an industrial site in southwestern Ontario, Canada (referred to as ISSO). The site geology consists of 3 to 6 m of clayey-silt overburden overlying a fractured carbonate bedrock aquifer system that includes cherty, fossiliferous, and argillaceous limestones and dolostones of the Bois Blanc Formation; the dolostones and shales of the Bertie Formation; and the underlying shales,

evaporites, and dolostones of the Salina Formation (Armstrong, 2007). The water table is located within the overburden at a depth of 1 to 2 m below the ground surface. Groundwater flow in the bedrock aquifer occurs primarily through subparallel bedding plane fractures, and also via secondary porosity features resulting from dissolution of calcite and gypsum. Maximum concentrations of TCE (>140 mg/L) have been detected in the bedrock groundwater. Significant concentrations of cDCE and VC also occur suggesting some degree of dechlorination by native microorganisms at the site.

In 2008, an EISB system was installed at the site. The EISB system consists of a recirculation loop, where groundwater is extracted from three wells located downgradient of the suspected source areas. The extracted groundwater is amended with electron donor (ethanol) and injected into the bedrock aquifer through recharge wells located upgradient of the extraction wells in the vicinity of the source area(s), as depicted in Figure 5-3. In October 2009, select recharge wells were bioaugmented with KB-1® microbial culture to enhance the reductive dechlorination of TCE and its degradation products (cDCE and VC) to ethene. Following startup, ethene concentrations in wells with strong hydraulic connectivity to the recirculating system increased to a maximum of 370 µg/L coincident with TCE, cDCE, and VC concentration decreases. Figure 5-4 shows changes in all compounds over time for the extraction wells. The concentration of ethene was expected to be higher based on observed molar losses of TCE, cDCE, and VC. Groundwater samples were thus collected for CSIA analysis to assess potential ethene degradation as a means to explain the mass balance issues.

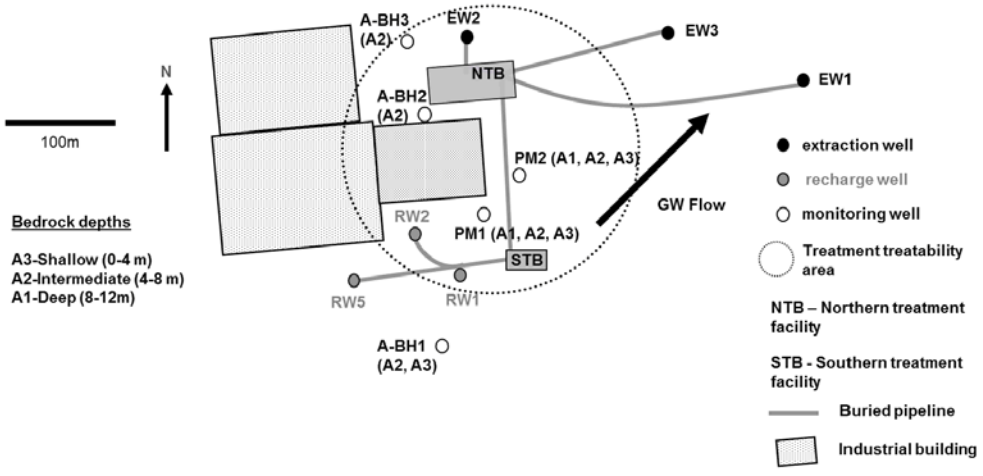

Figure 5-3: Sketch of the field site (ISSO). Groundwater is extracted in the vicinity of the northern property boundary (EW wells) and transferred through buried piping to the northern treatment building (NTB) where it is combined into a central manifold and directed through a filter system to remove particulates. Following filtration, the groundwater is amended (continuously or periodically depending on system operation) with chlorine dioxide (ClO_2) to control biofouling through a central forcemain to the southern treatment building (STB) where the groundwater is amended with electron donor (ethanol) and distributed to individual recharge wells through a manifold to stimulate the indigenous microorganisms.

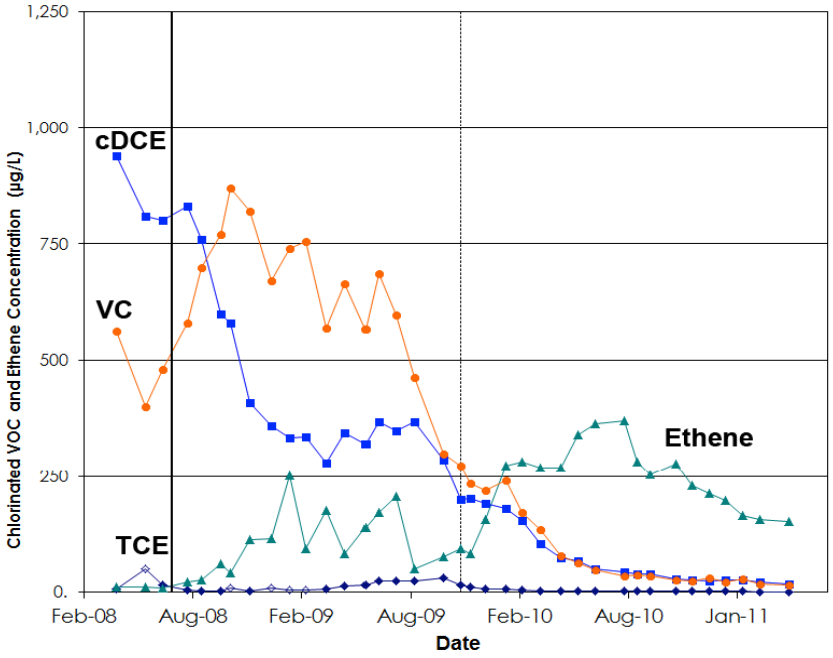

Figure 5-4: Concentration versus time for chlorinated contaminants and ethene in extraction wells with hydraulic connection to the recirculating system at an industrial site in southwestern Ontario, Canada (ISSO). Electron donor addition began in July 2008 (solid vertical line). Bioaugmentation with 100L of KB-1® began in October 2009 (dashed vertical line). Samples were collected for isotopic analysis in February 2010.

Groundwater field samples were collected in 40 mL volatile organic compound (VOA) vials treated with 1 mL of 6 N hydrochloric acid to avoid further biodegradation after sampling (Hunkeler, Meckenstock *et al.*, 2008). The samples were shipped and stored at 4°C. The samples were analyzed for VOCs at a commercial laboratory. CSIA was completed using a purge and trap Teledyne-Tekmar XPT concentrator coupled to an Agilent 5890 and a Finnigan Delta XP mass spectrometer via a combustion interface. The GC was fitted with a 60 m × 0.25 mm GSQ column with a temperature program of 35°C for 3 minutes, increasing at 10°C/min to 90 °C, then increasing at 25°C/min to 210°C, and holding for 5 min. Depending on the concentration of the sample, 5 to 80 mL of groundwater was injected into the purge and trap concentrator using a gastight syringe. The sample was purged for 11 minutes with a helium flow of 40 mL/min. The trap was then purged with dry helium for 1 minute, followed by heating the trap to 250°C. The desorbed compounds were injected over the course of 4 minutes into the GC through a heated line (260°C) with a flow rate of 50 mL/min. The split varied from 1:1 to 20:1 as a function of the concentration of compounds in each sample (Mundle, Johnson *et al.*, 2012).

5.3.6 Field Studies - Results

In February 2010, CSIA of groundwater samples from 12 wells (Table 5-2) was used to assess whether the deficient ethene mass balance was due to biodegradation of ethene or due to other processes such as volatilization during sampling. Undegraded TCE $\delta^{13}C$ values from the literature range from −34‰ to −22‰ with a mean value of −28‰ (Hunkeler, Meckenstock *et al.*, 2008; Beneteau, Aravena *et al.*, 1999; Holt, Sturchio *et al.*, 1997; Hunkeler and Aravena, 2000). Because CSIA sampling took place after the EISB was initiated at the site, some degradation of TCE had already occurred. Although the $\delta^{13}C$ value for undegraded TCE is not known at this site, we can limit the range of possible values from the literature. The least enriched $\delta^{13}C$ value for TCE (−21.5‰) was observed in A-BH1(A2), a background well that throughout the study also contained the highest concentrations of TCE, an order of magnitude less cDCE, and nondetectable VC. Based on assuming all the cDCE in this well is from TCE degradation, and converting to µM, the % degradation of TCE in this well over those dates is 10−20%. The largest reported ε value for biodegradation of TCE by KB-1® is −13.6‰ (Slater, Lollar *et al.*, 2001). If the TCE in this well has already been biodegraded by 10−20% with a maximum ε value of −13.6, an estimate of the $\delta^{13}C$ value for undegraded TCE of −27% to −21.5% can be calculated, well within the range of reported values in the literature of −34% to −22%. $\delta^{13}C$ values for cDCE and VC ranged from −28.4‰ to +8.5‰ and from −48.3‰ to −2.5‰, respectively, with the most enriched values for both compounds (and the lowest remaining levels of TCE and cDCE) occurring in the same treatment monitoring wells.

Table 5-2: $\delta^{13}C$ values (‰) of TCE, cDCE, VC, and ethene from ISSO[a]

		TCE		cDCE		VC		ethene	
monitoring well	hydraulic connection to recirculation system based on Br tracer tests	concn ($\mu g\ L^{-1}$)	$\delta^{13}C$	concn ($\mu g\ L^{-1}$)	$\delta^{13}C$	concn ($\mu g\ L^{-1}$)	$\delta^{13}C$	concn ($\mu g\ L^{-1}$)	$\delta^{13}C$
EW 1	high	7	bd	152	−8.0	197	−2.5	183	−28.6
EW 2	high	2.8	bd	151	−7.9	110	−6.4	236	−29.0
EW 3	high	3.2	bd	165	5.2	236	−8.0	200	−29.3
A-BH3(A2)	high	na	bd	na	−6.2	na	−20.4	na	−28.8
A-BH2(A2)	high	na	bd	na	−21.4	na	−33.9	na	−28.7
PM1 (A3)	low	1380	−18.0	4470	−22.2	245	−48.3	<5	bd
PM1 (A2)	high	<10	bd	1240	−10.5	645	−33.0	133	−28.9
PM1 (A1)	moderate	746	−15.7	7200	−22.1	498	−34.4	118	−29.1
PM2 (A3)	moderate	2890	−19.9	8600	−22.7	723	−39.4	277	−29.0
PM2 (A2)	high	4.8	bd	100	8.5	123	−29.2	257	−29.1
PM2 (A1)	low	47	bd	877	−16.3	328	−30.6	19.8	bd
A-BH1(A3)[c]	low	na	−19.3	na	−24.7	na	bd	na	−29.3
A-BH1(A2)[c]	low	na	−21.5	na	−28.4	na	−39.1	na	−29.7
A-BH2(A2)[b]	high	na	−4.5	na	−23.2	na	−40.7	na	−29.2

[a]Samples Collected for Isotopic Analysis in February 2010. na = not analyzed, bd = below detection limits. [b]Well was sampled in March 2010. [c]Background well A-BH1(A2, A3) not analyzed for VOC concentrations in February 2010 but quarterly monitoring concentrations provided in Table S1.

Together with the concentration decreases for the extraction wells shown in Figure 5-4, the CSIA data from February 2010 indicate significant biodegradation of all of the chlorinated ethenes is taking place at this site. In contrast, ethene $\delta^{13}C$ values show a very narrow range of −29.7‰ to −28.6‰ throughout the site (Table 5-2) that approach the range of $\delta^{13}C$ values expected for undegraded TCE. The uniformity of the ethene $\delta^{13}C$ values combined with agreement with the predicted range of undegraded TCE indicates that there is no evidence to attribute lack of VOC mass balance at this site to biodegradation of ethene. The range of $\delta^{13}C$ values for ethene at this site is most consistent with the undegraded ethene scenario (lower horizontal rectangle) depicted in Figure 5-5.

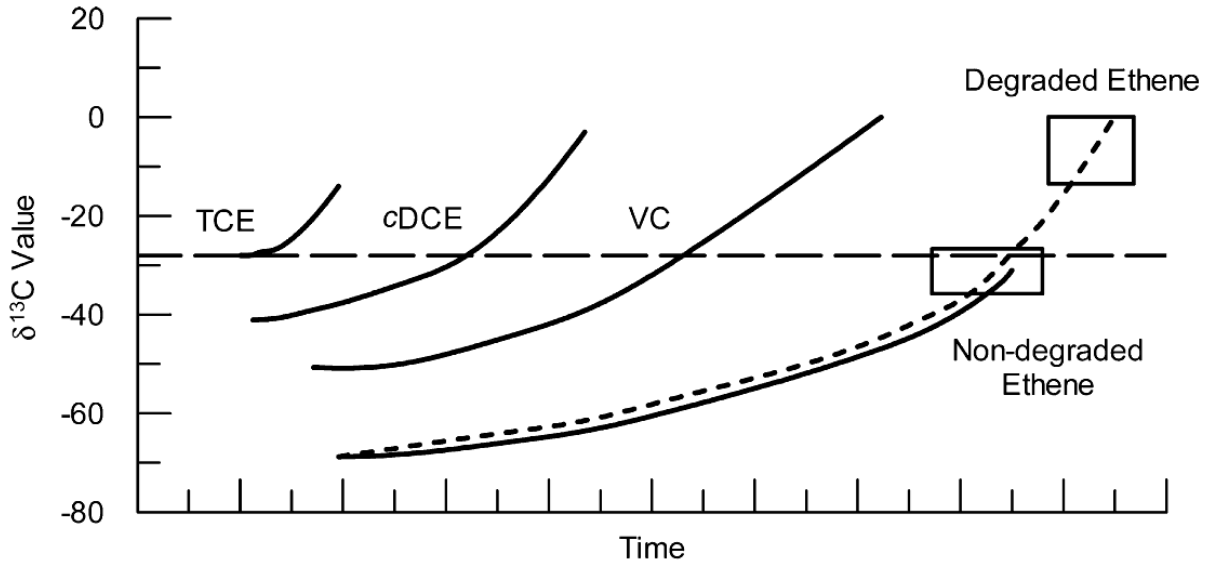

Figure 5-5: Schematic of $\delta^{13}C$ values versus time for microbial reductive dechlorination of TCE to ethene by KB-1®. Adapted from Slater *et al.* (Slater, Lollar *et al.*, 2001), used to conceptualize remediation at ISSO by KB-1®. The solid lines represent changes in the $\delta^{13}C$ values of TCE as it degrades to cDCE, VC, and ethene and the changes in $\delta^{13}C$ of the daughter products as each is produced by dechlorination and then subsequently degraded. The right-hand most solid curve represents the expected $\delta^{13}C$ values of ethene if no further biodegradation of this compound is taking place. In this case, the final $\delta^{13}C$ value of ethene is identical to the $\delta^{13}C_0$ of the TCE parent (horizontal dashed line). This is effectively a closed system with respect to reductive dechlorination. In contrast, if ethene is undergoing further degradation, $\delta^{13}C$ values of ethene (hatched curve) may become progressively more enriched than the $\delta^{13}C_0$ value of TCE. The lower horizontal rectangle represents the maximum (most enriched) $\delta^{13}C$ values for ethene in the first case, while the vertical open rectangle indicates a typical range for the latter case, i.e., a site where not only complete dechlorination of chlorinated ethenes but biodegradation of ethene has occurred.

Although the hydrogeology at ISSO involves contaminated water recirculation, $\delta^{13}C$ values can also be used to assess ethene biodegradation in other hydrogeological scenarios including sites without artificial recirculation and with other parent contaminants. For example, Hunkeler *et al.* (Hunkeler, Aravena *et al.*, 1999) reported $\delta^{13}C$ values for PCE, TCE, cDCE, VC, and ethene at a contaminated site (groundwater flow ~0.2−2 m/y) in Toronto, Canada. $\delta^{13}C$ values ranged from −31.7‰ to −25.7‰ (PCE), −30.7‰ to −29.5‰ (TCE), −31.5‰ to +4.2‰ (cDCE), and −40.4‰ to +25.4‰ (VC), with the most enriched values for cDCE and VC occurring in the same wells. The highest PCE concentration (~ 54 mg/L) corresponded with the least enriched $\delta^{13}C$ value (−31.7‰), which the authors suggested closely resembled the $\delta^{13}C$ value expected for the undegraded PCE (Hunkeler, Meckenstock *et al.*, 2008). The $\delta^{13}C$ values for ethene showed a broad range of −51.8‰ to −31.9‰ compared to the narrow range observed at ISSO; however, the most enriched $\delta^{13}C$ value for ethene similarly approached the expected value for undegraded parent contaminant.

5.3.7 Conclusions and Implications for Future Research / Implementation

We have shown that isotope fractionation of carbon occurs in both anaerobic and aerobic microbial degradation of ethene. We have demonstrated that the isotopic composition of the final daughter product of dechlorination (ethene) can be used to assess the effectiveness of remediation of contaminated sites – particularly in the case where there is a lack of VOC mass balance. In such cases it can be challenging to distinguish between lack of VOC mass balance due to incomplete dechlorination versus lack of mass balance due to degradation of ethene occurring simultaneously with dechlorination. Both processes decrease the measured concentrations of ethene, but only the latter (degradation of ethene) is likely to involve isotopic fractionation due to cleavage of the carbon-carbon double bond in ethene.

The results of this work are published in Mundle *et al.* (Mundle, Johnson *et al.*, 2012).

5.3.8 Literature Cited

Armstrong, D. K. (2007). "Paleozoic Geology of the Southern Niagara Peninsula Area; Open File Report 6213." Ontario Geological Survey 15-1 to 15-8.

Beneteau, K. M., R. Aravena and S. K. Frape. (1999). "Isotopic characterization of chlorinated solvents- laboratory and field results." Organic Geochemistry **30**(8): 739−753.

Holt, B. D., N. C. Sturchio, T. A. Abrajano and L. J. Heraty. (1997). "Conversion of chlorinated volatile organic compounds to carbon dioxide and methyl chloride for isotopic analysis of carbon and chlorine." Analytical Chemistry **69**(14): 2727−2733.

Hunkeler, D. and R. Aravena. (2000). Determination of compound-specific carbon isotope ratios of chlorinated methanes, ethanes, and ethenes in aqueous samples. Environmental Science & Technology **34**(13): 2839−2844.

Hunkeler, D., R. Aravena and B. J. Butler. (1999). “Monitoring microbial dechlorination of tetrachloroethene (PCE) in groundwater using compound-specific stable carbon isotope ratios: Microcosm and field studies.” Environmental Science & Technology **33**(16): 2733−2738.

Hunkeler, D., R. U. Meckenstock, B. Sherwood Lollar, T. C. Schmidt and J. T. Wilsont. A Guide for Assessing Biodegradation and Source Identification of Organic Groundwater Contaminants Using Compound Specific Isotope Analysis (CSIA); EPA 600/R-08/148; U.S. Environmental Protection Agency: Ada, OK, Dec. 2008; p 68.

Mundle, S. O. C., T. Johnson, G. Lacrampe-Couloume, A. Pérez-de-Mora, M. Duhamel, E. A. Edwards, M. McMaster, E. Cox, K. Révész, and B. Sherwood Lollar (2012). “Monitoring Biodegradation of Ethene and Bioremediation of Chlorinated Ethenes at a Contaminated Site Using Compound-Specific Isotope Analysis (CSIA).” Environmental Science & Technology **46**(3): 1731-1738.

Slater, G. F., B. Sherwood Lollar, B. E. Sleep and E. A. Edwards. (2001). “Variability in carbon isotopic fractionation during biodegradation of chlorinated ethenes: Implications for field applications.” Environmental Science & Technology **35**(5): 901−907.

6. MODULE 5 - SABRE

6.1 Introduction

At SERDP's request, Geosyntec added Module 5 to the ER1557 proposal. This module involved support of the Remediation Technology Development Forum (RTDF) Source Area BioREmediation (SABRE) project. The SERDP-funded portion of the SABRE field demonstration included:

- Installation and operation of a pH control system for the test cell (Section 6.2);
- Tracer testing (Section 6.3); and
- Molecular characterization for the test cell (Section 6.4).

6.1.1 SABRE Project Description

The SABRE project comprises laboratory and field-pilot scale development of an accelerated anaerobic bioremediation process based on reductive dechlorination by dehalorespiring bacteria for dense non-aqueous phase liquid (DNAPL) source areas in groundwater. This novel development is based on the controlled addition of growth substrates (electron donors) to support dehalorespiring bacteria under conditions that ensure the maximum rate of reductive dechlorination to ethene. The project aims to provide confidence in the viability of this technology through scientifically robust datasets.

To accomplish these objectives, the SABRE project includes field demonstration projects, based on field experiments conducted in two closely coordinated test cells: one contained test cell (30 meters long by 5 meters wide) with a comprehensive 3-dimensional groundwater monitoring array to assess treatment processes; and an uncontained test area with more conventional monitor well systems that represents a practical model of how treatment processes can be implemented at future sites. The conceptual design of the contained cell is shown in Figure 6-1, with a detailed layout of the instrumentation shown in Figure 6-2.

The influent trench is constructed the full width of the test cell through the majority of the aquifer and backfilled with gravel, located at the upgradient end of the test cell. The influent trench contains three wells. The influent trench system was originally designed to be used for continuous, or at least frequent, delivery of soluble electron donor, should this be the chosen donor type. Following laboratory trials, an emulsified vegetable oil (EVO) donor was selected, which resulted in redundancy of the influent trench because the EVO had to be injected directly into the treatment zone. However, following the decision to engineer a provision for pH control the influent trench system was the obvious choice for delivery of bicarbonate.

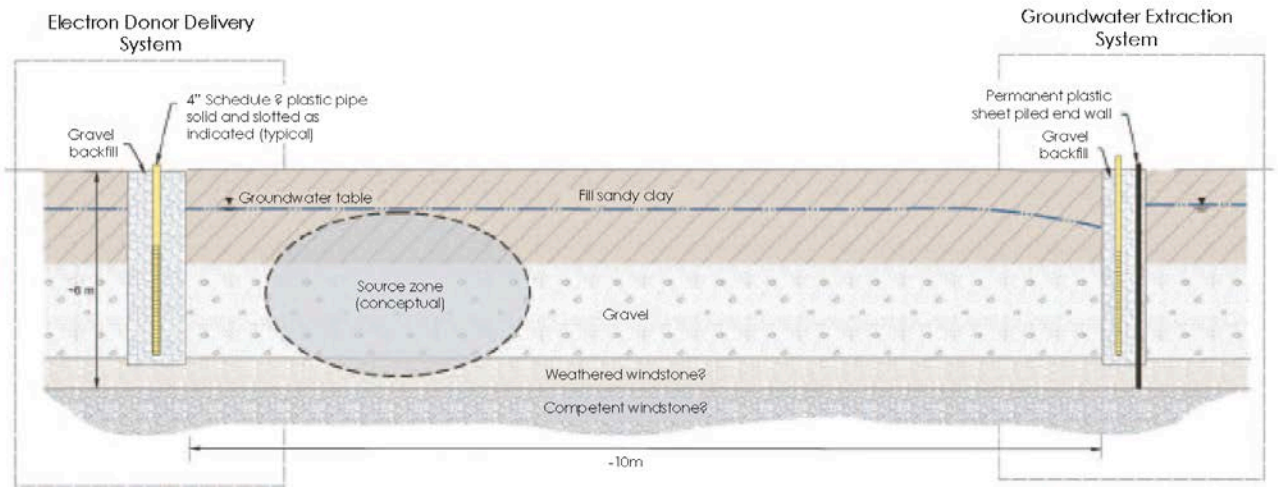

Figure 6-1: Conceptual test cell layout

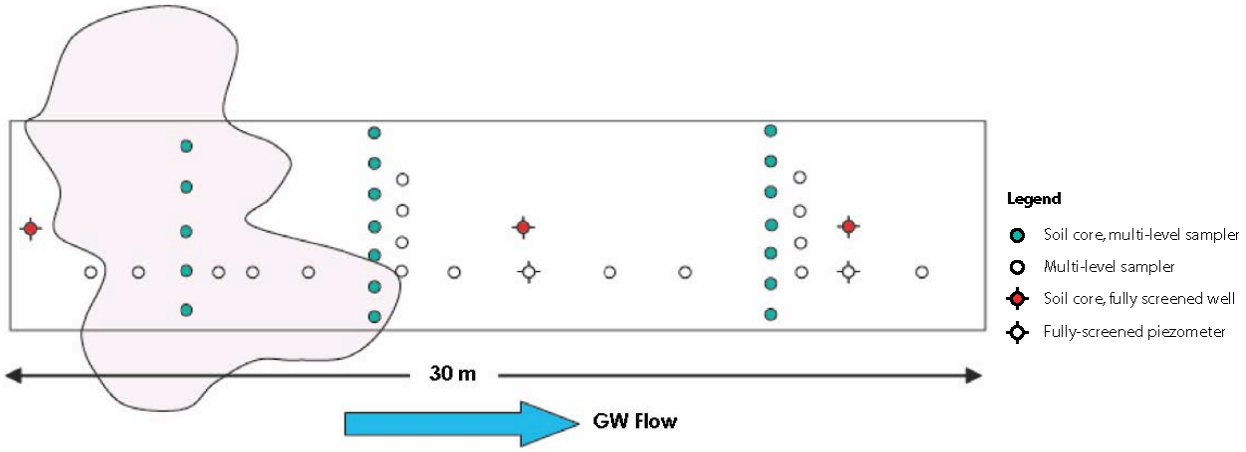

Notes: 9-14 ports in each multi-level sampler, total of over 400 sample points plus 15 oil injection wells with 1m long screens

*Monitoring network composed of both SABRE flux fences and an additional "Streamtube" network installed as part of a University of Birmingham Project

Figure 6-2: Test cell instrumentation layout

The test cell experiment comprises a baseline monitoring period, whereby groundwater was pumped through the cell at a constant rate, followed by a treatment period which continued the constant rate of groundwater flow and where injection of an EVO electron donor (Terra Systems Inc. "SRS") was conducted at multiple points in the test cell. The baseline period started on 8 January 2007 and the operational period started on 2 May 2007. The rate of controlled groundwater flow through the test cell was 1.4 liters per minute (Lpm), which was equivalent to an average groundwater residence time of 60 days.

6.2 Installation and Operation of pH Control System for Test Cell

6.2.1 Background

A pH control system for the test cell was installed to allow a bicarbonate buffer to be introduced to the test cell should the pH of the cell decrease significantly due to acid-generating reductive dechlorination activity. The infrastructure associated with the pH control system was also used for the tracer sub-task described below (Section 6.3).

Following electron donor amendment, biological activity in the test cell increased markedly, with significant biofouling of extraction and monitor wells, and associated hydrogeochemical changes. The hydrogeochemical changes included a significant pH reduction. The pH, which had started at about 7, approached a value of pH 6, at which point it was decided that control was necessary to maintain optimum conditions for biological activity. The pH control system was put into operation on 20 August 2007 to maintain optimum conditions for biological activity.

6.2.2 Research Objectives

Discussions at the SABRE Annual Technical Conference in September 2006 had identified the potential need for pH control during the operational (post donor injection) phase of the SABRE field experiment in the Test Cell. It had been agreed that the most effective method of delivering pH control amendments would be by continuous injection of bicarbonate into the "influent trench," using a methodology that would ensure good mixing throughout the influent trench.

6.2.3 Materials & Methods

Design and Specification

The design specification for pH control called for uniform delivery of bicarbonate over the full width and depth of the upgradient end of the test cell. This was implemented via the influent trench. Further, the design specification also required that the groundwater flow system, and associated boundary conditions at either end of the test cell, remain constant throughout the baseline and operational periods.

In order to ensure uniform bicarbonate delivery, groundwater was continuously extracted from the outer wells and re-injected into the center well of the influent system. Bicarbonate solution was added using a metered dosing pump before the groundwater was re-injected.

Recirculation of groundwater in the influent trench system was started during the baseline period in order that the boundary conditions at the inflow end of the test cell would not change if, and when, pH control was started.

The quantity of bicarbonate required to buffer pH was calculated using a geochemical model in conjunction with estimates of contaminant mass degradation rates. It was calculated that approximately 3 to 12 g of potassium bicarbonate per liter of groundwater flow through the test cell would be required to maintain optimum pH.

The specification originally required the use of potassium bicarbonate. Potassium bicarbonate was chosen because it was readily available, relatively inexpensive and unlikely to result in significant changes in aquifer hydraulic conductivity. Sodium bicarbonate was initially not selected because of concerns that sodium may exchange onto clay minerals in the aquifer matrix, resulting in clay swelling and reduction in aquifer hydraulic conductivity. However, following discussions at the SABRE Annual Technical Conference in September 2007 it was agreed that a mixture of potassium and sodium bicarbonate ($KHCO_3$ and $NaHCO_3$) would be used to avoid potential toxicity effects of using only one bicarbonate salt at the relatively high concentration considered to be required.

Installation and Commissioning

The influent recirculation pump was installed and started to operate on 10 February 2007. Injection of bicarbonate for pH control was started on 20 August 2007, with the injection of 3 g/L $KHCO_3$, which was soon after increased to 4 g/L. The injection rate was varied subsequently and the dosing solution changed to a mixture of potassium and sodium bicarbonate, as shown in Figure 6-3. The $KHCO_3$ and $NaHCO_3$ dose rate shown on Figure 6-3 is expressed as the fraction of the total mass of bicarbonate injected.

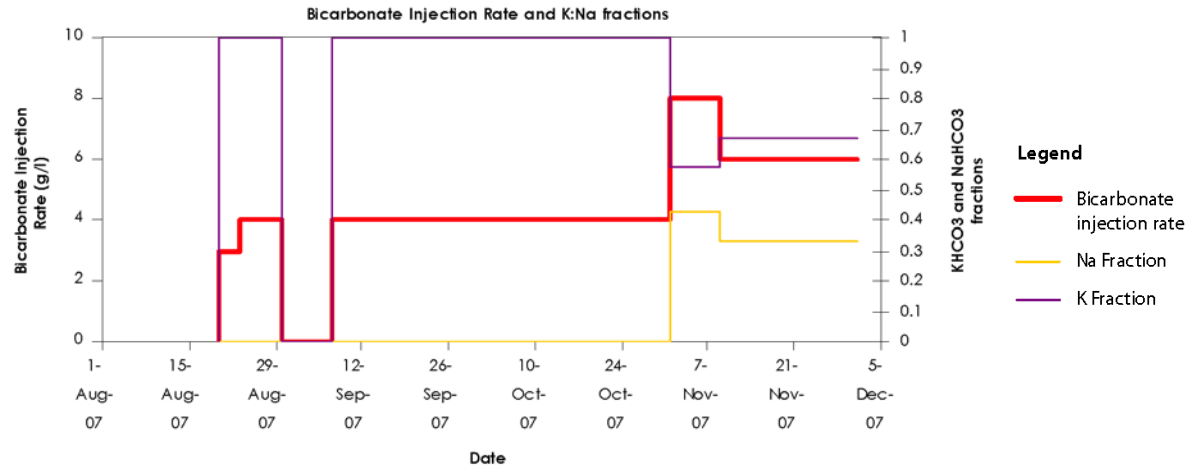

Figure 6-3: Bicarbonate dosing log

Monitoring

Field parameters, pH, electrical conductivity and redox potential, were measured weekly in the influent system ("Influent"), and also two monitor wells in the test cell (SW70 and SW75) and in the groundwater discharged from the test cell ("Effluent"). Figure 6-4 shows the pH at these monitoring points.

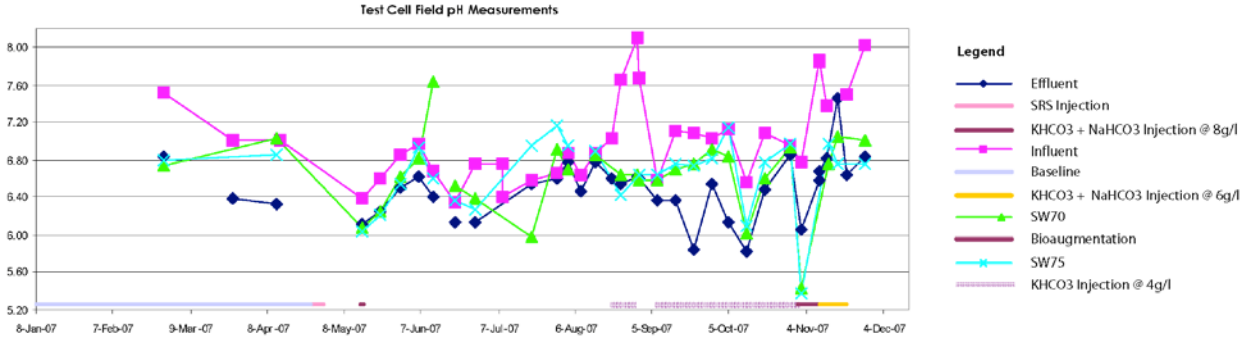

Figure 6-4: pH trends in test cell

6.2.4 Results & Discussion

Injection of bicarbonate for pH control was started on 20 August 2007, with the injection of 3 g $KHCO_3$ per liter of groundwater entering the test cell. This was soon after increased to 4 g/L. As can be seen from Figure 6-4, the measured pH fluctuated over a wide range throughout the period of operation. The fluctuation was partly measurement error, and partly the result of actual

pH variation. The injection rate was varied subsequently, and the dosing solution changed to a mixture of potassium and sodium bicarbonate on 7 September 2007, as shown in Figure 6-5. Throughout October and November 2007, the pH followed a generally rising trend, as a result of bicarbonate amendment.

Between October 2007 and January 2008, groundwater levels exhibited a continuing decline as the hydraulic performance of the test cell deteriorated, resulting in a loss of saturated thickness, difficulty in maintaining a constant extraction rate, and also in mobilization of DNAPL. In early January 2008, DNAPL reached ABS1, the effluent extraction well, and damaged the pump, resulting in its failure.

Bicarbonate injection was suspended on 7 January 2008 at the same time as the failure of the extraction pump.

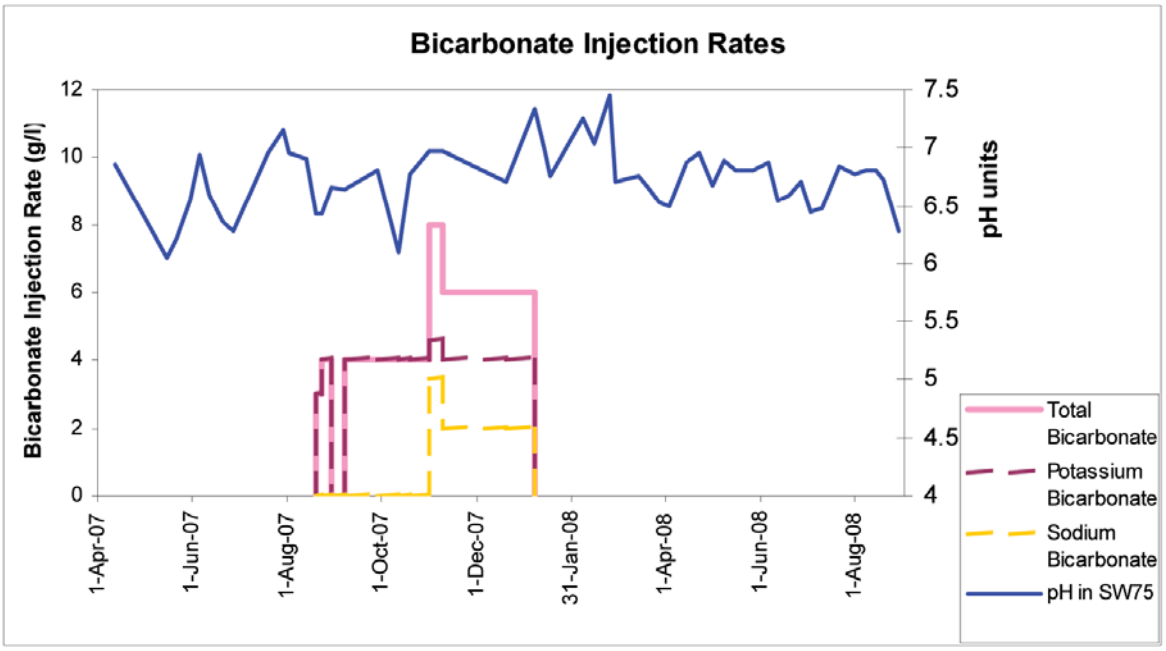

Figure 6-5: Bicarbonate dosing log

Investigations were carried out to determine the cause of the groundwater level decline and hydraulic deterioration. It was concluded that bicarbonate injection may have contributed to hydraulic deterioration, either directly through precipitation of carbonate minerals, or indirectly through enhanced biological activity, clay mineral expansion or other effects. Investigations were not conclusive and bicarbonate injection was not identified as a confirmed cause of the decline in hydraulic performance.

As a precautionary measure, it was decided not to recommence bicarbonate injection when extraction was re-started in March 2008. No further bicarbonate injection was carried out.

Field parameters, pH, electrical conductivity and redox potential were measured weekly in the influent system ("Influent"), and also two monitor wells in the test cell (SW70 and SW75) and in the groundwater discharged from the test cell ("Effluent"). Figure 6-6 shows the pH at these two monitoring points. As can be seen from Figure 6-6, the measured pH has fluctuated over a wide range throughout the period of operation.

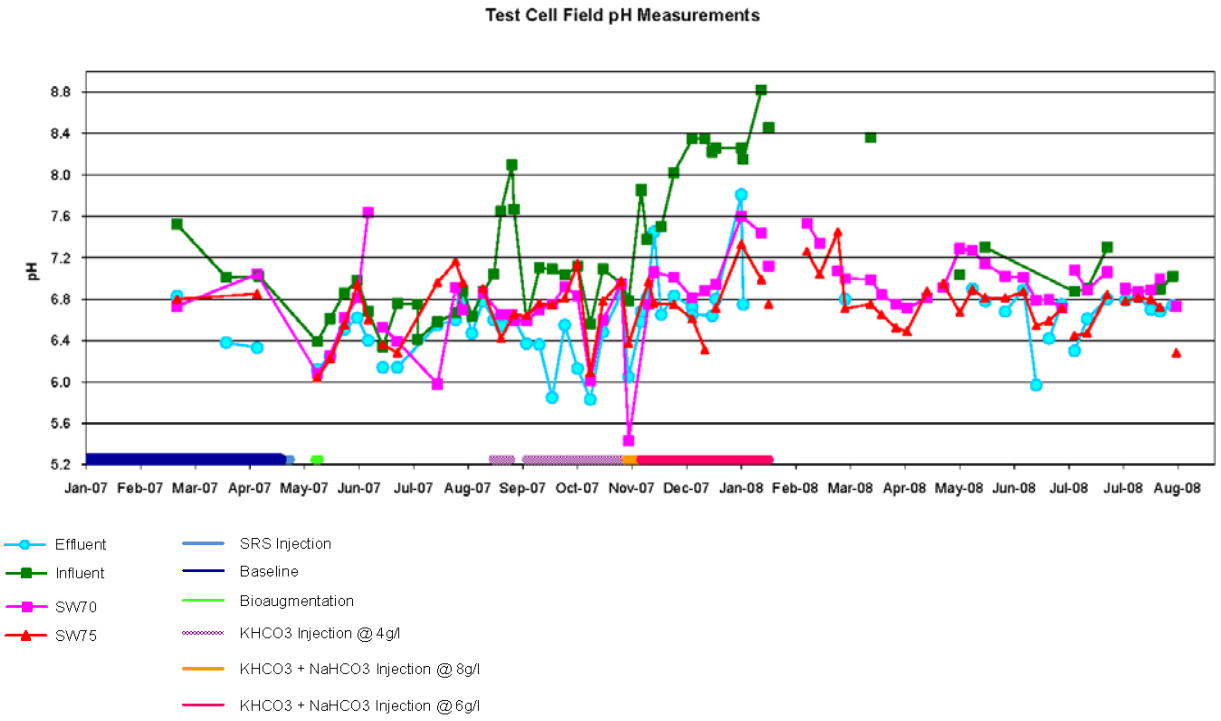

Figure 6-6: pH trends in the test cell

6.2.5 Conclusions and Implications for Future Research / Implementation

Initial results indicate successful delivery of bicarbonate to the test cell as evidenced by the generally rinsing trend in pH observed throughout October and November 2007. The pH control system (bicarbonate injection) was operational until January 2008 and remained off for the remainder of the demonstration.

6.2.6 Literature Cited

No literature was cited in Section 6.2.

6.3 Tracer Test

6.3.1 Background

Estimating VOC mass flux requires a detailed understanding of fluid flow through the test cell. The conceptual design of the tracer test included introduction of a bromide pulse using the upgradient trench recirculation system and detailed monitoring of the multi-level monitoring network to measure the break-through of this pulse along various flow paths within the test cell.

6.3.2 Research Objectives

A forced-gradient conservative tracer test was undertaken during the 'operational phase' of the SABRE enhanced bioremediation experiment, following biostimulation (emulsified vegetable oil, "SRS" from Terra Systems Inc.) and bioaugmentation (KB-1® culture). The data from the tracer test therefore represent a flow field which is influenced by the presence of DNAPL, SRS and KB-1®, essentially the conditions that would be observed in the field at this and other sites during bioremediation. The results of the tracer test were used to infer the spatial flow field characteristics of the surficial aquifer at the site, and guided operational aspects of the SABRE experimental cell and provided input parameters to the inverse modeling of performance monitoring data

6.3.3 Materials & Methods

The study involved the release of a lithium bromide (LiBr) conservative tracer in forced gradient flow field in the SABRE experimental cell. Break-through curve data, from groundwater monitoring at specific multilevel sampler ports, was interpreted by a number of methods, including: 1) Break-through Curve (BTC) analytical solutions (van Genuchten and Alves, 1982); 2) Longitudinal 'snapshots' method of moments (Freyberg, 1986); and 3) BTCs numerical inverse modeling. Interpretation activities 1) and 2) were undertaken within this scope of work by the British Geological Survey and University of Birmingham respectively, whereas activity 3) was undertaken by the SABRE Modeling Work Package to support the modeling and interpretation of the field experiment results. The results of the study were conveyed in a separate technical report, comprising a summary of the experimental method, the field data (BTCs), interpretative outputs and recommendations.

Following field trials (small-scale hydraulic tests) in the SABRE cell, an experimental method was developed to provide *a priori* hydraulic data that would be of considerable benefit in optimizing the tracer test sampling schedule. Additional testing in the remaining multilevel samplers was undertaken to characterize the hydraulic conductivity field and optimize the tracer test.

The tracer test layout was modified to reflect pore clogging issues identified at the influent end of the SABRE test cell. In summary, the new influent wells (Zone II) were used to release the

KBr tracer (Figure 6-7) with the central well also being used to release a second conservative tracer (potassium fluoride [KF]) to study the effects of mixing in the aquifer immediately downgradient of the release wells. Tracer arrival was monitored at the Streamtube T1 (Zone III) to determine the spatial distribution and vertical velocity characteristics prior to arrival at the sampling transect T2a (Zone IV). Transverse monitoring at the Transect 2a, was defined by monitoring all multi-level sampler (MLS) ports at each sampling event (Figure 6-8). Longitudinal monitoring in the Streamtube T4 MLS wells (Zone V) comprised one snapshot. The tracer injection wells were monitored until the tracer concentrations were depleted below detection limits and the extraction well was monitored throughout the tracer test.

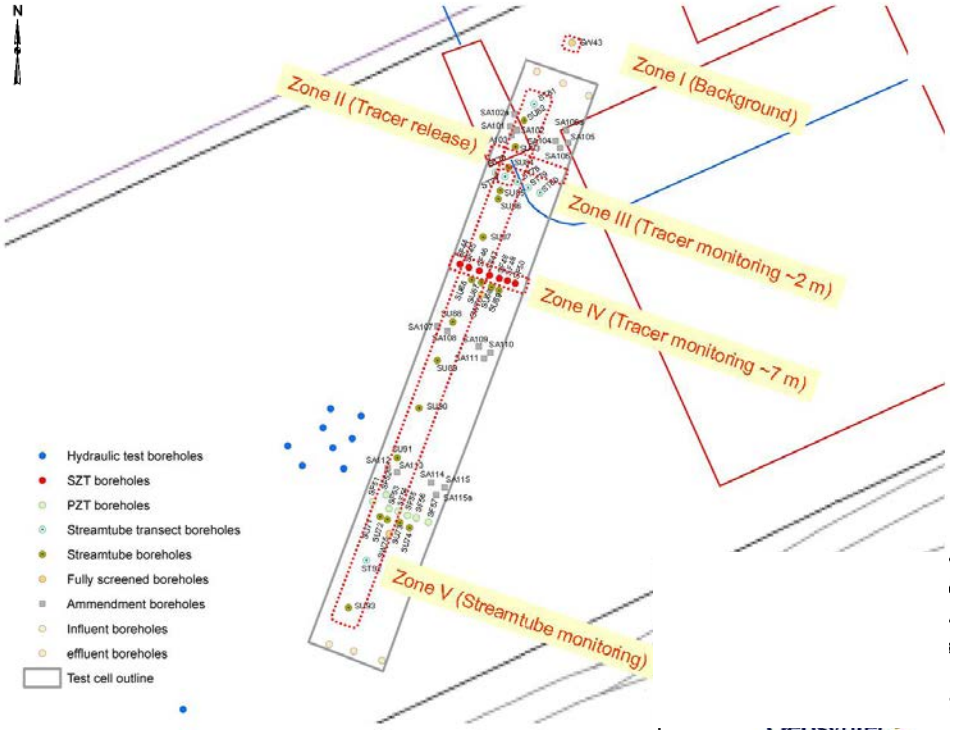

Figure 6-7: Sampling and tracer monitoring zone layout

Figure 6-8: Photograph of groundwater sampling during the SABRE tracer test

A conservative (potassium bromide [KBr]) tracer was released in the three wells of the influent well transect from individual vessels (Figure 6-9) containing tracer at concentration of about 15.15 g/L and KF was released in the central well at a concentration of 3.09 g/L. Concentrations within the injection wells were anticipated to be 500 mg/L KBr and 100 mg/L KF after dilution with the influent water. A 10-hour duration injection pulse delivered a volume of tracer solution to the test cell, resulting in an anticipated pulse of about 41 cm width which occupied an aquifer volume of approximately 3.3 cubic meters.

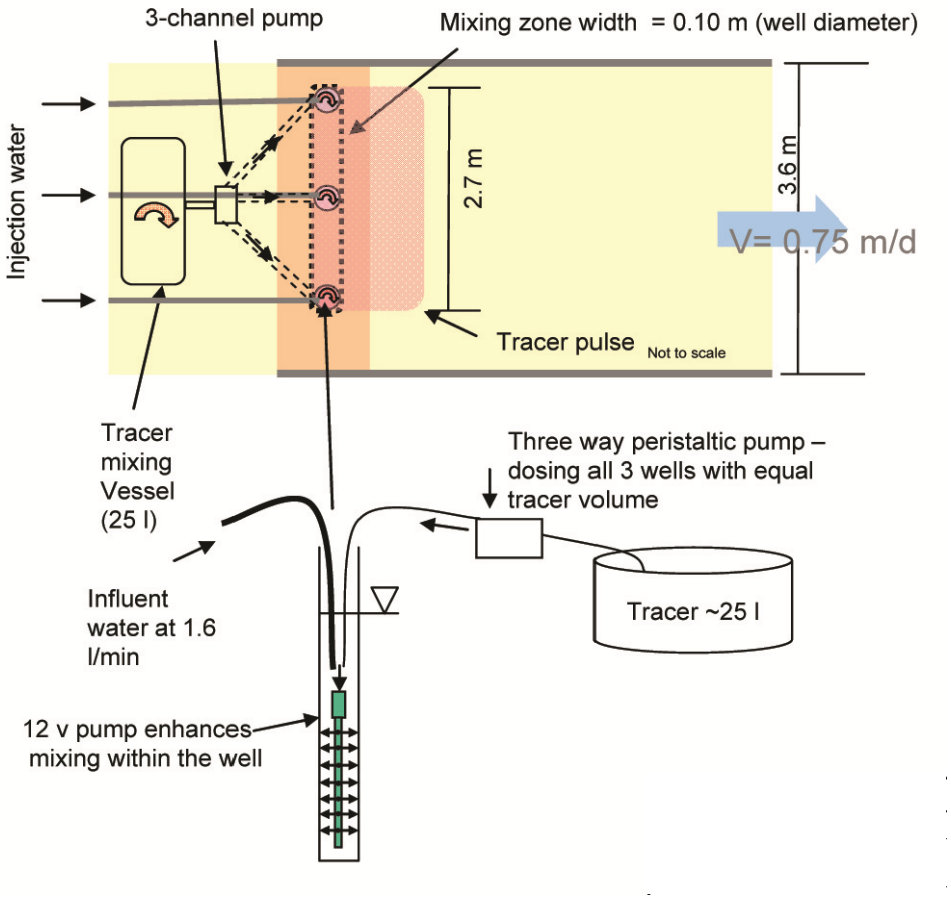

Figure 6-9: Schematic of tracer test delivery method

6.3.4 Results & Discussion

A break-through curve dataset from SF45 (Figure 6-10) illustrates that the majority of the ports recorded the complete tracer profile. The data show a range of arrival times (initial and peak) and concentration values, indicating a spatially variable flow field, even at one borehole location.

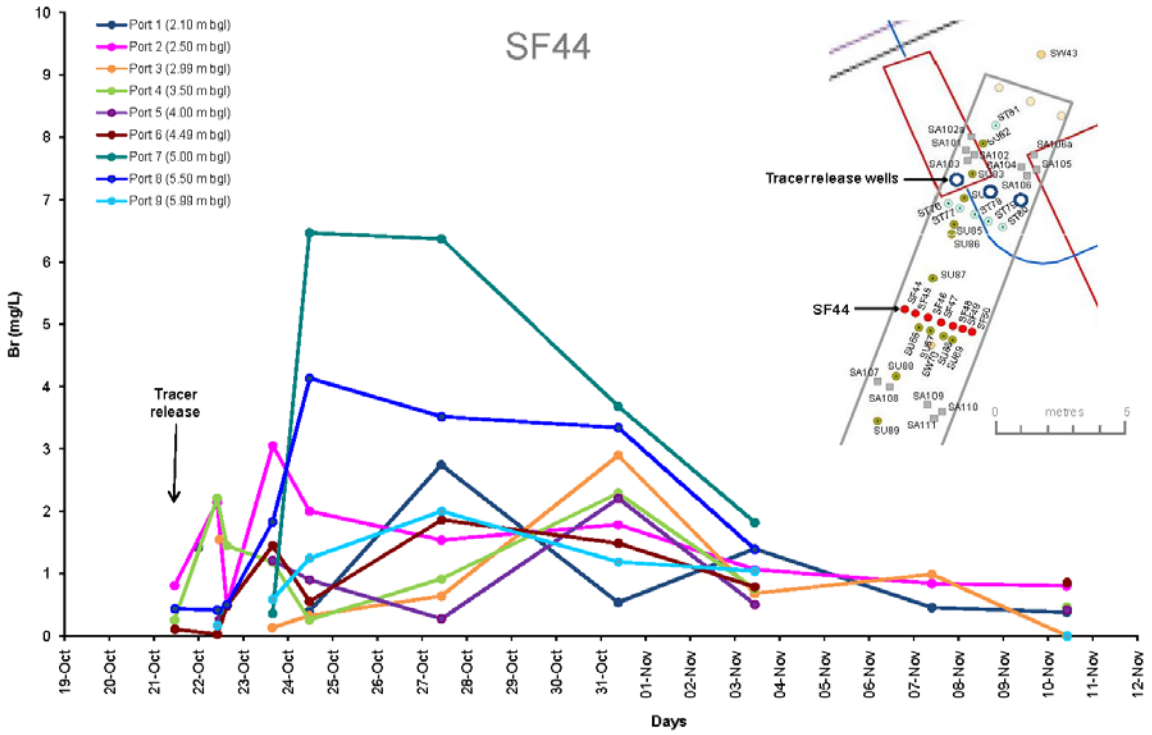

Figure 6-10: Tracer test break-through curve profiles at SF45

The tracer test was implemented from October to November 2008. A report prepared by the British Geological Survey (Dearden *et al.*, 2010) was submitted to SERDP during the second quarter of 2010 that summarized the findings related to: i) determining the spatial characteristics of the flow across the cell; and ii) estimating transport properties (velocity and dispersivity) for an inverse numerical modeling study. The tracer test results generated enhanced deliverables, which are additional to the SABRE research program, including conference presentations, a combined geophysics-hydrogeology manuscript submission, and an expanded SERDP-funded report that grew beyond the initial scope, in part due to collaboration with the University of Toronto (Robinson, *et al.*, 2009; Brovelli *et al.*, 2010; Harkness, *et al.*, 2010).

6.3.5 Conclusions and Implications for Future Research / Implementation

The aim of the tracer test in the SABRE test cell was to estimate field-scale transport parameters (seepage velocity and dispersivity) applicable to the aquifer unit within the SABRE test cell and hence better understand contaminant transport and remediation processes within the cell. Analysis of the transect tracer test data succeeded in developing an improved understanding of contaminant transport and remediation processes within the cell in several areas. The use of both transverse and longitudinal transect monitoring through contaminated source zone areas can enhance both transport and remediation performance understanding. Establishing the presence

of high velocity discrete pathways through a source area that may significantly limit the flushing of adjoining lower permeability areas of potentially much higher contamination or the conveyance of remediation fluids beyond the source zone is seen as particularly important.

6.3.6 Literature Cited

Brovelli, A., Barry, D. A. and J. I. Gerhard (2010). "Optimization of buffer injection during enhanced reductive dechlorination in presence of heterogeneous hydraulic conductivity distribution." Journal of Contaminant Hydrology. *In preparation*.

Dearden, R., Wealthall, G., Chambers, J. and M. Rivett (2010). "Forced Gradient Conservative Tracer Test in the SABRE Research Cell." British Geological Survey CR/09/054: 73pp.

Freyberg, D.L. (1986). "A natural gradient experiment on solute transport in a sand aquifer, 2, Spatial moments and the advection and dispersion of nonreactive tracers." Water Resources Research **22**(13): 2031–2046.

Harkness, M., Fisher, A., Lee, M., Mack, E. E., Payene, J. A., Roberts, J., Dworatzek, S., Possolo, A., and C. Acheson (2012). "Use of Statistical Tools to Evaluate the Reductive Dechlorination of High Levels of TCE in Microcosm Studies." Journal of Contaminant Hydrology. *In press*.

Robinson, C., Barry, D. A., McCarty P. L., Gerhard, J. I. and I. Kouznetsov. (2009). "pH control for enhanced reductive bioremediation of chlorinated solvent source zones." Science of the Total Environment **407**(16): 4560-4573.

van Genuchten, M., Th. and W.J. Alves (1982). "Analytical Solutions of the One-Dimensional Convective-Dispersive Solute Transport Equation." U. S. Department of Agriculture, Technical Bulletin No. 1661 151 p.

6.4 Molecular Characterization for Pilot Test

6.4.1 Background

A key objective of the SABRE project was to provide a quantitative understanding of the remediation of DNAPLs by reductive dechlorination. SABRE approached this objective by collecting detailed measurements during the pilot test, using these measurements to develop a detailed, quantitative process model. To properly construct the model, characterization of the microbial communities that become established in the cell was required. In particular, the biomass and community structure both within and outside of the DNAPL zone must be known. An array of appropriate molecular analyses was performed on groundwater samples collected throughout the pilot test.

6.4.2 Research Objectives

The objective of the field microbial characterization program was to monitor the distribution and growth of *Dehalococcoides* (*Dhc*) dechlorinating bacteria and changes in the overall microbial community throughout the test cell over the duration of the experiment. This included areas that

were proximate to DNAPL as well as areas in the general plume where bacteria were exposed to variable concentrations of TCE and daughter products.

6.4.3 Materials & Methods

Groundwater samples were collected at prescribed intervals through the field test from both fully-screened wells and multi-level sampling points within the test cell. These samples were sent to Scientifics Laboratory in the United Kingdom, where they were filtered to remove the biomass. The filters containing the biomass were frozen and sent to SiREM Laboratory in Guelph, Ontario, Canada and the US EPA Laboratories in Cincinnati, United States, where the biomass samples underwent microbial characterization. Characterization techniques applied by SiREM included quantitative polymerase chain reaction (PCR) to measure *Dhc* and VC reductase gene (VC-R) and denaturing gradient gel electrophoresis (DGGE) to qualitatively assess the community composition. The US EPA used phospholipid fatty acid analysis (PLFA) to measure total biomass (the US EPA work was not funded by SERDP).

In total, about 400 water samples were collected from the test cell during the baseline and operational period (operational day 527).

6.4.4 Results & Discussion

Results indicate levels of VC-R in the test cell generally increased 1 to 2 orders of magnitude over the first 180 days of the study. Subsequent variability in results corresponded with pH excursions and operational disruptions throughout the first six months of 2008. This increase in VC-R correlated with increasing production of VC and when ethene was first observed to increase in the test cell between days 90 and 150.

Results from the fully screened well (SW75) in the plume zone of the test cell indicated, despite several system operation upsets, that TCE was degraded to cDCE and VC with significant amounts of ethene produced (Figure 6-11). Initial increases in *dhc* counts were from 10^3 gene copies/L to 10^6. After September 2008, where data showed further increases in *Dhc* concentration to 10^8 gene copies/L, *Dhc* concentrations declined in areas of the test cell in the final months of operation.

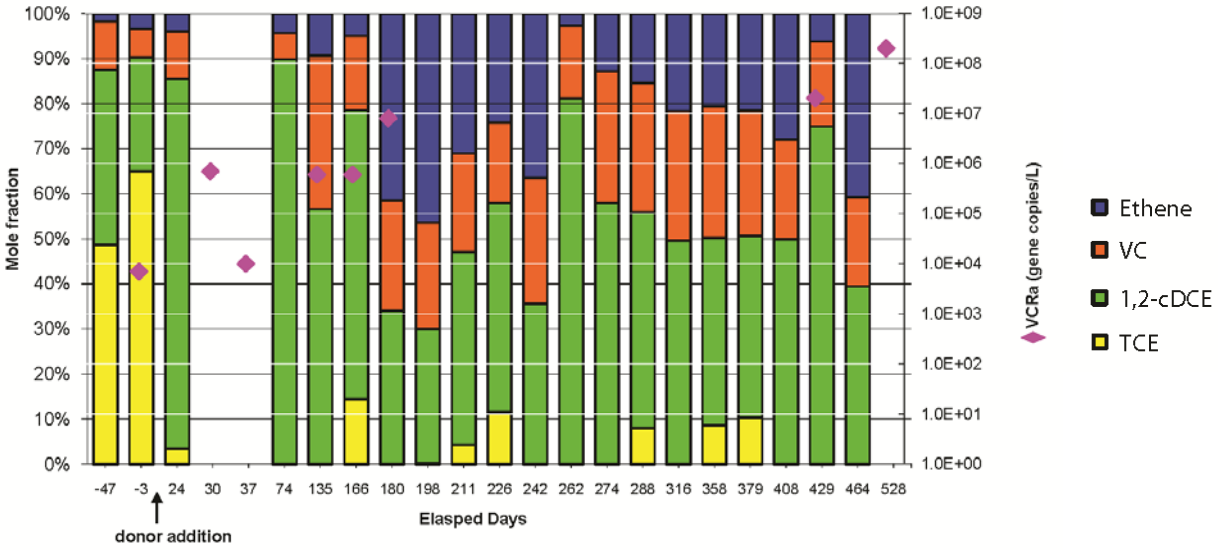

Figure 6-11: Microbial characterization trend plot

6.4.5 Conclusions and Implications for Future Research / Implementation

Results indicated successful stimulation of the biomass within the test cell as evidenced by the VC-R levels that increased 1 to 2 orders of magnitude during the study and approached close to 10^8 gene copies/L in some areas.

6.4.6 Literature Cited

No literature was cited in Section 6.4.

7. CONCLUSIONS AND IMPLICATIONS FOR FUTURE RESEARCH

The overall goal of this research program was to generate information and tools to help DoD RPMs and remediation practitioners better understand and quantify the frequency of occurrence, relative contribution, and overall environmental relevance of the various cDCE and VC degradation processes in field settings. In particular, the technical objectives of this research program were to:

i) elucidate the aerobic oxidation pathway and reaction kinetics for cDCE in JS666 and any other aerobic cDCE-oxidizing bacteria that could be isolated (Module 1);

ii) identify and isolate organisms capable of anaerobic oxidation of cDCE and VC, and if isolated, elucidate the pathways and reaction kinetics for these reactions (Module 2);

iii) improve the understanding of isotopic fractionation signatures related to cDCE and VC reductive dechlorination, and assess the isotopic signatures associated with ethene degradation (Module 3);

iv) develop and validate MBTs, including CSIA and DNA-based analyses, for assessment of the degradation mechanisms (Modules 1-3); and

v) determine the relevance of the various biodegradation mechanisms at field scale so that DoD RPMs and remediation practitioners can better design, implement, monitor, and validate MNA and EISB remedies (Modules 1-3).

The findings of this research program go a long way to resolving our understanding of the various mechanisms of cDCE and VC degradation under field settings relevant to MNA and EISB remedies.

The results of Module 1 confirm that JS666 remains the only isolated organism known to mediate aerobic oxidation of cDCE to CO_2, and MBTs exist to track its presence and fate during bioaugmentation (EISB) projects. Furthermore, significant advancements were made during this project in understanding the pathway, mechanisms and enzymes associated with aerobic oxidation of cDCE in JS666. Results suggest that cytochrome P450 carries out the first step of cDCE degradation by JS666, but that dehydrogenases (probably ChnA and/or ChnD) in the cyclohexanol pathway might play important roles in succeeding steps (e.g., in transforming alcohol and aldehyde intermediates). The critical involvement of metabolic genes from separate pathways under separate regulation might explain often-encountered difficulty in initiating cDCE degradation by JS666. The results also suggest that the cDCE degradation pathway in JS666 is recently evolved because the genes for cDCE degradation are not in an organized operon and are not highly upregulated. Lack of a well-regulated operon could account for the various behaviors (good versus bad) observed in cDCE-grown JS666 cultures, as well as the long lag times often seen before cDCE degradation begins. In the case of the cDCE pathway, it appears that at least

some of the genes were from an alkane degradation pathway (the cytochrome P450 gene), a DCA-degradation pathway, and a cyclohexanol degradation pathway. It appears that multiple pathways might be involved and that competing processes might divert some of the carbon skeleton. The evolution, regulation and potential for improvement of the cDCE pathway are compelling mysteries that can be explored now that the basic biochemistry and molecular biology of the pathway has been established.

In total, the information related to JS666 gained through this and prior research provide DoD RPMs with a viable microbial culture that could be used to treat cDCE in aerobic aquifers via bioaugmentation, as well as CSIA and DNA-based MBTs that can be used to track the introduction, spread, growth and survival of the JS666 microorganisms, though not necessarily their current, in situ activity. Since successful remediation of a cDCE-contaminated site through bioaugmentation with JS666 has yet to be demonstrated, the technology remains preliminary. A field test of bioaugmentation using JS666 was conducted at Site 21, St. Julien's Creek Annex in Chesapeake, Virginia under ESTCP funding (ESTCP ER-0516; *Enhancing Natural Attenuation through Bioaugmentation with Aerobic Bacteria that Degrade cDCE; January 2010*). The results of this project demonstrated successful introduction, spread and stability of the JS666 organisms in bioaugmented plots, and activity of JS666 over the course of the demonstration. Though the levels of JS666 were low (i.e., 3×10^3 to 10^4 colony forming units per mL), they were adequate to effect cDCE degradation, if suitable environmental conditions (adequate oxygen, pH and absence of inhibitory levels of TCE) were present. The reader is referred to the ESTCP report for ER-0516 for detailed results of this JS666 field bioaugmentation. While no other organisms capable of growth-coupled cDCE oxidation have been identified despite significant effort, it is possible that such other organisms exist in cDCE-impacted aquifers. However, given the difficulty in identifying such sites, remediation practitioners should be cautious in invoking aerobic oxidation of cDCE to CO_2 at sites where cDCE mass balance is poor. At such sites, microcosm studies still likely remain as the best method to prove that this mechanism may be occurring and contributing to MNA or EISB remedies.

The results of Module 2 suggest that anaerobic oxidation of cDCE and/or VC under iron- or manganese-reducing conditions may not occur, but that the apparent loss of at least VC from what are thought to be anaerobic sites might in fact be due to aerobic oxidation under conditions of low oxygen flux (e.g., via diffusion from surrounding aerobic regions and/or from recharge events). Very little oxygen would be required for aerobic degradation to have significant impact. For example, a VC concentration of 100 ppb would require only 0.1 mg/L DO for its complete degradation by aerobes. Reports suggest that aerobic VC-oxidizers are common at chloroethene-contaminated sites, and that they can survive prolonged exposure to truly anaerobic conditions. Many cases of anaerobic oxidation of VC in laboratory and field studies may in fact be aerobic oxidation at very low oxygen levels. From the standpoint of the remediation practitioner, this may not matter significantly, since aerobic oxidation of VC can be invoked as the responsible mechanism at sites that are generally perceived as anaerobic. If this conclusion needs to be validated for MNA or EISB projects, our research has developed an appropriate microcosm approach to test VC oxidation at low oxygen flux. It is also anticipated that DNA-based tools

will soon be available (developed as part of research by others) to determine the presence of aerobic VC-oxidizers, and potentially to detect VC oxidation activity itself. In the case of cDCE, where the results of Module 1 suggest that cDCE oxidation is not a widespread occurrence in field settings, it is possible that cDCE disappearance could be due to co-oxidation occurring at low oxygen levels, in the presence of a suitable co-substrate such as methane. While not tested during this study, the findings related to vinyl chloride suggest that this could be a possibility.

Based on the results of Module 2, remediation practitioners are cautioned against invoking anaerobic oxidation of cDCE and VC under anaerobic conditions as an explanation for disappearance of these VOCs, at least until such time as more concrete data supporting their occurrence is available. Instead, practitioners should explore whether disappearances might be related to aerobic oxidation or co-oxidation at very low oxygen levels using the microcosm approach developed in this project.

The results of Module 3 provide remediation practitioners with information and a CSIA tool that can be used to evaluate and explain poor ethane mass balance at chlorinated ethene MNA and EISB sites. As indicated in this report, poor ethene mass balance can often erode the credibility of MNA and EISB remedies. At some sites, ethene is not a conservative end product of VC dechlorination – ethene can be further reduced to ethane, or oxidized to CO_2. The results of our research clearly show that carbon isotope fractionation occurs during both anaerobic and aerobic microbial degradation of ethene. Through case studies at 2 separate EISB sites, we have demonstrated that the isotopic composition of ethene can be used to demonstrate why ethene mass balance may be poor at a given site. In at least one of the field cases tested, the CSIA analyses demonstrated that ethene was being degraded, thereby explaining the poor mass balance. These results will help to strengthen the credibility of the EISB remedy at this site.

The objectives of our research program have been effectively achieved. First, we have collected substantial information and developed a CSIA tool to help elucidate the aerobic oxidation pathway and reaction kinetics for cDCE (objectives 1 and 4). Second, while our research could not identify and isolate an organism capable of anaerobic oxidation of cDCE or VC, we have provided compelling evidence that such activity may in fact be aerobic oxidation or co-oxidation at very low oxygen levels (objective 2). Third, we have developed a CSIA tool to assess isotopic signatures associated with ethene degradation, which will help remediation practitioners explain poor ethane mass balance (objectives 3 and 4). Finally, the information and tools developed through this research program will help DoD RPMs and remediation practitioners determine the relevance of the various biodegradation mechanisms at field scale so that practitioners can better design, implement, monitor, and validate MNA and EISB remedies (objective 5).

Several research questions related to this topic remain. First, there are still components of the cDCE oxidation pathway that remain to be elucidated, and the search for cDCE oxidizers other than JS666 continues. However, we now have a viable set of tools for bioaugmentation for cDCE plumes, absent answering the above questions. Second, the search for organisms capable of anaerobic oxidation of cDCE and VC continues. However, we now have a plausible alternate explanation and viable set of tools to explain cDCE and VC mass loss under apparent anaerobic

conditions, by processes other than reductive dechlorination. Furthermore, it is likely that the phenomenon of aerobic oxidation of VC at low oxygen levels applies to other contaminants relevant to DoD, such as RDX, chlorobenzenes, nitrotoluenes, etc, and this should be investigated. Finally, increased use of the information and tools developed by this study will build a database and acceptance of these processes and tools that is likely to improve the credibility and use of MNA and EISB remedies for chlorinated ethenes.

APPENDIX A

SUPPORTING DATA

APPENDIX A-1

SUPPORTING DATA: PROTOCOLS FOR iTRAQ

Protein digestion and iTRAQ labeling

A total of 100 µg protein of each sample was denatured, reduced with 5 mM tris-(2-carboxylethyl) phosphine at 37 ºC for 1 hour, and the cysteine residues were blocked with 8 mM methyl methanethiosulfonate for 10 min at room temperature. Protein samples were digested with 10 µg of sequence-grade-modified trypsin at 37ºC for 16 hours. Efficiency of protein digestion was assessed by SDS-PAGE using undigested and digested samples. Tryptic peptides from four different samples (WT grown in cDCE and CAP, WT grown in CAP, KO grown in cDCE and CAP, KO grown in CAP) were each labeled with iTRAQ reagents 114, 115, 116, and 117, respectively according to the manufacturer's protocols (document #4351918A and 4350831C downloaded from http://docs.appliedbiosystems.com/search.taf; Applied Biosystems, Foster City, CA). The labeled samples were then combined and fractionated via high pH reverse phase liquid chromatography as described below.

High pH reverse phase (hpRP) fractionation

The pooled iTRAQ-labeled peptides were pretreated with SCX cartridges (AB Sciex, Framingham, MA) and desalted by Sep-Pak SPE for hpRP separation. The hpRP chromatography was carried out using a Dionex UltiMate 3000 HPLC system with a built-in micro fraction collection option in its autosampler and UV detection (Sunnyvale, CA). The iTRAQ-tagged tryptic peptides were reconstituted in buffer A (20 mM ammonium formate pH 9.5 in water), and loaded onto an XTerra MS C18 column (3.5 µm, 2.1x150 mm, Waters) with 20 mM ammonium formate (NH_4FA), pH 9.5 as buffer A and 80% ACN/20% 20 mM NH_4FA as buffer B. The LC was performed using a gradient from 10-45% of buffer B in 30 min at a flow rate 200 µL/min.(Gilar et al., 2005a; Gilar et al., 2005b) Forty-eight fractions were collected at 1 min intervals and pooled into a total of 24 fractions based on the UV absorbance at 214 nm. All of the fractions were dried and reconstituted in 20 µL of 2% ACN/0.5% FA for nanoLC-MS/MS analysis**.** Fractions were pooled into the final 10 fractions by disparate first dimension fractions (retention time multiplexing) as reported recently[3]. All ten pooled peptide fractions were dried and reconstituted in 2% ACN, 0.5% formic acid for subsequent nanoLC-MS/MS.

Nano-scale reverse phase chromatography and tandem mass spectrometry (nanoLC-MS/MS)

The nanoLC-MS/MS analysis was carried out using a LTQ-Orbitrap Velos (Thermo-Fisher Scientific, San Jose, CA) mass spectrometer equipped with nano ion source using high energy collision dissociation (HCD). The Orbitrap was interfaced with an UltiMate3000 RSLCnano system (Dionex, Sunnyvale, CA). An aliquot of hpRP peptide fractions (2.0 – 10.0 µL) was injected onto a PepMap C18 trap column (5 µm, 300 µm × 5 mm, Dionex) at 20 µL/min flow rate for on-line desalting and then separated on a PepMap C-18 RP nano column (3 µm, 75µm x

15cm), and eluted in a 90 min gradient of 5% to 38% acetonitrile (ACN) in 0.1% formic acid at 300 nL/min., followed by a 3-min ramping to 95% ACN-0.1%FA and a 5-min holding at 95% ACN-0.1%FA. The column was re-equilibrated with 2% ACN-0.1%FA for 20 min prior to the next run.

The eluted peptides were detected by Orbitrap through a nano ion source containing a 10-µm analyte emitter (NewObjective, Woburn, MA). The Orbitrap Velos was operated in positive ion mode with nano spray voltage set at 1.5 kV and source temperature at 275 °C. Either internal calibration using the background ion signal at *m/z* 445.120025 as a lock mass or external calibration for FT mass analyzer was performed. The instrument was operated in data-dependent acquisition (DDA) mode using FT mass analyzer for one survey MS scan for precursor ions, followed by ten data-dependent HCD-MS/MS scans for precursor peptides with multiple charged ions above a threshold ion count of 7500 with normalized collision energy of 45%. MS survey scanned at a resolution of 30,000 (fwhm at *m/z* 400), for the mass range of *m/z* 400-1400, and MS/MS scanned at 7,500 resolution for the mass range, m/z 100-2000. All data were acquired under Xcalibur 2.1 operation software (Thermo-Fisher Scientific).

Data processing, protein identification and data analysis

All MS and MS/MS raw spectra from iTRAQ experiments were processed using Proteome Discoverer 1.2 (PD1.2, Thermo), and the spectra from each DDA file were output as an MGF file for subsequent database search using in-house license Mascot Deamon (version 2.3.02, Matrix Science, Boston, MA). The *bacteria"* protein none redundancy" sequence database was used, containing 10,348,164 sequence entries downloaded from NCBI (http://www.NCBI.com) on Jan. 21st, 2010. "Combine with customized mutant sequences" was used for database search. The default search settings used for 4-plex iTRAQ quantitative processing and protein identification in Mascot server were: one mis-cleavage for full trypsin with fixed MMTS modification of cysteine, fixed 4-plex iTRAQ modifications on lysine and N-terminal amines and variable modifications of methionine oxidation and 4-plex iTRAQ on tyrosine.

The peptide mass tolerance and fragment mass tolerance values were 30 ppm and 100 mmu, respectively. To estimate the false discovery rate (FDR) for a measure of identification certainty in each replicate set, an automatic decoy database search was performed in Mascot by choosing the decoy checkbox in which a random sequence of database is generated and tested for raw spectra along with the real database. To reduce the probability of false peptide identification, the significant scores at 99% confidence interval for the peptides defined by a Mascot probability analysis (www.matrixscience.com/help/scoring_help.html#PBM) greater than "identity" were used as a filter and the resulting peptides are considered to be confidently identified peptides and used for protein identifications. Furthermore, proteins identified in all four iTRAQ experiments, which contained at least two peptides with a p value of < 0.001 (expectation value) as determined by Mascot probability analysis were further analyzed. Intensities of the reporter ions from iTRAQ tags upon fragmentation were used for quantification, and the relative quantitation ratios were normalized to the median ratio for the 4-plex in each set of experiments.

APPENDIX A-2

SUPPORTING DATA: SELECTED PROTEINS REPORTED IN iTRAQ STUDIES

Notes: (*) indicates ratio that is significantly different from 1 at a 95% confidence level. Percentage errors with brackets [ ] indicate that the peptide match ratios do not appear to come from a sample with a normal distribution; p is number of peptides.

Locus Tag	Protein Description	115/114	p	%error	116/114	p	%error	117/114	p	%error
Bpro_5301	cytochrome P450	1.587	7	1.193*	0.180	7	1.524*	0.370*	7	1.180*
Bpro_5566	Alpha/beta hydrolase fold-3	10.493	3	1.819*	0.282	3	1.653*	0.485*	3	1.283*
Bpro_5565	flavin-containing monooxygenase FMO	2.994	9	[1.182]	0.140	6	[2.421]	0.148*	7	1.371*
Bpro_5563	zinc-binding alcohol dehydrogenase	0.770	5	1.104*	0.100	5	1.535*	0.139*	5	1.319*
Bpro_5186	haloacid dehalogenase, type II	0.155	12	[1.212]	0.142	12	1.160*	0.150*	12	1.142*
Bpro_0056	haloacid dehalogenase, type II	0.804	2	1.023*	0.651	2	1.007*	0.828	2	1.030
Bpro_2101	isocitrate lyase	2.494	9	[1.088]	2.114	9	1.075*	2.177	9	[1.102]
Bpro_0645	glutathione S-transferase-like	0.724	1	[1.000]	0.017	1	[1.000]	0.024	1	[1.000]
Bpro_0646	pyridoxamine 5'-phosphate oxidase	1.165	1	[1.000]	0.450	1	[1.000]	0.401	1	[1.000]
Bpro_4442	DNA-directed RNA polymerase subunit beta	1.088	22	1.077*	0.949	22	1.090*	0.909	22	[1.088]
Bpro_0086	2,5-dioxopentanoate dehydrogenase (NAD+)	0.738	3	1.022*	0.702	3	1.059*	0.654	3	1.234
Bpro_4478	alpha/beta hydrolase fold	0.507	1	[1.000]	0.806	1	[1.000]	1.033	1	[1.000]
Aldehyde and alcohol dehydrogenases										
Bpro_3952	aldehyde dehydrogenase	0.385	23	1.081*	0.055	22	1.380*	0.081	23	1.228*
Bpro_2290	aldehyde dehydrogenase	1.141	6	1.046*	1.057	6	1.038*	1.061	6	1.061
Bpro_3422	aldehyde dehydrogenase	1.379	2	1.178	1.038	3	1.136	1.014	2	1.081
Bpro_4691	aldehyde dehydrogenase	0.849	1	[1.000]	1.334	1	[1.000]	1.329	1	[1.000]
Bpro_2298	aldehyde dehydrogenase	0.824	2	1.036	0.828	2	1.481	0.854	2	1.387

Bpro_4702	aldehyde dehydrogenase	0.934	2	1.064	1.377	2	1.482	1.655	2	1.057*
Bpro_3129	zinc-binding alcohol dehydrogenase	0.387	1	[1.000]	0.906	1	[1.000]	0.757	1	[1.000]
Bpro_2526	iron-containing alcohol dehydrogenase	0.546	3	1.178*	0.834	3	1.070*	1.081	3	1.074
Bpro_0360	zinc-binding alcohol dehydrogenase	0.735	1	[1.000]	1.176	1	[1.000]	1.132	1	[1.000]
Bpro_5563	zinc-binding alcohol dehydrogenase	0.770	5	1.104*	0.100	5	1.535*	0.139	5	1.319*
Bpro_3853	zinc-binding alcohol dehydrogenase	0.800	7	1.055*	1.907	8	1.113*	1.987	8	1.120*
Bpro_3259	zinc-binding alcohol dehydrogenase	0.806	5	[1.053]	0.710	4	1.051*	0.789	5	1.060*
Bpro_2634	zinc-binding alcohol dehydrogenase	1.122	5	1.043*	5.900	5	1.201*	5.295	5	1.187*
Bpro_4700	iron-containing alcohol dehydrogenase	1.129	4	1.094	1.604	4	1.123*	1.857	4	1.114*
Bpro_2565	zinc-binding alcohol dehydrogenase	1.536	4	1.157*	1.400	4	1.126*	1.438	4	1.182*
Bpro_3062	zinc-containing alcohol dehydrogenase	2.949	2	1.173	1.519	2	1.23	1.545	2	1.17
Bpro_2135	zinc-binding alcohol dehydrogenase	3.422	4	1.170*	0.901	4	1.042*	0.859	4	[1.068]
Proteins from suicide vector										
108796622	neomycin phosphotransferase	0.190	1	[1.000]	10.142	1	[1.000]	4.632	1	[1.000]
53793959	oriT-binding protein	---	0	---	79.075	2	2.407	84.455	2	2.359
Ribosomal proteins										
Bpro_4443	50S ribosomal protein L7/L12	1.470	8	1.243*	0.686	8	1.134*	0.675	8	1.123*
Bpro_4445	50S ribosomal protein L1	1.187	9	1.059*	0.603	9	1.052*	0.669	9	1.062*
Bpro_0259	50S ribosomal protein L2	0.975	5	1.020*	0.605	5	[1.049]	0.677	5	[1.111]
Bpro_1292	50S ribosomal protein L25P	1.186	9	1.063*	0.526	9	1.111*	0.581	8	1.068*
Bpro_0257	50S ribosomal protein L4	1.039	12	1.050*	0.552	12	1.125*	0.635	12	1.049*
Bpro_4113	50S ribosomal protein L13	1.020	8	[1.101]	0.576	7	1.077*	0.557	8	1.102*
Bpro_0487	50S ribosomal protein L5	1.088	9	1.025*	0.638	9	1.061*	0.607	8	1.032*
Bpro_2105	50S ribosomal protein L20	1.126	4	1.068*	0.493	4	1.046*	0.470	4	1.139*
Bpro_0485	50S ribosomal protein L14P	1.017	4	1.245	0.553	4	1.248*	0.625	4	1.197*

Bpro_3034	50S ribosomal protein L9P	1.018	9	1.069	0.560	9	1.084*	0.527	9	1.160*
Bpro_0493	50S ribosomal protein L30P	1.139	3	1.036*	0.502	3	[1.104]	0.592	3	1.057*
Bpro_0256	50S ribosomal protein L3P	1.098	7	1.085*	0.588	6	1.128*	0.650	7	[5.488]
Bpro_3802	50S ribosomal protein L28	1.116	5	1.022*	0.562	5	1.035*	0.590	5	1.040*
Bpro_0838	50S ribosomal protein L27	1.077	3	1.058	0.442	3	1.220*	0.464	3	1.111*
Bpro_1101	50S ribosomal protein L11P methyltransferase	0.787	3	1.207	0.823	3	1.173	0.874	3	1.122
Bpro_0490	50S ribosomal protein L6P	1.053	6	[1.408]	0.493	6	1.155*	0.569	6	1.091*
Bpro_2261	50S ribosomal protein L31P	1.146	4	1.052*	0.479	4	1.120*	0.585	3	1.045*
Bpro_0258	50S ribosomal protein L23P	0.947	2	1.068	0.600	2	1.027	0.470	2	1.021*
Bpro_0494	50S ribosomal protein L15P	0.929	2	1.101	0.584	2	1.241	0.472	2	1.226
Bpro_4444	50S ribosomal protein L10	1.120	2	1.079	0.683	2	1.393	0.662	2	1.026*
Bpro_0839	50S ribosomal protein L21P	1.262	1	[1.000]	0.558	1	[1.000]	0.474	1	[1.000]
Bpro_0027	50S ribosomal protein L19	1.118	2	1.747	2.883	2	1.214	4.030	2	1.115*
Bpro_0260	30S ribosomal protein S19P	0.304	4	[2.160]	0.704	4	1.192*	0.382	4	1.322*
Bpro_2695	30S ribosomal protein S2P	1.099	5	1.120	0.736	5	1.163*	0.721	4	1.065*
Bpro_3570	30S ribosomal protein S20P	0.413	1	[1.000]	1.101	1	[1.000]	0.934	1	[1.000]
Bpro_0499	30S ribosomal protein S11	0.687	3	1.322	0.792	3	1.122	0.677	3	1.185
Bpro_0252	30S ribosomal protein S7	0.928	7	1.032*	0.754	7	1.043*	0.638	7	1.033*
Bpro_0262	30S ribosomal protein S3	0.847	5	1.169	0.624	5	1.130*	0.646	5	1.108*
Bpro_1789	30S ribosomal protein S1	0.521	5	[1.193]	0.902	5	1.039*	0.813	5	1.064*
Bpro_0492	30S ribosomal protein S5	0.996	3	1.463	0.636	3	1.217	0.457	3	1.174*
Bpro_3261	30S ribosomal protein S15	0.959	5	1.021*	0.634	5	1.062*	0.662	5	1.036*
Bpro_0255	30S ribosomal protein S10	0.958	3	1.029	0.703	3	1.014*	0.753	3	1.018*
Bpro_0500	30S ribosomal protein S4	1.042	1	[1.000]	0.594	1	[1.000]	0.620	1	[1.000]
Bpro_4112	ribosomal protein S9	0.980	1	[1.000]	0.758	1	[1.000]	0.755	1	[1.000]
Bpro_2692	ribosome recycling factor	0.992	4	1.052	1.192	4	1.102*	1.178	4	1.091*
Bpro_0771	ribosome biogenesis GTP-binding protein YsxC	0.827	1	[1.000]	1.143	1	[1.000]	1.199	1	[1.000]

Central metabolism										
Bpro_0086	2,5-dioxopentanoate dehydrogenase (NAD+)	0.738	3	1.022*	0.702	3	1.059*	0.654	3	1.234
Bpro_0195	6-phosphogluconate dehydrogenase, NAD-binding	1.041	5	1.065	0.726	5	[1.079]	0.745	5	1.090*
Bpro_1231	Beta-ketoadipyl CoA thiolase	0.888	9	1.079*	0.124	9	1.354*	0.134	8	1.327*
Bpro_1287	fructose-bisphosphate aldolase	1.647	1	[1.000]	0.556	1	[1.000]	0.568	1	[1.000]
Bpro_0753	glucose-6-phosphate isomerase	0.738	2	1.016*	0.801	2	1.133	0.774	2	1.227
Bpro_4517	malate synthase G	0.556	8	[1.062]	0.594	8	1.124*	0.684	8	1.204*
Bpro_0643	NADPH-glutathione reductase	0.862	2	1.124	0.869	2	1.075	0.843	2	1.274
Bpro_0160	phosphoenolpyruvate carboxykinase	0.452	7	1.314*	0.666	7	[1.350]	0.792	7	1.142*
Bpro_3665	phosphoenolpyruvate carboxylase	0.789	16	[1.064]	1.444	16	1.055*	1.324	16	[1.089]
Bpro_4634	pyruvate kinase	0.936	1	[1.000]	0.347	1	[1.000]	0.403	1	[1.000]
Bpro_4827	transketolase	0.833	4	1.100*	0.985	4	1.146	1.037	3	1.056
Bpro_2140	acetyl-CoA acetyltransferase	1.122	18	[1.099]	2.674	21	[2.289]	2.245	20	[2.334]
Bpro_3678	L-lactate dehydrogenase (cytochrome)	1.056	1	[1.000]	0.928	1	[1.000]	0.821	1	[1.000]
Bpro_2055	hydroxyacylglutathione hydrolase	0.785	2	1.052	1.162	2	1.086	1.065	2	1.163
Bpro_0187	glycolate oxidase FAD binding subunit	1.153	1	[1.000]	1.757	1	[1.000]	1.404	1	[1.000]
Bpro_3592	aconitate hydratase	0.870	7	1.041*	1.794	8	1.073*	1.929	8	1.042*
Bpro_2942	isocitrate dehydrogenase	0.765	9	[1.294]	0.933	9	1.027*	0.763	9	[1.119]
Proteins involved in biological stresses										
Bpro_3126	molecular chaperone DnaK	0.802	20	[1.091]	0.593	20	1.075*	0.627	20	1.062*
Bpro_2031	ATP-dependent protease ATP-binding subunit ClpX	0.864	2	1.231	0.935	2	1.422	0.753	2	1.742
Bpro_1400	Ferritin and Dps	1.148	2	1.098	3.526	2	1.151	3.733	2	1.176
Bpro_0759	chaperonin GroEL	1.040	38	[1.128]	0.553	37	[1.099]	0.677	37	[1.094]
Bpro_1032	heat shock protein HtpX	1.290	1	[1.000]	1.153	1	[1.000]	1.067	1	[1.000]
Bpro_1303	heat-inducible transcription repressor	1.138	1	[1.000]	1.167	1	[1.000]	1.246	1	[1.000]

Bpro_1199	heat shock protein Hsp20	0.551	10	1.064*	1.970	10	1.054*	2.175	10	1.061*
Bpro_2651	putative heat shock protein	0.943	2	1.280	0.487	3	1.349	0.485	2	1.017*
Bpro_0614	heat shock protein 90	1.255	1	[1.000]	1.003	1	[1.000]	1.330	1	[1.000]
Bpro_0948	DNA repair protein RadC	0.772	1	[1.000]	1.260	1	[1.000]	0.929	1	[1.000]
Bpro_3337	DNA mismatch repair protein MutS	1.362	3	[1.229]	0.846	3	1.136	0.999	3	1.105
Bpro_3097	sigma 70 (RpoD)	1.423	5	1.046*	1.128	5	1.136	1.166	5	1.055*
Bpro_3187	Hsp33 protein	0.927	1	[1.000]	1.019	1	[1.000]	1.140	1	[1.000]
Bpro_2396	heme peroxidase	2.414	2	1.066	0.407	2	1.057	1.345	2	1.009
Bpro_0678	catalase/peroxidase HPI	0.979	1	[1.000]	1.054	1	[1.000]	0.939	1	[1.000]
Bpro_4841	peroxidase	1.051	3	1.056	2.994	3	1.074*	2.870	3	1.063*
Bpro_4561	glyoxylate carboligase	0.293	1	[1.000]	0.335	1	[1.000]	0.335	1	[1.000]
Bpro_4563	2-hydroxy-3-oxopropionate reductase	0.239	2	1.094*	0.051	5	3.652*	0.060	4	3.210*
Bpro_4562	hydroxypyruvate isomerase	0.009	1	[1.000]	0.059	2	1.989	0.053	2	2.182
Bpro_3549	glyoxalase I	0.830	1	[1.000]	0.524	1	[1.000]	0.637	1	[1.000]
Bpro_0266	alkyl hydroperoxide reductase/ Thiol specific antioxidant/ Mal allergen	0.936	3	1.054	1.417	4	1.3	1.447	4	1.087*
Bpro_2187	alkyl hydroperoxide reductase/ Thiol specific antioxidant/ Mal allergen	0.892	6	1.050*	0.817	6	1.053*	0.868	6	1.031*
Bpro_2856	glutaredoxin	0.836	5	1.066*	1.427	5	1.295*	1.468	4	1.129*
Bpro_0848	glutaredoxin-like protein	0.676	1	[1.000]	0.747	1	[1.000]	0.802	1	[1.000]
Bpro_2337	phosphoadenylylsulfate reductase (thioredoxin)	0.949	1	[1.000]	0.578	1	[1.000]	0.676	1	[1.000]
Bpro_2263	thioredoxin	0.847	7	1.136*	1.059	7	1.172	1.016	7	1.244
Bpro_3369	thioredoxin	1.267	1	[1.000]	0.846	1	[1.000]	0.889	1	[1.000]
Bpro_4628	thioredoxin	1.031	4	1.291	1.246	4	1.128*	1.184	4	1.056*
Bpro_3801	thioredoxin reductase	0.732	5	1.049*	0.966	5	1.041	1.015	5	1.037

Proteins involved in iron-sulfur cluster assembly

Bpro_4271	FeS assembly protein SufD	0.656	1	[1.000]	1.120	1	[1.000]	1.514	1	[1.000]
Bpro_4109	iron-sulfur cluster insertion protein ErpA	0.793	3	1.079*	0.839	3	1.049*	0.905	3	1.049
Bpro_3557	(2Fe-2S)-binding	0.865	1	[1.000]	0.890	1	[1.000]	0.984	1	[1.000]
Bpro_2178	cysteine desulfurase IscS	0.907	2	1.038	0.689	2	1.076	0.912	2	1.030
Bpro_2335	sulfate adenylyltransferase subunit 1	0.916	5	[1.089]	0.421	4	1.049*	0.558	5	1.138*
Bpro_2628	sulfur compound chelating protein SoxZ	0.924	2	1.01	0.815	2	1.037	0.915	2	1.084
Bpro_2337	phosphoadenylylsulfate reductase (thioredoxin)	0.949	1	[1.000]	0.578	1	[1.000]	0.676	1	[1.000]
Bpro_2182	Fe-S protein assembly chaperone HscA	0.976	2	1.043	0.940	2	1.003*	1.195	2	1.176
Bpro_2336	sulfate adenylyltransferase subunit 2	1.019	2	1.339	0.444	2	1.095	0.548	2	1.167
Proteins involved in glutathione synthesis										
Bpro_3399	glutamate-cysteine ligase	0.803	1	[1.000]	1.161	1	[1.000]	1.085	1	[1.000]
Bpro_2178	cysteine desulfurase IscS	0.907	2	1.038	0.689	2	1.076	0.912	2	1.030
Bpro_2417	glutathione-dependent formaldehyde-activating, GFA	0.708	8	1.184*	2.187	8	1.101*	2.310	8	1.084*
Bpro_0824	glutathione S-transferase-like	1.612	6	1.090*	1.164	6	1.081*	1.178	6	[1.070]
Bpro_2563	putative glutathione S-transferase-related protein	1.924	6	1.119*	1.538	4	1.013*	1.284	5	1.044*
Bpro_0643	NADPH-glutathione reductase	0.862	2	1.124	0.869	2	1.075	0.843	2	1.274
Bpro_0243	glutathione S-transferase-like	0.976	3	1.025	1.034	3	1.052	1.053	3	1.002*
Bpro_4661	glutathione S-transferase-like	0.961	1	[1.000]	1.156	1	[1.000]	1.309	1	[1.000]
Bpro_4540	glutathione synthetase	0.804	1	[1.000]	1.027	1	[1.000]	1.136	1	[1.000]
Bpro_0387	glutathione S-transferase-like	0.733	1	[1.000]	0.412	1	[1.000]	0.486	1	[1.000]
Bpro_2168	lactoylglutathione lyase	0.913	1	[1.000]	1.349	1	[1.000]	1.239	1	[1.000]
Bpro_2055	hydroxyacylglutathione hydrolase	0.785	2	1.052	1.162	2	1.086	1.065	2	1.163
Bpro_4156	D-isomer specific 2-hydroxyacid dehydrogenase, NAD-binding	0.861	1	[1.000]	0.982	1	[1.000]	1.052	1	[1.000]

APPENDIX B

LIST OF SCIENTIFIC / TECHNICAL PUBLICATIONS

APPENDIX B

LIST OF SCIENTIFIC / TECHNICAL PUBLICATIONS

Scientific and technical publications produced during the course of SERDP Project ER1557 *Elucidation of the Mechanisms and Environmental Relevance of cis-Dichloroethene and Vinyl Chloride Biodegradation* are summarized below.

1. Articles in Peer-Reviewed Journals

Mundle, S. O. C., T. Johnson, G. Lacrampe-Couloume, A. Pérez-de-Mora, M. Duhamel, E. A. Edwards, M. McMaster, E. Cox, K. Révész, and B. Sherwood Lollar (2012). "Monitoring Biodegradation of Ethene and Bioremediation of Chlorinated Ethenes at a Contaminated Site Using Compound-Specific Isotope Analysis (CSIA)." Environmental Science & Technology **46**(3): 1731-1738.

Gossett, J. M. (2010). "Sustained Aerobic Oxidation of Vinyl Chloride at Low Oxygen Concentrations." Environmental Science & Technology **44**(4): 1405-1411.

Giddings, C. G. S., L. K. Jennings, and J. M. Gossett (2010). "Microcosm Assessment of a DNA Probe Applied to Aerobic Degradation of cis-1,2- Dichloroethene by Polaromonas sp. strain JS666." Ground Water Monitoring & Remediation **30**(2): 97-105.

Jennings, L. K., M. M. G. Chartrand, G. Lacrampe-Couloume, B. Sherwood Lollar, J. C. Spain, and J. M. Gossett (2009). "Proteomic and transcriptomic analyses reveal genes upregulated by cis-dichloroethene in Polaromonas sp. strain JS666." Applied and Environmental Microbiology **75**(11): 3733-3744.

Shin, K. A., J. M Gossett, and J.C Spain. Initial Steps of cis-Dichloroethene Biodegradation by Polaromonas sp. JS666. To be submitted to Applied and Environmental Microbiology – *in process*.

2. Technical Reports

Cox, E., C. Austrins, J. Gossett, J. Spain, E. Edwards, and B. Sherwood Lollar. (2010). "Elucidation of the Mechanisms and Environmental Relevance of cis-Dichloroethene and Vinyl Chloride Biodegradation." 2010 Annual Report – Year 4 prepared for SERDP Project ER-1557.

Cox, E., C. Austrins, J. Gossett, J. Spain, E. Edwards, and B. Sherwood Lollar. (2009). "Elucidation of the Mechanisms and Environmental Relevance of cis-Dichloroethene and Vinyl Chloride Biodegradation." 2009 Annual Report – Year 3 prepared for SERDP Project ER-1557.

Cox, E., C. Austrins, J. Gossett, J. Spain, E. Edwards, and B. Sherwood Lollar. (2008). "Elucidation of the Mechanisms and Environmental Relevance of cis-Dichloroethene and Vinyl Chloride Biodegradation." 2008 Annual Report prepared for SERDP Project ER-1557.

Cox, E., C. Austrins, J. Gossett, J. Spain, E. Edwards, and B. Sherwood Lollar. (2007). "Elucidation of the Mechanisms and Environmental Relevance of cis-Dichloroethene and Vinyl Chloride Biodegradation." 2007 Annual Report prepared for SERDP Project ER-1557.

3. Conference or Symposium Proceedings

Cox, E., C. Austrins, J. Spain, K. Shin, S. Nishino, J. Gossett, C. Giddings, L. Jennings, E. Edwards, T. Johnson, M. Duhamel, and B. Sherwood Lollar, "The Truth is Out There: Unraveling the Mystery of the Missing DCE, Vinyl Chloride, and Ethene," presented at the Seventh International Conference on Remediation of Chlorinated and Recalcitrant Compounds," Monterey CA (May 24-27, 2010).

Giddings, C. G. S. and J. M. Gossett, "Dynamic Expression of Putative Genes in the Aerobic, *cis*-1,2-Dichlorothene Degradation Pathways of *Polaromonas* sp. Strain JS666," presented at the Seventh International Conference on Remediation of Chlorinated and Recalcitrant Compounds," Monterey CA (May 24-27, 2010).

Giddings, C. G. S., L. K. Jennings, and J. M. Gossett, "Microcosm Assessment of a DNA-Probe Applied to Aerobic Degradation of cis-1,2-Dichloroethene by *Polaromonas* sp. Strain JS666," presented at the Seventh International Conference on Remediation of Chlorinated and Recalcitrant Compounds," Monterey CA (May 24-27, 2010).

Sherwood Lollar, B., J. McKelvie, M. Elsner, S. Mancini, T. Johnson, M. Simpson, A. Simpson, E. Edwards, J. Gossett, L. Jennings, J. Spain, and E. Cox, "New Developments in Forensic Evaluation of Contaminant Sources and Microbial Degradation Pathways Using CSIA," presented at the Seventh International Conference on Remediation of Chlorinated and Recalcitrant Compounds," Monterey CA (May 24-27, 2010).

Wan Johari, W. L. and J. M. Gossett, "The Involvement of a Cyclohexanone Monooxygenase Gene of *Polaromonas* sp. JS666 during Aerobic *cis*-Dichloroethene Degradation," presented at the Seventh International Conference on Remediation of Chlorinated and Recalcitrant Compounds," Monterey CA (May 24-27, 2010).

Cox, E., J. M. Gossett, J. C. Spain, E. Edwards, and B. Sherwood Lollar, "The Truth is Out There: Unraveling the Mystery of the Missing DCE, Vinyl Chloride & Ethene," *Partners in Environmental Technology Technical Symposium & Workshop, SERDP/ESTCP*, Washington, D.C. (December 1-3, 2009).

Gossett, J. M., "Characterization of a Novel Aerobic Bacterium Capable of Growth on the Aerobic Oxidation of cis-Dichloroethene." Spring 2009 Distinguished Lecturer, Georgia Institute of Technology's Association of Environmental Engineers and Scientists (AEES) (April 18, 2009).

Cox, E., C. Austrins, J. Gossett, J. Spain, E. Edwards, and B. Sherwood Lollar, "Elucidation of the Mechanisms and Environmental Relevance of cis-Dichloroethene and Vinyl Chloride Biodegradation," *Partners in Environmental Technology Technical Symposium & Workshop, SERDP/ESTCP*, Washington, D.C. (December 2-4, 2008).

Gossett, J. M., "Polaromonas sp. Strain JS666 as a potential bioaugmentation agent for aerobic, cDCE-contaminated sites," presented at the Third International Joint Workshop: Tsinghua University and Cornell University, Ithaca NY (April 29-30, 2008).

Jennings, L. K., J. M. Gossett, and J. C. Spain, "Deciphering cDCE Degradation Pathways in *Polaromonas* sp. Strain JS666," presented at Ninth International In Situ and On-Site Bioremediation Symposium, Baltimore, MD (May 7-10, 2007).

4. Conference or Symposium Abstracts

Liu, Fang, E. Wood, and J. M. Gossett, "Kinetics of the Aerobic Degradation of Chloroethene Mixtures by Polaromonas sp. JS666," Abstract 09-GM-A-2658-ASM, 109th General Meeting, American Society for Microbiology, Philadelphia, PA (May 17-21, 2009).

Jennings, L. K., S. F. Nishino, R. B. Payne, J. C. Spain, and J. M. Gossett. "Proteomic and transcriptomic analyses reveal genes upregulated by cis-dichloroethene in Polaromonas sp. JS666," Abstracts of the 108th General Meeting of the Amer. Soc. for Microb., Boston, MA (June 1-5, 2008).

5. Text Books or Book Chapters

Jennings, L. K., C. G. S. Giddings, J. C. Spain, and J. M. Gossett (2012). "Bioaugmentation for Aerobic Degradation of cis-1,2-Dichloroethene," Chapter 7 in *Bioaugmentation for Groundwater Remediation*, Volume 4 of the SERDP and ESTCP Remediation Technology Monograph Series, Springer Publishers – *publication pending*.

APPENDIX C

OTHER SUPPORTING MATERIALS

TECHNICAL AWARDS AND HONORS

Understanding cis-DCE and VC Biodegradation

Longstanding scientific question now resolved, knowledge enables DoD to improve management of chlorinated solvent-contaminated sites.

Dr. James Gossett, Co-Performer

Mr. Evan Cox, Geosyntec Consultants, Inc.
Elucidation of the Mechanisms and Environmental Relevance of *cis*-Dichloroethene and Vinyl Chloride Biodegradation

Chlorinated solvents are the most common source of contaminated groundwater on DoD lands. Over the last decade, tremendous progress has been made in understanding the fundamental processes that drive cost-effective remediation at these sites. The cleanup approach used today bears little resemblance to the approaches used 20 year ago. Due to the effort of many SERDP and ESTCP investigators, most DoD sites are cleaned up by either introduced or natural biological processes that break down these contaminants to the point where the harmful chemicals are fully degraded and the site is remediated. These approaches have saved the Department of Defense billions of dollars.

But at a significant number of sites, the process may appear to stall at a point where the solvents have been degraded into the toxic chemicals *cis*-dichloroethene (DCE) and vinyl chloride (VC). The possible routes and rate for the continued degradation of these chemicals have been a subject of great debate in the scientific literature with significant economic and risk consequences.

Mr. Evan Cox and his colleagues Jim Gossett (Cornell University), Jim Spain (Georgia Institute of Technology), and Elizabeth Edwards and Barbara Sherwood Lollar (the University of Toronto) succeeded in identifying the organisms and elucidating the pathways by which these toxic chemicals may continue to break down at these sites. Through a series of elegant experiments, they determined that micropockets of oxygen, at very low concentration, do in fact exist in groundwater at sites that appear to be anaerobic, promoting aerobic biodegradation of *cis*-DCE and VC, thus resolving a longstanding scientific question.

This knowledge will directly reduce DoD costs for cleaning up chlorinated solvent sites and improve management of these sites. Managers will now be able to predict with confidence if a site will continue to remediate itself or if they need to introduce other processes to fully degrade these toxic chemicals.

For this work, Mr. Cox and his team received a Project-of-the-Year award at the annual Partners in Environmental Technology Technical Symposium & Workshop held November 30 – December 2, 2010, in Washington, D.C.

Related Resources

Elucidation of the Mechanisms and Environmental Relevance of *cis*-Dichloroethene and Vinyl Chloride Biodegradation

Strategic Environmental Research and Development Program (SERDP)
Environmental Security Technology Certification Program (ESTCP)
Phone (703) 696-2127 | Fax (703) 696-2114
901 North Stuart Street, Suite 303 Arlington, VA 22203

Geosyntec consultants

130 Research Lane, Suite 2
Guelph, Ontario, Canada
N1G 5G3
PH 519.822.2230
FAX 519.822.3151
www.geosyntec.com

MEMORANDUM

Date: 30 September 2010

To: Dr. Jeffery A. Marqusee/SERDP and ESTCP

Copies to: Ms. Alicia Shepard/HGL

From: Carey Austrins, Evan Cox – Geosyntec Consultants

Subject: SERDP Project of the Year – List of co-performers.

ER-1557: Elucidation of the Mechanisms and Environmental Relevance of cis-Dichloroethene and Vinyl Chloride Biodegradation

---

This memorandum provides a list of co-performers as requested for the SERDP Project of the Year. The lead investigators are listed below, along with the co-performers:

1. Evan Cox (PI) – Geosyntec Consultants, Inc.
    a. Carey Austrins
2. Dr. Elizabeth Edwards (CO-PI) – University of Toronto
    a. Alfredo Pérez-de-Mora
    b. Melanie Duhamel
    c. Winnie Chan
    d. Tiffany Johnson
3. Dr. James Gossett (CO-PI) – Cornell University
    a. Laura Jennings
    b. Cloelle Giddings
    c. Wan Lutfi Wan Johari
4. Dr. Barbara Sherwood-Lollar (CO-PI) – University of Toronto
    a. George Lacrampe-Couloume

b. Scott Mundle

5. Dr. Jim Spain (CO-PI) - Georgia Institute of Technology

   a. Shirley Nishino

   b. Rayford Payne

   c. Kwanghee Shin

   d. Sarah Craven